Design, Synthesis and Evaluation of Macrocyclic Antifungal Peptides

Monique Priscilla Catharina Mulder

Design, Synthesis and Evaluation of Macrocyclic Antifungal Peptides
M.P.C. Mulder

ISBN: 978-94-6182-165-2

Printed by: Offpage, Amsterdam

Cover design: Monique Mulder and Jeroen van der Meer
"Defeat of the fungi"

Design, Synthesis and Evaluation of Macrocyclic Antifungal Peptides

Ontwerp, synthese en evaluatie van macrocyclische antischimmel peptides

(met een samenvatting in het Nederlands)

Proefschrift

ter verkrijging van de graad van doctor aan de Universiteit Utrecht op gezag van de rector magnificus, prof.dr. G.J. van der Zwaan, ingevolge het besluit van het college voor promoties in het openbaar te verdedigen op vrijdag 9 november 2012 des ochtends te 10.30 uur

door

Monique Priscilla Catharina Mulder

geboren op 1 november 1983, te Zeist

Promotor: Prof. dr. R. M. J. Liskamp

Co-promotor: Dr. ir. J. A. W. Kruijtzer

The printing of this thesis was financially supported by:
JEOL (Europe) B.V. Nieuw-Vennep, The Netherlands

Voor mijn moeder

Table of contents

List of abbreviations

Amino acids

Ala	Alanine
Alg	Allylglycine
Asp	Aspartic acid
Cys	Cysteine
Hyp	Hydroxyproline
HSe	Homoserine
hSec	Selenohomocysteine
hTyr	Homotyrosine
Lys	Lysine
Orn	Ornithine
Thr	Threonine
VGly	Vinylglycine

General

A.	Aspergillus
Ac	acetyl
AccuTOF	accurate time of flight
AcOH	acetic acid
AmB	Amphotericin B
APT	attached proton test
Ar	aromatic
Boc	tert-butyloxycarbonyl
BOP	benzotriazol-1-yl-oxy-tris-(dimethylamino)-phosphonium hexaflurophosphate
*t*Bu	*tert*-butyl
C.	Candida
cat	catalytic
CBS	centraalbureau voor Schimmelcultures
Cbz	benzyloxycarbonyl
CD	circular dichroism
Cfu	colony forming unit
CNS	central nervous system
COSY	correlation spectroscopy
δ	chemical shift
d	doublet
dd	double doublet
DART	direct analysis in real time
DCBC	2,6-dichlorobenzoyl chloride
DCC	*N*,*N*-dicyclohexyl-carbodiimide
DCM	dichloromethane
DCU	*N*,*N*-dicyclohexylurea
DIBAL	diisobutylaluminium hydride
DiPEA	*N*,*N*-diisopropylethyl-amine
DMA	dimethylacetal
DMAP	4-dimethylaminopyridine
DMF	*N*,*N*-dimethylformamide
DMSO	dimethylsulfoxide
DMT-Myr	(10*R*,12*S*)-dimethyl-myristoyl
DNA	deoxyribonucleic acid
ECBN	Echinocandin B
ESI-MS	electro spray ionization mass spectrometry
EtOAc	ethyl acetate
EtOH	ethanol
5-FC	5-fluorouracil
FDA	food and drug administration
Fmoc	9-fluorenylmethyl-oxycarbonyl
GS	glucan synthase
h	hour
HATU	*O*-(7-azabenzotriazol-1-yl)-*N*,*N*,*N'*,*N'*-tetramethyluronium hexafluorophosphate
HFIP	hexafluoro-isopropanol
HOBt	*N*-hydroxy-benzotriazole
HONSu	hydroxy succinimide
HPLC	high pressure liquid chromatography
HRMS	high resolution mass spectrometry
HSQC	heteronuclear single quantum correlation

IvDde	1-(4,4-dimethyl-2,6-dioxocyclohex-1-ylidene)-3-methylbutyl
KDa	kilo dalton
LDA	lithium diisopropylamide
LHMDS	lithium hexamethyl disilazide
m	multiplet
MALDI-TOF	matrix-assisted laser desorption ionisation time of flight
MeCN	acetonitrile
MeOH	methanol
Me-Myr	(12*S*)-methyl-myristoyl
mg	milligram
MHz	megahertz
MIC	minimum inhibitory concentration
min	minutes
mL	milliliter
mmol	millimol
MeOH	methanol
MS	mass spectrometry
MTBE	*tert*-butyl methyl ether
Mtt	4-methyltrityl
MW	microwave
Myr	myristoyl
m/z	mass to charge ratio
nm	nanometer
NMI	*N*-methylimidazole
NMO	*N*-methylmorpholine *N*-oxide
NMP	*N*-methyl-2-pyrrolidine
NMR	nuclear magnetic resonance
NOE	nuclear Overhauser effect
NOESY	nuclear Overhauser effect spectroscopy
µM	micromolar
Palm	palmitoyl
PIFA	phenyliodine bistrifluoroacetate
Pkc1	protein kinase C
ppm	parts per million
Psoc	(2-phenyl-2-trimethylsilyl) ethoxycarbonyl
q	quartet
RCM	ring closing metathesis
R_f	retardation factor
RNA	ribonucleic acid
ROESY	rotating-frame Overhauser effect spectroscopy
R_t	retention time
s	singlet
SAR	structure activity relationship
S.	Saccharomyces
spp	species
SPPS	solid phase peptide synthesis
Su	succinimide
t	triplet
TEA	triethylamine
Ter	terphenyl
TFA	trifluoroacetic acid
TFE	trifluoroethanol
THF	tetrahydrofuran
THP	tetrahydropyran
TIS	triisopropylsilane
TLC	thin layer chromatography
TMS	tetramethylsilane (NMR)
TMS	trimethylsilyl
TOCSY	total correlation spectroscopy
TOF	time of flight
Tol	toluene
UV	ultra violet
YPD	yeast extract peptone dextrose

CHAPTER 1

General Introduction

1.1 Fungal infections

Invasive fungal infections represent a growing threat and over the past two decades the incidence and diversity of fungal infections has increased enormously, especially among immunocompromised patients and patients hospitalized with serious underlying diseases.[1,2,3] Despite advances in antifungal therapies, the morbidity and mortality associated with these severe opportunistic fungal infections is substantial.[2-4] The still expanding population of immunocompromised patients as well as resistance against and toxicity of the current antifungal agents underscores the urgent need for development of new antifungal compounds preferentially acting on novel targets.[5,6]

Fungal infections, also called mycoses, are classified as superficial, subcutaneous and systemic infections depending on the type and degree of tissue involvement and the host response to the pathogen.[7,8] Superficial and subcutaneous fungal infections affect the skin, keratinous tissues (e.g. nails) or mucous membranes. These infections include some of the most frequently occurring skin diseases. Most of them are easily diagnosed and treated. However, systemic infections, affecting deeper tissues and organs, can be life threatening and are associated with high morbidity and mortality. Opportunistic systemic fungal pathogens require a compromised host in order to establish infection.[7,8] The number of patients having this condition is increasing because of the complications of advanced HIV infection but also due to developments in modern medicine, such as intensive chemotherapy and the use of immunosuppressive drugs for organ transplant recipients.[2]

There are two kinds of fungi: yeasts and moulds (Figure 1). Most moulds and higher fungi are filamentous forms known as hyphae. Hyphae grow by elongation at their tips. At the end of some of these hyphae are conidia or spores that can be compared to seeds, which may develop into new fungi. Examples of filamentous fungi are *Aspergillus* spp., *Fusarium* spp. and *Zygomycota*. Yeasts (e.g. *Candida* spp.) are small rounded forms that reproduce by budding (or fission). Also, some species of *Candida* can develop into different forms, such as yeast and hyphae, depending on infection sites or different culture conditions. These so-called dimorphic fungi can assume both morphological forms.[9]

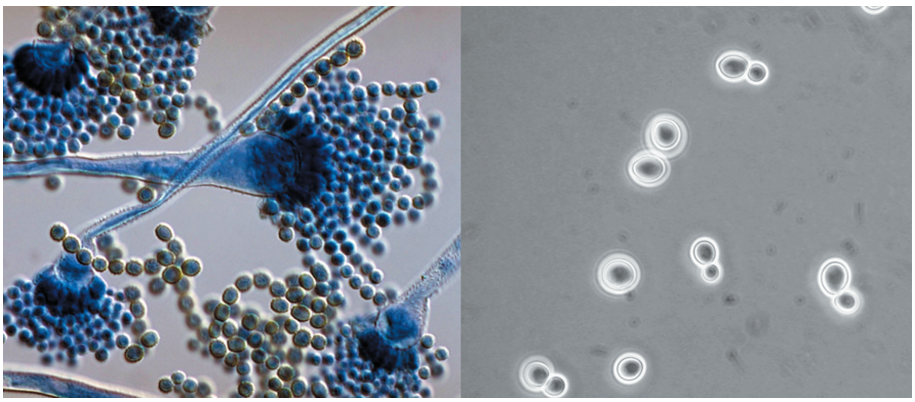

Figure 1. Left: Microscopic view of conidia of *Aspergillus flavus* mould, with the budding conidiospores and the releasing conidia. Right: Microscopical view of budding yeast *Candida albicans*.

Candida spp. and *Aspergillus* spp. account for most of the life-threatening systemic infections.[2,7,8] Candidiasis is a fungal infection of any of the *Candida* species, of which *Candida albican* is the most common. An emergence of *non-albicans Candida* spp., such as *C. krusei*, *C. parapsilosis*, *C. tropicalis* and *C. glabrata* has been seen in recent years.[10] These Candida species represent the most common cause of invasive fungal infection in humans, producing infections that range from non-life threatening mucocutaneous disorders to invasive diseases that can involve any organ. Blood stream infection is the most common clinical manifestation of invasive candidiases.[2]

The incidence of invasive aspergillosis has increased significantly in highly immuno-compromised patients.[2] The most common cause is *Aspergillus fumigatus*, accounting for approximately 90% of infections.[11] *Aspergillus fumigatus* is widely distributed in nature and the hospital environment and its main portal is the respiratory tract. This filamentous fungus is inhaled as unicellular conidia and can develop into branching hyphae in the lungs. However, injuries to the skin may also introduce the organism into susceptible hosts.[7,8] Healthy individuals are naturally immune and do not develop disease against Aspergillus. In addition to *Candida* and *Aspergillus* spp., *Cryoptococcus neoformans*, *Pneumocystis carinii* and *Histoplasma capsulatum* are becoming a growing danger to human health.[10] Moreover, other newly discovered moulds such as *Fusarium* spp., *Scedosporium* spp., and *Zygomycetes* have emerged as leading causes of various mycotic infections.[11] Limited treatment is only possible with currently available antifungal compounds.[2]

1.2 Antifungal agents

Herein, both systemic and superficial fungicides, which have been or are currently under evaluation for use in combating invasive fungal pathogens, are broadly classified into sterol inhibitors (polyenes, azoles and allylamines), DNA synthesis inhibitors (fluoropyrimidines) and β-glucan synthase inhibitors (e.g. echinocandins). An overview of the targets of these inhibitors is presented in Figure 2.[12-14]

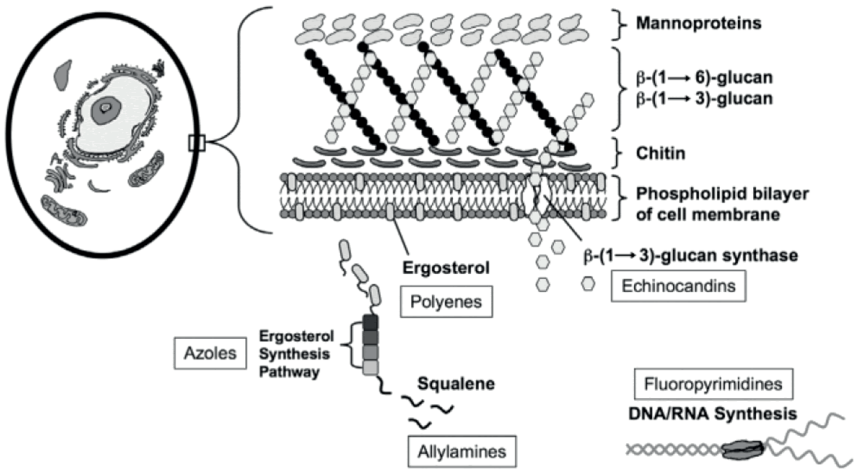

Figure 2. Main targets of antifungal agents.[15]

1.2.1 Sterol inhibitors

The polyenes, azoles and allylamines all owe their antifungal activities to inhibition of the biosynthesis of ergosterol, the predominant component of the fungal cell wall, or direct an interaction with it (Figure 3).[13]

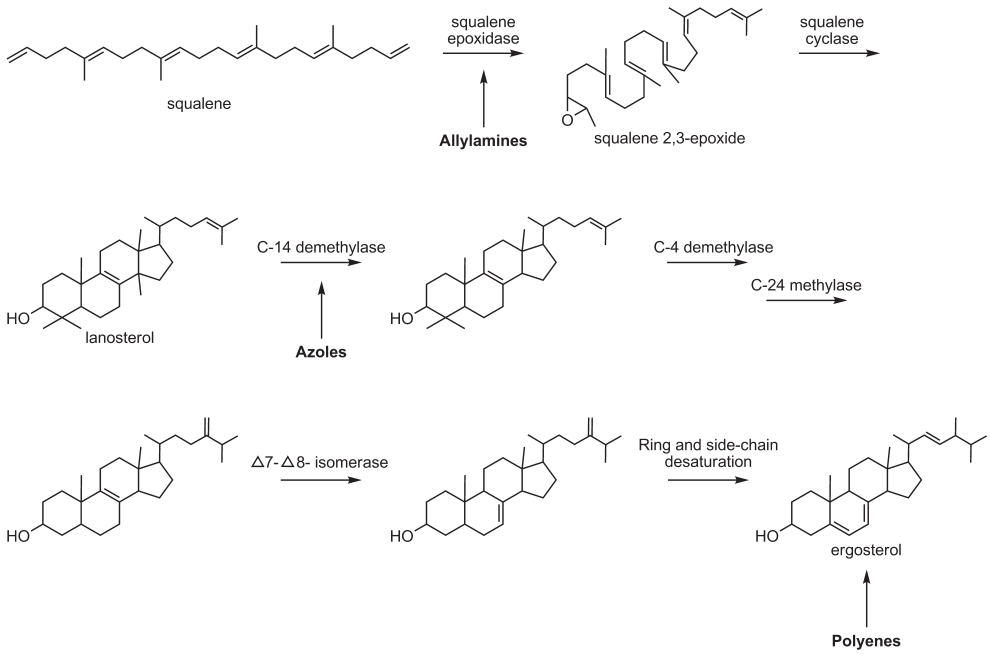

Figure 3. Inhibition and interaction sites of the sterol inhibitors in the ergosterol biosynthesis pathway.

Polyenes

The polyenes constitute the major class of fungal antibiotics. The first member of the polyene family, nystatin was discovered in 1950.[16] Like many other antifungals and antibiotics, nystatin is of bacterial origin and it was isolated from *Streptomyces noursei*. A broad screening of streptomycete cultures for antifungal activity was therefore instituted and led to the discovery of Amphotericin B (AmB), a drug produced by *Streptomyces nodosus*, in 1956.[17] Although many polyenes have been isolated from *Streptomyces* species, only AmB and nystatin are currently widespread used.[14]

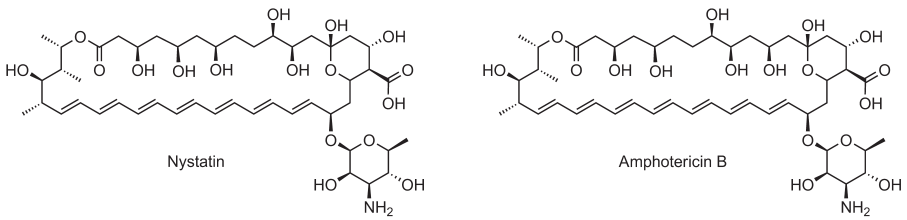

Figure 4. Structures of the polyenes nystatin and Amphotericin B.

Polyene antibiotics display an atypical mode of action for an antimicrobial molecule: instead of inhibiting an enzyme, they bind to ergosterol, the principal sterol in fungal membranes. This interaction leads to the formation of a complex of the polyene with the hydrophobic outer core of the fungal membrane. The inner core of the polyene-sterol complex is hydrophilic due to the presence of hydroxyl groups, and provides an aqueous pore, thereby making the fungal cell membranes permeable to ions and other small molecules. This finally results in fungal cell death.[18]

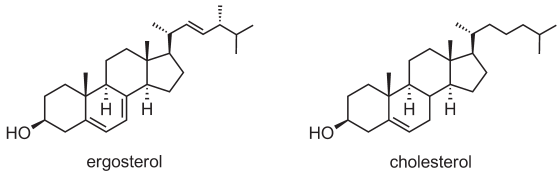

Figure 5. Chemical structures of the sterols in fungi (ergosterol) and in mammalian cells (cholesterol).

Unfortunately, as predicted on the basis of its mechanism of action, polyenes are toxic to mammalian cells due to a considerable interaction of this drug with cholesterol containing membranes (Figure 5).[19] In general, the polyene macrolides may cause such serious side-effects as acute renail failure[20] and thrombophlebitis (inflammation of a vein caused by a blood clot)[21], especially upon intravenous administration. Despite these side effects, broad spectrum of activity and low frequency of appearance of resistant pathogens make polyene antibiotics, like Amphotericin B, the drugs of choice when dealing with life-threatening systemic fungal infections. To reduce these unwanted side-effects, Amphotericin B has been formulated in liposomes resulting in reduced toxicity and therefore larger doses can be administered.[22,14]

Azoles

The azoles represent the second largest class of compounds active against fungal infections.[14] In the late 1960s the first imidazole-based drugs, such as clotrimazole and miconazole, were introduced.[23] Ketoconazole (Figure 6), the first available compound for the oral treatment of systemic fungal infections, was discovered in the late 1970s.[24] The limitations of these imidazoles, such as their toxicity and limited efficacy, led to the development of a second chemical group of azole derivatives, the triazole containing antifungal compounds. There are currently four commercially available triazoles: fluconazole, itraconazole, voriconazole, and posaconazole (Figure 6).[25,26]

Fluconazole and itraconazole were the first triazoles introduced into clinical practice. They displayed a broader spectrum of activity than the imidazoles and a considerably improved safety profile compared to Amphotericin B.[27] Unfortunately, fluconazole lacks activity against filamentous fungi *(e.g. Aspergillus*) and itraconazole has been hindered by poor absorption. These clinically important limitations related to their suboptimal range of activity, but also the development of resistance and some toxicity has led to a search for new analogues and a so-called 'second generation' of triazoles, including voriconazole and posaconazole, has been developed.[14] The structure of voriconazole is related to fluconazole, whereas posaconazole is structurally similar to itraconazole (Figure 6). Voriconazole was approved by the FDA in 2002 and revolutionized the treatment of aspergillosis in severely immunocompromised

patients.[14] However, its use is hampered by complicated pharmacokinetics, notable drug interactions, and relatively significant side-effects.[25] Finally, posaconazole is the last addition to the azole armamentarium, approved by the FDA in 2006.[28] As was the case with voriconazole, it also showed interaction with other drugs, but to a lesser degree relative to other triazoles. Moreover, it displayed a broader antifungal spectrum, significant activity against the *Zygomycetes*, and an optimal safety profile. However, multiple daily dosing, a need for fatty foods to assure adequate bioavailability, and absence of an intravenous formulation restricted its use to selected populations of patients.[25,28]

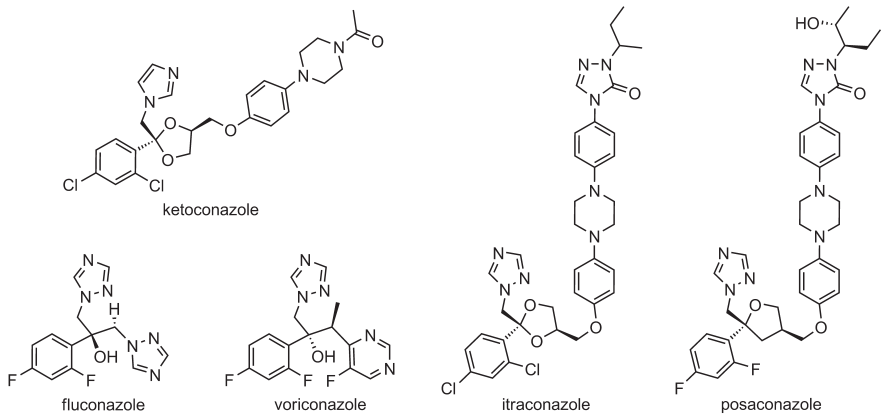

Figure 6. The azole class of antifungal agents.

Azole antifungal drugs inhibit the enzyme lanosterol 14α-demethylase; the enzyme necessary to convert lanosterol to ergosterol (Figure 3). Depletion of ergosterol coupled with an accumulation of sterol precursors, including 14α-methyl sterols, results in impaired fungal cell growth. The triazoles owe their antifungal activity mainly to inhibition of P450-dependent 14α sterol demethylase.[12-14] Their ability to interact with the heme of many host cytochrome P450 enzymes, particularly mammalian CYP3A4, makes the antifungal agents potentially toxic.[29] In humans, CYP3A comprises the largest fraction of the total CYP content and is responsible for the metabolism of a broad range of drugs, such as immunosuppressive and chemotherapeutic drugs. Thus, azoles exhibit a wide range and variety of drug-drug interactions that limit their use.[30,31]

Allylamines

Allylamines such as naftifine and terbinafine (Figure 7) are synthetic fungicidal inhibitors and inhibit ergosterol synthesis at the level of squalene epoxidase.[12-14] This is another enzyme in the biosynthetic pathway leading to ergosterol; together with squalene cyclase it converts squalene to lanosterol, the precursor of ergosterol in the fungal cell (Figure 3).[32] So the activity of the antifungal allylamines is conceptually related to that of the azole antifungal agents.

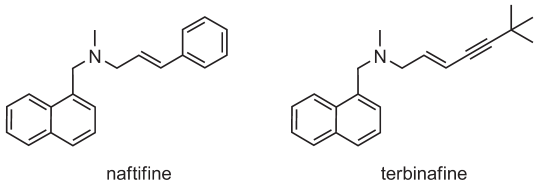

Figure 7. The allylamine antifungal agents naftifine and terbinafine.

The first member of the allylamines, naftifine, was discovered by chance while the scientists were working on spironaphthalenones with the aim of finding compounds that acted on the central nervous system (CNS).[32,34] A screening programme in the Sandoz Research Institute (Vienna, Austria) revealed the antifungal activity of this compound.[35] Intensive structure activity relationship studies aimed at modification of the allylamine side chain led to the discovery of terbinafine.[34]

These agents are highly selective for the fungal enzyme and have a minimal effect on mammalian cholesterol biosynthesis.[36] They show activity against many filamentous fungi but they are not very effective against pathogenic yeasts involved in invasive aspergillosis and systemic candidiasis. However, terbinafine was found to be very effective against species of *Candida*, *Aspergillus* and *Zygomycota*, and even against *Candida* isolates with resistance to fluconazole as well as effective against itraconazole-resistant *Aspergillus* strains, when administrated with azoles and Amphotericin B.[37]

1.2.2 DNA synthesis inhibitor

Flucytosine, a fluorinated pyrimidine analogue, was first synthesized in 1957[38] but its antifungal properties were discovered in 1963. Several years later flucytosine was successfully used for the treatment of systemic candidiasis and of cryptococcal meningitis.[39] It is the only available antimetabolite type of an antimycotic drug. Its mode of action is very unique within the antifungal agents. Flucytosine is taken up into fungal cells by a cytosine permease and is converted to its antimetabolite 5-fluorouracil (Figure 8) by cytosine deaminase (CD).[40] The absence of CD in mammalian cells makes flucytosine non-toxic for humans. The antimetabolite fluorouracil is then incorporated in fungal RNA by replacing uracil with 5-flurouracil, thereby disrupting protein synthesis. Moreover, it inhibits thymidylate synthetase via 5-fluorodeoxy-uridine monophosphate and thus interferes with fungal DNA synthesis.[40]

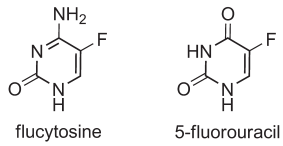

Figure 8. Pyrimidine class of antifungal agents, flucytosine and the antimetabolite 5-fluorouracil.

This mechanism of action requires the presence of several enzymes in the target cells; cytosine permease to internalize the flucytosine molecule, cytosine deaminase to convert it to 5-fluorouracil, and uracil phosphoribosyltransferase to convert 5-fluorouracil into a substrate for nucleic acid synthesis. Most filamentous fungi lack these enzymes, and

hence the useful spectrum of this drug is limited to pathogenic yeast (*Candida* spp. and *Cryptococcus neoformans*).[14] 5-fluorouracil itself cannot be used as an antimycotic drug due to its high toxicity to mammalian cells and also because it has a poor adsorption profile by fungal cells.[39]

The use of flucytosine alone in treatment frequently resulted in the emergence of resistance owing to the multitude of enzymes involved in the metabolic pathway.[39] Thus, flucytosine is never used as monotherapy but always in combination with another antifungal compound and usually combined with Amphotericin B or fluconazole or with both as combination therapy.[39]

Side effects in the form of gastrointestinal intolerance and bone marrow depression have been observed. Rash, hepatoxicity, headache, confusion, hallucinations, sedation and euphoria have also been reported.[14] Since flucytosine is commonly combined with amphotericin B, the renal impairment caused by amphotericin B may further increase flucytosine hepatoxicity. The toxicity of flucytosine is presumably due to 5-fluorouracil which is produced from flucytosine by bacteria in gut lumen. Therefore 5-FC is more often used in combination therapy with azole drugs.[39]

1.2.3 β-*glucan synthase inhibitors*

The most recent additions to the arsenal of antifungal compounds are the β-glucan synthase inhibitors. β-(1,3)-glucan is a major component of the framework of the fungal cell wall. There are several families of antifungal drugs that interfere with β-(1,3)-glucan synthesis by inhibiting the β-(1,3)-glucan synthase enzyme (Figure 2).[9] These inhibitors include the papulacandins, echinocandins and the acidic terpenoids. To date, only the echinocandin compounds caspofungin, micafungin and anidulafungin have been approved for treatment of invasive fungal infections.

Papulacandins

The papulacandins (Figure 9), first described in 1977, are a series of naturally occurring glycolipid antifungal agents. This group consists of five members, i.e., papulacandins A, B, C, D and E and is isolated from the fermentation broths of *Papularia sphaerosperma*.[41] These amphipatic compounds have a unique structure, described as a spirocyclic diglycoside.[42] Here, the lactose disaccharide has its *gluco*-sugar converted to a spirocyclic arylglycoside. The spirocyclic diglycoside is esterified by two long-chain unsaturated fatty acids. With the exception of papulacandin D, the compounds only differ from another in the nature of the unsaturated fatty acid side chains. Papulacandin D, the simplest member of the family, contains only one carbohydrate residue and one fatty acid side chain.[42]

The papulacandins have demonstrated potent *in vitro* antifungal activity against pathogens such as *Candida albicans* and *Saccharomyes cerivisiae*[43], *Pneumocystis carinii* etc. However, they are largely inactive against filamentous fungi, bacteria and protozoa. Although the papulacandins showed acceptable *in vitro* inhibition of β-1,3-glucan synthase, little or no efficacy in animal models was found.[41] The high degree of selective activity towards fungi and the fascinating structure of the papulacandins have led to several attempts to develop

papulacandin derivatives as drugs either by chemical modification or by total synthesis approaches.[44,45] Despite these efforts, the papulacandins have not yet been developed for treatment of invasive fungal infections because they showed limited potency in animal models.

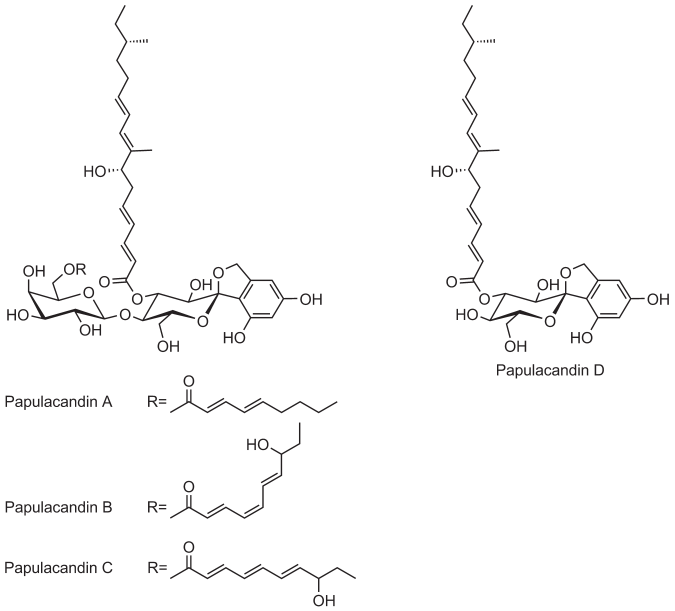

Figure 9. Structures of the Papulacandin family.

Echinocandins

The echinocandins represent the most recent class of antifungal drugs that have reached the market in the last decade. These fungal secondary metabolites are composed of a complex cyclic hexapeptide core whose *N*-terminus is acetylated by a lipid side chain.[46] An echinocandin compound is grouped into one of the three families of these antifungal agents (i.e. echinocandins, aculeacins and pneumocandins) based on the type of fatty acid side chain that is present in the compound (Table 1).

The first group of the echinocandin family consists of a group of related cyclic peptides, isolated from *Aspergillus nidulans* and *A. Rugulosus* each possessing an *N*-linoleyol side chain but having different hydroxylation patterns.[47,48] The second group consists of the aculeacins from *Aspergillus aculeatus*, which have the same peptide nucleus as echinocandin B but an *N*-palmitoyl side chain.[49] The closely related lipopeptides isolated from *Coleophoma empetri (*e.g. WF 11899) also differ from the echinocandins by having a sulphate moiety on the homotyrosine residue (R^7, Table 1) thus rendering them more soluble than the other echinocandins.[50] In addition the latter group has a different amino acid at position R^5.[50] The third group is that of the pneumocandins from *Zalerion arboricula*, having a dimethylmyristoyl side chain attached to the peptide ring.[51]

Table 1. Echinocandin family

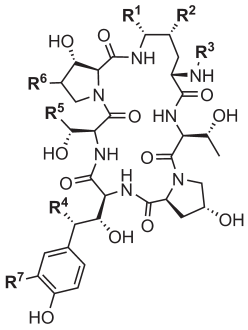

Year		R^1	R^2	R^3	R^4	R^5	R^6	R^7
1974	Echinocandin B	OH	OH	Linoleoyl	OH	Me	Me	H
1979	Echinocandin C	OH	OH	Linoleoyl	H	Me	Me	H
1979	Echinocandin D	H	H	Linoleoyl	H	Me	Me	H
1977	Aculeacine A	OH	OH	Palmitoyl	OH	Me	Me	H
1993	WF11899A (FR901379)	OH	OH	Palmitoyl	OH	CH_2CONH_2	Me	OSO_3H
1993	WF11899B	OH	OH	Palmitoyl	H	CH_2CONH_2	Me	OSO_3H
1993	WF11899C	OH	H	Palmitoyl	H	CH_2CONH_2	Me	OSO_3H
1989	Pneumocandin A	OH	OH	DiMe-Myr	OH	CH_2CONH_2	Me	H
1989	Pneumocandin B	OH	OH	DiMe-Myr	OH	CH_2CONH_2	H	H

None of these natural echinocandins have been used clinically. Their limitations for human therapeutics were lack of oral bioavailability, poor water solubility and toxicity problems such as haemolysis.[46] Due to the encountered limitations, extensive semisynthetic structure-activity relationship (SAR) studies have been carried out on the natural echinocandins to improve their pharmacokinetic profiles and tolerability.[52] Lipophilic side chain replacement has been employed primarily to improve potency and reduce the haemolytic properties associated with some members of the echinocandin class.[53-57] This work demonstrated that the entire intact echinocandin molecule is necessary for inhibition of antifungal growth, neither solely the cyclic peptide nucleus nor the fatty acid chain or a mixture thereof showed significant antifungal activity.[55] Alteration of the cyclic peptide core affects chemical stability, aqueous solubility, pharmacokinetic profile, potency and in vivo efficacy.[52] Among sites for chemical alterations of the cyclic peptide structure, the ornithine hemiaminal function has been the most successful. The hemiaminal group of the echinocandins is responsible for its instability and results in a ring opened, inactive product (**3**, Figure 10).[59,60] With respect to this part of the structure, several studies have reported on derivatization (e.g. reduction, substitution and alkylation) of the hemiaminal to improve stability and water solubility.[61-65]

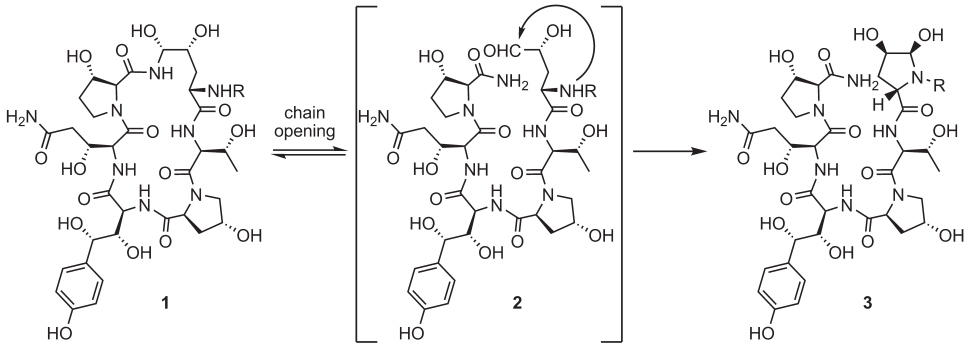

Figure 10. Base catalyzed ring-opening reaction of an echinocandin (**1**), providing an aldehyde intermediate (**2**) wich recyclizes to a thermodynamically more favourable five-membered N-acyl hemiaminal (**3**) incorporating the side chain amide.

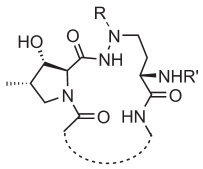

4 R= Me
5 R= $COCH_2NH_2$
6 R= *n*-Pr

R' = pentyloxyterphenyl

Figure 11. Acyl hydrazides prepared using an ornithine excision/replacement strategy.

These medicinal chemistry efforts have led to the discovery of the first generation of clinically used echinocandins, resulting from either side chain (micafungin[67] and anidulafungin[60]) or cyclic peptide core (caspofungin[68]) modification (Figure 12). The development of another semi-synthetic derivative of echinocandin with an altered fatty acid side chain, cilofungin[53-55], was abandoned after Phase II clinical trials due to toxicity of the vehicle that was used to dissolve the compound, as well as low oral efficacy and a narrow spectrum of activity.[46] A new generation of echinocandin analogues (e.g. aminocandin) bearing modifications of both core and side chain is currently under clinical investigation (Figure 12).[69,70]

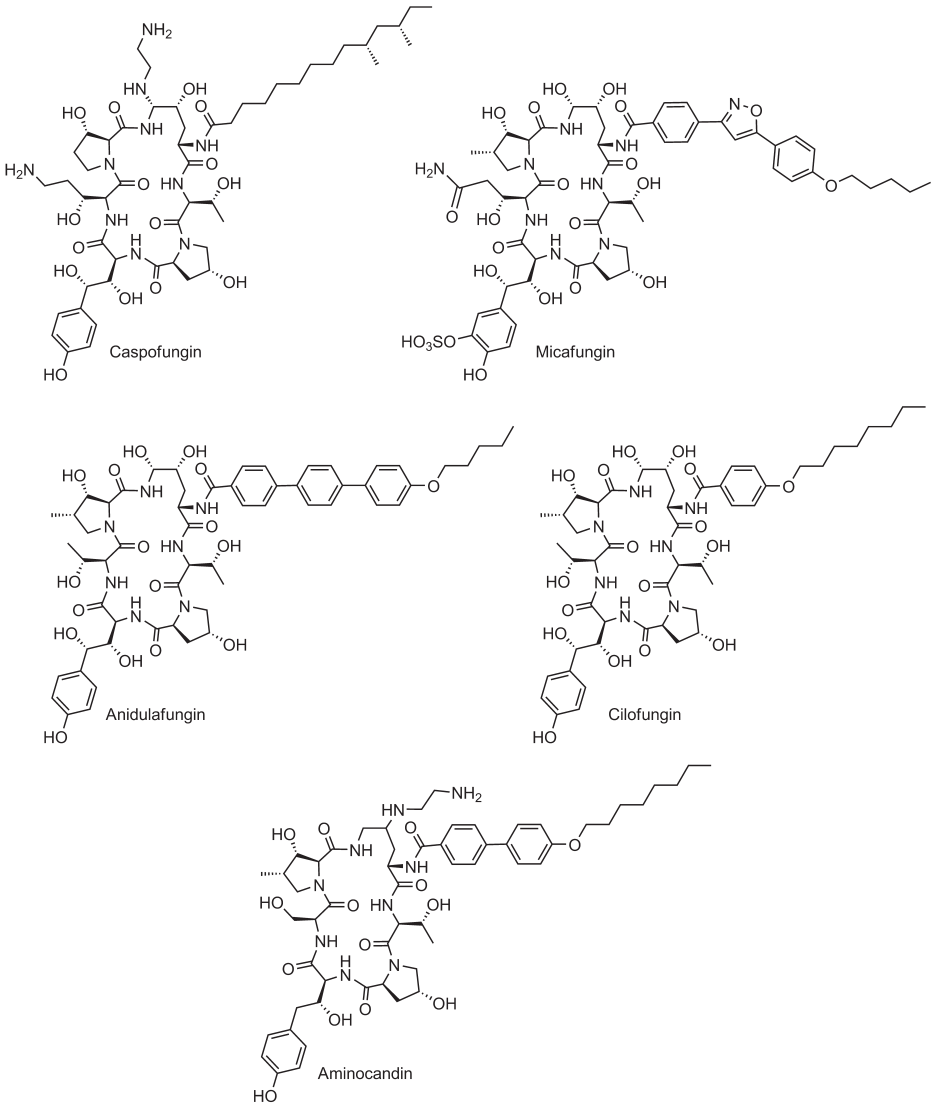

Figure 12. The semi-synthetic echinocandin class of antifungal drugs.

Caspofungin, the first approved agent from this class in 2001, is a semisynthetic derivative of pneumocandin B prepared by chemical modification at two sites of the peptide core, a reduction of the primary amide of the hydroxyglutamine residue to an amine and condensation of the hemiaminal moiety with ethylenediamine (Figure 13).[68] It is a well-tolerated antifungal compound active against invasive candidiasis, oesophageal candidiasis and invasive aspergillosis.[79] In 2005, the second antifungal agent of the echinocandin class was approved, that is micafungin in 2005, a water soluble semisynthetic derivative of the natural occurring FR901379.[80] Enzymatic deacetylation of the natural sulphated echinocandin derivative and reacetylation of the peptide nucleus, with an isoxazole containing benzoyl like side chain,[81] provided micafungin (Figure 14).[67] The third approved echinocandin derivative is anidulafungin in 2006.[82] It is a semisynthetic derivative of echinocandin B in which the lineoyl side chain was replaced by a terphenyl head and a C5 alkyl tail (Figure 14).[60]

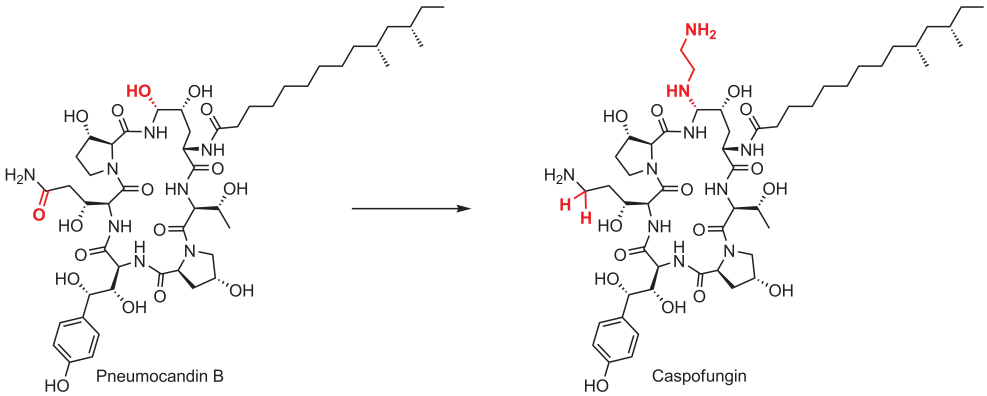

Figure 13. Preparation of caspofungin from pneumocandin B by chemical modification at two sites of the peptide core.

All three antifungal compounds are used intravenously and approved for treatment of oesophageal candidiasis, candidaemia and other forms of invasive candidiasis. They are fungicidal *in vitro* and *in vivo* against a broad range of *Candida* spp. and fungistatic against *Aspergillus* spp., where they block the growing tips of hyphae.[83] Despite the occurrence of spontaneous resistance to echinocandins of *Candida* spp. *in vitro*, the clinical resistance remains rare.[83] In combination with their unique mode of action and thereby their safety profile they present a valuable addition to the arsenal of antifungal compounds.

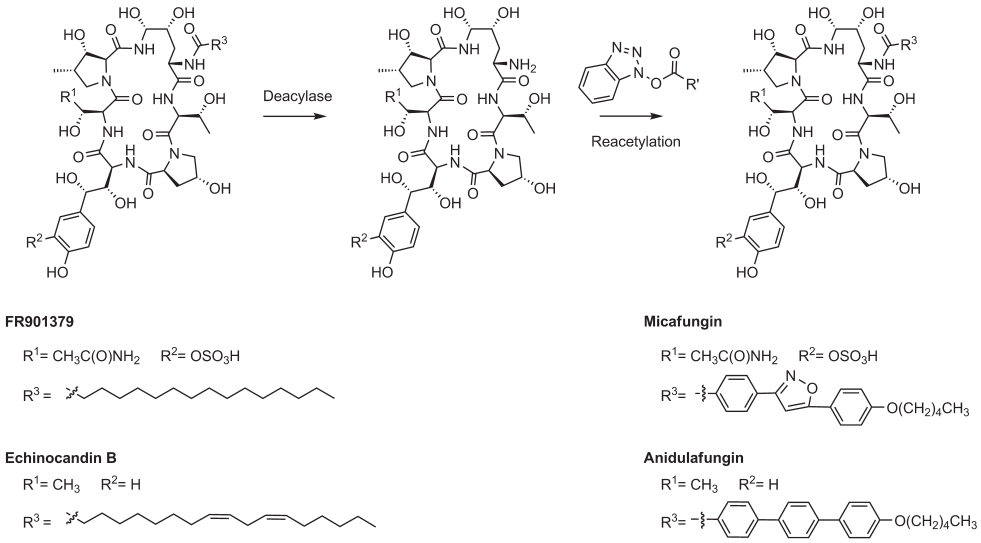

Figure 14. Semisynthetic approach to micafungin and anidulafungin

To date, only a few studies have been focused on the total synthesis of echinocandin derivatives. The first total synthesis of echinocandin D was reported in the mid 1980s.[71-73] Further attempts on the synthesis of echinocandin C have failed due to problems with the hemiaminal bond formation (Figure 15).[71,73] For their attempted synthesis of echinocandin C, linear hexapeptide **7** containing a fully oxygenated ornithine residue with a terminal dimethoxy acetal was synthesized. Unmasking this protected aldehyde was expected to initiate macrocyclization, thereby generating the desired hemiaminal function of echinocandin C. Instead the uncyclized aldehyde was obtained as its hydrate (**8**) and all further attempts failed yielding the pyrrolidine **9** instead.

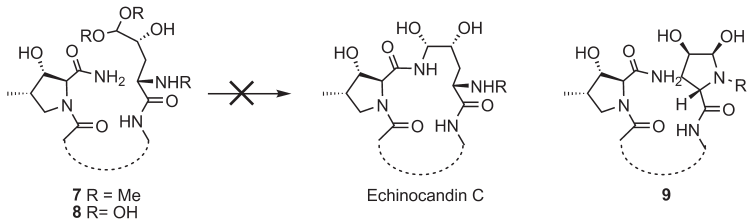

Figure 15. Attempted ring-closing reaction to form echinocandin C.

Later, potential issues surrounding the hemiaminal linkage were avoided by preparing simplified analogues with a stable amide connection between proline and ornithine.[74-76] In 1992 the first total synthesis of simplified echinocandin analogues (**10**, Figure 16) using solid-phase techniques was reported by Zambias et al.[74] In this work, the 4-octyloxybenzoyl side chain of Cilofungin was combined with cyclic hexapeptides of varying complexity. The unusual amino acids present in the echinocandins were replaced with more readily accessible natural amino acids. Structure activity relationship (SAR) data from this work showed that

several of the functional groups, primarily the hydroxyl groups, were not necessary for antifungal activity. In addition, the L-homotyrosine residue turned out to be crucial for antifungal activity. Notably, analogues bearing a tyrosine residue (**10**) were inactive while analogues bearing homotyrosine retained antifungal activity.[74]

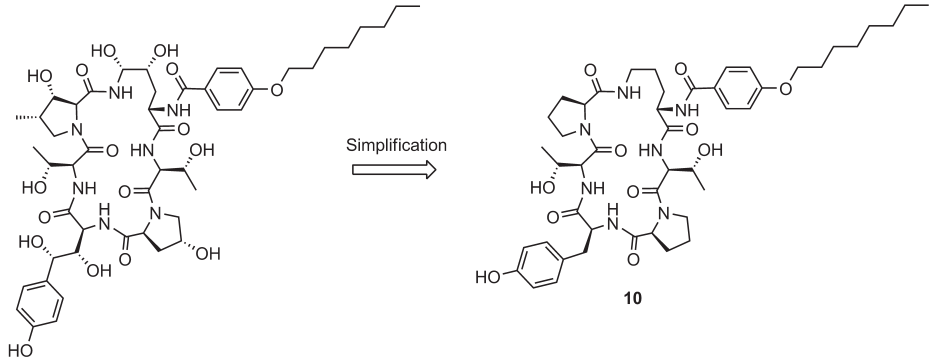

Figure 16. Simplified analogues of Cilofungin.

Klein et al. reported a similar study in 2000. They extended the approach of Zambias et al. in a more comprehensive manner toward simplification of the hexapeptide nucleus. The effects on antifungal activity was explored by further modifications of several amino acid residues in the peptide nucleus (A-C, Figure 17) and the lipophilic side chain (G, Figure 17). Here, solid phase synthesis of the analogues was utilized for initial stages of their work and a solution phase approach ('3 + 3' format) to obtain larger quantities of analogues for biological testing. SAR data from this work showed that the (2S, 3S, 4S)-3-hydroxy-4-methyl proline residue can be replaced with 4β-amino proline. Related analogues, such as 4-guanidino proline, possess improved solubility and good activity.[75] From this study the optimal groups were chosen and combined in a new analogue A199930, which displayed excellent anti-*Candida* activity *in vitro* and *in vivo* in a mouse chronic candidiasis model (Figure 17).[77] Unfortunately, subsequent pre-clinical safety evaluations of A199930 showed undesirable cardiovascular (CV) effects in rat and monkey that were linked to a histamine releasing effect. It was found that this effect was associated with clustered basic sites (e.g. neighbouring guanidine and amino groups). Further chemical optimization made in light of these findings led to the improved analogue A192411 (Figure 17).[77] Here the basic site of ornithine is replaced by threonine and an additional basic amine is introduced at the 3' position of the homotyrosine aromatic ring. Efficacy was demonstrated against *Candida albicans* and an improved CV safety profile in both rodents and monkeys.[78]

More recently, Yao et al. reported a SAR study on Caspofungin in 2012 (Figure 18).[76] The strategy employed was similar to work presented by Klein et al. The effects on antifungal activity were explored by modification of six parts of the molecule (A, B, D, E, G; Figure 18). Again a [3+3] coupling strategy for the preparation of analogues was used. The findings in this work indicated that hydrophilic amino acids were favoured for the 'left' tripeptide fragment (A-C), whereas the 'right' lipotripeptide segment (D-G) was preferred as a hydrophobic core.

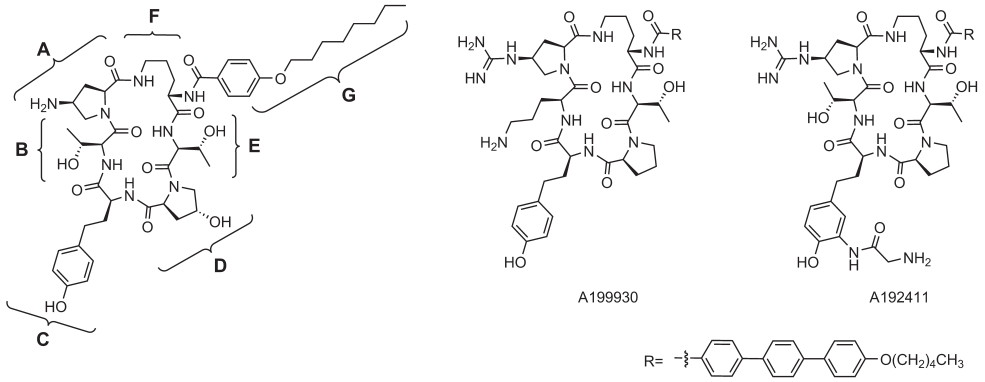

Figure 17. SAR studies of Klein et al. and the optimized analogues A199930 and A192411.

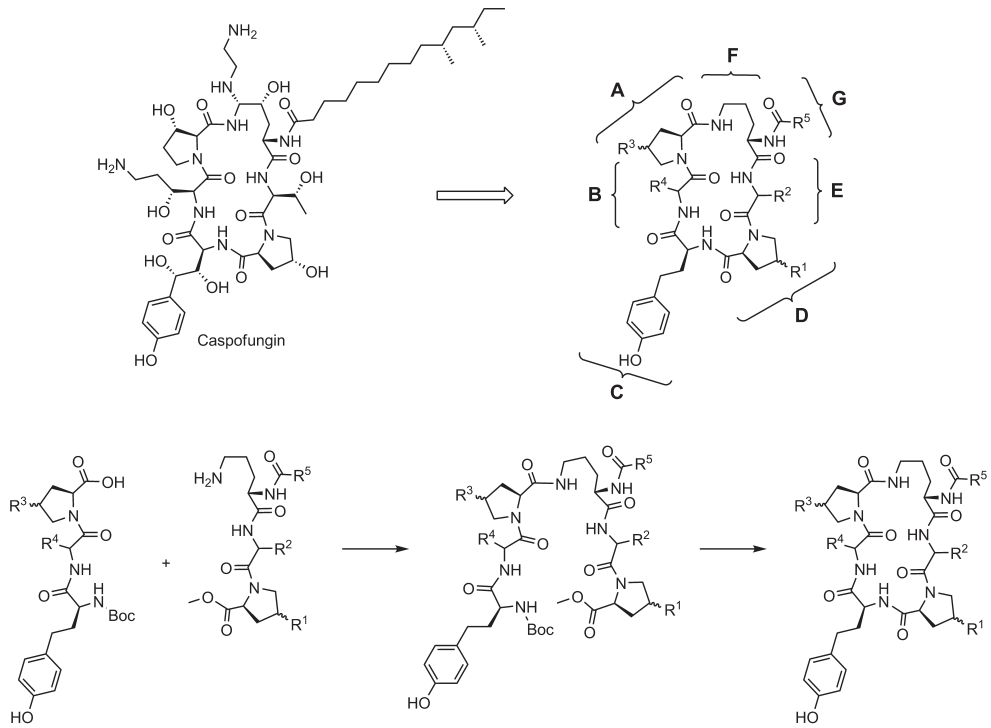

Figure 18. Design of the caspofungin analogues and the [3+3] coupling strategy.

Unfortunately, although these syntheses gave valuable SAR information (Figure 19) that could not be provided by direct chemical modification of the natural product, none of the synthesized analogues have been used clinically so far.

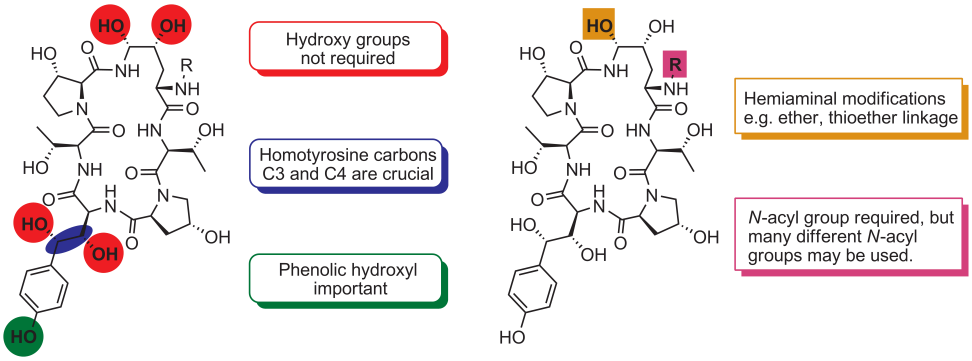

Figure 19. Summary of Structure-Activity Relationships studies of the echinocandins. Left: based on total synthesis; Right: based on semisynthetic work.

Acidic terpenoids

Despite their advantages, the echinocandin class of compounds show low oral absorption. Therefore, screening efforts for new chemical entities that inhibit (1,3)-β-glucan synthase with improved pharmacokinetic properties as compared to those of the papulacandins and the lipopeptides have been performed in several laboratories.[84] These natural-product screening efforts have resulted in a new class of inhibitors, the acidic terpenoids.

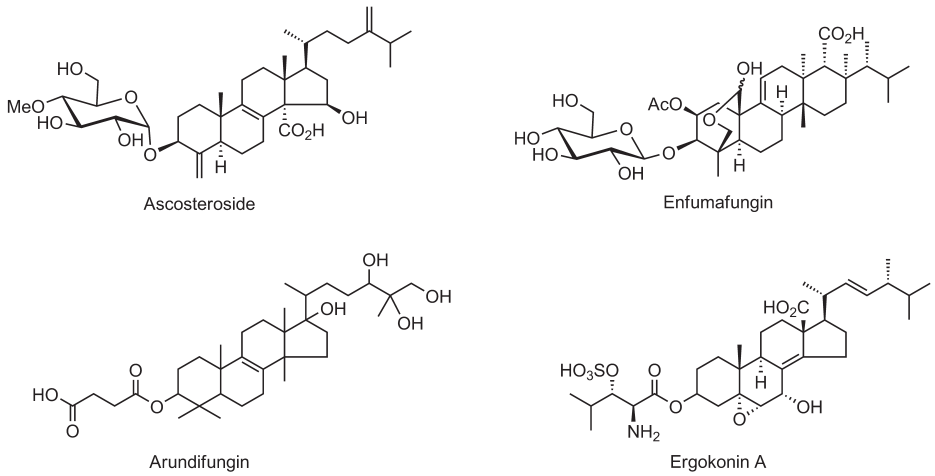

Figure 20. Structures of the acidic terpenoids.

Members of this new class of antifungal triterpenes with a polar (-acidic-) moiety include the glycosidic triterpene ascosteroside A[85] and the related glycoside, enfumafungin.[86] Other members are arundifungin[87] containing a succinate moiety and Ergokonin A[88], a sulfate-derivatized amino acid containing terpenoid (Figure 20).

Studies on the mode of action of these compounds have shown that they do inhibit glucan synthesis in whole cells and in (1,3)-β-glucan synthase assays. The in vitro antifungal activity of enfumafungin, is comparable to that of the echinocandin class of compounds.[84] Because of their good solubility in water, the acidic terpenoids represent new promising lead structures for the development of oral active antifungal drugs.

1.3 Mechanism of action - Target

Considering the mode of action, pharmacological, and toxicological profiles of the antifungal agents described here, the echinocandin class of the antifungals exhibit the most promising target selectivity, as β-(1,3)-glucan is only found in fungi not in mammalian cells. This imminently results in less toxic effects, as compared to the other classes.[89]

Fungal cell walls consist of glycoproteins and polysaccharides, mainly glucan and chitin.[90] The chains of the glucans and chitin are interconnected by covalent cross-links and form a strong three-dimensional matrix, which gives the cell wall its shape and mechanical strength.[91,92] Glucan is the major structural polysaccharide of the fungal cell wall, constituting approximately 50-60% of the wall by dry weight. Polymers of glucan are composed by repeating glucose residues that are assembled into chains through a variety of chemical linkages.[91] Chitin, a long linear homopolymer of β-1,4-linked N-acetyl glucosamine accounts for only 1-2% of the yeast cell wall by dry weight,[93] whereas the cell walls of filamentous fungi, such as *Aspergillus*, are reported to contain 10-20% chitin.[90]

Different fungi have varying amounts of chitin and glycoproteins. Therefore, some species are more susceptible to the echinocandins than others. Since β-(1,3)-D-glucan is a major cell wall component of *Candida* and *Aspergillus* species, these species are more sensitive to echinocandins. In general, between 65% and 90% of the cell wall glucan is β-1,3-glucan.[91] However, in *Cryptococcus neoformans*, β-(1,3)-linked glucose units may not have a structural role in the cell wall because they only occur as side chains on β-(1,6)-glucan polymers.[94] Studies in the yeast *S. cerivisiae* and *Candida albicans* demonstrated that the glycosyl units within their cell walls are arranged as long coiling chains of β-(1,3)-linked residues, with occasional side chains that involve β-(1,6)-linkage.[95,96] Cell walls of many filamentous fungi, including *A. fumigatus*, do not contain β-1,6-glucan.[97]

β-1,3-Glucans are synthesized by the plasma membrane-bound protein complex glucan synthase. This enzyme complex uses UDP-glucose on its intracellular side as a substrate for polymerization to glucan fibrils, followed by extrusion of the linear β-1,3-glucan chains through the membrane into the cell wall space.[98,99] When synthesis of β-(1,3)-D-glucan is inhibited, the resulting disorganization of the fungal cell wall leads to a weakened cell wall, which is the cause of lysis of the cells by osmotic pressure. Another effect is that by blockade of the cell wall synthesis, fungal growth is reduced.[89]

The glucan synthase protein complex contains both catalytic and regulatory subunits. The putative catalytic subunit of the GS-complex (>200 KDa) is encoded by either of two homologue genes designated FKS1 and FKS2 (>200 KDa). The resulting proteins of both genes are targets of antifungal lipopeptides. The cell cycle-regulated FKS1 gene is expressed during

normal vegetative growth and linked to cell-wall remodelling, while FKS2 is transcriptionally regulated by calcineurin and is preferentially expressed during sporulation.[89]

FKS proteins are an essential component of the GS-complex, their large size and integral membrane character may explain why β-1,3-D-glucan synthase has been so difficult to purify. The glucan synthesis complex in yeast (e.g. *S. cerevisiae*[100], *C. albicans*[101] and *A. fumigatus*[102]) has been partially purified via product entrapment. The product entrapment procedure consists of incubating the dissolved glucan synthesis complex with substrate under conditions that allow synthesis of the insoluble glucan product. The enzyme is trapped within the microfibril network and is recovered by differential centrifugation.[101] In this way the polypeptides that are components of the complex were identified.

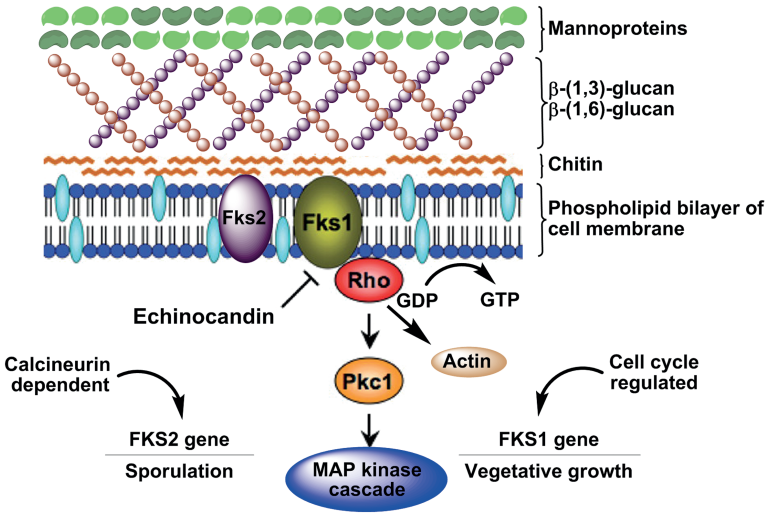

Figure 21. Model of FKS1p and Fks2p regulation of the glucan synthase protein complex.

The key regulatory subunit is Rho, which interacts not only with FKS proteins but also with protein kinase C (Pkc1) (Figure 21). Pkc1 is a known regulator of the MAPK cascade and actin cytoskeleton assembly pathway in yeast.[98] Because of the interaction with multiple proteins, Rho is thought to be a key switch, driving or arresting the synthesis of β-1,3-glucan.[89] It switches between a GDP-bound inactive state and a GTP-bound active state via conformational changes.[92]

Reduced susceptibility to echinocandins has been attributed to mutations in either FKS1 or FKS2. Predominantly FKS1 mutations decrease the sensitivity of glucan synthase for echinocandin drugs by 1000-fold or more.[103] This resistance is associated with amino acid substitutions in two 'hot-spot' regions of FKS1. FKS1 mutations confer resistance in both yeasts and moulds.[103,104] Therefore, it was suggested that the echinocandin class of inhibitors interact with the FKS1 protein. However, photoaffinity studies with a photoactivatable cross linking analog of Anidulafungin demonstrated that the echinocandins interact directly with at least two proteins (40 and 18-kDa) in *C. Albicans*, and neither one is the Candida FKS homolog.[105] These findings led to a further diminishment of understanding of the

exact mechanism of action of the echinocandin class of compounds. In addition to point mutations in FKS1, exposure to echinocandins can induce a salvage mechanism involving the up regulation of chitin synthesis. This physiological adaption enables a fungus to survive at otherwise lethal-concentrations of echinocandins.[104,106]

In conclusion, targeting the synthesis of β-(1,3)-glucan, the major structural polysaccharide of the fungal cell wall, still provides the most promising mechanism of action for current antifungal treatments. To date, only the echinocandins have been approved for treatment of invasive fungal infections by this unique mechanism of action. Although, substantial work has been devoted to attempts for understanding of the binding sites of the antifungal lipopeptides to the glucan synthase complex, so far this has not been very successful.

1.4 Aim and outline of this Thesis

From these paragraphs it is may be clear that very few antifungal agents can be used for life-threatening fungal infections. Despite the introduction of more effective, less toxic triazole agents and new formulations of Amphotericin B the need for new antifungal agents with a novel mode of action remains. A substantial number of patients fail to respond to either therapy and the broad clinical application of the few antifungal agents has resulted in severe drug resistance. The development of echinocandin related cyclic lipohexapeptides for the treatment of invasive fungal infections represented a breakthrough in antifungal chemotherapy. Considering the mode of action, pharmacological, and toxicological profiles of the described classes of compounds, the echinocandins exhibit the most promising target selectivity, as β-1,3-glucan is only found in fungi not in mammalian cells. As a consequence fewer toxic side effects are observed, as compared to the other classes of antifungal agents. Moreover, the clinically approved agents for this class have rarely shown fungal resistance selection. Despite these advantages, the echinocandin class of compounds has its own limitations. Firstly, due to their semisynthetic nature, they are costly. Secondly their mechanism of action is still unknown. The interaction site of FKs1p/FKs2p with echinocandins has not yet been determined. Elucidating the mode of action of echinocandins on β-(1,3)-glucan synthase will efficiently lead to the development of improved drugs.

The aim of the research described in this thesis was therefore to explore the crucial structural features necessary for the antifungal activity of the echinocandin compounds, by synthesizing new derivatives for evaluation of their antifungal activity. This information can be used for the development of improved drugs and can help in the elucidation of their mode of action. Efforts to obtain new echinocandins are relevant, since these compounds are active against a distinctive target.

The chemistry to synthesize new echinocandin derivatives was developed and is described in **chapter 2** of this thesis. The newly designed echinocandin mimics by ring closing metathesis or disulfide formation have been synthesized on the solid support and their antifungal activity has been evaluated by determining their minimum inhibitory concentration. It was found that ring size is an important factor for antifungal activity.

Next, the scope and limitations of the use of vinylglycine for the preparation of echinocandin derivatives is explored in **chapter 3**. The synthesis of vinylglycine and its tendency to isomerize to the conjugated α,β-unsaturated derivative is described herein. Therefore, the direct incorporation of vinylglycine into peptides turned out to be problematic. Alternatively, facile, site-specific and chemoselective incorporation of vinylglycine into peptides could be achieved via a 'masked' amino acid.

The research described in **chapter 4** entails an approach to echinocandin based photoaffinity analogues. Due to the structural importance of the cyclic hexapeptide nucleus of the echinocandins, the chemical probe was constructed as part of the fatty acid side chain. The synthesis of photoreactive side chains and its application in the preparation of echinocandin analogues is described.

Chapter 5 reports on the role of methyl groups in the lipophilic tail of analogues of caspofungin. Based on findings described in chapter 2 regarding the low activity of palmitoyl containing analogues, a simplified analog of caspofungin, containing its natural dimethylmyristoyl chain, was synthesized and evaluated for its antifungal activity. Also analogues were included with either one or no methyl groups. The results of this investigation suggest that the top-left proline residue somehow plays an important role in the bio-active conformation of the macrocyclic peptide ring structure.

In **chapter 6** the conformational behaviour of the echinocandin analogues was evaluated. In the previous chapters it became clear that the size, choice of the fatty acid side chain as well as crucial substituents are determining factors for antifungal activity. Here, it was attempted to evaluate the conformational behaviour and possible ensuing influence of ring size on antifungal activity. To elucidate solution conformations of the analogues described earlier in this thesis nuclear magnetic resonance (NMR) and circular dichroism (CD) techniques were applied. Moreover, attempts were made for the crystallization of our analogues.

References and notes

1. Pfaller, M.A.; Diekema, D.J. *Clin. Microbiol. Rev.*, **2007**, *20*, 133-163.
2. Lai, C.-C.; Tan, C.-K.; Huang, Y.-T.; Shao, P.-L.; Hsueh, P-R. *J. Infect. Chemother.*, **2008**, *14*, 77-85.
3. Gullo, A. *Drugs*, **2009**, *69 Suppl. 1*, 65-73.
4. Kanafani, Z.A.; Perfect, J.R. *Clin. Infect. Dis.*, **2008**, *46*, 120-128.
5. Chen, S.C-A.; Playford, E.G.; Sorrel, T.C. *Curr. Opin. Pharmacol.*, **2010**, *10*, 522-530.
6. Pfaller, M.A. *Am. J. Med.*, **2012**, *125*, S3-S13.
7. Garber, G. *Drugs*, **2001**, *61 Suppl. 1*, 1-12.
8. Walsh, T.J.; Dixon, D.M. *Spectrum of Mycoses* In: *Medical Microbiology* (S. Baron eds.), 4th edition, **1996**, Univ of Texas Medical Branch (via NCBI Bookshelf).
9. Hector, R.F. *Clin. Microbiol. Rev.*, **1993**, *6*, 1-21.
10. Pfaller, M.A.; Diekema, D.J. *Clin. Microbiol. Rev.*, **2007**, *20*, 133-163.
11. Cornely, O.A. *Infection*, **2008**, *36*, 296-312.
12. Odds, F.C.; Brown, A.J.P., Gow, N.A.R. *Trends Microbiol.*, **2003**, *11*, 272-279.
13. Ruge, E.; Korting, H.C.; Borelli, C. *Int. J. Antimicrob. Agents*, **2005**, *26*, 427-441.

14. Mathew, B.P.; Nath, M. *ChemMedChem*, **2009**, *4*, 310-323.
15. Reprinted from *Aspergillosis: from diagnosis to prevention*, Thompson, G.R.; copyright **2009**, with permission from Springer (license date: Feb, 16, 2012).
16. Hazen, E.L.; Brown, R. *Science,* **1950**, *112*, 423.
17. Dutcher, J.D. *Dis. Chest.*, **1968**, *54*: *Suppl 1*, 296-298.
18. de Kruiff, B.; Demel, R.A. *Biochim. Biophys. Acta*, **1974**, *339*, 57-70.
19. Baginski, M.; Resat, H.; Borowski, E. *Biochim. Biophys. Acta*, **2002**, *1567*, 63-78.
20. Bates, D.W.; Su, L.; Yu, D.T.; Chertow, G.M.; Seger, D.L.; Gomes, D.R.J.; Dasbach, E.J.; Platt, R. *Clin. Infect. Dis.*, **2001**, *32*, 686-693.
21. Ullmann, A.J.; Sanz, M.A.; Tramarin, A.; Barnes, R.A.; Wu, W. Gerlach, B.A.; Krobot, K.J.; Gerth, W.C. *Clin. Infect. Dis.*, **2006**, *43*, e29-e38.
22. Brajtburg, J.; Powderly, W.G..; Kobayashi, G.S.; Medoff, G. *Antimicrob. Agents Chemother.*, **1990**, *34*, 183-188.
23. Sheehan, D.J.; Hitchcock, C.A.; Sibley, C.M. *Clin. Microbiol. Rev.*, **1999**, *12*, 40-79.
24. Heeres, J.; Backx, L.J.J.; Mostmans, J.H.; Cutsem van, J. *J. Med. Chem.*, **1979**, *22*, 1003-1005.
25. Zonios, D.I.; Bennett, J.E. *Semin. Respir. Crit. Care Med.*, **2008**, *29*, 198-210.
26. Girmenia, C. *Expert Opin. Investig. Drugs*, **2009**, *18*, 1279-1295.
27. Maertens, J.A. *Clin. Microbiol. Infect.*, **2004**, *10 Suppl. 1*, 1-10.
28. Nagappan, V.; Deresinski, S. *Clin. Infect. Dis.*, **2007**, *45*, 1610-1617.
29. Slama, J.T.; Hancock, J.L.; Rho, T.; Sambucetti, L.; Bachmann, K.A. *Biochem. pharmacol.*, **1998**, *55*, 1881-1892.
30. Saad, A.H.; DePestel, D.D.; Carver, P.L. *Pharmacotherapy*, **2006**, *26*, 1730-1744.
31. Brüggemann, R.J.M.; Alffenaar, J-W., C.; Blijlevens, N.M.A.; Billaud, E.M.; Kosterink, J.G.W.; Verweij, P.E.; Burger, D.M. *Clin. Infect. Dis.*, **2009**, *48*, 1441-1458.
32. Ryder, N.S. *Ann. NY Acad. Sci.*, **1988**, *544*, 208-220.
33. Mieth, H. *J. Dermatolog. Treat.*, **1990**, *1 Suppl 2*, 5-6.
34. Stütz, A. *Angew. Chem. Int. Ed.*, **1987**, *26*, 320-328.
35. Paltauf, F.; Daum, G.; Zuder, G.; Högenauer, G.; Schulz, G.; Seidl, G. *Biochim. Biophys. Acta.*, **1982**, *712*, 268-273.
36. Favre, B.; Ryder, N.S. *Arch. Biochem. Biophys.*, **1997**, *340*, 265-269.
37. Cuenca-Estrella, M.; Rodriguez-Tudela, J. L. *Terbinafine* In: *Aspergillosis: From Diagnosis to Prevention*, Comarú Pasqualotto, A. (Eds.), **2010**, 317-325 Springer Netherlands.
38. Duschinsky, R.; Pleven, E.; Heidelberger, C. *J. Am. Chem. Soc.*, **1957**, *79*, 4559-4560.
39. Vermes, A.; Guchelaar, H.-J.; Dankert, J. *J. Antimicrob. Chemother.*, **2000**, *46*, 171-179.
40. Waldorf, A.R.; Polak, A. *Antimicrob. Agents and Chemother.*, **1983**, *23*, 79-85.
41. Traxler, P.; Gruner, J.; Auden, J.A.L. *J. Antibiot.*, **1977**, *30*, 289-296.
42. Traxler, P.; Fritz, H.; Fuhrer, H.; Richter, W.J. *J. Antibiot.*, **1980**, *33*, 967-978.
43. Römmele, G.; Traxler, P.; Wehrli, W. *J. Antibiot.*, **1983**, *36*, 1539-1542.
44. Traxler, P.; Tosch, W.; Zak, O. *J. Antibiot.*, **1987**, *40*, 1146-1164.
45. Denmark, S.E.; Kobayashi, T.; Regens, C.S. *Tetrahedron*, **2010**, *66*, 4745-4759.
46. Turner, W.W.; Current, E.L., *Echinocandin Antifungal Agents* In: Drugs and the Pharmaceuticall Sciences, *Biotechnology of antibiotics*, Strohl, W.R. (Eds.), **1997**, 315-334 Marcel Dekker, Inc..
47. Benz, F.; Knüsel, F.; Nüesch, J.; Treichler, H.; Voser, W.; Nyfeler, R.; Keller-Schierlein, W. *Helv. Chim. Acta.*, **1974**, *57*, 2459-2477.

48. Traber, R.; Keller-Juslén, C.; Loosli, H-R.; Kuhn, M.; Wartburg von, A. *Helv. Chim. Acta.*, **1979**, *62*, 1252-1267.
49. a) Mizuno, K.; Yagi, A.; Satoi, S.; Takada, M.; Hayashi, M.; Asano, K.; Matsuda, T. *J. Antiobiot.*, **1977**, *30*, 297-302; b) Satoi, S.; Yagi, A.; Asano, K.; Mizuno, K.; Watanabe, T. *J. Antibiot.*, **1977**, *30*, 303-307; c) Mizoguchi, J.; Saito, T.; Mizuno, K.; Hayano, K. *J. Antibiot.*, **1977**, *30*, 308-313.
50. Iwamoto, T.; Fujie, A.; Sakamoto, K.; Tsurumi, Y.; Shigematsu, N.; Yamashita, M.; Hashimoto, S.; Okuhara, M.; Kohsaka, M. *J. Antibiot.*, **1994**, *47*, 1084-1091.
51. a) Schwartz, R.E.; Giacobbe, R.A.; Bland, J.A.; Monaghan, R.L. *J. Antibiot.*, **1989**, *42*, 163-167; b) Wichmann, C.F.; Liesch, J.M.; Schwartz, R.E. *J. Antibiot.*, **1989**, *42*, 168-173; c) Fromtling, R.A.; Abruzzo, G.K. *J. Antibiot.*, **1989**, *42*, 174-178.
52. For an excellent review of the total and semisynthetic approaches, see Renslo, A.R. *Anti-Infect. Agents Med. Chem.*, **2007**, *6*, 201-212.
53. Debono, M.; Abbott, B.J.; Turner, J.R.; Howard, L.C.; Gordee, R.S.; Hunt, A.S.; Barnhart, M.; Molloy, R.M.; Willard, K.E.; Fukuda, D.; Butler, T.F.; Zeckner, D.J. *Ann. NY Acad. Sci.*, **1988**, *544*, 152-163.
54. Debono, M.; Abbott, B.J.; Fukuda, D.S.; Barnhart, M.; Willard, K.E.; Molloy, R.M.; Michel, K.H.; Turner, J.R.; Butler, T.F.; Hunt, A.H. *J. Antibiot.*, **1989**, *XLII*, 389-397.
55. Taft, C.S.; Selitrennikoff, C.P. *J. Antibiot.*, **1990**, *XLIII*, 433-437.
56. Debono, M.; Turner, W.W.; LaGrandeur, L.; Burkhardt, F.J.; Nissen, J.S.; Nichols, K.K.; Rodriguez, M.J.; Zweifel, M.J.; Zeckner, D.J.; Gordee, R.S.; Tang, J.; Parr, T.R. *J. Med. Chem.*, **1995**, *38*, 3271-3281.
57. Jamison, J.A. ; Rodriguez, M.J. *PCT Int. Appl. WO 1996/037512*, November 28, **1996**.
58. Jamison, J.A.; Zeckner, D.J.; Rodriguez, M.J. *J. Antibiot.*, **1997**, *50*, 562-566.
59. Bouffard, F.A.; Hammond, M.L.; Arison, B.H. *Tetrahedron Lett.*, **1995**, *36*, 1405-1408
60. Norris, T.; VanAlsten, J.; Hubbs, S.; Ewing, M.; Cai, W.; Jorgensen, M.L.; Bordner, J.; Jensen G.O. *Org. Process Res. Dev.*, **2008**, *12*, 447-455.
61. Balkovec, J.M.; Dropinski, J.F.; Bouffard, F.A. *United States Patent 5.741.775*, April 21, **1998**.
62. Jamison, J.A.; LaGrandeur, L.M.; Rodriguez, M.J.; Turner, W.W.; Zeckner, D.J. *J. Antibiot*, **1997**, *51*, 239-242.
63. Rodriguez, J.M.; Nesler, M.J.; Zwelfel, M.J. *PCT Int. Appl. WO 2000035945*, June 22, **2000**.
64. Lal, B.; Gund, V.G.; Gangopadhyay, A.K.; Nadkarni, S.R.; Dikshit, V.; Chatterjee, D.K.; Shirvaikar, R. *Bioorg. Med. Chem.*, **2003**, *11*, 5189-5198.
65. Lal, B.; Gund, V.G. *Bioorg. Med. Chem. Lett.*, **2004**, *14*, 1123-1128.
66. Borromeo, P.S.; Cohen, J.D.; Gregory, G.S.; Henle, S.K.; Hitchcock, S.A.; Jungheim, L.N.; Mayhugh, D.R.; Shepherd, T.A.; Turner, W.W. *PCT Int. Appl. WO 2000/011023*, March 2, **2000**.
67. Tomishima, M.; Ohki, H.; Yamada, A.; Maki, K.; Ikedia, F. *Bioorg. Med. Chem. Lett.*, **2008**, *18*, 2886-2890.
68. Leonard, W.R.; Belyk, K.M.; Conlon, D.A.; Bender, D.R.; DiMichele, L.M.; Liu, J.; Hughes, D.L. *J. Org. Chem.*, **2007**, *72*, 2335-2343.
69. Warn, P.A.; Sharp, A.; Morrissey, G.; Denning, D.W. *Int. J. Antimicrob. Agents*, **2010**, *35*, 146-151.
70. Di Santo, R. *Nat. Prod. Rep.*, **2010**, *27*, 1088.

71. Kurokawa, N.; Ohfune, Y. *J. Am. Chem. Soc.*, **1986**, *108*, 6041-6043.
72. Evans, D.A.; Weber A.E., *J. Am. Chem. Soc.*, **1987**, *109*, 7151-7157.
73. Kurokawa, N.; Ohfune Y., *Tetrahedron*, **1993**, *49*, 6195-6222.
74. Zambias, R.A.; Hammond, M.L.; Heck, J.V.; Bartizal, K.; Trainor, C.; Abruzzo, G.; Schmatz, D.M.; Nollstadt, K. M. *J. Med. Chem.*, **1992**, *35*, 2843-2855.
75. Klein, L.L.; Li, L.; Chen, H.; Curty, C.B.; DeGoey, D.A.; Grampovnik, D.J.; Leone, C.L.; Thomas, S.A.; Yeung, C.M.; Funk, K.W.; Kishore, V.; Lundell, E.O.; Wodka, D.; Meulbroek, J.A.; Alder, J.D.; Nilius, A.M.; Lartey, P.A.; Plattner, J.J. *Bioorg. Med. Chem. Lett.*, **2000**, *8*, 1677-1696.
76. a) Yao, J.; Liu, H.; Zhou, T.; Chen, H.; Miao, Z.; Dong, G.; Wang, S.; Sheng, C.; Zhang, W. *Tetrahedron*, **2012**, *68*, 3074-3085; b) Yao, J.; Liu, H.; Zhou, T.; Chen, H.; Miao, Z.; Sheng, C.; Zhang, W. *Eur J. Med. Chem.*, **2012**, *50*, 196-208.
77. Wang, W.; Li, Q.; Hasvold, L.; Steiner, B.; Dickman, D.A.; Ding, H.; Clairborne, A.; Chen, H.-J.; Frost, D.; Goldman, R.C.; Marsh, K.; Hui, Y.-H.; Cox, B.; Nilius, A.; Balli, D.; Lartey, P.; Plattner, J.J.; Bennani, Y.L. *Bioorg. Med. Chem. Lett.*, **2003**, *13*, 489-493.
78. Meulbroek, J.A.; Nilius, A.M.; Li, Q.; Wang, W.; Hasvold, L.; Steiner, B.; Dickman, D.A.; Ding, H.; Frost, D.; Goldman, R.C.; Lartey, P.; Plattner, J.J.; Bennani, Y.L. *Bioorg. Med. Chem. Lett.*, **2003**, *13*, 495-497.
79. Kartsonis, N.A.; Nielsen, J.; Douglas, C.M. *Drug Resist. Update*, **2003**, *6*, 197-218.
80. Hashimoto, S. *J. Antiobiot.*, **2009**, *62*, 27-35.
81. Ohigashi, A.; Kanda, A.; Tsuboi, H.; Hashimoto, N. *Org. Process Res. Dev.*, **2005**, *9*, 179-184.
82. Estes, K.E.; Penzak, S.R.; Calis, K.A.; Walsh, T.J. *Pharmacotherapy*, **2009**, *29*, 17-30.
83. Chen, S.C.-A.; Slavin, M.A.; Sorrell, T.C. *Drugs*, **2011**, *71*, 11-41.
84. Onishi, J.; Meinz, M.; Thompson, J.; Curotto, J.; Dreikorn, S.; Rosenbach, M.; Douglas, C.; Abruzzo, G.; Flattery, A.; Kong, L.; Cabello, A.; Vicente, F.; Pelaez, F.; Diez, M.T.; Martin, I.; Bills, G.; Giacobbe, R.; Dombrowski, A.; Schwartz, R.; Morris, S.; Harris, G.; Tsipouras, A.; Wilson, K.; Kurtz, M.B. *Antimicrob. Agents Chemother.*, **2000**, *44*, 368-377.
85. a) Gorman, J.A.; Chang, L.-P.; Clark, J.; Gustavson, D.R.; Lam, K.S.; Mamber, S.W.; Pirnik, D.; Ricca, C.; Fernandes, P.B.; O'Sullivan, J. *J. Antibiot.*, **1996**, *49*, 547-552; b) Leet, J.E.; Huang, S.; Klohr, S.E.; McBrien, K.D. *J. Antibiot.*, **1996**, *49*, 553-559.
86. Schwartz, R.E.; Smith, S.K.; Onishi, J.C.; Meinz, M.; Kurtz, M.; Giacobbe, R.A.; Wilson, K.E.; Liesch, J.; Zink, D.; Horn, W.; Morris, S.; Cabello, A.; Vicente, F. *J. Am. Chem. Soc.*, **2000,** *122*, 4882-4886.
87. Cabello, M.A.; Platas, G.; Collado, J.; Díez, M.T.; Martin, I.; Vicente, F.; Meinz, M.; Onishi, J.C.; Douglas, C.; Thompson, J. ; Kurtz, M.B.; Schwartz, R.E.; Bills, G.F.; Giacobbe, R.A.; Abruzzo, G.K.; Flattery, A.M.; Kong, L.; Peláez, F. *Int. Microbiol*., **2001**,*4*, 93-102.
88. Vicente, M.F.; Cabello, A.; Platas, G. Basilio, A.; Díez, M.T.; Dreikorn, S.; Giacobbe, R.A.; Onishi, J.C.; Meinz, M.; Kurtz, M.B.; Rosenbach, M.; Thompson, J.; Abruzzo, G.; Flattery, A.; Kong, L.; Tsipouras, A.; Wilson, K.E., Peláez, F. *J. Appl. Microbiol.*, **2001**, *91*, 806-813.
89. Kurtz, M.B.; Douglas, C.M. *J. Med. Vet. Mycol.*, **1997**, *35*, 79-86.
90. Bartnicki-Garcia, S. *Annu. Rev. Microbiol.*, **1968**, *22*, 87-108.
91. Bowman, S.M.; Free, S.J. *BioEssays*, **2006**, *28*, 799-808.
92. Latgé, J.-P., *Mol. Microbiol.*, **2007**, *66*, 279-290.
93. Klis, F.M.; Mol, P.; Hellingwerf, K.; Brul, S. *FEMS Microbiol. Rev.*, **2002**, *26*, 239-256.

94. James, P.G.; Cherniak, R.; Jones, R.G.; Stortz, C.A. *Carbohydr. Res.*, **1990**, *198*, 22-38.
95. Smits, G.J.; Kapteyn, J.C.; Ende, van den H.; Klis, F.M. *Curr. Opin. Microbiol.*, **1999**, *2*, 348-352.
96. Kapteyn, J.C.; Hoyer, L.L; Hecht, J.E.; Müller, W.H.; Andel, A.; Verkleij, A.J.; Makarow, M.; Ende, van den H., Klis, F.M. *Mol. Microbiol.*, **2000**, *35*, 601-611.
97. Fontaine, T.; Simene, C.; Dubreucq, G.; Adam, O.; Delepierre, M.; Lemoine, J.; Vorgias, C.E.; Diaquin, M.; Latgé, J.-P. *J. Biol. Chem.* **2000**, *275*, 27594-27607.
98. Douglas, C.M. *Medical Mycology*, **2001**, *39*, 55-66.
99. Liu, J.; Balasubramanian, M.K. *Curr. Drug Targets: Infect. Disord.*, **2001**, *1*,159-169.
100. Inoue, S.B.; Takewaki, T.; Mio, T.; Adachi, M.; Fujii, Y.; Miyamoto, C.; Arisawa, M.; Furuichi, Y.; Watamabe, T. *Eur. J. Biochem.*, **1995**, *231*, 845-854.
101. Frost, D.; Brandt, K.; Estill, C.; Goldman, R. *FEMS Microbiol Lett*, **1997**, *146*, 255-261.
102. Beauvais, A.; Bruneau, J.M.; Mol, P.C.; Buitrago, M.J.; Legrand, R.; Latgé, J.P. *J. Bacteriol.*, **2001**, *183*, 2273-2279.
103. Perlin, D.S. *Drug Resist Update*, **2007**, *10*, 121-130.
104. Walker, L.A.; Gow, N.A.R.; Munro, C.A. *Fungal Genet Biol*, **2010**, *47*, 117-126.
105. Radding, J.A.; Heidler, S.A.; Turner, W.W. *Antimicrob. Agents Chemother.*, **1998**, 1187-1194.
106. Walker, L.A.; Munro, C.A.; de Bruijn, I.; Lenardon, M.D.; McKinnon, A.; Gow, N.A.R. *PloS*

CHAPTER 2

Synthesis and Evaluation of Novel Macrocyclic Antifungal Peptides

Parts of this chapter have been published:

Mulder, M.P.C.; Kruijtzer, J.A.W.; Breukink, E.J.; Kemmink, J.; Pieters, R.J.; Liskamp, R.M.J., *Bioorg. Med. Chem.*, **2011**, *19*, 6505-6517.

2.1 Introduction

There is currently an urgent need for the development of new antifungal agents. The echinocandins represent the most recent class of antifungal drugs that reached the market in the last decade[1] and act on a novel target [2].

As was described in chapter 1 only three echinocandins have been approved by the Food and Drug Administration (FDA). These echinocandins are all semisynthetic derivatives of the natural fermentation products.[3-5] Due to the large number of hydroxyl groups in these lipopeptides, total synthesis of the echinocandins is extremely challenging. In addition these synthetic limitations led to a semi-synthetic approach in which isolation of the natural echinocandin was followed by synthetic modifications. These derivatives were used for most of the structure activity relationship (SAR) studies.[6] However, in 1992 the first total synthesis of simplified echinocandin analogues was described by Zambias et al.[7] These structure activity relationship data showed that several of the functional groups, primarily the hydroxyl groups, were not essential for antifungal activity. Klein et al. reported a similar study in 2000.[8] Both papers described derivatives that were obtained by peptide head-to-tail cyclization. Inspired by these reports, we became interested in the synthesis of novel echinocandin analogues by employing alternative peptide cyclization approaches.

In this chapter the synthesis and activity of novel echinocandin analogues (Figure 1) obtained by ring closing metathesis (**6**) and disulfide formation (**7**) is described. Using these approaches, the impact of the size and character of the macrocyclic peptide backbone on antifungal activity can be investigated more extensively. In addition, these new mimics may be attractive alternatives since they also contain a position for further modification (i.e. the C-terminus; substituent R^2). Moreover the analogues obtained by ring closing metathesis (**6**) possess an additional site for modification, namely the double bond.

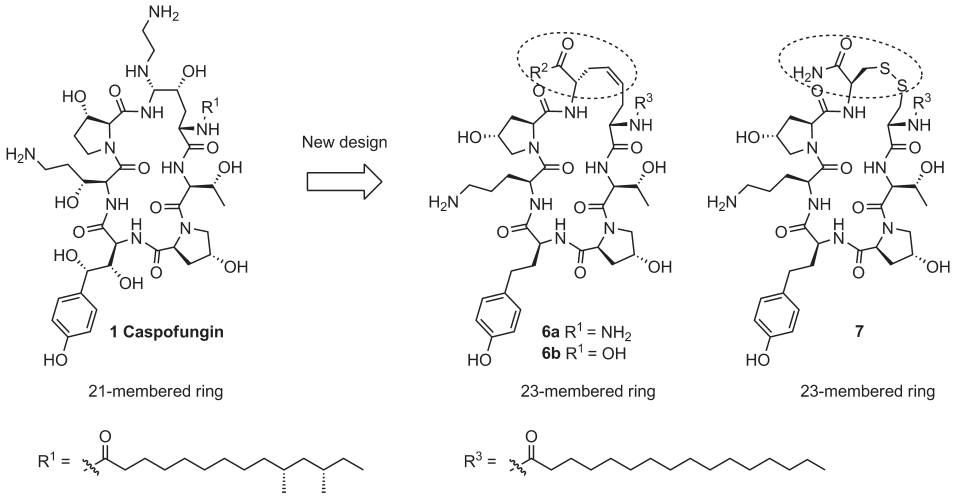

Figure 1. Structures of the designed synthetic echinocandin analogues compared to caspofungin (**1**).

In comparison to caspofungin **1**, mimics **6** and **7** were designed to contain several modifications (Figure 1). Consistent with SAR studies[7,8] a number of functional groups which are not necessary for antifungal activity, were omitted. Moreover, the lipophilic chain (R^1 in **1**) was replaced by a palmitoyl group (R^3 in **6a**, **6b** and **7**), which closely mimics the fatty acid tail of caspofungin. Earlier SAR studies showed that a C12-C18 fatty acid chain gave an optimal activity.[9] In addition, the ornithine derived residue at the top of the caspofungin structure (**1**) was replaced by an allylglycine residue together with introduction of an allylglycine residue at the C-terminus leading to precursor **8**. Similarly, replacement by a cysteine residue at these positions gave precursor **11**. Cyclization of these precursors slightly enlarged the ring to a 23-membered ring as compared to the original 21-membered ring of caspofungin. According to the literature[10] there was room for alterations at this site of the molecule. Borromeo et al. reported an approach in which the ring of the hexapeptide was opened at the hemiaminal function and the ornithine residue was replaced to generate new cyclic hexapeptides.[10]

2.2 Results and Discussion

Ring-closing metathesis (RCM) reactions have been previously carried out on peptides linked to a solid support.[11] However, these RCM reactions required long reaction times (18-48h). Recently, Robinson et al. reported large acceleration of RCM on resin-bound peptides by microwave heating in the presence of chaotropic reagents.[12] This procedure was also applied to the preparation of our mimic **6**. As shown in Scheme 1, linear precursors were prepared by SPPS using either the Rink or Wang resin, ultimately providing the peptide amide (**6a**) or carboxylic acid (**6b**), respectively.

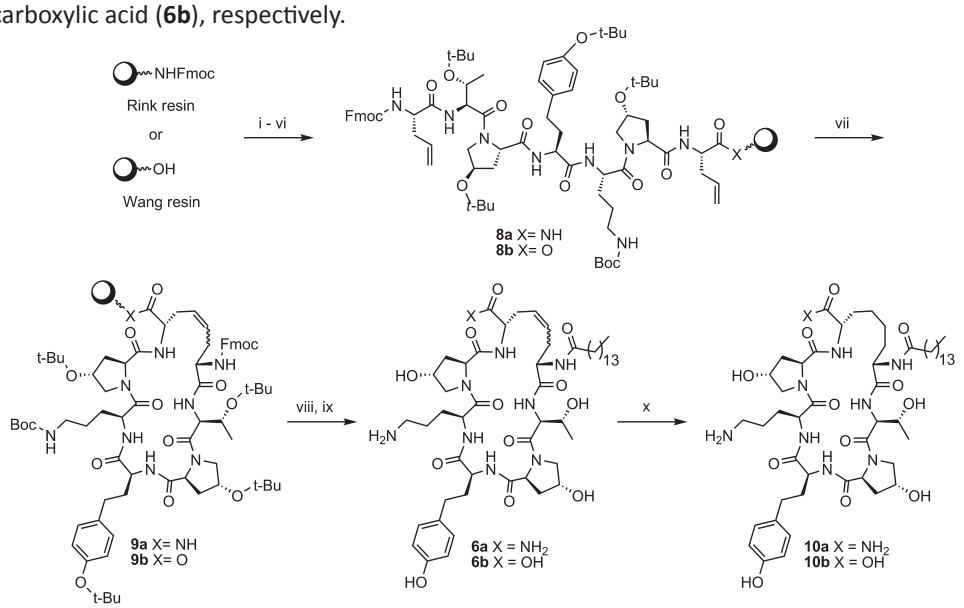

Scheme 1. Reagents and conditions: (i) Rink resin: (1) 20% piperidine in NMP; (2) Fmoc-Alg-OH, BOP, DIPEA, NMP; Wang resin: (1) Fmoc-Alg-OH, pyridine, DCBC, DMF; (2) Ac_2O/NMI/DiPEA/DMF (2/1/1/6, v/v/v); (ii-vi) (1) 20% piperidine in NMP; (2) Fmoc-Xxx-OH, BOP, DiPEA, NMP; (vii) Grubbs II (15 mol%), 10 vol% LiCl/DMA (0.4M), MW, 75 min, 100 °C, DCM; (viii) (1) 20% piperidine in NMP; (2) palmitic acid, HATU, DiPEA, NMP; (ix) TFA/TIS/H_2O (95/2.5/2.5, v/v/v); (x) H_2, 10% Pd/C, EtOH, rt, 36h.

Then, RCM reaction of resin-bound peptide **8** was performed using a 15 mol% solution of Grubbs II in DCM (containing 10 vol% LiCl/DMA 0.4M) and microwave irradiation to provide the ring-closed product **9**. Removal of the Fmoc group, coupling of palmitic acid, and acidolytic cleavage from the resin with concomitant removal of the side chain protecting groups, gave the cyclic peptide **6** as a mixture of *cis/trans* isomers (Figure 2a) in an overall yield of 11% after purification by preparative HPLC. Attempted RCM reactions without microwave irradiation were less successful. For example, treatment of the linear resin-bound peptide with second generation Grubbs catalyst (20 mol%) in DCM containing 10 vol% LiCl/DMA (0.4M) at 50 °C for 24h gave only trace amounts of the cyclized product. After reduction of unsaturated peptides **6a** and **6b** macrocyclic peptides **10a** and **10b** were obtained.

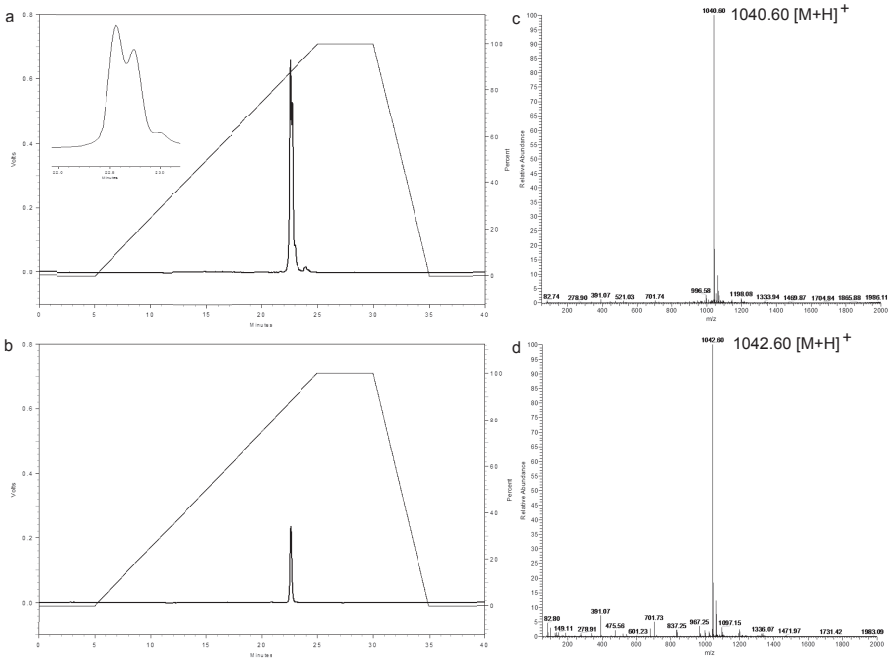

Figure 2. Analysis of **6a** and **10a**. (a) HPLC of **6a** (220 nm); (c) ESI-MS **6a**; (b) HPLC of **10a** (220 nm); (d) ESI-MS **10a**.

For the synthesis of disulfide mimic **7** the synthesis strategy outlined in scheme 2 was applied. The linear precursor was prepared by SPPS on the Rink resin. Removal of the Fmoc group followed by introduction of the palmitoyl chain and cleavage from the resin yielded the deprotected peptide **11,** which was then cyclized via disulfide formation by oxidation with aq. DMSO[13] yielding peptide **7** in an overall yield of 22% after purification by preparative HPLC.

The antifungal activity of each macrocyclic peptide analogue was evaluated by broth microdilution using Caspofungin **1**[14] as a reference compound. Minimum inhibitory concentrations (MICs) were determined visually and thereby quantified as the lowest concentration of compound resulting in inhibition of yeast growth after overnight incubation at 30 °C (Table 1). Unfortunately, mimics **6, 7** and **10** did not show antifungal activity up to 100 μg/mL (corresponding to 96 μM).

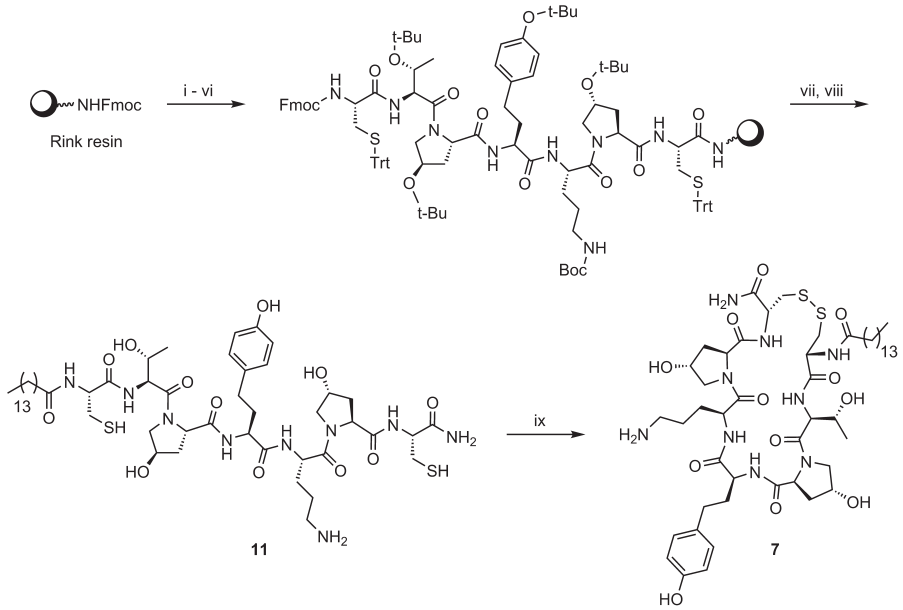

Scheme 2. Reagents and conditions: (i) (1) 20% piperidine in NMP; (2) Fmoc-Cys(Trt)-OH, BOP, DiPEA, NMP; (ii-vi) (1) 20% piperidine in NMP; (2) Fmoc-Xxx-OH, BOP, DiPEA, NMP; (vii) (1) 20% piperidine in NMP; (2) palmitic acid, HATU, DiPEA, NMP; (viii) TFA/TIS/H_2O (95/2.5/2.5, v/v/v); (x) H_2O, NH_4OAc, DMSO, pH 6.

Table 1. Antifungal activity of analogues

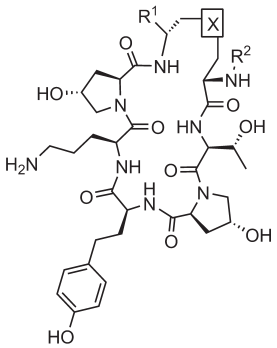

				Candida albicans
	R^1	**X**	**R^2**	CBS 9975
Caspofungin (1)				0.025
6a	$C(O)NH_2$	CH=CH	Palm	>100
6b	C(O)OH	CH=CH	Palm	>100
7	$C(O)NH_2$	S-S	Palm	>100
10a	$C(O)NH_2$	CH_2CH_2	Palm	>100
10b	C(O)OH	CH_2CH_2	Palm	>100

To obtain a better understanding of the observed lack of antifungal activity, further investigations were performed by varying the lipophilic "tail" (substituent R^2, Figure 3A), introduction of modifications at the C-terminus (Figure 3B) and at the double bond (Figure 3C) and changing the peptide ring size (Figure 3D).

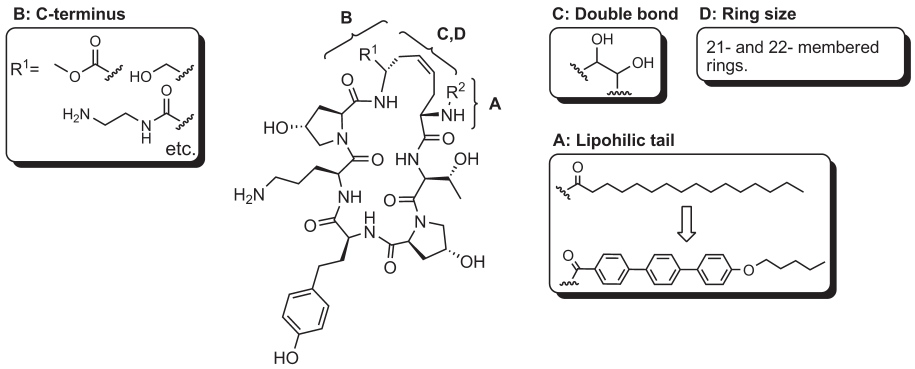

Figure 3. Structural variations for study of their influence on antifungal activity.

2.2.1 Influence of the lipophilic "Tail"

The nature of the fatty acid chain and its influence on the activity of the echinocandins has been studied extensively. Several reports have described the preparation of semi-synthetic echinocandin analogues by enzymatic de-acylation and chemical re-acylation with alternative fatty acids.[9,15-19] It has been shown that neither the macrocyclic peptide itself, the fatty acid, nor a mixture of both show significant antifungal activity. These results clearly demonstrated that the intact echinocandin molecule is required for inhibition of antifungal growth.[16] Moreover, the nature of the fatty acid side chain plays a very important role in the biological activity (see chapter 5). In this regard, side chain length, overall lipophilicity, and other geometric factors such as rigidity, contribute to the SAR of these analogues.

These previous studies have shown that the lipophilic chain in the echinocandins is a crucial determinant for antifungal potency. To determine if the choice of the lipophilic tail for mimics **6**, **7** and **10** might be partly responsible for the loss of antifungal activity, a series of fatty acid derivatives (**12a**,**b** and **13a**,**b**; Scheme 5), based on previous work by Klein et al., were prepared.[8] Their work established that head-to-tail backbone mimics bearing a terphenyl ("Ter") chain showed considerable biological activity.

The required terphenyl acid building block **14**, was synthesized as outlined in Scheme 3.[17] First the alkoxy tail of **16** was introduced in 87% yield by a Williamson ether synthesis using 1-bromopentane. Then, the organolithium derivative was prepared with *n*-butyllithium, reacted with triisopropyl borate and subsequently hydrolyzed to boronic acid **17** in 78% yield. In a Suzuki reaction, 4-iodobenzoic acid was coupled to boronic acid **17** in the presence of $Pd(PPh_3)_4$ to give the terphenyl side chain containing "fatty" acid derivative **14**.

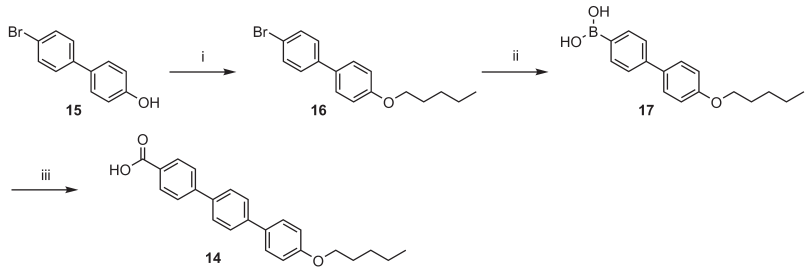

Scheme 3. Reagents and conditions: (i) 1-bromopentane, K_2CO_3, KI, DMF, 87%; (ii) (1) *n*BuLi, $B[OCH(CH_3)_2]_3$, THF; (2) H_2O, 78%; (iii) 4-iodobenzoic acid (**18**), Na_2CO_3, $Pd(PPh_3)_4$, Tol/EtOH (3/1, v/v), Δ, 25-43%.

This synthesis proceeded smoothly until the Suzuki reaction.[20] The product of this reaction had a grey color and was not soluble in any protic (e.g. ethanol, methanol, acetic acid) or aprotic (e.g. DCM, DMF, MeCN, DMSO) solvent. Characterization by NMR and ESI-MS was not possible for this product. However, a simple test coupling reaction with DCC of **14** and H-Ala-O*t*Bu was successful, indicating that **14** had been indeed obtained. In a further attempt to characterize our product a relatively new mass spectrometry technique was used. The DART (Direct Analysis in Real Time) has been developed in 2003[21] and works by simply placing a sample, in its native form, between the atmospheric DART ion source and the AccuTOF mass spectrometer inlet (Figure 4) measuring high-resolution mass spectra.

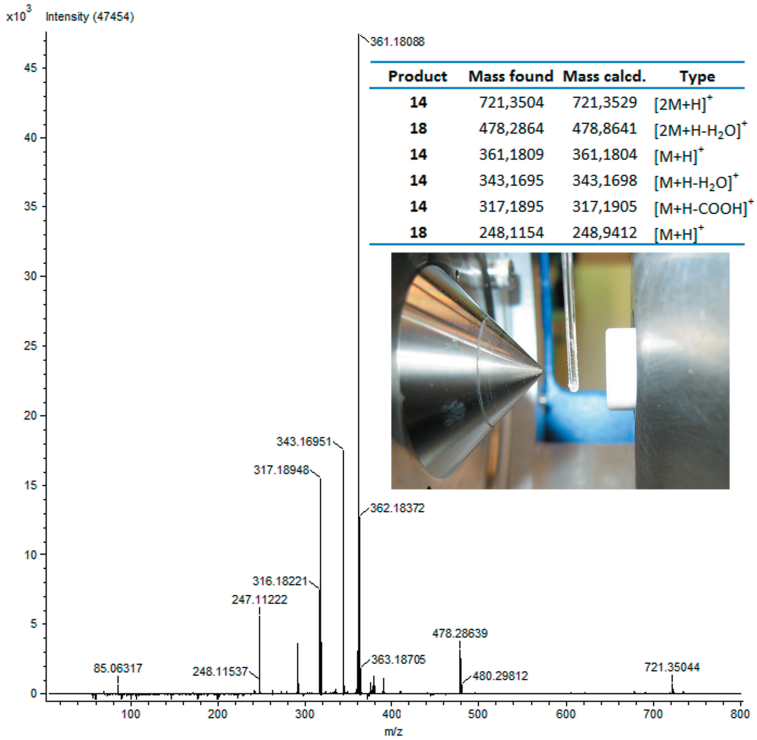

Product	Mass found	Mass calcd.	Type
14	721,3504	721,3529	$[2M+H]^+$
18	478,2864	478,8641	$[2M+H-H_2O]^+$
14	361,1809	361,1804	$[M+H]^+$
14	343,1695	343,1698	$[M+H-H_2O]^+$
14	317,1895	317,1905	$[M+H-COOH]^+$
18	248,1154	248,9412	$[M+H]^+$

Figure 4. DART mass spectrum and mass table of **14** (insert). Picture of the sample, on a glass rod, being analyzed is held in the sample chamber between the DART ion source (right) and the spectrometer inlet (cone on left).

This allowed us to measure neat **14** since solvents or sample preparations were not required (Figure 4). The presence of the $[M+H]^+$ ion in the DART mass spectrum clearly showed that the product was formed. Nevertheless, the reproducibility of the Suzuki reaction was problematic. Optimization attempts with different bases, solvent systems and Pd catalysts were unsuccessful. In addition, possibly Pd is complexed by **14**, explaining its grey color and insolubility. Therefore, the route of Scherer et al.[22] as is shown in scheme 4 was used for a larger scale production of **14**. Boronic acid **21** was prepared from 4-bromophenol **19**. Thus, Williamson etherification of **19** with 1-bromopentane afforded **20** in 92% yield, followed by synthesis of the boronic acid **21** in 63% yield similar to the preparation of **17**. For the preparation of the biphenyl iodide **23**, the biphenyl carboxylic acid **22** was treated with iodine and the hypervalent iodine reagent phenyliodine bistrifluoroacetate (PIFA) affording **23** in 83% yield. Finally, Suzuki coupling, in the presence of $PdCl_2(PPh_3)_2$, of boronic acid **21** and iodide **23** gave **14** as a white solid in 42% yield.

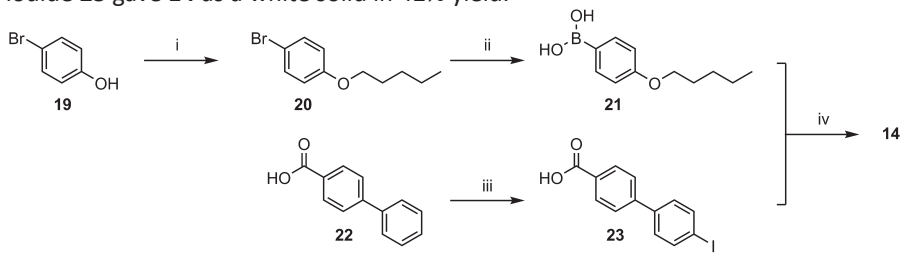

Scheme 4. Reagents and conditions: (i) 1-bromopentane, K_2CO_3, KI, DMF, 92%; (ii) (1) *n*BuLi, $B[OCH(CH_3)_2]_3$, THF; (2) H_2O, 63%; (iii) Phenyliodine bistrifluoroacetate (PIFA), I_2, CCl_4, 83%; (iv) biphenyl-4-carboxylic acid, Na_2CO_3, $PdCl_2(PPh_3)_2$, DMSO, 80°C, 42%.

Despite the poor solubility of terphenyl carboxylic acid **14** characterization by NMR in DMSO was feasible, for product **14** obtained through this optimized route, next to DART-MS (Figure 5). Although the latter Suzuki coupling gave a modest yield, this method proved to be reproducible and could be performed on a larger scale. In addition, in the spectra of **14** obtained by the method of Scherer et al. (Figure 5) starting material was absent and lower intensities of ions were found between m/z 250-400. Thus, the purity of **14** was higher than when using the former synthesis method, as was also apparent from the white color of the product.

Now that we had terphenyl carboxylic acid **14** in hand, the attention was turned to the synthesis of the head-to-tail mimics with the palmitoyl (**12**) and the terphenyl (**13**) fatty acid chain. The synthesis of these mimics proceeded readily and is outlined in Scheme 5 for mimic **12b**. Linear precursor **24** was prepared by SPPS using the trityl resin. Removal of the ε-Fmoc group from ornithine, followed by mild acidolytic cleavage of the protected peptide from the resin followed by cyclization gave the protected macrocyclic peptide **25** in an overall yield of 90%. Removal of the IvDde-group[23] from ornithine with hydrazine and subsequent coupling of the fatty acid chain, followed by global deprotection and purification, gave cyclic peptides **12** and **13** in overall yields of 17-23% corresponding to 87 % on the average per step.

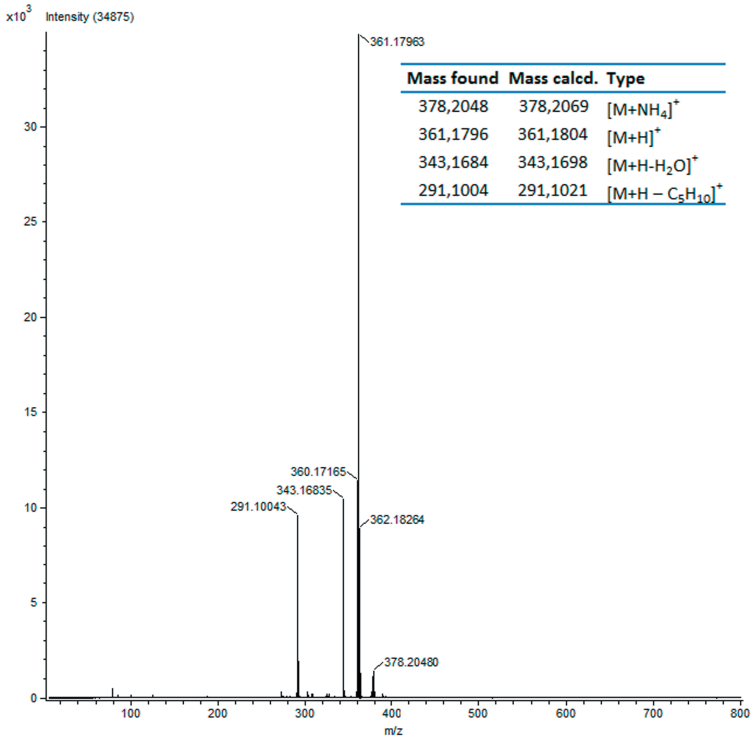

Figure 5. DART mass spectrum and mass table of **14** (insert) obtained by the route of Scherer et al.

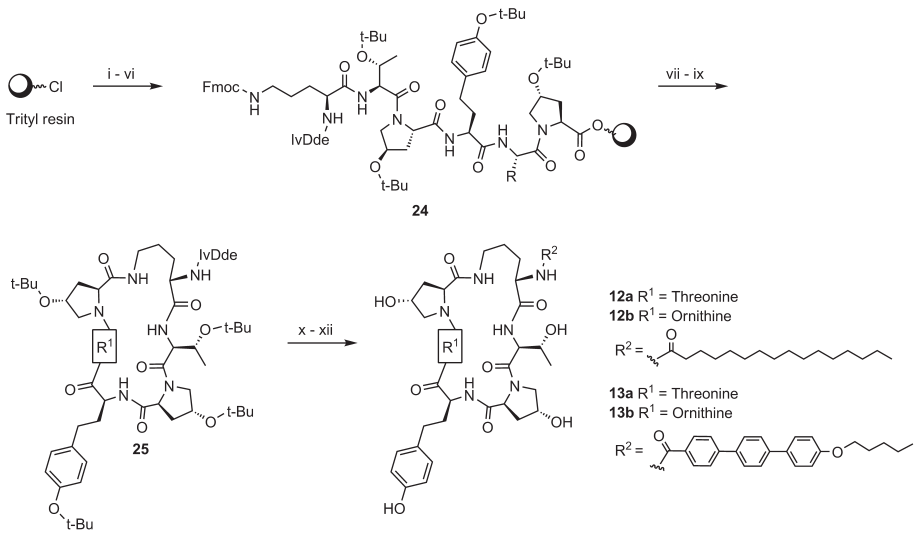

Scheme 5. Reagents and conditions: (i) (1) Fmoc-Hyp(*t*Bu)-OH, DIPEA, DCM; (2) DCM/MeOH/DiPEA (17/2/1, v/v/v); (ii-vi) (1) 20% piperidine in NMP; (2) Fmoc-Xxx-OH, BOP, DiPEA, NMP; (vii) 20% piperidine in NMP; (viii) HFIP/DCM (1/1, v/v); (ix) BOP, DiPEA, DMF; (x) NH_2NH_2/DMF (5 vol%); (xi) for **12**: palmitic acid, DCC, HOBt, DCM; for **13** Ter chain, DCC, HOBt, DCM; (xii) TFA/TIS/H_2O (95/2.5/2.5, v/v/v).

Minimum inhibitory concentrations (MICs) were evaluated and are given in Table 2. These results showed that mimic **13a** with a terphenyl lipophilic tail is 50-fold more active than **12a** with a palmitoyl chain. Moreover, mimics containing an ornithine (**12b**, **13b**) residue were 5-fold more active than the mimics containing a threonine (**12a**, **13a**) residue at this position as is consistent with previously described results by Klein et al.[8]

Table 2. Antifungal activity of head-to-tail analogues.

			Candida albicans
	R^1	**R^2**	CBS 9975
Caspofungin (1)	-	-	0.025
12a	Threonine	Palm	25
12b	Ornithine	Palm	4.38
13a	Threonine	Ter	0.47
13b	Ornithine	Ter	0.14

Thus, compounds **12** and **13** having a terphenyl tail gave us a clue about the high importance of the lipophilic tail in general. This finding enticed us to synthesize from thereon all compounds with a terphenyl chain. For example **6b** containing terphenyl chain became **26**. For the synthesis of RCM mimic **26** with a terphenyl chain, the used RCM conditions required optimization. Employing Hoveyda-Grubbs II catalyst, longer reaction times, and adding the catalyst in portions did not improve the rate of conversion to the ring-closed product. The results are summarized in Table 3.

Table 3. Attempted conditions for optimization of the RCM reaction.

				Conversion rates [a]	
Entry	**Catalyst**	**mol %**	**Time**	**Linear**	**E/Z**
1	Grubbs II	15	1 h	40%	60%
2	Grubbs II	10	1 h	42%	58%
3	Hoveyda Grubbs II	10	1 h	38%	62%
4	Grubbs II	2 x 5	2 x 30 min	45%	55%
5	Grubbs II	10	2 h	41%	59%
6[b]	Grubbs II	10	1 h	22%	78%

[a] Conversion is assessed by analytical HPLC. [b] RCM was not performed with Fmoc precursor **8** as for entry's 1-5, but with the linear peptide with a Ter side chain.

However, we found that changing the sequence of the reactions led to success in the RCM step (entry 6, Table 3). Thus, RCM was performed after coupling of the fatty acid chain instead of using the Fmoc precursor **8** as in Scheme 1 (step vii and viii were switched). Linear precursor **8** was prepared by SPPS on the Wang resin. Removal of the N-terminal Fmoc group, coupling of the terphenyl chain followed by RCM reaction of the resin-bound peptide using a 10 mol% solution of Grubbs II in DCM (containing 10 vol% 0.4M LiCl in DMA) under microwave irradiation resulted in the ring-closed product. Cleavage from the resin with concomitant removal of side chain protecting groups gave cyclic peptide **26** as a mixture of

cis/trans isomers in an overall yield of 15% after purification by preparative HPLC. After Pd/C assisted reduction of the double bond macrocyclic peptide **27** was obtained.

The disulfide mimic **7** was also synthesized with a terphenyl chain, leading to **28**. Synthesis of this mimic **28** proceeded analogously to the synthesis of mimic **7** in Scheme 2. For the preparation of **28** terphenyl carboxylic acid **14** was coupled in step vii instead of palmitic acid as shown in Scheme 2. The minimum inhibitory concentrations (MICs) were evaluated and are shown in Table 4.

Table 4. Antifungal activity of analogues

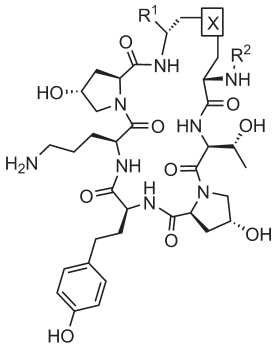

				Candida albicans
	R^1	**X**	**R^2**	CBS 9975
Caspofungin (1)	-	-	-	0.025
26	C(O)OH	CH=CH	Ter	>100
27	C(O)OH	CH_2CH_2	Ter	>100
28	$C(O)NH_2$	S-S	Ter	>100

Although these results showed that mimics **26** - **28** with a terphenyl chain did not reach their MIC-values at 100 μg/mL (corresponding to 87 μM), a difference in growth of *C. albicans* cells was visible starting at 5 μg/mL (Figure 6).

Further investigation of this observation by light microscopy has led to a clearer view of the difference in growth that was observed (Figure 7). A clear-dose-dependent effect of our compounds in the growth pattern of *C. albicans* cells was visible. Higher concentrations of **26** resulted in enlarged rounded cells that agglutinated, showing large vacuoles and distorted cytoplasms. There was a clear reduction in the number of budding cells and when these appeared more buds were formed simultaneously. Although **26** was not fully active at concentrations up to 100 μg/mL a clear effect on yeast growth was observed. At first glance the microtiter plate (Figure 6) may show the presence of more cells present at higher concentration of compound. However, this is not the case since the agglutinated, deformed cells are more spread out.

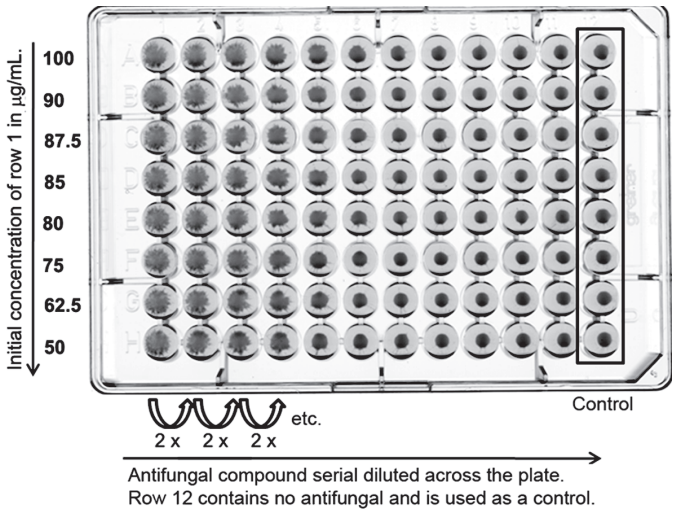

Figure 6. Minimum Inhibitory concentration (MIC) determination of **26** by microbroth dilution technique, in a 96-well microtiter plate. A clear dose-dependent change in the growth pattern of *C. albicans* cells is visible for the first five columns.

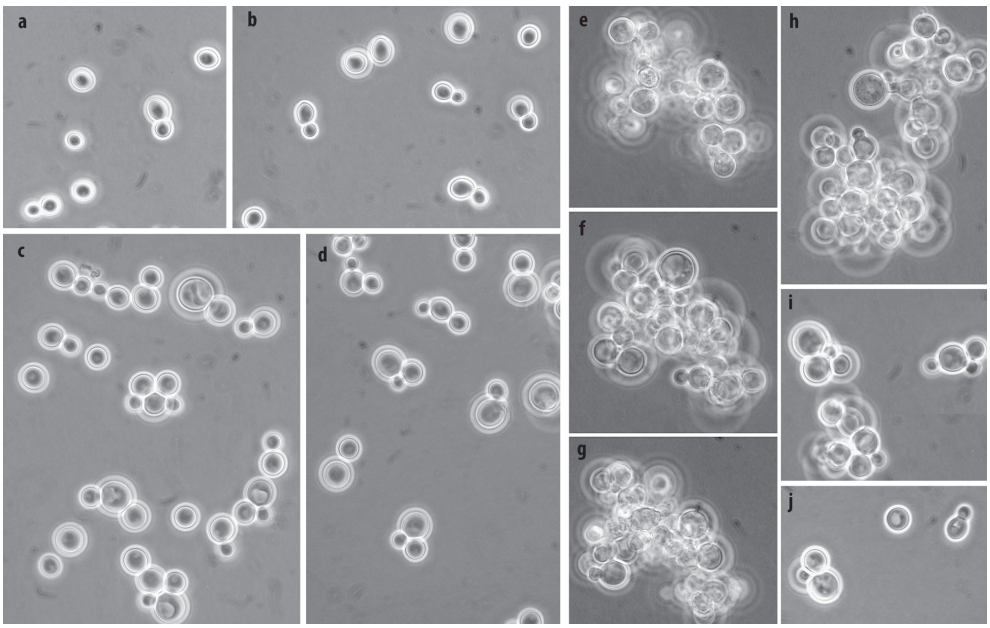

Figure 7 Visualization of yeast cells, in microtiter plate of **26**, by light microscopy. (**a**)-(**b**): Control, healthy yeast cells (well E-12); (**c**)-(**d**): yeast cells in well E-5; (**e**)-(**j**): yeast cells in well B1. In all images the same magnification is used.

2.2.2 Influence of C-terminal modifications

RCM mimic **26** contains a C-terminal moiety allowing for modification, which is convenient for the preparation of additional analogues. This moiety replaces the site of the hemiaminal group present in most echinocandins (Figure 1, R^1 = OH), which is known to be unstable at pH>7.[24,25,5] The instability of the hemiaminal hydroxyl group at the C-5 position of ornithine at pH>7 results in a facile base catalyzed ring opening and rearrangement to the 5-membered ring hemiaminal isomer with substantial loss in activity[25] (Figure 10, chapter 1). This has led to several studies on derivatization of the hemiaminal moiety to improve stability.[26-32] In particular, these studies showed that aminoalkylethers (e.g. R^1 = $OCH_2CH_2NH_2$) bearing a basic amino group had enhanced antifungal properties.[26] Further optimization led to the closely related *N*-alkylamino aminal series[32] including clinically used caspofungin **1**.

In view of the importance of this part of the structure two C-terminally modified analogues incorporating basic groups **32** and **34** were synthesized (Scheme 6). Moreover, a few other relatively easy accessible mimics were prepared (**30** and **33**). Synthesis of these mimics proceeded largely as described for mimic **26**, except for the last step. The resin-bound ring-closed product was cleaved from the resin with KCN in MeOH to give the fully *t*Bu/Boc protected methylester **29**. Saponification of **29** gave carboxylic acid **31**, which was coupled to Boc-protected ethylene diamine followed by acidolysis affording **32**. Reduction of methylester **29** followed by removal of the protecting groups gave macrocyclic peptide alcohol **33**. Reacting **29** with hydrazine followed by acidolysis afforded **34** (Scheme 6). For the acidolysis of the hydrazine mimic we used different cleavage conditions. When the peptide was treated with the standard TFA conditions, the TFA adduct of the hydrazine mimic (**35**) was formed. By employing HCl/Et_2O conditions this side reaction was circumvented.

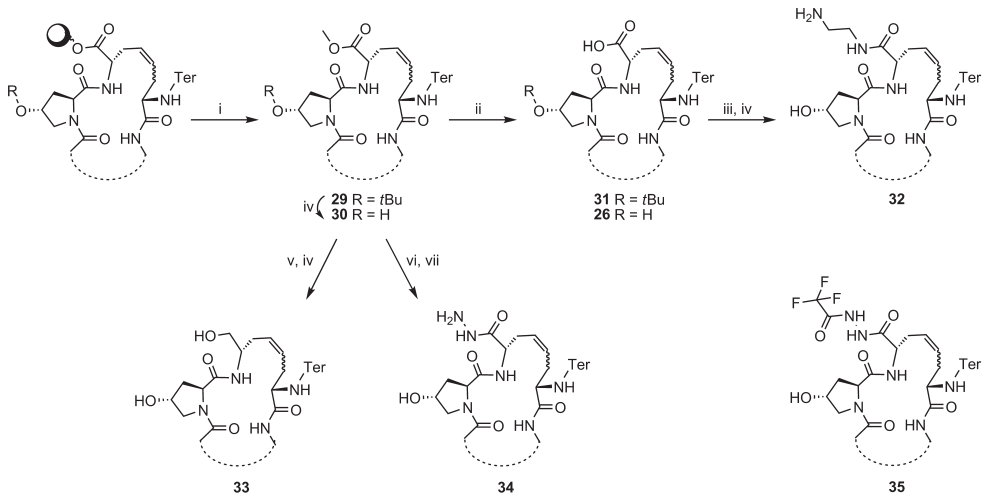

Scheme 6. Reagents and conditions: (i) KCN, MeOH; (ii) LiOH, THF; (iii) *N*-Boc-ethylene-diamine, HATU, DiPEA, NMP; (iv) TFA/TIS/H_2O (95/2.5/2.5, v/v/v); (v) $LiBH_4$, THF; (vi) $N_2H_4.H_2O$, DMF; (vii) HCl/Et_2O.

The minimum inhibitory concentrations (MICs) of mimics **30**, **32**, **33** and **34** were evaluated and are shown in Table 5. Although these results showed that these mimics did not reach their MIC-values at 100 μg/mL, the same dose-dependent change in the growth pattern of the *C. albicans* cells was observed for mimics **32**, **33** and **34** as was the case for **26**.

Table 5. Antifungal activity of analogues

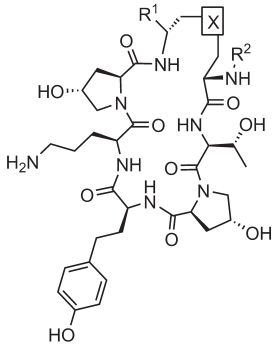

	R^1	X	R^2	*Candida albicans* CBS 9975
Caspofungin (1)	-	-	-	0.025
30	$C(O)OCH_3$	CH=CH	Ter	>100
32	$C(O)NHCH_2CH_2NH_2$	CH=CH	Ter	>100
33	CH_2OH	CH=CH	Ter	>100
34	$C(O)NHNH_2$	CH=CH	Ter	>100

2.2.3 Oxidation of the double bond

The double bond resulting from the RCM approach presented an additional site for derivatization. Therefore we decided to study modifications at this site. Beside the hydrogenated mimics, like **27**, we were interested in an oxidized mimic. These oxidized mimics would have more similarities with the highly oxidized echinocandins. Hydroxylation of the double bond of the RCM mimic **29** is shown in Scheme 7.

Hydroxylation was carried out by treatment with NMO and OsO_4. Partial saponification was observed and therefore the methyl ester was completely saponified followed by acidolysis affording the oxidized mimic **36** as a mixture of diastereoisomers. The minimum inhibitory concentration (MIC) of these analogues was evaluated and turned out to be >100 μg/mL. Due to the absence of activity, no attempts were undertaken to separate diastereoisomers.

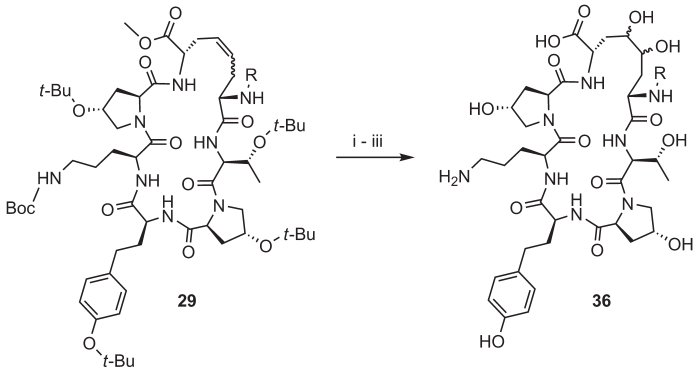

Scheme 7. Reagents and conditions: (i) OsO_4, NMO, *t*-BuOH/H_2O; (ii) LiOH/THF; (iii) TFA/TIS/H_2O (95/2.5/2.5, v/v/v).

2.2.4 The ring size is crucial

The ring size of the RCM compounds (23-membered rings) is slightly larger than that of the natural echinocandins (21-membered rings). However, the resulting compounds were completely devoid of biological activity. This somewhat unexpected finding enticed us to investigate the influence of ring size on activity, and a 22-membered ring containing analogue **39** of echinocandin was synthesized by head-to-tail cyclization as is outlined in Scheme 8.

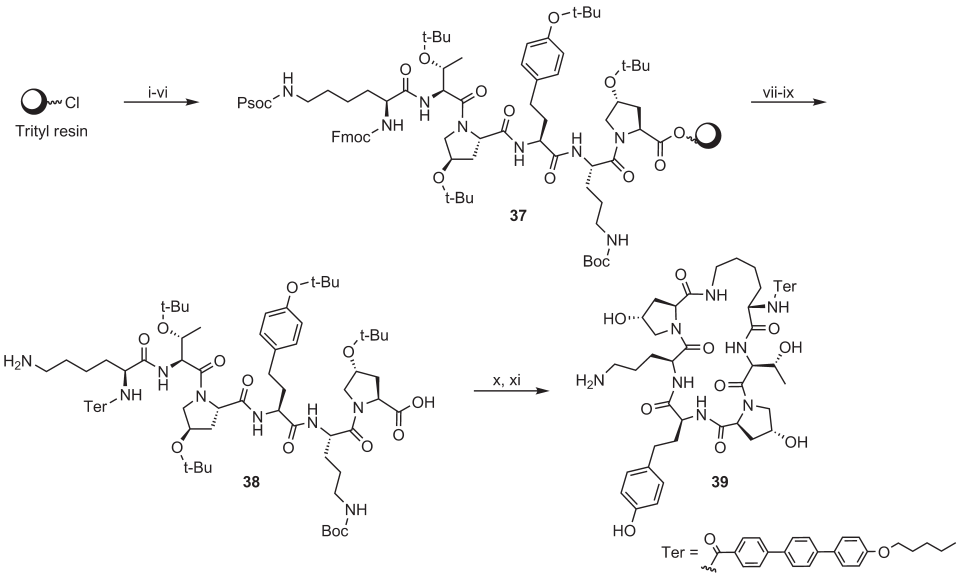

Scheme 8. Reagents and conditions: (i) Fmoc-Hyp(*t*Bu)-OH, DIPEA, DCM; (ii-vi) (1) 20% piperidine in NMP; (2) Fmoc-Xxx-OH, BOP, DiPEA, NMP; (vii) (1) 20% piperidine in NMP; (2) ter tail, HATU, DiPEA, NMP; (viii) TBAF.H_2O, DCM; (ix) HFIP/DCM (1/1; v/v); (x) BOP, DiPEA, DMF; (xi) TFA/TIS/H_2O (95/2.5/2.5, v/v/v).

Linear precursor **37** was prepared by SPPS on the trityl resin. Removal of the Fmoc group on lysine, coupling of the Ter chain, removal of the Psoc-protecting group[33] and mild acid cleavage from the resin gave protected linear peptide **38**. Solution-phase cyclization followed by protecting group removal afforded the macrocyclic peptide **39** in an overall yield of 21%. The minimum inhibitory concentration (MIC) of this echinocandin homolog was evaluated and turned out to be >100 μg/mL.

Even expansion of the peptide macrocycle by just one carbon atom completely abolished antifungal activity which we had not expected in view of the limited added flexibility to the peptide macrocycle.
To assure that the low activities of our compounds are not strain dependent and hence the conclusions regarding the importance of the ring size are more general, we have tested a representative selection of the compounds against a panel of common *Candida* species.[34] This panel included *C. dubliensis*, *C. glabrata*, *C. tropicalis*, *C. parapsilosis*, *C. krusei* and two strains of *C. albicans*. The results were in the same order of magnitude as shown in Table 6.

Table 6. Screen against a panel of candida strains. (MIC value in μg/mL).

	Candida albicans CBS9975	*Candida albicans* CBS8758	*Candida dubliniensis* CBS7987	*Candida glabrata* CBS138	*Candida krusei* CBS573	*Candida parapsilosis* CBS604	*Candida tropicalis* CBS94
Caspofungin	0.025	0.039	0.013	0.023	0.004	0.281	0.006
6b	>100	>100	>100	>100	>100	>100	>100
13b	0.14	0.156	0.063	0.188	0.078	>4	0.063
26	>100	>100	>100	>100	>100	>100	>100
28	>100	>100	>100	>100	>100	>100	>100
32	>100	>100	>100	>100	>100	>100	>100
33	>100	>100	>100	>100	>100	>100	>100
36	>100	>100	>100	>100	>100	>100	>100
39	>100	>100	>100	>100	>100	>100	>100

2.3 Conclusions

A series of new echinocandin analogues were synthesized by RCM and disulfide bond formation to explore the influence of the macrocyclic peptide ring structure of the echinocandins on antifungal activity. Evaluation of the antifungal properties of the resulting compounds showed no measurable activity for mimics **6**, **7** and **10**. It is also known that the fatty acid chain plays a crucial role in relation to antifungal potency, therefore analogues **26**-**28**, bearing a terphenyl lipophilic chain, were synthesized. These analogues showed a dose-dependent effect on antifungal growth at concentrations starting at 5 μg/mL. The C-terminus and double bond represent other sites for modification. The corresponding analogues (**32-34**) with a modified C-terminus and analog **36** with an oxidized double bond were prepared and had the same dose-dependent effect on fungal growth. Remarkably, a slight enlargement of the macrocyclic peptide ring from a 21- (**13b**) to a 22-membered

system (**39**) completely abolishes antifungal activity. Therefore, the preparation of other larger derivatives by either RCM or disulfide formation seems an unattractive avenue. Attempts towards the preparation of smaller RCM mimics will be described in chapter 3.

The mimics described in this chapter comprise a novel set of echinocandin-based analogues. The possible influence of ring size on the conformation(s) of the macrocyclic lipopeptides and impact on antifungal activity will be described in chapter 6.

2.4 Experimental section

2.4.1 Reagents, materials and analysis methods

Unless stated otherwise, all chemicals were obtained from commercial sources and used as supplied, with the exception of DMF, NMP and DCM, which were dried on molecular sieves (4Å) prior to use. HPLC grade solvents were purchased from Biosolve B.V. (Valkenswaard, The Netherlands). Fmoc protected amino acids were purchased from GL Biochem Ltd. (Shanghai, China). The *tert*-butyl side chain protected homotyrosine (H-hTyr(*t*Bu)-OH) was purchased from Advanced Chemtech (Louisville, United States) and subsequently protected with the Fmoc group. The 2-chlorotritylchloride PS resin was purchased from Hecheng Chemicals (Shanghai, China). Tentagel S PHB and Rink resin were purchased from RAPP Polymere (Tübingen, Germany). All other reagents were purchased from Merck (Darmstadt, Germany), Sigma-Aldrich (Munich, Germany) and Acros (Geel, Belgium) and were used without further purification.

All Reactions were carried out at room temperature unless stated otherwise. Solid phase synthesis was performed in plastic syringes with a polyethylene frit. Microwave reactions were carried out on a Biotage Initiator system. Reactions in solution were monitored by TLC on Merck pre-coated Silica 60 plates. Spots were visualized by UV light, ninhydrin or K_2CO_3/$KMnO_4$. Solid phase reactions were monitored with the chloranil test[35] in case of secondary amines or with the Kaiser test[36] in case of primary amines. Column chromatography was performed using Silicycle UltraPure silicagel (40-63 μm).

^{1}H NMR spectra were recorded on a Varian G-300 (300 MHz) spectrometer and chemical shifts are given in ppm relative to TMS (0.00 ppm). ^{13}C NMR spectra were recorded using the attached proton test (APT) sequence on a Varian G-300 (75.5 MHz) spectrometer and chemical shifts are given in ppm relative to $CDCl_3$ (77.0 ppm). For the peptides ^{1}H NMR, TOCSY, ^{1}H-^{13}C HSQC and ROESY spectra were recorded using a Varian INOVA-500 spectrometer (500 MHz); chemical shifts (δ) were obtained in ppm relative to TMS. For measurements in DMSO, the residual solvent peak was used as a reference.

Analytical HPLC was performed on a Shimadzu automated HPLC system equipped with an evaporative light scattering detector (PL-ELS 1000) and a UV/Vis detector operated at 220/254 nm. Preparative HPLC runs were performed on an Applied Biosystems 400 solvent delivery system with an Applied Biosystems 757 UV/VIS absorbance detector. Two buffer systems were used for HPLC. The first will be referred to as TFA MeCN/H_2O buffer and consists out of buffer A: 0.1 % TFA in MeCN/H_2O, 5/95, v/v and buffer B: 0.1% TFA in MeCN/

H_2O, 95/5, v/v. For analytical HPLC a flow rate of 1.0 mL/min with a linear gradient of buffer B (100% in 20 min) from 100% buffer A was used. Preparative runs used a flow rate of 12 ml/min with a linear gradient of buffer B (100% in 40 min) from 100% buffer A. The second will be referred to as *i*-PrOH/MeOH/H_2O buffer and consists out of buffer A: 0.1 % TFA in *i*-PrOH/MeOH/H_2O, 5/5/90, v/v/v and buffer B: 0.1% TFA in *i*-PrOH/MeOH/H_2O, 45/50/5, v/v/v. For analytical HPLC a flow rate of 0.5 mL/min with a linear gradient of buffer B (100% in 40 min) from 100% buffer A was used. Preparative runs used a flow rate of 6 ml/min with a linear gradient of buffer B (100% in 80 min) from 100% buffer A.

ESI-MS spectra were obtained in the positive ion mode on a Shimadzu QP8000 single quadrupole mass spectrometer. DART mass spectra were obtained in the positive mode on a JEOL AccuTOF JMS-T100LP with DART interface. Peptides were characterized by high resolution mass spectrometry (HRMS) analyses performed on a MALDI TOF/TOF (Applied Biosystems).

2.4.2 Chemistry

General Procedures

Solid phase peptide synthesis: Peptides were synthesized manually. Each synthetic cycle consisted of the following steps:

Fmoc removal: The resin was treated with a 20% solution of piperidine in NMP (3×, each 10 min). The solution was removed by filtration and the resin was washed with NMP (3×, each 3 min) and DCM (3×, each 3 min).

Coupling step: A mixture of Fmoc-Xxx-OH (3 equiv.), BOP (3 equiv.) and DiPEA (6 equiv.) in NMP (10 mL/mmol)) was added to the resin and N_2 was bubbled through the mixture for 2h. The solution was removed by filtration and the resin washed with NMP (3×, each 3 min) and DCM (3×, each 3 min). Completion of the coupling was checked with Kaiser or chloranil test.

Capping of the remaining free amines: Capping solution [Ac_2O (50 mmol, 4.7 mL), HOBt (1.9 mmol, 220 mg), DiPEA (12.5 mmol, 2.2 mL) in 100 mL NMP] was added to the resin and N_2 was bubbled through the mixture for 20 min The solution was removed by filtration and the resin was washed with NMP (3×, each 3 min) and DCM (3×, each 3 min).

TFA cleavage: The resin was shaken in a mixture of TFA/TIS/H_2O (95/2.5/2.5, v/v/v) for 2h. The peptide was precipitated in MTBE/hexane (1/1), the supernatant was removed and the crude peptide was washed twice with MTBE/hexane (1/1) and lyophilized from *tert*-BuOH/H_2O (1/1, v/v). The isolated peptide was analyzed by HPLC and characterized by MS.

Microwave-assisted RCM: A microwave vessel containing a magnetic stirrer bead was loaded under argon with resin peptide, catalyst and solvent. The vessel was capped and irradiated at 100 °C. At the end of the reaction period the resin-bound peptide was washed with DMF (3× 3 mL, each 3 min) DCM (3× 3 mL, each 3 min) and MeOH (3× 3 mL, each 3 min).

Hydrogenation: To a solution of the olefenic peptide in *t*BuOH/H_2O (1 mL, 3/1, v/v) 10% Pd/C was added. The reaction mixture was stirred under H_2 at atmospheric pressure overnight. The mixture was then filtered through a path of celite and washed extensively with *t*BuOH.

The mixture was concentrated and lyophilized from *tert*-BuOH/H_2O (1/1, v/v).

Head-to-tail cyclization: The peptide was dissolved in dry DMF (2 mL/μmol) and BOP (4 equiv.) and DiPEA (8 equiv.) were added. The mixture was stirred overnight followed by evaporation *in vacuo*. The product was redissolved in EtOAc and washed with 1M $KHSO_4$ (2×), $NaHCO_3$ (2×) and H_2O (2×). The organic layer was dried over Na_2SO_4, filtered and concentrated *in vacuo*.

Cleavage IvDde group: The peptide was dissolved in dry DMF (70 mL/mmol) and N_2H_4. H_2O/DMF (5 v/v%) was added. The mixture was stirred for 2 h. Followed by the addition of brine and extraction with EtOAc (2×). The organic layer was washed with H_2O, dried over Na_2SO_4, filtered and concentrated *in vacuo*. The crude peptide was purified by column chromatography (DCM/MeOH 20/1, v/v/v).

***Cyclo*[-(Palm)-Alg-Thr-Hyp-hTyr-Orn-Hyp-Alg]-NH_2 (6a)**

The linear peptide Fmoc-Alg-Thr-Hyp-hTyr-Orn-Hyp-Alg-NH_2 (**8a**) was synthesized on Fmoc-Rink-Tentagel resin (1 g; 0.25 mmol) according to the general procedure for solid phase peptide synthesis. ESI-MS calcd for TFA deprotected **8a** $C_{54}H_{69}N_9O_{13}$: 1051.50, found: m/z 1052.20 $[M+H]^+$. The resulting resin-bound peptide **8a** was subjected to the general microwave-assisted RCM procedure under the following conditions: Resin-bound peptide (421 mg; 105.2 μmol), DCM (3.8 mL), LiCl/DMA (degassed; 0.4M; 0.38 mL), Grubbs II (15 mol%; 13.4 mg; 15.8 μmol), 100 °C for 75 min. ESI-MS calcd for TFA deprotected **9a** $C_{52}H_{65}N_9O_{13}$: 1023.47, found: m/z 1024.15 $[M+H]^+$. The Fmoc group was cleaved and palmitic acid (108 mg; 421 μmol) was coupled overnight in the presence of HATU (160 mg; 421 μmol) and DIPEA (147 μL; 842 μmol) in NMP (3 mL). The resin was washed with NMP (3× 3 mL, each 3 min) and DCM (3× 3 mL, each 3 min) and subjected to the TFA-mediated cleavage procedure followed by lyophilization. The crude peptide was purified by column chromatography (*i*-PrOH/NH_4OH/H_2O, 15/1/1, v/v/v). After lyophilization peptide **6a** (12 mg; 11%) was obtained as a white solid. Purity was confirmed by analytical HPLC (Adsorbosphere C8, 40 min run, TFA MeCN/H_2O buffers) and was found to be higher than 95% for a mixture of *E/Z* stereoisomers (R_t = 22.6 min and 22.8 min). ESI-MS calcd for $C_{53}H_{85}N_9O_{12}$: 1039.63, found: m/z 1040.61 $[M+H]^+$; HRMS calcd for $C_{53}H_{85}N_9O_{12}$ $[M+H]^+$ 1040.6396, found 1040.6403; ^{1}H-NMR (DMSO, 500 MHz): δ Alg-1: 8.05 (NH), 4.16 (αCH), 2.36/2.16 (βCH), 5.74 (γCH); Thr-2: 7.354 (NH), 4.61 (αCH), 4.32 (βCH), 1.09 (γCH); Hyp-3: 4.43 (αCH), 2.13/1.79 (βCH), 4.30 (γCH), 3.64/3.56 (δCH); hTyr-4: 7.75 (NH), 6.95/6.65 (Ar-H); 4.00 (αCH), 2.04/1.90 (βCH), 2.46/2.36 (γCH); Orn-5: 7.23 (NH), 4.49 (αCH), 1.65/1.53 (βCH), 1.47 (γCH), 2.75 (δCH); Hyp-6: 4.46 (αCH), 2.02/1.87 (βCH), 4.37 (γCH), 3.78/3.66 (δCH); Alg-7: 7.93 (NH), 4.093 (αCH), 2.29 (βCH), 5.74 (γCH); Palm: 2.11 (CH_2), 1.45 (CH_2), 1.26 (CH_2), 1.23 (CH_2), 0.86 (CH_3) ppm. ^{13}C-NMR (DMSO, 125 MHz): δ Alg-1: 52.2 (αCH), 34.5 (βCH), 126.2 (γCH); Thr-2: 56.6 (αCH), 66.0 (βCH), 19.4 (γCH); Hyp-3: 58.3 (αCH), 37.3 (βCH), 68.7 (γCH), 55.7 (δCH); hTyr-4: 52.4 (αCH), 32.6 (βCH), 31.1 (γCH); 115.5 (Ar-H), 129.8 (Ar-H); Orn-5: 52.8 (αCH), 28.0 (βCH), 24.0 (γCH), 39.0 (δCH); Hyp-6: 59.3 (αCH), 37.9 (βCH), 69.2 (γCH), 55.7 (δCH); Alg-7: 52.9 (αCH), 33.8 (βCH), 126.2 (γCH); Palm: 35.2 (CH_2), 28.9 (CH_2), 25.4 (CH_2), 22.2 (CH_2), 14.0 (CH_3).

***Cyclo*[-(Palm)-Alg-Thr-Hyp-hTyr-Orn-Hyp-Alg]-OH (6b)**

Peptide **6b** was obtained analogous to peptide **6a,** on Wang-Tentagel resin (1 g; 0.26 mmol),

except for the loading step. For that Tentagel S PHB (1.0 g, 0.26 mmol) and Fmoc-Alg-OH (364 mg, 1.04 mmol) were dried *in vacuo* overnight over P_2O_5. DMF (5 mL) and pyridine (114 μL, 1.42 mmol) were added and the resin was shaken for 10 min untill total dissolution. DCBC (149 μL, 1.04 mmol) was added and the resin was shaken over the weekend. The resin was drained and washed with DMF (5× 3 mL, each 2min) and DCM (5× 3 mL, each 2 min). Subsequently, unreacted hydroxyl functions of the resin were acetylated by treatment with Ac_2O/NMI/DiPEA/DMF (5 mL; 2/1/1/6; v/v/v) for 30 min. The resin was drained and washed with DMF (3× 3 mL, each 2 min) and DCM (3× 3 mL, each 2 min). Hyp was coupled as the dipeptide Fmoc-Orn(Boc)-Hyp(*t*Bu)-OH. ESI-MS calcd for TFA deprotected **8b** $C_{54}H_{68}N_8O_{14}$: 1052.49, found: m/z 1053.10 $[M+H]^+$. ESI-MS calcd for TFA deprotected **9b** $C_{52}H_{64}N_8O_{14}$: 1024.45, found: m/z 1025.00 $[M+H]^+$. The crude peptide was purified by column chromatography (*i*-PrOH/NH_4OH/H_2O, 10/1/1, v/v/v). After lyophilization peptide **6b** (12.2 mg; 11%) was obtained as a white solid. Purity was confirmed by analytical HPLC (Adsorbosphere C8, 40 min run, TFA MeCN/H_2O buffers) and was found to be higher than 95% for a mixture of *E/Z* stereoisomers (R_t = 22.60 min and 22.81 min). ESI-MS calcd for $C_{53}H_{84}N_8O_{13}$: 1040.62, found: m/z 1041.15 $[M+H]^+$; HRMS calcd for $C_{53}H_{84}N_8O_{13}$ $[M+H]^+$ 1041.6236, found 1041.6243; ^{1}H-NMR (CD_3OH, 500 MHz): δ Alg-1: 7.87 (NH), 4.17 (αCH), 2.60/2.13 (βCH), 5.48 (γCH); Thr-2: 7.95 (NH), 4.70 (αCH), 4.32 (βCH), 1.14 (γCH); Hyp-3: 4.37 (αCH), 2.18/1.73 (βCH), 4.40 (γCH), 3.68/3.61 (δCH); hTyr-4: 7.64 (NH), 6.91/6.56 (Ar-H); 4.02 (αCH), 2.14/1.93 (βCH), 2.48 (γCH); Orn-5: 7.64 (NH), 4.62 (αCH), 2.00/1.52 (βCH), 1.58 (γCH), 2.86 (δCH); Hyp-6: 4.51 (αCH), 2.20/1.99 (βCH), 4.34 (γCH), 3.68/3.42 (δCH); Alg-7: 8.23 (NH), 2.47/2.18 (βCH), 5.48 (γCH) ppm. ^{13}C-NMR (CD_3OH, 125 MHz): δ Alg-1: 54.1 (αCH), 35.4 (βCH), 128.9 (γCH); Thr-2: 56.8 (αCH), 67.8 (βCH), 18.7 (γCH); Hyp-3: 61.1 (αCH), 37.2 (βCH), 70.2 (γCH), 55.7 (δCH); hTyr-4: 54.3 (αCH), 32.3 (βCH), 31.7 (γCH); 115.5 (Ar-H), 129.8 (Ar-H); Orn-5: 50.8 (αCH), 28.5 (βCH), 23.7 (γCH), 39.2 (δCH); Hyp-6: 59.3 (αCH), 37.9 (βCH), 69.8 (γCH), 55.5 (δCH); Alg-7: 54.7 (αCH), 34.3 (βCH), 128.9 (γCH).

***Cyclo*[-(Palm)-Cys-Thr-Hyp-hTyr-Orn-Hyp-Cys]-NH_2 (7)**

The linear peptide Fmoc-Cys-Thr-Hyp-hTyr-Orn-Hyp-Cys-NH_2 was synthesized on Fmoc-Rink-Tentagel resin (211 mg; 50.6 μmol) according to the general procedure for solid phase peptide synthesis. The Fmoc group was cleaved and palmitic acid (52 mg; 202.6 μmol) was coupled overnight in the presence of HATU (77 mg; 202.6 μmol) and DiPEA (71 μL; 405.2 μmol) in NMP (2 mL). The resin was washed with NMP (3× 2 mL, each 3 min) and DCM (3× 2 mL, each 3 min) and subjected to the TFA cleavage procedure and lyophilized. Mass spectral analysis (ESI-MS calcd for **11** $C_{51}H_{85}N_9O_{12}S_2$: 1079.58, found: m/z 1079.90 $[M+H]^+$) confirmed the formation of the linear peptide **11** and the peptide was cyclized by oxidation with DMSO. Peptide **11** (43.2 mg; 40 μmol) was dissolved in aq. 2.5% AcOH (50 mL). The pH was adjusted to 6 with aq. NH_4OH (25%). To this solution DMSO (10 mL) was added. After stirring at RT overnight, the solution was partially concentrated *in vacuo* and remaining DMSO was removed by a speedvac apparatus (42 °C, overnight). After preparative HPLC and lyophilization, peptide **7** (12.2 mg; 22%) was obtained as a white solid. Purity was confirmed by analytical HPLC (Alltima C8, 65 min run, *i*-PrOH/MeOH/H_2O buffers) and was found to be higher than 99% (R_t = 40.71 min). ESI-MS calcd for $C_{51}H_{83}N_9O_{12}S_2$: 1077.56, found: m/z 1078.35 $[M+H]^+$; HRMS calcd for $C_{51}H_{83}N_9O_{12}S_2$ $[M+H]^+$ 1078.5681, found 1078.5721; ^{1}H-NMR (DMSO, 500 MHz): δ Cys-1: 8.18 (NH), 4.76 (αCH), 3.29/2.85 (βCH); Thr-2: 7.63 (NH), 4.70 (αCH), 4.29 (βCH), 1.05 (γCH); Hyp-3: 4.24 (αCH), 2.12/1.80 (βCH), 4.37 (γCH), 3.80/3.59

(δCH); hTyr-4: 7.34 (NH), 6.96/6.66 (Ar-H); 3.90 (αCH), 1.96/1.89 (βCH), 2.52/2.47 (γCH); Orn-5: 7.25 (NH), 7.24 (εNH), 4.45 (αCH), 1.80/1.61 (βCH), 1.51 (γCH), 2.80 (δCH); Hyp-6: 4.55 (αCH), 1.94 (βCH), 4.28 (γCH), 3.56/3.18 (δCH); Cys-7: 8.25 (NH), 4.30 (αCH), 2.85 (βCH); Palm: 2.11 (CH_2), 1.47 (CH_2), 1.26 (CH_2), 1.23 (CH_2), 0.86 (CH_3) ppm. ^{13}C-NMR (DMSO, 125 MHz): δ Cys-1: 51.1 (αCH), 43.4 (βCH); Thr-2: 56.1 (αCH), 66.7 (βCH), 19.3 (γCH); Hyp-3: 61.0 (αCH), 37.1 (βCH), 69.3 (γCH), 55.9 (δCH); hTyr-4: 53.5 (αCH), 32.4 (βCH), 31.2 (γCH); 115.5 (Ar-H), 129.9 (Ar-H); Orn-5: 49.6 (αCH), 27.6 (βCH), 23.5 (γCH), 38.5 (δCH); Hyp-6: 59.0 (αCH), 37.8 (βCH), 68.5 (γCH), 53.5 (δCH); Cys-7: 51.5 (αCH), 43.4 (βCH); Palm: 35.3 (CH_2), 29.0 (CH_2), 25.4 (CH_2), 22.1 (CH_2), 14.0 (CH_3).

***Cyclo*[-(Palm)-Alg-Thr-Hyp-hTyr-Orn-Hyp-Alg]-NH_2 (10a)**

Hydrogenation of the cyclic unsaturated peptide **6a** (3.2 mg; 3.07 μmol) was carried out using the hydrogenation procedure in the presence of 3 mg 10% Pd/C. The saturated peptide **10a** (3.1 mg; quant) was obtained as a white solid. Purity was confirmed by analytical HPLC (Adsorbosphere C8, 40 min run, TFA MeCN/H_2O buffers) and was found to be higher than 99% (R_t = 22.62 min). ESI-MS calcd for $C_{53}H_{87}N_9O_{12}$: 1041.65, found: m/z 1042.59 $[M+H]^+$; HRMS calcd for $C_{53}H_{87}N_9O_{12}$ $[M+H]^+$ 1042.6552, found 1042.6530.

***Cyclo*[-(Palm)-Alg-Thr-Hyp-hTyr-Orn-Hyp-Alg]-OH (10b)**

Hydrogenation of the cyclic unsaturated peptide **6b** (4.7mg; 4.52 μmol) was carried out using the hydrogenation procedure in the presence of 5 mg 10% Pd/C. The saturated peptide **10b** (4.6 mg; quant.) was obtained as a white solid. Purity was confirmed by analytical HPLC (Adsorbosphere C8, 40 min run, TFA MeCN/H_2O buffers) and was found to be higher than 95% (R_t = 22.57 min). ESI-MS calcd for $C_{53}H_{86}N_8O_{13}$: 1042.63, found: m/z 1043.59 $[M+H]^+$; HRMS calcd for $C_{53}H_{86}N_8O_{13}$ $[M+H]^+$ 1043.6393, found 1043.6416.

***Cyclo*[-(Palm)-Orn-Thr-Hyp-hTyr-Thr-Hyp] (12a)**

A polystyrene resin functionalized with a 2-chloro Trityl linker (600 mg; initial loading: 1.1 mmol/g) was loaded with Fmoc-Hyp(*t*Bu)-OH (810.8 mg; 1.98 mmol) in DCM (5 mL) in the presence of DiPEA (690 μL; 3.96 mmol) for 16h. Subsequently, unreacted tritylchloride moieties were capped with methanol (DCM/MeOH/DiPEA; 3× 5 mL, each 2 min; 17/2/1; v/v/v). After drying *in vacuo* overnight, the amount of Fmoc-Hyp(*t*Bu)-OH coupled to the resin was determined by a Fmoc determination according to Meienhofer[37] and was found to be 0.536 mmol/g. The peptide sequence was synthesized according to the general procedure for solid phase peptide synthesis. The Fmoc group was cleaved and the linear peptide was released from the resin by treatment of the resin with HFIP/DCM (6 mL, 1/1, v/v) for 2h. This treatment was repeated once for 1h. The mixture was concentrated to obtain the linear peptide. A portion of the linear peptide (187 mg; 0.15 mmol) was subjected to head-to-tail cyclization and the IvDde group was cleaved following the general procedures. The free amine of the linear peptide (54.2 mg; 54.2 μmol) was coupled with palmitic acid by dissolving the peptide in dry DCM (4 mL) and adding palmitic acid (15.3 mg; 59.6 μmol), DCC (12.3 mg; 59.6 μmol) and HOBt (8.0 mg; 59.6 μmol). The mixture was stirred overnight and the DCU filtered off over celite. The crude peptide was purified by column chromatography (DCM/MeOH 30/1, v/v/v), Followed by treatment with a mixture of TFA/TIS/H_2O (3 mL, 95/2.5/2.5, v/v/v) for 2h. The mixture was concentrated *in vacuo*, redissolved in a small amount of TFA and precipitated in MTBE/hexane (1/1). The supernatant was removed and the crude

peptide washed twice with MTBE/hexane (1/1). After lyophilization, peptide **12a** (15.6 mg; 19%) was obtained as a white solid. Purity was confirmed by analytical HPLC (Alltima C8, 65 min run, *i*-PrOH/MeOH/H_2O buffers) and was found to be higher than 99% (R_t = 42.18 min). ESI-MS calcd for $C_{49}H_{79}N_7O_{12}$: 957.58, found: m/z 958.95 $[M+H]^+$; HRMS calcd for $C_{49}H_{79}N_7O_{12}$ $[M+H]^+$ 958.5865, found 958.5819; ^{1}H-NMR (DMSO, 500 MHz): δ Orn-1: 7.80 (NH), 4.30 (αCH), 1.69/1.38 (βCH), 1.39 (γCH), 2.98 (δCH); Thr-2: 7.88 (NH), 4.23 (αCH), 4.01 (βCH), 1.21 (γCH); Hyp-3: 4.42 (αCH), 2.11/1.82 (βCH), 4.40 (γCH), 3.76 (δCH); hTyr-4: 8.46 (NH), 6.93/6.65 (Ar-H), 3.62 (αCH), 2.19/2.11 (βCH), 2.43/2.34 (γCH); Thr-5: 7.45 (NH), 4.12 (βCH), 1.02 (γCH); Hyp-6: 2.11/1.82 (βCH), 4.27 (γCH), 3.61 (δCH); Palm: 0.85 (CH_3), 1.26 (CH_2), 1.24 (CH_2), 1.44 (CH_2), 2.07 (CH_2) ppm. ^{13}C-NMR (DMSO, 125 MHz): δ Orn-1: 50.9 (αCH), 28.9 (βCH), 24.0 (γCH), 37.9 (δCH); Thr-2: 58.5 (αCH), 66.5 (βCH), 19.1 (γCH); Hyp-3: 60.0 (αCH), 37.7 (βCH), 69.1 (γCH), 56.4 (δCH); hTyr-4: 53.7 (αCH), 31.0 (βCH), 31.2 (γCH), 129.8, 115.5 (Ar-H); Thr-5: 56.5 (αCH), 67.3 (βCH), 18.9 (γCH); Hyp-6: 59.3 (αCH), 37.7 (βCH), 69.0 (γCH), 56.2 (δCH); Palm: 13.9 (CH_3), 22.0 (CH_2), 25.3 (CH_2), 29.0 (CH_2), 31.4 (CH_2), 35.1 (CH_2).

***Cyclo*[-(Palm)-Orn-Thr-Hyp-hTyr-Orn-Hyp] (12b)**

Peptide **13a** was obtained analogously to peptide **12a** except for the amino acid sequence. The second amino acid coupled was Fmoc-Orn(Boc)-OH instead of Fmoc-Thr(*t*Bu)-OH. The loading of the resin determined after first coupling was 0.543 mmol/g. After lyophilization, peptide **12b** (18.5 mg; 22%) was obtained as a white solid. Purity was confirmed by analytical HPLC (Alltima C8, 40 min run, TFA MeCN/H_2O buffers) and was found to be higher than 99% (R_t = 23.18 min). ESI-MS calcd for $C_{50}H_{82}N_8O_{11}$: 970.61, found: m/z 971.20 $[M+H]^+$; HRMS calcd for $C_{50}H_{82}N_8O_{11}$ $[M+H]^+$ 971.6181, found 971.6187; ^{1}H-NMR (DMSO, 500 MHz): δ Orn-1: 7.92 (NH), 7.67 (εNH), 4.14 (αCH), 1.64/1.56 (βCH), 1.54 (γCH), 2.79 (δCH); Thr-2: 8.27 (NH), 4.74 (αCH), 4.36 (βCH), 1.09 (γCH); Hyp-3: 4.39 (αCH); hTyr-4: 7.59 (NH), 6.95/6.66 (Ar-H), 4.03 (αCH), 1.86/1.75 (βCH), 2.43/2.37 (γCH); Orn-5: 7.70 (NH), 7.59 (εNH), 4.52 (αCH), 1.89/1.62 (βCH), 1.56 (γCH), 3.40/2.66 (δCH); Hyp-6: 4.40 (γCH), 3.76/3.51 (δCH); Palm: 2.02 (CH_2), 1.46 (CH_2), 1.32 (CH_2), 1.26 (CH_2), 0.86 (CH_3) ppm. ^{13}C-NMR (DMSO, 125 MHz): δ Orn-1: 50.6 (αCH), 28.3 (βCH), 23.5 (γCH), 38.3 (δCH); Thr-2: 56.1 (αCH), 66.2 (βCH), 20.4 (γCH); Hyp-3: 60.8 (αCH); hTyr-4: 53.2 (αCH), 28.1 (βCH), 30.9 (γCH); 115.2 (Ar-H), 129.5 (Ar-H); Orn-5: 50.6 (αCH), 28.4 (βCH), 22.2 (γCH), 35.2 (δCH); Hyp-6: 69.3 (γCH), 55.4 (δCH); Palm: 35.2 (CH_2), 27.8 (CH_2), 25.9 (CH_2), 25.0 (CH_2), 13.6 (CH_3).

***Cyclo*[-(Ter)-Orn-Thr-Hyp-hTyr-Thr-Hyp] (13a)**

Peptide **13a** was obtained analogously to peptide **12a** until the coupling of the tail. Loading of the resin determined after first coupling: 0.536 mmol/g. The free amine of the linear peptide (34.7 mg; 34.7 μmol) was coupled with the Ter chain by dissolving the peptide in DCM (4 mL) and adding terphenyl acid **14** (13.8 mg; 38.2 μmol), DCC (7.9 mg; 38.2 μmol) and HOBt (5.2 mg; 38.2 μmol). The mixture was stirred overnight and then the DCU was filtered off over celite. The crude peptide was purified by column chromatography (DCM/MeOH 30/1, v/v/v), Followed by treatment with a mixture of TFA/TIS/H_2O (95/2.5/2.5; 3 mL) for 1h. The mixture was concentrated *in vacuo*, redissolved in a small amount of TFA and precipitated in MTBE/hexane (1/1). The supernatant was removed and the crude peptide washed twice with MTBE/hexane (1/1). After lyophilization, peptide **13a** (13.1 mg; 23%) was obtained as a white solid. Purity was confirmed by analytical HPLC (Alltima C8, 65 min run, *i*-PrOH/MeOH/H_2O buffers) and was found to be higher than 99% (R_t = 39.72 min). ESI-

MS calcd for $C_{57}H_{71}N_7O_{13}$: 1061.51, found: m/z 1062.65 $[M+H]^+$; HRMS calcd for $C_{57}H_{71}N_7O_{13}$ $[M+H]^+$ 1062.5188, found 1062.5227; ^{1}H-NMR (DMSO, 500 MHz): δ Orn-1: 8.38 (NH), 7.46 (εNH), 4.53 (αCH), 1.91/1.54 (βCH), 1.53 (γCH), 3.09/3.02 (δCH); Thr-2: 7.95 (NH), 4.32 (αCH), 4.08 (βCH), 1.25 (γCH); Hyp-3: 4.43 (αCH), 2.14/1.84 (βCH), 4.40 (γCH), 3.77 (δCH); hTyr-4: 8.40 (NH), 6.95/6.66 (Ar-H), 3.68 (αCH), 2.18/2.13 (βCH), 2.44/2.36 (γCH); Thr-5: 7.48 (NH), 4.80 (αCH), 4.16 (βCH), 1.06 (γCH); Hyp-6: 4.38 (αCH), 2.11/1.84 (βCH), 4.29 (γCH), 3.64 (δCH); Ter: 0.91 (CH_3), 1.37 (CH_2), 1.42 (CH_2), 1.74 (CH_2), 4.01 (OCH_2) 7.66/7.04 (Ar-H Ph-3), 7.80/7.74 (Ar-H Ph-2), 7.99/7.81 (Ar-H Ph-1) ppm. ^{13}C-NMR (DMSO, 125 MHz): δ Orn-1: 52.1 (αCH), 28.2 (βCH), 24.1 (γCH), 38.0 (δCH); Thr-2: 58.4 (αCH), 66.6 (βCH), 19.2 (γCH); Hyp-3: 60.1 (αCH), 37.6 (βCH), 69.2 (γCH), 56.4 (δCH); hTyr-4: 53.6 (αCH), 31.2 (βCH), 31.2 (γCH), 129.8/ 115.5 (Ar-H); Thr-5: 56.5 (αCH), 67.3 (βCH), 19.0 (γCH); Hyp-6: 59.3 (αCH), 37.6 (βCH), 69.1 (γCH), 56.2 (δCH); Ter: 13.8 (CH_3), 21.9 (CH_2), 27.7 (CH_2), 28.4 (CH_2), 67.7 (OCH_2), 128.2/115.4 (Ar-C Ph-3), 127.8/127.2 (Ar-C Ph-2), 128.8/126.6 (Ar-C Ph-1).

***Cyclo*[-(Ter)-Orn-Thr-Hyp-hTyr-Orn-Hyp] (13b)**

Peptide **13b** was obtained analogously to peptide **13a** except for the amino acid sequence. The second amino acid coupled was Fmoc-Orn(Boc)-OH instead of Fmoc-Thr(*t*Bu)-OH. Loading of the resin determined after first coupling: 0.543 mmol/g. After lyophilization, peptide **13b** (9.4 mg; 17%) was obtained as a white solid. Purity was confirmed by analytical HPLC (Alltima C8, 65 min run, *i*-PrOH/MeOH/H_2O buffers) and was found to be 90% (R_t = 38.95 min). ESI-MS calcd for $C_{58}H_{74}N_8O_{12}$: 1074.54, found: m/z 1075.69 $[M+H]^+$; HRMS calcd for $C_{58}H_{74}N_8O_{12}$ $[M+H]^+$ 1075.5504, found 1075.5529; ^{1}H-NMR (DMSO, 500 MHz): δ Orn-1: 8.62 (NH), 8.01 (εNH), 4.60 (αCH), 1.83/1.65 (βCH), 1.60 (γCH), 3.47/2.72 (δCH); Thr-2: 8.34 (NH), 4.78 (αCH), 4.39 (βCH), 1.13 (γCH); Hyp-3: 4.34 (αCH), 2.00/1.86 (βCH), 4.38 (γCH), 3.75/3.69 (δCH); hTyr-4: 7.60 (NH), 6.95/6.66 (Ar-H), 4.07 (αCH), 2.09/1.87 (βCH), 2.46/2.38 (γCH); Orn-5: 7.50 (NH), 4.69 (αCH), 1.83/1.65 (βCH), 1.60 (γCH), 2.90/2.84 (δCH); Hyp-6: 4.38 (αCH), 2.16/1.77 (βCH), 4.37 (γCH), 3.72/3.49 (δCH); Ter: 0.91 (CH_3), 1.37 (CH_2), 1.42 (CH_2), 1.75 (CH_2), 4.02 (OCH_2) 7.66/7.04 (Ar-H Ph-3), 7.81/7.75 (Ar-H Ph-2), 8.03/7.82 (Ar-H Ph-1) ppm. ^{13}C-NMR (DMSO, 125 MHz): δ Orn-1: 51.8 (αCH), 29.0 (βCH), 22.9 (γCH), 35.7 (δCH); Thr-2: 56.5 (αCH), 66.5 (βCH), 19.5 (γCH); Hyp-3: 60.9 (αCH), 37.7 (βCH), 69.2 (γCH), 55.9 (δCH); hTyr-4: 52.2 (αCH), 33.4 (βCH), 31.1 (γCH), 129.9/ 115.5 (Ar-H); Orn-5: 49.7 (αCH), 29.0 (βCH), 22.9 (γCH), 38.9 (δCH); Hyp-6: 59.2 (αCH), 37.3 (βCH), 69.2 (γCH), 56.1 (δCH); Ter: 13.9 (CH_3), 21.9 (CH_2), 27.7 (CH_2), 28.4 (CH_2), 67.7 (OCH_2), 128.2/115.4 (Ar-C Ph-3), 127.9/127.2 (Ar-C Ph-2), 128.9/126.6 (Ar-C Ph-1).

4-bromo-4'-(pentyloxy)biphenyl (16)

4-(4-bromophenyl)phenol (**15**)(3.44 g; 13.81 mmol), 1-bromopentane (2.50 g; 16.57 mmol), K_2CO_3 (3.82 g; 27.62 mmol) and KI (458 mg; 2.76 mmol) were stirred in dry DMF (34 mL) at 150°C for 3.5h. The reaction was cooled and filtered. Subsequently, the solid was washed with acetone. The amount of DMF was reduced by evaporation to ~25% of the volume. The concentrated solution was precipitated by aqueous 1M HCl and extracted with DCM (2x 50 mL). The combined organic layers were washed with 1N HCl (2x 50 mL) and H_2O (2x 50 mL), dried (Na_2SO_4), filtered and concentrated in *vacuo*, yielding a brownish solid. Product **16** (3.95 g; 90%) was obtained after recrystallization from EtOH as an off-white solid. R_f = 0.93 (DCM/MeOH), 50/1, v/v); ^{1}H-NMR ($CDCl_3$, 300 MHz): δ = 7.53-7.38 (m, 6H, Ar-H), 6.95 (d, 2H, Ar-H), 3.98 (t, J=6.6 Hz, 2H, OCH_2), 1.85-1.76 (m, 2H, CH_2CH_3), 1.48-1.38 (m, 4H, OCH_2CH_2,

$OCH_2CH_2CH_2$), 0.94 (t, J= 7.0 Hz, 3H, CH_3) ppm; ^{13}C-NMR ($CDCl_3$, 75.5 MHz): δ = 159.2 (CO), 140.0 and 132.4 (Ar-C), 132.0, 128.5, 128.1 and 115.1 (Ar-CH), 120.9 (C-Br), 68.3 (OCH_2), 29.2, 28.4 and 22.7 (CH_2), 14.2 (CH_3) ppm.

4'-(pentyloxy)biphenyl-4-ylboronic acid (17)
To a solution of **16** (3.93 g; 12.31 mmol) in freshly distilled THF (50 mL), flushed with nitrogen and cooled to -78°C, a solution of *sec*-BuLi (1.4 M in cyclohexane, 10.55 mL, 14.77 mmol) was added dropwise. The obtained reaction mixture was stirred at -78°C for 20 min. Then, triisopropylborate (5.68 mL; 24.62 mmol) was added and this reaction mixture was stirred for 2h and then slowly warmed to room temperature. The reaction mixture was diluted with Et_2O (100 mL) and washed with 2N HCl (100 mL) and H_2O (100 mL). The organic layer was dried (Na_2SO_4), filtered and evaporated to dryness. The residue was precipitated in Et_2O yielding the boronic acid **17** (2.52 g; 72%) as a white solid. R_f = 0.54 (DCM/MeOH), 50/1, v/v); ^{1}H-NMR (CD_3OD, 300 MHz): δ = 7.79 (d, J= 7.7 Hz, 1H, Ar-H), 7.65 (d, J= 7.7 Hz, 1H, Ar-H), 7.54 (d, J= 8.8 Hz, 4H, Ar-H), 6.96 (d, J= 8.8 Hz, 2H, Ar-H), 3.98 (t, J=6.5 Hz, 2H, OCH_2), 1.80-1.73 (m, 2H, CH_2CH_3), 1.49-1.37 (m, 4H, OCH_2CH_2, $OCH_2CH_2CH_2$), 0.95 (t, J= 7.0 Hz, 3H, CH_3) ppm.

4-(4''-pentyloxy-1,1':4',1''-terphenyl)-carboxylic acid (14)
A schlenk vessel, flushed with argon, was loaded with boronic acid **17** (568 mg; 2 mmol) and 4-iodobenzoic acid **18** (451 mg; 1.82 mmol). Subsequently, degassed toluene and EtOH (16 mL; 3/1; v/v) were added followed by aqueous 2M Na_2CO_3 (1.82 mL; 3.64 mmol) and $Pd(PPh_3)_4$ (105.2 mg; 9.1 μmol). The obtained reaction mixture was heated at 100°C for 20 hours. Then, the reaction mixture was acidified with 1N HCl. The reaction mixture was diluted with H_2O (20 mL) and the water layer was extracted with EtOAc (3x 20 mL). The combined organic layer was washed with H_2O and brine. In the organic layer a grey solid was present. This was filtered off and the organic layer was dried (Na_2SO_4), filtered and concentrated in *vacuo*. The organic layer showed to contain only starting material and DART analysis of the grey solid confirmed the presence of desired **14** (278.8 mg; 43%), in addition to the presence of starting material 4-iodobenzoic acid **18**. DART MS calcd for $C_{24}H_{24}O_3$: 361.1804, found: m/z 361.1809 $[M+H]^+$.

1-bromo-4-(pentyloxy)benzene (20)
The reaction was carried out following the procedure for the preparation of **16**, using 10 g of bromophenol **19** (57.8 mmol), 8.6 mL of bromopentane (69.4 mmol), 15.98 g K_2CO_3 (115.6 mmol) and 1.92 g KI (11.56 mmol) in 150 mL dry DMF. Pure product **20** (12.98 g; 92%) was obtained after column chromatography (DCM/ MeOH, 200/1, v/v) as a clear oil. R_f = 0.95 (DCM/MeOH), 100/1, v/v); ^{1}H-NMR ($CDCl_3$, 300 MHz): δ = 7.38-7.32 (m, 2H, Ar-H), 6.78-6.75 (m, 2H, Ar-H), 3.90 (t, J=6.5 Hz, 2H, OCH_2), 1.81-1.72 (m, 2H, CH_2CH_3), 1.45-1.34 (m, 4H, OCH_2CH_2, $OCH_2CH_2CH_2$), 0.93 (t, J= 7.0 Hz, 3H, CH_3) ppm; ^{13}C-NMR ($CDCl_3$, 75.5 MHz): δ = 158.5 (CO), 132.4 and 116.5 (Ar-CH), 112.7 (C-Br), 68.5 (OCH_2), 29.1, 28.4 and 22.7 (CH_2), 14.2 (CH_3) ppm.

hydroxy(4-(pentyloxy)phenyl)borane (21)
The reaction was carried out following the procedure for the preparation of **17**, using 11.89 g of **20** (48.90 mmol), 41.9 mL of *sec*BuLi (58.68 mmol) and 22.57 mL triisopropylborate

(97.80 mmol) in 200 mL freshly distilled THF. Pure product **21** (6.41 g; 63%) was obtained as a white solid after precipitation in hexane. R_f = 0.27 (DCM/MeOH), 100/1, v/v); ^{1}H-NMR ($CDCl_3$, 300 MHz): δ = 8.14 (d, J= 8.5 Hz, 2H, Ar-H), 7.0 (d, J= 8.5 Hz, 2H, Ar-H), 4.03 (t, J=6.6 Hz, 2H, OCH_2), 1.87-1.78 (m, 2H, CH_2CH_3), 1.54-1.37 (m, 4H, OCH_2CH_2, $OCH_2CH_2CH_2$), 0.95 (t, J= 7.0 Hz, 3H, CH_3) ppm; ^{13}C-NMR ($CDCl_3$, 75.5 MHz): δ = 163.0 (CO), 137.7 and 114.2 (Ar-CH), 68.1 (OCH_2), 29.2, 28.4 and 22.7 (CH_2), 14.3 (CH_3) ppm.

4'-iodobiphenyl-4-carboxylic acid (23)

To a suspension of biphenyl carboxylic acid (**22**) (10 g; 50.45 mmol) in CCl_4 (100 mL) PIFA (23.86 g; 55.49 mmol) was added and the color of the suspension changed to pink. Then, finely ground molecular iodine (12.80 g; 50.45 mmol) was added and the color changed to purple. After ca 35 min of stirring, a gel was formed and more CCl_4 (50 mL) was added. Stirring was continued for another hour. The suspension was filtered and the solids were washed extensively with Et_2O to yield pure product **23** (13.54 g; 83%) as a yellowish solid. ^{1}H-NMR (DMSO, 300 MHz): δ = 8.04 (d, J= 7.7 Hz, 2H, Ar-H), 7.87 (d, J= 8.0 Hz, 2H, Ar-H), 7.80 (d, J = 7.7 Hz, 2H, Ar-H), 7.55 (d, J= 7.7 Hz, 2H, Ar-H) ppm; ^{13}C-NMR (DMSO, 75.5 MHz): δ = 167.0 (COOH), 143.1 and 138.5 (Ar-C), 137.8, 130.0, 129.1 and 126.6 (Ar-CH), 94.9 (CI) ppm.

Route 2: 4-(4"-pentyloxy-1,1':4',1"-terphenyl)-carboxylic acid (14)

A schlenk vessel, flushed with argon, was loaded with boronic acid **21** (1.58 g; 7.6 mmol) 4-iodobiphenyl carboxylic acid **23** (1.97 g; 6.08 mmol), Na_2CO_3 (966 mg; 9.11 mmol) and $Pd(Cl_2(PPh_3)_2$ (4.21 mg; 6 μmol). Subsequently, degassed DMSO (19 mL) was added and the obtained reaction mixture was heated at 80°C for 20 hours. Then, the reaction mixture was filtered and the solid resuspended in H_2O (20 mL). The suspension was acidified with H_2SO_4 and heated to 95°C for 30 min after which the solid was filtered off. The solid was then resuspended in DMF (20 mL), heated to 100°C and cooled. Final filtration of the solid and drying in *vacuo* yielded pure product **14** (924 mg; 42%) as a white solid. DART MS calcd for $C_{24}H_{24}O_3$: 361.1804, found: m/z 361.1796 $[M+H]^+$; ^{1}H-NMR (DMSO, 300 MHz): δ = 8.03 (d, J= 8.3 Hz, 2H, Ar-H), 7.85-7.73 (m, 4H, Ar-H), 7.66 (d, J=8.5 Hz, 2H, Ar-H), 7.04 (d, J= 8.5 Hz, 2H, Ar-H), 4.01 (t, J=6.2 Hz, 2H, OCH_2), 1.74-1.72 (m, 2H, CH_2CH_3), 1.39 (m, 4H, OCH_2CH_2, $OCH_2CH_2CH_2$), 0.91 (t, J= 6.6 Hz, 3H, CH_3) ppm.

***Cyclo*[-(Ter)-Alg-Thr(*t*Bu)-Hyp(*t*Bu)-hTyr(*t*Bu)-Orn(Boc)-Hyp(*t*Bu)-Alg]-OMe (29)**

Wang-Tentagel S PHB resin (4 g; 1.04 mmol) and Fmoc-Alg-OH (1.09 g, 4.16 mmol) were dried *in vacuo* overnight over P_2O_5. DMF (20 mL) and pyridine (555 μL, 6.86 mmol) were added and the resin was shaken for 10 min until total dissolution. DCBC (596 μL, 4.16 mmol) was added and the resin was shaken for two days. The resin was drained and washed with DMF (5× 30 mL, each 2 min) and DCM (5× 30 mL, each 2 min). Subsequently, unreacted hydroxyl functions of the resin were acetylated by treatment with Ac_2O/NMI/DiPEA/DMF (30 mL; 2/1/1/6; v/v/v) for 30 min. The resin was drained and washed with DMF (3× 30 mL, each 2 min) and DCM (3× 30 mL, each 2 min). The peptide sequence was synthesized according to the general procedure for solid phase peptide synthesis. Hyp was coupled as part of the dipeptide Fmoc-Orn(Boc)-Hyp(*t*Bu)-OH. ESI-MS calcd for TFA deprotected **8b** $C_{54}H_{68}N_8O_{14}$: 1052.49, found: m/z 1053.52 $[M+H]^+$. Removal of the Fmoc group was followed by coupling overnight of the ter tail (1.44 g; 4 mmol) in the presence of HATU (1.52 g; 4 mmol) and DIPEA (1.39 mL; 8 mmol) in NMP (30 mL). The resin was washed with NMP (3× 30 mL, each

3 min) and DCM (3× 30 mL, each 3 min). The resin-bound peptide was subjected to the microwave-assisted RCM procedure under the following conditions: Resin peptide (3.3 g; 0.86 mmol), DCM (27.5 mL), LiCl/DMA (degassed; 0.4M; 2.7 mL), Grubbs II (9 mol%; 64 mg; 75.4 μmol), 100 °C for 60 min (performed in three batches due to the size (10 mL) of the microwave vessel). The fully protected peptide **29** was obtained by cleavage from the resin by treatment with a catalytic amount of KCN in MeOH (20 mL) for 16h. The resin was filtered and washed with MeOH (3× 15 mL) and the filtrate was concentrated *in vacuo* to yield the crude peptide. The peptide was purified by column chromatography (DCM/MeOH, 50/1, v/v). After lyophilization peptide **29** (191.5 mg; 15%) was obtained as a white solid. Purity was confirmed by analytical HPLC (Alltima C8, 65 min run, *i*-PrOH/MeOH/H_2O buffers) and was found to be higher than 99% (R_t = 50.05 min). ESI-MS calcd for $C_{83}H_{118}N_8O_{16}$: 1482.87, found: m/z 1483.79 $[M+H]^+$; HRMS calcd for $C_{83}H_{118}N_8O_{16}$ $[M+H]^+$ 1483.8744, found 1483.8715; ^{1}H-NMR ($CDCl_3$, 500 MHz): δ *t*Bu: 1.53-1.37 (CH_3), 1.25-1.11(CH_3); hTyr-4: 7.57/7.00 (Ar-H); Me ester: 3.71 (OCH_3); Ter: 0.95 (CH_3), 1.31 (CH_2), 1.41 (CH_2), 1.82 (CH_2), 4.01 (OCH_2) ppm. ^{13}C-NMR ($CDCl_3$, 125 MHz): δ *t*Bu: 28.6 (CH_3), 28.2 (CH_3); hTyr-4: 128.7/115.5 (Ar-H); Me ester: 52.7 (OCH_3); Ter: 14.1 (CH_3), 22.6 (CH_2), 28.9 (CH_2), 29.2 (CH_2), 68.5 (OCH_2). Full NMR characterization of the protected peptide **29** was not possible due to the high intensity of the *t*Bu/Boc signals and the broadened amino acid signals. However, full NMR characterization of the deprotected peptide can be found at the experimental details of cyclic peptide **30**.

***Cyclo*[-(Ter)-Alg-Thr-Hyp-hTyr-Orn-Hyp-Alg]-OH (26)**

Peptide **26** was obtained analogous to peptide **29** except for the last step and obtained by using the TFA cleavage procedure for a small aliquot of resin. After preparative HPLC and lyophilization, peptide **26** was obtained as a white solid. Purity was confirmed by analytical HPLC (Alltima C8, 65 min run, *i*-PrOH/MeOH/H_2O buffers) and was found to be higher than 95% for a mixture of *E/Z* stereoisomers (R_t = 40.25 min and 40.43 min). ESI-MS calcd for $C_{61}H_{76}N_8O_{14}$: 1144.55, found: m/z 1145.67 $[M+H]^+$; HRMS calcd for $C_{61}H_{76}N_8O_{14}$ $[M+H]^+$ 1145.5559, found 1145.5547; ^{1}H-NMR (DMSO, 500 MHz): δ Alg-1: 8.15 (NH), 4.19 (αCH), 2.35 (βCH), 5.46 (γCH); Thr-2: 7.66 (NH), 4.68 (αCH), 4.26 (βCH), 1.09 (γCH); Hyp-3: 4.23 (αCH), 1.79 (βCH), 4.36 (γCH), 3.78/3.58 (δCH); hTyr-4: 7.33 (NH), 6.95/6.65 (Ar-H), 3.87 (αCH), 1.95/1.88 (βCH), 2.52/2.47 (γCH); Orn-5: 7.62 (εNH), 7.21 (NH), 4.46 (αCH), 1.83/1.56 (βCH), 1.51 (γCH), 2.83 (δCH); Hyp-6: 4.28 (αCH), 1.91 (βCH), 4.53 (γCH), 3.58/3.16 (δCH); Alg-7: 8.62 (NH), 4.73 (αCH), 2.88/2.55 (βCH), 5.46 (γCH); Ter: 0.89 (CH_3), 1.21 (CH_2), 1.39 (CH_2), 1.73 (CH_2), 4.01 (OCH_2), 7.65/7.03 (Ar-H Ph-3), 7.79/7.73 (Ar-H Ph-2), 7.98/7.81 (Ar-H Ph-1) ppm.

***Cyclo*[-(Ter)-Alg-Thr-Hyp-hTyr-Orn-Hyp-Alg]-OH (27)**

Hydrogenation of the cyclic unsaturated peptide **26** (3.5 mg; 3.06 μmol) was carried out using the hydrogenation procedure in the presence of 3 mg of 10% Pd/C. The saturated peptide **27** (quant.) was obtained as a white solid. Purity was confirmed by analytical HPLC (Alltima C8, 65 min run, *i*-PrOH/MeOH/H_2O buffers) and was found to be higher than 95% (R_t = 41.99 min). ESI-MS calcd for $C_{61}H_{78}N_8O_{14}$: 1146.56, found: m/z 1147.53 $[M+H]^+$; HRMS calcd for $C_{61}H_{78}N_8O_{14}$ $[M+H]^+$ 1147.5710, found 1147.5707; ^{1}H-NMR (DMSO, 500 MHz): δ Alg-1: 8.60 (NH), 4.55 (αCH), 1.76 (βCH), 1.35 (γCH); Thr-2: 7.44 (NH), 4.64 (αCH), 4.30 (βCH), 1.14 (γCH); Hyp-3: 4.37 (αCH), 2.17/1.81 (βCH), 4.32 (γCH), 3.67/3.44 (δCH); hTyr-4: 7.68 (NH), 6.95/6.67 (Ar-H), 3.97 (αCH), 2.11/1.89 (βCH), 2.47/2.38 (γCH); Orn-5: 7.65 (εNH),

7.64 (NH), 4.64 (αCH), 1.89/1.62 (βCH), 1.54 (γCH), 2.57/2.83 (δCH); Hyp-6: 4.47 (αCH), 2.46/1.85 (βCH), 4.38 (γCH), 3.73 (δCH); Alg-7: 8.33 (NH), 4.32 (αCH), 1.80/1.60 (βCH), 1.376 (γCH); Ter: 0.91 (CH_3), 1.36 (CH_2), 1.42 (CH_2), 1.75 (CH_2), 4.02 (OCH_2), 7.67/7.05 (Ar-H Ph-3), 7.81/7.76 (Ar-H Ph-2), 8.04/7.83 (Ar-H Ph-1) ppm. ^{13}C-NMR (DMSO, 125 MHz): δ Alg-1: 54.0 (αCH), 31.4 (βCH), 24.0 (γCH); Thr-2: 56.1 (αCH), 66.3 (βCH), 19.1 (γCH); Hyp-3: 60.5 (αCH), 37.1 (βCH), 68.4 (γCH), 55.2 (δCH); hTyr-4: 52.1 (αCH), 32.2 (βCH), 30.7 (γCH), 129.6/115.2 (Ar-H); Orn-5: 49.3 (αCH), 28.6 (βCH), 23.2 (γCH), 38.4 (δCH); Hyp-6: 58.0 (αCH), 37.6 (βCH), 68.9 (γCH), 55.5 (δCH); Alg-7: 49.5 (αCH), 29.6 (βCH), 24.2 (γCH); Ter: 13.6 (CH_3), 21.6 (CH_2), 27.4 (CH_2), 28.1 (CH_2), 67.4 (OCH_2), 127.9/115.1 (Ar-H Ph-3), 127.6/126.9 (Ar-H Ph-2), 128.6/126.3 (Ar-H Ph-1) ppm.

***Cyclo*[-(Ter)-Cys-Thr-Hyp-hTyr-Orn-Hyp-Cys]-NH_2 (28)**

Peptide **28** was prepared analogously to peptide **7** except for the coupling step of the fatty acid after Fmoc cleavage. Resin bound linear peptide (280 mg; 67.2 μmol) was subjected to the Fmoc cleavage procedure. Then, the free amine was coupled with terphenyl acid **14** (97 mg; 269 μmol) overnight in the presence of HATU (102.2 mg; 269 μmol) and DiPEA (94 μL; 538 μmol) in NMP (2 mL). The resin was washed with NMP (3× 2 mL, each 3 min) and DCM (3× 2 mL, each 3 min) and subjected to the TFA cleavage procedure and lyophilized. Then, the linear peptide (33.6 mg; 28.4 μmol) was cyclized by oxidation with DMSO analogously to **7.** After preparative HPLC and lyophilization, peptide **28** (6 mg; 18%) was obtained as a white solid. Purity was confirmed by analytical HPLC (Alltima C8, 65 min run, *i*-PrOH/MeOH/H_2O buffers) and was found to be higher than 99% (R_t = 41.12 min). ESI-MS calcd for $C_{59}H_{75}N_9O_{13}S_2$: 1181.49, found: m/z 1182.72 $[M+H]^+$; HRMS calcd for $C_{59}H_{75}N_9O_{13}S_2$ $[M+H]^+$ 1182.5004, found 1182.5013; ^{1}H-NMR (DMSO, 500 MHz): δ Cys-1: 8.74 (NH), 4.98 (αCH), 3.43/3.16 (βCH); Thr-2: 7.73 (NH), 4.73 (αCH), 4.29 (βCH), 1.05 (γCH); Hyp-3: 4.25 (αCH), 2.11/1.81 (βCH), 4.37 (γCH), 3.80/3.61 (δCH); hTyr-4: 7.35 (NH), 6.95/6.65 (Ar-H); 3.90 (αCH), 1.96/1.89 (βCH), 2.52/2.46 (γCH); Orn-5: 7.28 (NH), 4.48 (αCH), 1.80/1.61 (βCH), 1.51 (γCH), 2.77 (δCH); Hyp-6: 4.60 (αCH), 2.00 (βCH), 4.30 (γCH), 3.59/3.21 (δCH); Cys-7: 8.36 (NH), 4.35 (αCH), 3.31/2.90 (βCH); Ter: 0.90 (CH_3), 1.36 (CH_2), 1.41 (CH_2), 1.74 (CH_2), 4.01 (OCH_2), 7.66/7.04 (Ar-H Ph-3), 7.81/7.75 (Ar-H Ph-2), 8.01/7.83 (Ar-H Ph-1) ppm. ^{13}C-NMR (DMSO, 125 MHz): δ Cys-1: 51.9 (αCH), 43.4 (βCH); Thr-2: 56.0 (αCH), 66.5 (βCH), 19.0 (γCH); Hyp-3: 60.8 (αCH), 36.9 (βCH), 69.2 (γCH), 55.8 (δCH); hTyr-4: 53.4 (αCH), 32.4 (βCH), 31.2 (γCH); 115.5 (Ar-H), 129.9 (Ar-H); Orn-5: 49.5 (αCH), 27.2 (βCH), 23.2 (γCH), 38.2 (δCH); Hyp-6: 59.0 (αCH), 37.8 (βCH), 68.5 (γCH), 53.5 (δCH); Cys-7: 51.4 (αCH), 43.4 (βCH); Ter: 13.8 (CH_3), 21.8 (CH_2), 27.6 (CH_2), 28.2 (CH_2), 67.6 (OCH_2), 128.1/115.3 (Ar-H Ph-3), 127.8/127.1 (Ar-H Ph-2), 128.7/126.6 (Ar-H Ph-1).

***Cyclo*[-(Ter)-Alg-Thr-Hyp-hTyr-Orn-Hyp-Alg]-OMe (30)**

Fully protected peptide **29** (19.9 mg; 13.41 μmol) was treated with a mixture of TFA/TIS/H_2O (2 mL, 95/2.5/2.5, v/v/v) for 2h. The mixture was concentrated *in vacuo*, re-dissolved in a small amount of TFA and precipitated in MTBE/hexane (1/1). The supernatant was removed and the crude peptide washed twice with MTBE/hexane (1/1). After preparative HPLC (Alltima C8 semiprep, 120 min run, *i*-PrOH/MeOH/H_2O buffers) and lyophilization, peptide **30** (9.3 mg; 60%) was obtained as a white solid. Purity was confirmed by analytical HPLC (Alltima C8, 65 min run, *i*-PrOH/MeOH/H_2O buffers) and was found to be higher than 99% (R_t = 42.62 min). ESI-MS calcd for $C_{62}H_{78}N_8O_{14}$: 1158.56, found: m/z 1159.52 $[M+H]^+$; HRMS calcd

for $C_{62}H_{78}N_8O_{14}$ $[M+H]^+$ 1159.5716, found 1159.5750; ^{1}H-NMR (DMSO, 500 MHz): δ Alg-1: 8.62 (NH), 4.73 (αCH), 2.88/2.55 (βCH), 5.46 (γCH); Thr-2: 7.65 (NH), 4.68 (αCH), 4.26 (βCH), 1.09 (γCH); Hyp-3: 4.22 (αCH), 2.02/1.83 (βCH), 4.36 (γCH), 3.79/3.59 (δCH); hTyr-4: 7.33 (NH), 6.94/6.64 (Ar-H), 3.88 (αCH), 1.94/1.88 (βCH), 2.52/2.46 (γCH); Orn-5: 7.63 (εNH), 7.21 (NH), 4.46 (αCH), 1.82/1.57 (βCH), 1.51 (γCH), 2.82 (δCH); Hyp-6: 4.53 (αCH), 1.93/1.88 (βCH), 4.28 (γCH), 3.58/3.17 (δCH); Alg-7: 8.27 (NH), 4.29 (αCH), 2.35 (βCH), 5.46 (γCH); Me ester: 3.61 (CH_3); Ter: 0.89 (CH_3), 1.22 (CH_2), 1.38 (CH_2), 1.72 (CH_2), 4.00 (OCH_2), 7.64/7.03 (Ar-H Ph-3), 7.79/7.73 (Ar-H Ph-2), 7.98/7.81 (Ar-H Ph-1) ppm.

***Cyclo*[-(Ter)-Alg-Thr(*t*Bu)-Hyp(*t*Bu)-hTyr(*t*Bu)-Orn(Boc)-Hyp(*t*Bu)-Alg]-OH (31)**

A solution of 0.2N LiOH (0.6 mL) was added drop-wise to a cooled (0 °C) solution of peptide **29** (61.8 mg; 41.7 μmol) in THF (1.5 mL). The reaction mixture was stirred at room temperature for 16h followed by evaporation *in vacuo*. The product was re-dissolved in H_2O and neutralized with 1N HCl, followed by lyophilization yielding peptide **31** (67 mg; quant.) as a white solid. Purity was confirmed by analytical HPLC (Alltima C8, 65 min run, *i*-PrOH/MeOH/H_2O buffers) and was found to be higher than 95% (R_t = 49.63 min). ESI-MS calcd for $C_{82}H_{116}N_8O_{16}$: 1468.85, found: m/z 1469.75 $[M+H]^+$; HRMS calcd for $C_{82}H_{116}N_8O_{16}$ $[M+H]^+$ 1469.8588, found 1469.8579; ^{1}H-NMR ($CDCl_3$, 500 MHz): δ *t*Bu: 1.48-1.33 (CH_3), 1.22-1.08(CH_3); hTyr-4: 7.53/6.96 (Ar-H); Ter: 0.92 (CH_3), 1.38 (CH_2), 1.28 (CH_2), 1.79 (CH_2), 3.98 (OCH_2) ppm. ^{13}C-NMR ($CDCl_3$, 125 MHz): δ *t*Bu: 28.1 (CH_3), 28.0 (CH_3); hTyr-4: 128.3/115.1 (Ar-H); Ter: 13.7 (CH_3), 22.2 (CH_2), 28.5 (CH_2), 28.7 (CH_2), 68.0 (OCH_2). Full NMR characterization of the protected peptide **31** was not possible due to the high intensity of the *t*Bu/Boc signals and the broadened amino acid signals. However, full NMR characterization of the deprotected peptide can be found at the experimental details of cyclic peptide **26**.

***Cyclo*[-(Ter)-Alg-Thr-Hyp-hTyr-Orn-Hyp-Alg]-NHCH$_2$CH$_2$NH$_2$ (32)**

To a solution of peptide **31** (12.3 mg; 8.37 μmol), *N*-boc-ethylene-diamine (2.68 mg; 16.74 μmol) and HATU (3.18 mg; 8.37 μmol) in DCM (1 mL) DIPEA (2.92 μL; 16.74 μmol) was added and the reaction mixture was stirred for 48h. As the reaction was not finished according to TLC (DCM/MeOH/AcOH, 19/1/0.1) another portion of *N*-boc-ethylene-diamine (2.7 mg; 17 μmol), HATU (3.2 mg; 8.4 μmol) and DIPEA (2.92 μL; 16.74 μmol) was added and the mixture was stirred for an additional 24h. The mixture was concentrated *in vacuo*, the residue re-dissolved in EtOAc (5 mL) and washed with 1N $KHSO_4$ (3× 5 mL), 5% $NaHCO_3$ (3× 5 mL) and brine (5 mL). The organic layer was dried over Na_2SO_4 and concentrated *in vacuo*. The crude peptide was purified by column chromatography (DCM/MeOH/AcOH, 30/1/0.1, v/v/v) yielding the protected peptide (8.0 mg; 59%) as a white solid. ESI-MS calcd for $C_{89}H_{130}N_{10}O_{17}$: 1610.96, found: m/z 1611.53 $[M+H]^+$. The protected peptide (12.7 mg; 7.8 μmol) was treated with a mixture of TFA/TIS/H_2O (1 mL, 95/2.5/2.5, v/v/v) for 2h. The mixture was concentrated *in vacuo*, the residue re-dissolved in a small amount of TFA and precipitated in MTBE/hexane (1/1). The supernatant was removed and the crude peptide washed twice with MTBE/hexane (1/1). After preparative HPLC (Alltima C8 semiprep, 120 min run, *i*-PrOH/MeOH/H_2O buffers) and lyophilization, peptide **32** (7.2 mg; 78%) was obtained as a white solid. Purity was confirmed by analytical HPLC (Alltima C8, 65 min run, *i*-PrOH/MeOH/H_2O buffers) and was found to be higher than 99% for a mixture of *E/Z* stereoisomers (R_t = 39.20 min and 39.48 min). ESI-MS calcd for $C_{63}H_{82}N_{10}O_{13}$: 1186.61, found: m/z 1187.65 $[M+H]^+$; HRMS calcd for $C_{61}H_{78}N_{10}O_{13}$ $[M+H]^+$ 1187.6141, found 1187.6152; ^{1}H-NMR (DMSO, 500

MHz): δ Alg-1: 8.15 (NH), 4.25 (αCH), 2.40/2.19 (βCH), 5.61 (γCH); Thr-2: 7.67 (NH), 4.65 (αCH), 4.31 (βCH), 1.14 (γCH); Hyp-3: 4.35 (αCH), 2.16/1.83 (βCH), 4.41 (γCH), 3.77/3.72 (δCH); hTyr-4: 7.74 (NH), 6.96/6.67 (Ar-H), 3.96 (αCH), 2.11/1.95 (βCH), 2.48/2.37 (γCH); Orn-5: 7.71 (εNH), 7.46 (NH), 4.66 (αCH), 1.84/1.68 (βCH), 1.54 (γCH), 2.87 (δCH); Hyp-6: 4.48 (αCH), 2.06/1.89 (βCH), 4.32 (γCH), 3.67/3.44 (δCH); Alg-7: 7.99 (NH), 4.23 (αCH), 2.34 (βCH), 5.47 (γCH); $NHCH_2CH_2NH_2$ amide: 3.32/3.23 (CH_2), 2.86/2.82 (CH_2); Ter: 0.92 (CH_3), 1.38 (CH_2), 1.43 (CH_2), 1.75 (CH_2), 4.03 (OCH_2), 7.67/7.06 (Ar-H Ph-3), 7.82/7.76 (Ar-H Ph-2), 8.01/7.84 (Ar-H Ph-1) ppm.

***Cyclo*[-(Ter)-Alg-Thr-Hyp-hTyr-Orn-Hyp-Alg]-Ψ[CH_2OH] (33)**

A $LiBH_4$ (11 μL; 22.17 μmol) solution (2.0 M in THF) was added to a solution of peptide **29** (18.8 mg; 12.67 μmol) in dry THF (2 mL) and the reaction mixture was stirred for 5h. The reaction mixture was quenched by addition of sat. aq. $NaHCO_3$ and stirred for an additional 10 min. The aqueous layer was extracted with Et_2O (10 mL) and EtOAc (10 mL). The combined organic layers were dried over Na_2SO_4, filtered and concentrated *in vacuo*. The crude peptide was purified by column chromatography (DCM/MeOH/AcOH, 20/1/0.1, v/v/v) yielding the protected peptide alcohol (10.2 mg; 55%) as a white solid. ESI-MS calcd for $C_{82}H_{118}N_8NaO_{15}$: 1477.86, found: m/z 1477.82 $[M+Na]^+$. The peptide (10 mg; 6.9 μmol) was treated with a mixture of TFA/TIS/H_2O (2 mL; 95/2.5/2.5; v/v/v) for 2h. The mixture was concentrated *in vacuo*, re-dissolved in a small amount of TFA and precipitated in MTBE/hexane (1/1). The supernatant was removed and the crude peptide washed twice with MTBE/hexane (1/1). After preparative HPLC (Alltima C8 semiprep, 120 min run, *i*-PrOH/MeOH/H_2O buffers) and lyophilization, peptide **33** (3.7 mg; 26%) was obtained as a white solid. Purity was confirmed by analytical HPLC (Alltima C8, 65 min run, *i*-PrOH/MeOH/H_2O buffers) and was found to be higher than 99% (R_t = 41.83 min). ESI-MS calcd for $C_{61}H_{78}N_8O_{13}$: 1130.57, found: m/z 1131.57 $[M+H]^+$; HRMS calcd for $C_{61}H_{78}N_8O_{13}$ $[M+H]^+$ 1131.5767, found 1131.5795; ^{1}H-NMR (DMSO, 500 MHz): δ Alg-1: 8.67 (NH), 4.63 (αCH), 2.55/2.43 (βCH), 5.58 (γCH); Thr-2: 7.70 (NH), 4.64 (αCH), 4.28 (βCH), 1.13 (γCH); Hyp-3: 4.32 (αCH), 2.13/1.81 (βCH), 4.31 (γCH), 3.66/3.41 (δCH); hTyr-4: 7.75 (NH), 6.95/6.66 (Ar-H), 3.91 (αCH), 2.08/1.93 (βCH), 2.46/2.38 (γCH); Orn-5: 7.64 (εNH), 7.45 (NH), 4.63 (αCH), 1.91/1.61 (βCH), 1.55 (γCH), 2.94/2.83 (δCH); Hyp-6: 4.39 (αCH), 2.00/1.82 (βCH), 4.39 (γCH), 3.74/3.71 (δCH); Alg-7: 7.69 (NH), 3.71 (αCH), 2.29/1.94 (βCH), 5.54 (γCH); alcohol: 3.28/3.13 (CH_2OH); Ter: 0.91 (CH_3), 1.37 (CH_2), 1.42 (CH_2), 1.75 (CH_2), 4.02 (OCH_2), 7.67/7.05 (Ar-H Ph-3), 7.82/7.75 (Ar-H Ph-2), 8.01/7.83 (Ar-H Ph-1) ppm. ^{13}C-NMR (DMSO, 125 MHz): δ Alg-1: 54.0 (αCH), 34.0 (βCH), 128.9 (γCH); Thr-2: 56.2 (αCH), 66.3 (βCH), 19.1 (γCH); Hyp-3: 60.5 (αCH), 36.9 (βCH), 68.4 (γCH), 55.1 (δCH); hTyr-4: 52.4 (αCH), 32.0 (βCH), 30.7 (γCH), 129.6/115.2 (Ar-H); Orn-5: 49.5 (αCH), 28.5 (βCH), 23.3 (γCH), 38.4 (δCH); Hyp-6: 58.2 (αCH), 38.0 (βCH), 69.0 (γCH), 55.5 (δCH); Alg-7: 50.0 (αCH), 33.0 (βCH), 127.7 (γCH); alcohol: 63.8 (CH_2OH); Ter: 13.6 (CH_3), 21.6 (CH_2), 27.4 (CH_2), 28.1 (CH_2), 67.4 (OCH_2), 127.9/115.1 (Ar-H Ph-3), 127.5/126.9 (Ar-H Ph-2), 128.5/126.3 (Ar-H Ph-1) ppm.

***Cyclo*[-(Ter)-Alg-Thr-Hyp-hTyr-Orn-Hyp-Alg]-$NHNH_2$ (34)**

To a solution of peptide **29** (9.0 mg; 6.06 μmol) in dry DMF (1 mL) $N_2H_4.H_2O$ (0.2 mL) was added and the reaction mixture was stirred for 24h. The volatiles were removed by evaporation *in vacuo* and coevaporation with MeOH (3×). Lyophilization yielded the protected peptide hydrazide (8.0 mg; 89%) as a white solid. ESI-MS calcd for $C_{82}H_{118}N_{10}NaO_{15}$: 1505.87, found:

m/z 1505.80 [M+Na]. The protected peptide (8.0 mg; 5.4 μmol) was treated with HCl/Et_2O[38] for 2h. The mixture was concentrated *in vacuo*, re-dissolved in a small amount of MeOH and precipitated in MTBE/hexane (1/1). The supernatant was removed and the crude peptide washed twice with MTBE/hexane (1/1). After preparative HPLC (Alltima C8 semiprep, 120 min run, *i*-PrOH/MeOH/H_2O buffers) and lyophilization, peptide hydrazide **34** (3 mg; 48%) was obtained as a white solid. Purity was confirmed by analytical HPLC (Alltima C8, 65 min run, *i*-PrOH/MeOH/H_2O buffers) and was found to be higher than 95% (R_t = 39.50 min). ESI-MS calcd for $C_{61}H_{78}N_{10}O_{13}$: 1158.57, found: m/z 1159.80 $[M+H]^+$; HRMS calcd for $C_{61}H_{78}N_{10}O_{13}$ $[M+H]^+$ 1159.5828, found 1159.5845; ^{1}H-NMR (DMSO, 500 MHz): δ Alg-1: 8.72 (NH), 4.62 (αCH), 2.52/2.46 (βCH), 5.62 (γCH); Thr-2: 7.57 (NH), 4.65 (αCH), 4.30 (βCH), 1.13 (γCH); Hyp-3: 4.46 (αCH), 2.21/2.32 (βCH), 4.40 (γCH), 3.66/3.42 (δCH); hTyr-4: 7.71 (NH), 6.95/6.66 (Ar-H), 3.95 (αCH), 2.10/1.92 (βCH), 2.47/2.37 (γCH); Orn-5: 7.67 (εNH), 7.45 (NH), 4.65 (αCH), 1.85/1.65 (βCH), 1.52 (γCH), 2.92/2.83 (δCH); Hyp-6: 4.34 (αCH), 2.03/1.83 (βCH), 4.30 (γCH), 3.74 (δCH); Alg-7: 8.30 (NH), 4.31 (αCH), 2.15 (βCH), 5.63 (γCH); Ter: 0.91 (CH_3), 1.37 (CH_2), 1.42 (CH_2), 1.74 (CH_2), 4.02 (OCH_2), 7.76/7.05 (Ar-H Ph-3), 7.84/7.67 (Ar-H Ph-2), 8.02/7.82 (Ar-H Ph-1) ppm. ^{13}C-NMR (DMSO, 125 MHz): δ Alg-1: 54.0 (αCH), 33.9 (βCH), 127.3 (γCH); Thr-2: 56.2 (αCH), 66.2 (βCH), 19.1 (γCH); Hyp-3: 58.0 (αCH), 34.1 (βCH), 69.0 (γCH), 55.1 (δCH); hTyr-4: 52.2 (αCH), 32.2 (βCH), 30.7 (γCH), 129.6/115.2 (Ar-H); Orn-5: 49.3 (αCH), 28.6 (βCH), 23.2 (γCH), 38.4 (δCH); Hyp-6: 60.6 (αCH), 37.6 (βCH), 68.4 (γCH), 55.5 (δCH); Alg-7: 50.5 (αCH), 37.0 (βCH), 129.3 (γCH); Ter: 13.5 (CH_3), 21.6 (CH_2), 27.4 (CH_2), 28.0 (CH_2), 67.4 (OCH_2), 126.9/115.1 (Ar-H Ph-3), 126.4/127.9 (Ar-H Ph-2), 128.5/127.5 (Ar-H Ph-1) ppm.

Hydroxylated caspofungin derivative (36)

To a solution of NMO (1.05 g; 779 μmol) and OsO_4 (7.3 μL; 22.9 μmol) in H_2O (5 mL), a solution of fully protected peptide **29** (34 mg; 22.9 μmol) in MeCN (5 mL) was added and the reaction mixture was stirred for 24h. The reaction was poured into an aqueous saturated $Na_2S_2O_3$ solution (20 mL) and extracted with EtOAc (2x 20 mL). The combined organic layers were dried (Na_2SO_4), filtered and concentrated in *vacuo*. The peptide was lyophilized. Then, the peptide was dissolved in MeOH (2 mL) and treated with aqeous 0.2 N LiOH (500 μL). The reaction mixture was stirred for 24h and concentrated in *vacuo*. Subsequently, the residue was treated with a mixture of TFA/TIS/H_2O (2 mL; 95/2.5/2.5; v/v/v) for 2h. The mixture was concentrated *in vacuo*, re-dissolved in a small amount of TFA and precipitated in MTBE/hexane (1/1). The supernatant was removed and the crude peptide washed twice with MTBE/hexane (1/1). After preparative HPLC (Alltima C8 semiprep, 120 min run, *i*-PrOH/MeOH/H_2O buffers) and lyophilization, peptide **36** (5 mg; 19% overall yield) was obtained as a white solid. Purity was confirmed by analytical HPLC (Alltima C8, 65 min run, *i*-PrOH/MeOH/H_2O buffers) and was found to be higher than 99% (R_t = 39.77 min). ESI-MS calcd for $C_{61}H_{78}N_8O_{16}$: 1178.55, found: m/z 1179.76 $[M+H]^+$; HRMS calcd for $C_{61}H_{78}N_8O_{16}$ $[M+H]^+$ 1179.5614, found 1179.5646.

***Cyclo*[-(Ter)-Lys-Thr-Hyp-hTyr-Orn-Hyp] (39)**

Linear peptide Fmoc-Lys(Psoc)-Thr(*t*Bu)-Hyp(*t*Bu)-hTyr(*t*Bu)-Orn(Boc)-Hyp(*t*Bu)-OH (**37**) was synthesized on trityl resin (200 mg; 93.8 μmol) according to the general procedure for solid phase peptide synthesis. The Fmoc group was cleaved and the Ter tail (101.4 mg; 281.4 μmol) was coupled overnight in the presence of HATU (107 mg; 281.4 μmol) and DiPEA

(98 μL; 562.8 μmol) in NMP (2 mL). The resin was washed with NMP (3× 3 mL, each 3 min) and DCM (3× 3 mL, each 3 min). The Psoc group was cleaved by treatment with TBAF.3 H_2O (88.8 mg; 281 μmol) for 15 min in DCM (2 mL). Peptide **38** was obtained by treatment of the resin with HFIP/DCM (3 mL, 1/1, v/v) for 3h. This was repeated once for 1h. The mixture was concentrated to obtain crude peptide **38** (121.4 mg; 90%) as a foam. Characterization was carried out by ESI-MS (calcd for $C_{80}H_{118}N_8O_{15}$: 1430.87, found: m/z 1431.89 $[M+H]^+$). Then, the crude linear peptide Ter-Lys-Thr(*t*Bu)-Hyp(*t*Bu)-hTyr(*t*Bu)-Orn(Boc)-Hyp(*t*Bu)-OH (**38**) was subjected to the head-to-tail cyclization according to the general procedure, followed by treatment with a mixture of TFA/TIS/H_2O (10 mL, 95/2.5/2.5, v/v/v) for 1h. The mixture was concentrated *in vacuo*, re-dissolved in a small amount of TFA and precipitated in MTBE/hexane (1/1). The supernatant was removed and the crude peptide washed twice with MTBE/hexane (1/1). After preparative HPLC (Alltima C8 semiprep, 120 min run, *i*-PrOH/MeOH/H_2O buffers) and lyophilization, peptide **39** (20.4 mg; 23%) was obtained as a white solid. Purity was confirmed by analytical HPLC (Alltima C8, 65 min run, *i*-PrOH/MeOH/H_2O buffers) and was found to be higher than 99% (R_t = 41.05 min). ESI-MS calcd for $C_{59}H_{76}N_8O_{12}$: 1088.56, found: m/z 1089.82 $[M+H]^+$; HRMS calcd for $C_{59}H_{76}N_8O_{12}$ $[M+H]^+$ 1089.5661, found 1089.5656; ^{1}H-NMR (DMSO, 500 MHz): δ Lys-1: 8.53 (NH), 7.90 (εNH), 4.66 (αCH), 2.14/1.72 (βCH), 1.60/1.33 (γCH), 1.58/1.32 (δCH), 3.56/2.71 (εCH); Thr-2: 7.79 (NH), 4.71 (αCH), 1.09 (βCH), 1.09 (γCH); Hyp-3: 4.23 (αCH), 2.12/1.78 (βCH), 4.37 (γCH), 3.80/3.59 (δCH); hTyr-4: 7.43 (NH), 6.96/6.66 (Ar-H), 3.98 (αCH), 1.99/1.87 (βCH), 2.52/2.46 (γCH); Orn-5: 7.69 (εNH), 7.33 (NH), 4.51 (αCH), 1.87/1.63 (βCH), 1.56 (γCH), 2.89 (δCH); Hyp-6: 4.40 (αCH), 1.98/1.77 (βCH), 4.30 (γCH), 3.66/3.31 (δCH); Ter: 0.91 (CH_3), 1.36 (CH_2), 1.41 (CH_2), 1.74 (CH_2), 4.01 (OCH_2) 7.65/7.03 (Ar-H Ph-3), 7.80/7.74 (Ar-H Ph-2), 8.03/7.81 (Ar-H Ph-1) ppm. ^{13}C-NMR (DMSO, 125 MHz): δ Lys-1: 53.4 (αCH), 31.0 (βCH), 23.3 (γCH), 26.9 (δCH), 38.4 (εCH); Thr-2: 55.7 (αCH), 66.4 (βCH), 19.2 (γCH); Hyp-3: 60.7 (αCH), 36.7 (βCH), 68.9 (γCH), 55.2 (δCH); hTyr-4: 53.0 (αCH), 32.3 (βCH), 30.7 (γCH), 129.1/ 114.6 (Ar-H); Orn-5: 49.4 (αCH), 27.7 (βCH), 23.3 (γCH), 38.3 (δCH); Hyp-6: 59.2 (αCH), 37.6 (βCH), 68.4 (γCH), 54.5 (δCH); Ter: 13.7 (CH_3), 21.6 (CH_2), 27.5 (CH_2), 28.1 (CH_2), 67.2 (OCH_2), 127.4/114.7 (Ar-C Ph-3), 127.1/126.4 (Ar-C Ph-2), 128.1/125.8 (Ar-C Ph-1).

2.4.3 Biology

Candida MIC Assay

Antifungal activity was evaluated by broth microdilution. The media used in this assay was Yeast Extract Peptone Dextrose (YPD) containing 1% yeast extract, 2% peptone, 1% dextrose in distilled water. Test compounds were dissolved in distilled water or 10% DMSO, depending on the solubility characteristics of the compounds, to a concentration of 1 mg/mL. After dissolving each compound solution was diluted 5 times in YPD medium rendering a stock solution of 200 μg/mL. Caspofungin[14], purchased from Merck Sharp & Dohme B.V. (Haarlem, Netherlands), was included as a reference. Serial 2-fold dilutions of the test compounds in YPD medium were prepared as followed. To each well of a sterile Greiner bio-one CellStar 96 well, U bottomed microtiter plate 100 μl of YPD was dispensed. Manually, 100 μl of stock compounds was delivered to each well in column 1. Then using a 8-channel pipette, compounds in column 1 were serially diluted 2-fold over the microtiter plate until column 11. The last column of the plate contained drug-free wells dedicated for growth and sterility controls for each organism tested.

The plates containing the diluted compounds were inoculated with 100µl of the appropriate microorganism. The yeast strains used were isolates obtained from the CBS-KNAW Fungal Biodiversity Centre (Utrecht, The Netherlands). The collection included *C. dubliensis*, *C. glabrata*, *C. tropicalis*, *C. parapsilosis*, *C. krusei* and two strains of *C. albicans*. Stock cultures of the yeast strains in liquid media (YPD + 15% glycerol) were maintained at -80°C. For use in this assay, yeast cultures were streaked on YPD agar plates and incubated for 24h at 30°C. Then, using a sterile disposable loop, cells from a colony were suspended in 5 mL of YPD media and aerated for 24h at 30°C on a shaker set at 300 rpm. The broth cultures were diluted 10 times with media and the optical density of this suspension was measured at a wavelength of 600 nm. The suspension was further diluted to an OD_{600} of 0.01 resulting in a concentration of (1-5) $\times$ 10^6 cfu/mL. This suspension was further diluted 1:100 in YPD media to yield (1-5) $\times$ 10^4 cfu/mL. This final dilution was used for inoculating the plates. Plates containing the diluted compounds were inoculated with 100 µL/ well of the appropriate microorganism using a 8-channel pipette. The final volume/well, including organism and compound was 200 µl. Thus, the final number of cells per well is approximately 5-25 x10^3 cfu/ml. Tests were incubated overnight at 30 °C prior to recording MICs. The in vitro activity was determined visually at 24h of incubation as the lowest concentration of compound resulting in full inhibition of yeast growth.

References and notes

1. Denning, D.W. *J. Antimicrob. Chemother*., **2002**, *49*, 889-891.
2. Examples of reviews discussing the β-(1,3)-D-glucan synthase complex: (*a*) Douglas, C.M. *Med. Mycol.*, **2001**, *39 Suppl. I*, 55-66; (*b*) Liu, J.; Balasubramanian, M.K. *Current Drug Targets – Infectious Disorders*, **2001**, *1*, 159-169; (*c*) Bowman, S.M.; Free, S.J. *BioEssays*, **2006**, *28*, 799-808; (*d*) Latgé, J.P. *Mol. Microbiol.*, **2007**, *66*, 279-290.
3. Leonard, W.R.; Belyk, K.M.; Conlon, D.A.; Bender, D.R.; DiMichele, L.M.; Liu, J.; Hughes, D.L. *J. Org. Chem.*, **2007**, *72*, 2335-2343.
4. Tomishima, M.; Ohki, H.; Yamada, A.; Maki, K.; Ikedia, F. *Bioorg. Med. Chem. Lett.*, **2008**, *18*, 2886-2890.
5. Norris, T.; VanAlsten, J.; Hubbs, S.; Ewing, M.; Cai, W.; Jorgensen, M.L.; Bordner, J.; Jensen G.O. *Org. Process Res. Dev.*, **2008**, *12*, 447-455.
6. For an excellent review of the total and semisynthetic approaches, see Renslo, A.R. *Anti-Infect. Agents Med. Chem.*, **2007**, *6*, 201-212.
7. Zambias, R.A.; Hammond, M.L.; Heck, J.V.; Bartizal, K.; Trainor, C.; Abruzzo, G.; Schmatz, D.M.; Nollstadt, K. M. *J. Med. Chem.*, **1992**, *35*, 2843-2855.
8. Klein, L.L.; Li, L.; Chen, H.; Curty, C.B.; DeGoey, D.A.; Grampovnik, D.J.; Leone, C.L.; Thomas, S.A.; Yeung, C.M.; Funk, K.W.; Kishore, V.; Lundell, E.O.; Wodka, D.; Meulbroek, J.A.; Alder, J.D.; Nilius, A.M.; Lartey, P.A.; Plattner, J.J. *Bioorg. Med. Chem. Lett.*, **2000**, *8*, 1677-1696.
9. Debono, M.; Abbott, B.J.; Turner, J.R.; Howard, L.C.; Gordee, R.S.; Hunt, A.S.; Barnhart, M.; Molloy, R.M.; Willard, K.E.; Fukuda, D.; Butler, T.F.; Zeckner, D.J. *Ann. N.Y. Acad. Sci.*, **1988**, *544*, 152-163.
10. Borromeo, P.S.; Cohen, J.D; Gregory, G.S.; Henle, S.K.; Hitchcock, S.A.; Jungheim, L.N.; Mayhugh, D.R.; Shepherd, T.A.; Turner, W.W. Jr., (Eli Lilly and Company). *US patent 6,653,281 B1*, **2003**.

11. Examples of on-resin RCM (*a*) Stymiest, J.L.; Mitchell, B.F.; Wong, S.; Vederas, J.C. *Org. Lett.* **2003**, *5*, 47-49; (*b*) Stymiest, J.L.; Mitchell, B.F.; Wong, S.; Vederas, J.C. *J. Org. Chem.*, **2005**, *70*, 7799-7809; (*c*) Elaridi, J.; Patel, J.; Jackson, W.R.; Robinson, A.J. *J. Org. Chem.*, **2006**, *71*, 7538-7545; (*d*) Jiang, S.; Li, P.; Lee, S.L.; Lin, C.Y.; Long, Y.; Johnson, M.D.; Dickson, R.B.; Roller, P.P. *Org. Lett.*, **2007**, *9*, 9-12; (*e*) Addona, D.D.; Carotenuto, A.; Novellino, E.; Piccand, V.; Reubi, J.C.; Cianni, A.D.; Gori, F.; Papini, A.M.; Ginanneschi, M. *J. Med. Chem.*, **2008**, *51*, 512-520.
12. Robinson, A.J.; Elaridi, J.; van Lierop, B.J.; Mujcinovic, S.; Jackson, W.R. *J. Pept. Sci.*, **2007**, *13*, 280-285.
13. Tam, J.P.; Wu, C.-R.; Liu, W.; Zhang, J.-W. *J. Am. Chem. Soc.*, **1991**, *113*, 6657-6662.
14. Caspofungin is present in and commercially available as “Cancidas” from Merck.
15. Debono, M.; Abbott, B.J.; Fukuda, D.S.; Barnhart, M.; Willard, K.E.; Molloy, R.M.; Michel, K.H.; Turner, J.R.; Butler, T.F.; Hunt, A.H. *J. Antibiot.*, **1989**, *XLII*, 389-397.
16. Taft, C.S.; Selitrennikoff, C.P. *J. Antibiot.*, **1990**, *XLIII*, 433-437.
17. Debono, M.; Turner, W.W.; LaGrandeur, L.; Burkhardt, F.J.; Nissen, J.S.; Nichols, K.K.; Rodriguez, M.J.; Zweifel, M.J.; Zeckner, D.J.; Gordee, R.S.; Tang, J.; Parr, T.R. *J. Med. Chem.*, **1995**, *38*, 3271-3281.
18. Jamison, J.A.; Rodriguez, M.J.; Vasudevan, V. *US Patent 6,670,324*, **2003**.
19. Jamison, J.A.; Zeckner, D.J.; Rodriguez, M.J. *J. Antibiot.*, **1997**, *50*, 562-566.
20. Miyaura, N.; Suzuki, A. *J. Chem. Soc. Chem. Commun.*, **1979**, 866-867.
21. Cody, R.B.; Laramée, J.A.; Durst, H.D. *Anal. Chem.*, **2005**, *77*, 2297–2302.
22. Scherer, S.; Haber, S. (Clariant GMBH), *Patent WO 00/50375*, **2000**.
23. Chhabra, S.R.; Hothi, B.; Evans, D.J.; White, P.D.; Bycroft, B.W.; Chan, W.C. *Tetrahedron Lett*., **1998**, *39*, 1603-1606.
24. Balkovec, J.M.; Black, R.M.; Hammond, M.L.; Hock, J.V.; Zambias, R.A.; Abruzzo, G.; Bartizal, K.; Kropp, H.; Trainor, C.; Schwartz, R.E; McFadden, D.C.; Nollstadt, K.H.; Pittarelli, L.A.; Powles, M.A.; Schmatz, D.M. *J. Med. Chem.*, **1992**, *35*, 194-198.
25. Bouffard, F.A.; Hammond, M.L.; Arison, B.H. *Tetrahedron Lett.*, **1995**, *36*, 1405-1408.
26. Bouffard, F.A; Zambias, R.A.; Dropinski, J.F.; Balkovec, J.M.; Hammond, M.L;, Abruzzo, G.K.; Bartizal, K.F.; Marrinan, J.A.; Kurtz, M.B.; McFadden, D.C.; Nollstadt, K.H.; Powles, M.A.; Schmatz, D.M. *J. Med.Chem.*, **1994**, *37*, 222-225.
27. Jamison, J.A.; LaGrandeur, L.M.; Rodriguez, M.J.; Turner, W.W.; Zeckner, D.J. *J. Antibiot.*, **1997**, *51*, 239-242.
28. Balkovec, J.M.; Dropinski, J.F.; Bouffard, F.A. *US Patent 5,741,775*, **1998**.
29. Rodriguez, J.M.; Nesler, M.J.; Zweifel, M.J. *US Patent 60/112,433*, **2000**.
30. Lal, B.; Gund, V.G.; Gangopadhyay, A.K.; Nadkarni, S.R.; Dikshit, V.; Chatterjee, D.K.; Shirvaikar, R. *Bioorg. Med. Chem.*, **2003**, *11*, 5189-5198.
31. Lal, B.; Gund, V.G. *Bioorg. Med. Chem. Lett.*, **2004**, *14*, 1123-1128.
32. Balkovec, J.M.; Dropinski, J.F.; Bouffard, F.A. *US Patent 6,268,338,* **1996**.
33. Wagner, M.; Heiner, S.; Kunz, H. *Synlett*, **2000**, *12*, 1753-1756.
34. Pfaller, M.A.; Diekema, D.J. *Clin. Microbiol. Rev.*, **2007**, *20*, 133-163.
35. Vojkovsky, T. *Pept. Res.*, **1995**, *8*, 236-237.
36. Kaiser, E.; Colescott, R.L.; Bossinger, L.D.; Cook, P.I. *Anal. Biochem.*, **1970**, *34*, 595-598.
37. Meienhofer, J.; Waki, M.; Heimer, E.P.; Lambros, T.J.; Makofske, R.C.; Chang, C.-D. *Int. J. Peptide Protein Res.,***1979**, *13*, 35.
38. When the peptide was cleaved using the standard TFA procedure, the TFA adduct of

the hydrazine amide was formed. Characterization of the TFA adduct was carried out by ESI-MS (calcd for $C_{63}H_{77}F_3N_{10}O_{14}$: 1254.56, found: m/z 1255.64 $[M+H]^+$).

CHAPTER 3

Approaches to the Use of Vinylglycine for the Preparation of Echinocandin Derivatives by Ring Closing Metathesis

3.1 Introduction

In the previous chapter it was found that a slight enlargement of the macrocyclic peptide backbone of the echinocandins has a tremendous influence on the antifungal activity. Even expansion of the peptide macrocycle by just one carbon atom completely abolished antifungal activity which was not expected in view of the resulting limited added flexibility to the peptide macrocycle.[1] This somewhat unexpected finding enticed us to investigate the synthesis of smaller RCM-derived mimics (**2**, Figure 1).

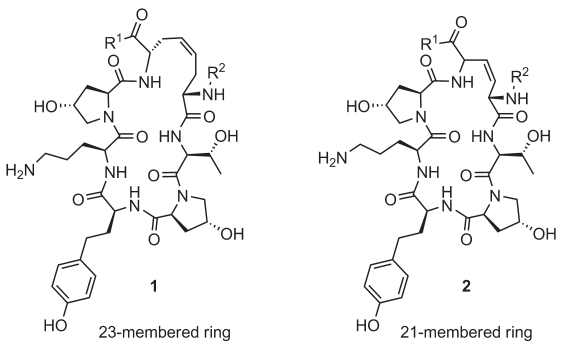

Figure 1. Previously described 23-membered RCM mimic (**1**)[1] and the new smaller 21-membered RCM mimic (**2**).

In mimic **2** the optimal 21-membered ring size is maintained. This new mimic (**2**) may be an attractive alternative since it still contains a position for further modification (i.e. the C-terminus; substituent R^1). This position could be interesting for the introduction of photolabels and as such these compounds can give more clues about the mechanism of action of the echinocandins.

To realize the synthesis of this mimic, RCM using vinylglycine containing precursors is envisioned. In this chapter attempts will be discussed towards the use vinylglycine in RCM reactions.

3.2 Results and Discussion

Several methods for the synthesis of vinylglycine (**3**) are available. Three years after the first racemic synthesis[2], the first synthesis producing the enantiomer **3** was published by Afzaliardakani and Rapoport[3]. In this approach, methionine was used as starting material for the synthesis of vinylglycine.[3-5] Many other syntheses of vinylglycine using optically active amino acids as starting chiral compound have been reported since then. Besides amino acids, such as homoserine[6,7], glutamic acid[8-10] and serine[11,12], also mannitol[13] and xylose[14] have been used as chiral building blocks for the synthesis of **3**.

The protocol of Rapoport et al.[3-5] was the first choice for the synthesis of vinylglycine (**3**) because it is short, efficient and more importantly, it avoids the use of poisonous reagents and heavy metal salts (Scheme 1) of other procedures.[6,7,10,14]

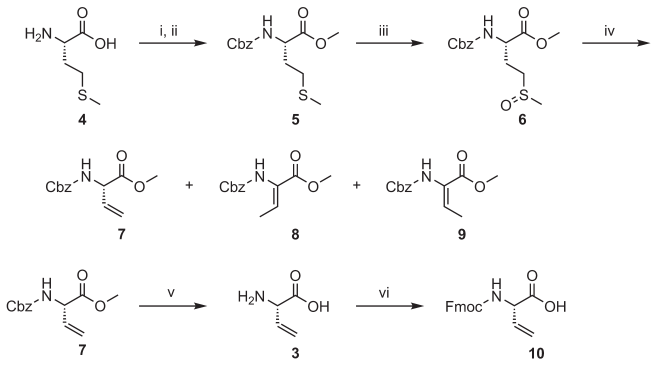

Scheme 1. Reagents and conditions: (i) $Me_2C(COMe)_2$, HCl, 87%; (ii) CbzCl, $NaHCO_3$, 88%; (iii) $NaIO_4$,MeOH, 0 °C, 99%; (iv) mesitylene, Δ, 65%; (v) 6 N HCl, Δ, 65%; (vi) FmocOSu, Et_3N, 74%.

Thus, L-methionine **4** was converted to its methyl ester and subsequent treatment with benzyl chloroformate under Schotten-Bauman conditions afforded the fully protected intermediate **5**. Then, oxidation of **5** was accomplished in quantitative yield to afford the sulfoxide **6**. Pyrolysis of sulfoxide **6** leading to elimination of methyl sulfenic acid gave the desired bond in **7** accompanied by the formation of *Z* and *E* isomers **8** and **9** by rearrangement of the double bond. The extent of this rearrangement could be limited by carrying out the elimination reaction in a solvent[15] rather than neat[3,4], to give the desired product in 65% yield after tedious separation by chromatography. Acid hydrolysis of **7** gave vinylglycine (VGly) **3** as its hydrochloride salt and final Fmoc protection afforded **10**.

Next, the obtained Fmoc-VGly-OH **10** was loaded onto the trityl resin. Unexpectedly, during the synthesis of our peptide **2** by SPPS it was found that the Kaiser test[16] was invariably positive when vinylglycine was incorporated into the sequence. As the resin sample has to be heated during the Kaiser test a possible explanation is migration of the double bond of vinylglycine **11** as is shown in Scheme 2. Then imine **13** is formed and will decompose to give carbamate **14** which will decompose to ammonia and react with ninhydrin in the Kaiser test.

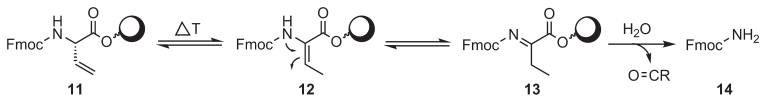

Scheme 2. Possible explanation of the false positive Kaiser test.

To verify if this migration occurs during SPPS or under Kaiser test conditions (Scheme 2), vinylglycine was coupled to the trityl resin (Scheme 3). Then the Fmoc group was cleaved, the *N*-terminus acetylated and the product cleaved from the resin. Subsequently the carboxylic acid was esterified and the product evaluated by NMR.

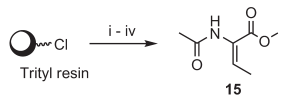

Scheme 3. Test reaction vinylglycine on trityl resin. Reagents and conditions: (i) Fmoc-VGly-OH (8), DIPEA, DCM; (ii) (1) 20% piperidine in NMP; (2) Capping solution: Ac_2O/HOBt/DiPEA/NMP; (iii) HFIP/DCM (1/4, v/v); (iv) MeOH, TMS-diazomethane.

By NMR the conjugated product **15** was found. Apparently the basic conditions used in the solid phase synthesis resulted in rearrangement of the double bond to the α,β-position. The rapid isomerization of the double bond can be explained by removal of the acidic Cα proton (Figure 2).

Figure 2. Base induced rearrangement of the double bond in vinylglycine.

To avoid this migration of the double bond and to avoid racemization vinylglycine was coupled as an amide to the rink resin and as a second residue on the trityl resin as is shown in Scheme 4. Since the α-proton is less acidic in amide, the amide of vinylglycine should be less sensitive to racemization and rearrangement of the double should be less likely to occur. In these cases predominantly (ca 60%) of the desired compounds **18** and **21** were formed.

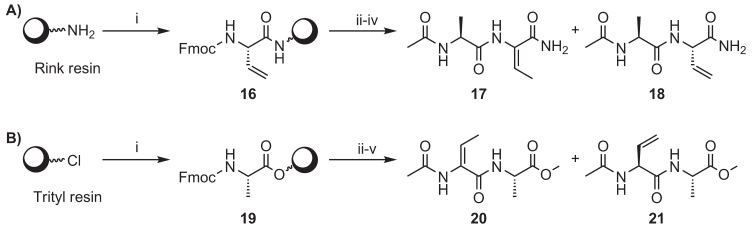

Scheme 4. Evaluation of effect on the migration of double bond when vinylglycine was coupled as an amide on solid phase.
A): As amide on the rink resin. Reagents and conditions: (i) (1) 20% piperidine in NMP; (2) Fmoc-VGly-OH (8), BOP, DiPEA, NMP; (ii) (1) 20% piperidine in NMP; (2) Fmoc-Ala-OH, BOP, DiPEA, NMP; (iii) (1) 20% piperidine in NMP; (2) Capping solution: Ac_2O/HOBt/DiPEA/NMP; (iv) TFA/TIS/H_2O (95/2.5/2.5; v/v/v).
B): As amide on the trityl resin. Reagents and conditions: (i) Fmoc-Ala-OH, DiPEA, DCM; (ii) (1) 20% piperidine in NMP; (2) Fmoc-VGly-OH (8), BOP, DiPEA, NMP; (iii) (1) 20% piperidine in NMP; (2) Capping solution: Ac_2O/HOBt/DiPEA/NMP; (iv) HFIP/DCM (1/4, v/v); (v) MeOH, TMS-diazomethane.

However, the tendency of vinylglycine to isomerize to the conjugated α,β unsaturated derivative complicated the synthesis of the echinocandin mimics severely. Therefore, a strategy was attempted in which the vinylglycine moiety is generated just before application of the metathesis conditions.

As discussed previously several methods exist for the synthesis of vinylglycine. For the 'masked' vinylglycine approach homoserine[7] was used as a starting chiral compound. Here *o*-nitrophenyl selenide **22** was used as a precursor for a terminal double bond as in vinylglycine. The *o*-nitrophenylselenoethyl functionality has proven to be a useful vinyl protecting group in other systems.[17,18] Moreover, deprotection can easily be accomplished under mild, non-basic conditions.[19,20] Therefore, *o*-nitrophenyl selenide **22** was used as a 'masked' vinylglycine derivative in solid phase synthesis. Problems with migration of the double bond in vinylglycine should be avoided and on resin selenium oxide elimination using H_2O_2 will give the olefin.

The 'masked' amino acid Fmoc-L-(2-nitro)phenylselenohomocysteine (Fmoc-hSec(*o*NO_2)Ph-OH) **22** could be easily prepared in three steps as shown in Scheme 5. In the first step, sodiumborohydride reduction of the isobutoxycarbonyl mixed anhydride of Boc-Asp-O*t*Bu

(**23**) proceeded smoothly and gave Boc-HSe-O*t*Bu (**24**) in 78% yield.[21] Subsequent treatment with Bu_3P, followed by addition of *o*-nitrophenyl selenocyanate of alcohol **24** afforded selenide **25**[20] in 74% yield by a Mitsunobu like reaction. Final deprotection of the Boc/*t*Bu protecting groups and subsequent protection with a Fmoc group gave 'masked' vinylglycine **22**.

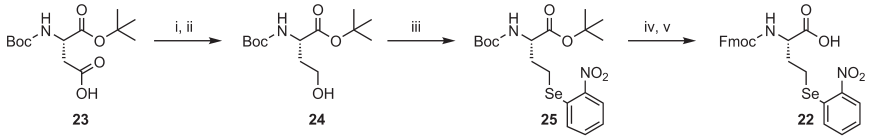

Scheme 5. Reagents and conditions: (i) $ClCO_2Bu$-*i*, NMM, THF; (ii) $NaBH_4$, MeOH, 0°C, 78%; (iii) 2-nitrophenylselenocyanate, Bu_3P, THF, 74%; (iv) TFA/DCM (1/1, v/v), 80%; (v) FmocOSu, Et_3N, 74%.

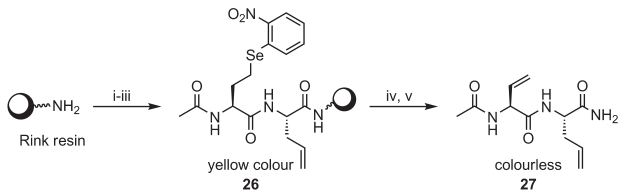

Scheme 6. Reagents and conditions: (i) (1) 20% piperidine in NMP; (2) Fmoc-Alg-OH, BOP, DiPEA, NMP; (ii) (1) 20% piperidine in NMP; (2) Fmoc-VGly(*o*NO_2PhSe)-OH (**22**), BOP, DiPEA, NMP; (iii) (1) 20% piperidine in NMP; (2) Capping solution: Ac_2O/HOBt/DiPEA/NMP; (iv) H_2O_2; (v) TFA/TIS/H_2O (95/2.5/2.5; v/v/v).

To test the use of 'masked vinylglycine' **22** in solid phase synthesis a dipeptide was synthesized on the rink resin as shown in Scheme 6. On Rink resin a dipeptide consisting of Fmoc-Alg-OH and 'masked' vinylglycine **22** was synthesized using SPPS. This resulted in a bright yellow coloured resin after the coupling of **22** to the resin. Then, the N-terminus was acetylated and the selenide oxidized with hydrogen peroxide to a selenoxide and elimination takes place with expulsion of *o*-nitrophenylselenol. This reaction can be easily monitored by the disappearance of the yellow colour from the resin after a few washing steps. Final cleavage from the resin gave the desired dipeptide **27**. None of the conjugated α,β unsaturated derivative was found proving that vinylglycine can be succesfully incorparated in a peptide sequence by using a 'masked' vinylglycine derivative (**22**).

For synthesis of peptide **2** the expensive building block homotyrosine needs to be used and therefore it was decided to use a different vinylglycine containing peptide test system for evaluation of the RCM conditions. For that the alkene-bridged B ring mimic of Nisin, which involved using a precursor containing two L-allylglycine residues, was choosen (Scheme 7).[22] Ring B of nisin is a cyclic pentapeptide with a Pro residue, which is known to induce β-turns. First, a precursor of a mimic of the Nisin ring B was synthesized having two Alg residues.[22] Second, a precursor of the Nisin B mimic was synthesized in which one Alg residue was replaced by a 'masked' vinylglycine **22** and a third Nisin B ring mimic precursor was synthesized with both Alg residues replaced by masked vinyl glycine derivative **22** as outlined in Scheme 7.

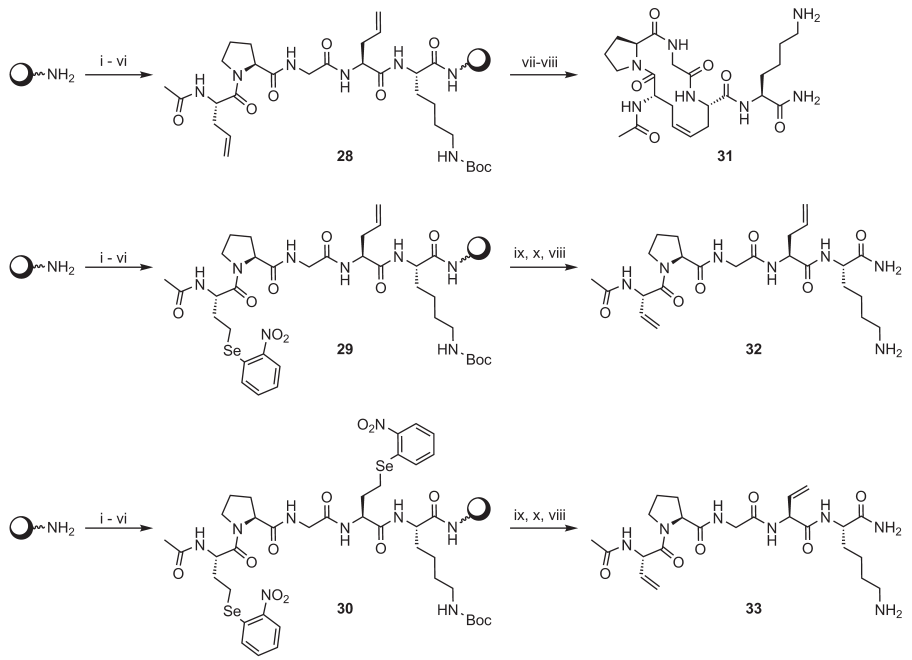

Scheme 7. Reagents and conditions: (i) (1) 20% piperidine in NMP; (2) Fmoc-Lys(Boc)-OH, BOP, DIPEA, NMP; (ii-v) (1) 20% piperidine in NMP; (2) Fmoc-Xxx-OH, BOP, DiPEA, NMP; (vi) (1) 20% piperidine in NMP; (2) Capping solution: Ac_2O/HOBt/DiPEA/NMP; (vii) Grubbs II (10 mol%), 10 vol% LiCl/DMA (0.4M), MW, 60 min, 100 °C, DCM; (viii) (1) TFA/TIS/H_2O (95/2.5/2.5, v/v/v); (ix) H_2O_2; (x) Grubbs II (10 mol%), 10 vol% LiCl/DMA (0.4M), MW, 75 min, 100 °C, DCM.

All three linear precursors (**28**-**30**) were synthesized on the rink resin by SPPS. Then, the two Nisin ring B mimics precursors **29** and **30** with 'masked' vinylglycine residues were treated with H_2O_2 to achieve liberation of vinylglycine. Subsequently, the three resin-bound peptides were treated with RCM conditions using a 10 mol% solution of Grubbs II in DCM (containing 10 vol% LiCl/DMA 0.4M) and exposed to microwave irradiation.[23] Finally, cleavage from the resin by acidolysis with concomitant removal of the side chain protecting groups, gave the desired cyclic peptide **31** as a mixture of *cis/trans* isomers and linear peptides **32** and **33**, which were not cyclized. Apparently, on resin RCM conditions for peptides containing VGly residues were unsuccessful. Employment of longer reaction times, larger amounts of catalyst and different catalysts (Grubbs I and Hoveyda Grubbs) did not lead to any cyclized product.

The lower reactivity of vinylglycine is probably due to steric effects. The sterically bulky amino acid moiety is hindering the approach of the catalytic ruthenium species to the double bond of the substrate.[24] This unreactivity in metathesis reactions of VGly residues was often attributed to the acidic Cα proton of the vinylglycine residue, leading to the formation of only α,β unsaturated compounds after exposure to the ruthenium based catalyst.[25] However, here in the NMR spectra this migration of the double bond in peptides **32** and **33** was not observed, as is apparent from Figure 3 showing the 500 MHz NMR spectrum of peptide **33**.

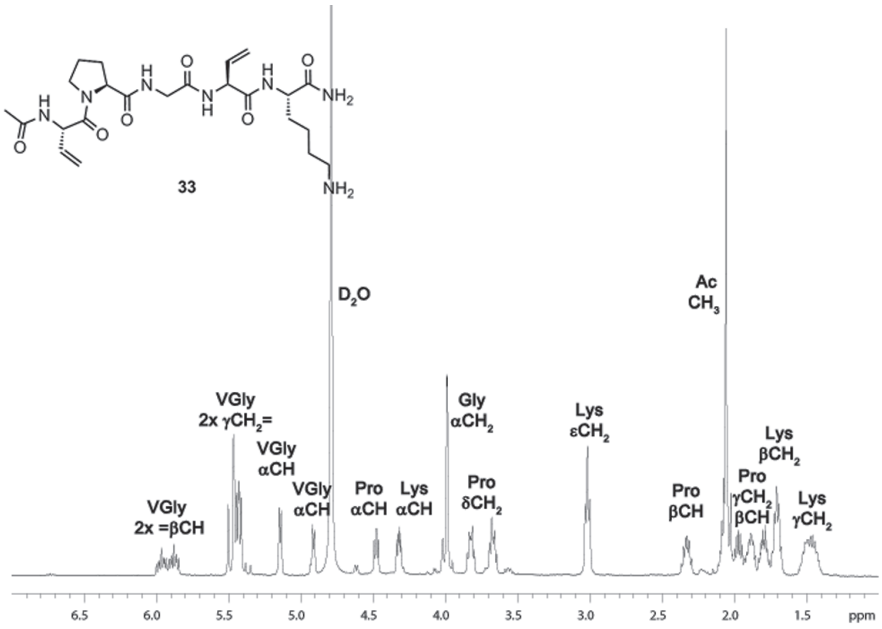

Figure 3. 500 MHz ^{1}H-NMR spectrum of the Nisin ring B precursor mimic **33** containing two VGly residues.

Due to these problems with RCM of vinylglycine residues we envisaged that our mimics might be prepared involving a cross metathesis reaction. Boons et al[26] have reported the cross metathesis reaction between a readily available allyl and vinyl glycine derivative (Scheme 8). This will give acces to a product (**37**) required for a 22-membered echinocandin mimic. For our desired 21-membered echinocandin mimic a cross metathesis reaction between two vinylglycine derivatives had to be performed. Due to the problems encountered earlier with vinylglycine residues the literature procedure of Boons leading to **37** (scheme 8) was followed first, after which the synthesis of a cross metathesis product between two vinylglycine residues was attempted.

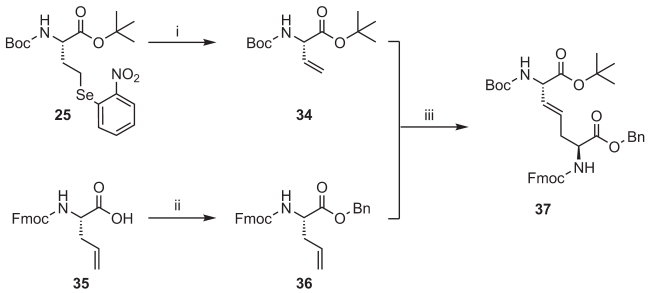

Scheme 8. Reagents and conditions: (i) H_2O_2, THF, 77%; (ii) BnBr, $NaHCO_3$, DMF, 91%; (iii) Grubbs II (10 mol%), DCM, 45%.

Boc-VGly-OtBu **34** was obtained by an oxidation/elimination step of **25**. Subsequently Fmoc-Alg-OH **35** was protected with a benzyl ester to afford **36.** Then, a reaction of Fmoc-Alg-OBn (**36**) with a two-fold excess of Boc-VGly-OtBu (**34**) in the presence of Grubbs II was attempted. Unfortunately, no product was found, only the homo-dimerized allylglycine and starting material **34**. After several unsuccessful attempts the group of Boons was contacted and it was found that the starting materials had to be very pure, especially vinylglycine **34**. Therefore, an additional purification was performed with column chromatography for compound **34**. The reaction now gave the expected cross coupling product **37** in 45% yield. Apart from the desired compound, unreacted vinylglycine was still present and homo-dimerized allylglycine was formed which could be easily separated from the product by column chromatography.

Now that the cross metathesis reaction described by Boons was moderately successful the desired cross metathesis reaction between two vinylglycine residues was carried out as is depicted in Scheme 9.

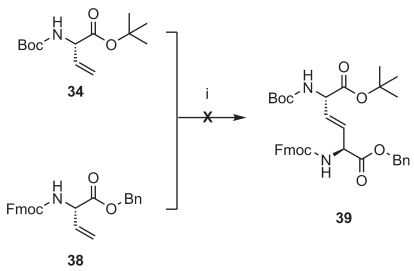

Scheme 9. Reagents and conditions: (i) Grubbs II (10 mol %), DCM.

As was already observed in the previous described cross metathesis reaction between Fmoc-Alg-OBn (**36**) and Boc-VGly-OtBu (**34**), the VGly residue was much less reactive than the Alg residue. Despite several attempts no desired compound (**39**) was obtained and only starting materials **34** and **38** were recovered. Employment of longer reaction times, larger amounts of catalyst and increasing reaction temperatures did not lead to any desired product.

Unfortunately the cross metathesis approach only gave access to a product (**37**) required for the synthesis of 22-membered echinocandin mimics. All attempts of cross metathesis reactions between two vinylglycine residues failed. In the previous chapter 2 it was shown that the ring size is crucial for activity and therefore further attempts to smaller echinocandin constructs by incorporating VGly in the sequence was terminated.

3.3 Conclusions

In summary, the use of vinylglycine for the construction of smaller caspofungin mimics involving RCM was studied. It was found that vinylglycine has a tendency to isomerize to the conjugated α,β-unsaturated derivative due to its acidic Cα proton. Therefore, the direct incorporation of vinylglycine into peptides turned out to be problematic. Alternatively, facile, site-specific and chemoselective incorporation of vinylglycine can be achieved via oxidative elimination of (2-nitro)-phenylselenohomocysteine. This 'masked'' amino acid was readily prepared in three steps and conveniently incorporated into peptides through SPPS. Convenient liberation of vinylglycine was accomplished by employing a chemoselective mild

oxidation with hydrogen peroxide. The reaction proved easy to monitor by a colour change from yellow to colorless upon oxidation of the resin bound peptide.

Although a successful strategy for the synthesis of vinylglycine containing peptides was described, their use in metathesis reactions, for the construction of smaller RCM echinocandin mimics by RCM, proved to be unsuccessful. It was found that the vinylglycine derivatives were not or less reactive under RCM and cross metathesis conditions as compared to allylglycine derivatives. Further attempts for the synthesis of 21-membered mimics by RCM were discontinued.

3.4 Experimental section

3.4.1 Reagents, materials and analysis methods

Unless stated otherwise, all chemicals were obtained from commercial sources and used as supplied, with the exception of DMF, NMP and DCM, which were dried on molecular sieves (4Å) prior to use. Fmoc protected amino acids were purchased from GL Biochem Ltd. (Shanghai, China). Rink resin was purchased from RAPP Polymere (Tübingen, Germany) and the 2-chlorotritylchloride PS resin was purchased from Hecheng Chemicals (Shanghai, China). All other reagents were purchased from Merck (Darmstadt, Germany), Sigma-Aldrich (Munich, Germany) and Acros (Geel, Belgium) and were used without further purification.

All Reactions were carried out at room temperature unless stated otherwise. Solid phase synthesis was performed in plastic syringes with a polyethylene frit. Microwave reactions were carried out on a Biotage Initiator system. Reactions in solution were monitored by TLC on Merck pre-coated Silica 60 plates. Spots were visualized by UV light, ninhydrin and K_2CO_3/$KMnO_4$. Solid phase reactions were monitored with the chloranil test[27] in case of secondary amines or with the Kaiser test[16] in case of primary amines. Column chromatography was performed using Silicycle UltraPure silicagel (40-63 μm).

^{1}H NMR spectra were recorded on a Varian G-300 (300 MHz) spectrometer and chemical shifts are given in ppm relative to TMS (0.00 ppm). ^{13}C NMR spectra were recorded using the attached proton test (APT) sequence on a Varian G-300 (75.5 MHz) spectrometer and chemical shifts are given in ppm relative to $CDCl_3$ (77.0 ppm). For measurements in DMSO, the residual solvent peak was used as a reference.

ESI-MS spectra were obtained in the positive ion mode on a Shimadzu QP8000 single quadrupole mass spectrometer.

3.4.2 Chemistry

General Procedures

<u>*Solid phase peptide synthesis:*</u> Peptides were synthesized manually. Each synthetic cycle consisted of the following steps:

Fmoc removal: The resin was treated with a 20% solution of piperidine in NMP (3×, each 10 min). The solution was removed by filtration and the resin was washed with NMP (3×, each

3 min) and DCM (3×, each 3 min).
Coupling step: A mixture of Fmoc-Xxx-OH (3 equiv.), BOP (3 equiv.) and DiPEA (6 equiv.) in NMP (10 mL/mmol resin bound peptide derivative)) was added to the resin and N_2 was bubbled through the mixture for 2h. The solution was removed by filtration and the resin washed with NMP (3×, each 3 min) and DCM (3×, each 3 min). Completion of the coupling reaction was verified with the Kaiser or chloranil test.
Capping of the remaining free amines: Capping solution [Ac_2O (50 mmol, 4.7 mL), HOBt (1.9 mmol, 220 mg), DiPEA (12.5 mmol, 2.2 mL) in 100 mL NMP] was added to the resin and N_2 was bubbled through the mixture for 20 min The solution was removed by filtration and the resin was washed with NMP (3×, each 3 min) and DCM (3×, each 3 min).

Microwave-assisted RCM: A microwave vessel containing a magnetic stirrer bead was loaded under argon with resin peptide, catalyst and solvent. The vessel was capped and irradiated at 100 °C. At the end of the reaction period the resin-bound peptide was washed with DMF (3× 3 mL, each 3 min) DCM (3× 3 mL, each 3 min) and MeOH (3× 3 mL, each 3 min).

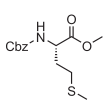

Cbz-(*S*)-methionine methyl ester (5)[3]
To a suspension of (*S*)-methionine **4** (17 g; 113.9 mmol) in 2,2-dimethoxypropane (575 mL) conc. aq. HCl (115 mL) was added. The solution was stirred over the weekend and concentrated in vacuo. Then, the crude product was dissolved in a minimal amount of MeOH and Et_2O was added until the product precipitated from the solution to afford pure methionine methyl ester hydrochloride (19.77 g; 87%). R_f = 0.47 (DCM/MeOH, 9/1, v/v); ^{1}H-NMR ($CDCl_3$, 300 MHz): δ = 8.80 (bd, 1H, NH), 4.40 (t, J=6.2 Hz, 1H, αCH), 3.84 (s, 3H, OCH_3), 2.86-2.71 (m, 2H, γCH_2), 2.44-2.35 (m, 2H, βCH_2), 2.13 (s, 3H, SCH_3) ppm; ^{13}C-NMR ($CDCl_3$, 75.5 MHz): δ = 170.0 (MeO-*C*O), 53.5 (αCH), 52.2 (OCH_3), 29.7 and 29.5 (CH_2), 15.2 (SCH_3).
Subsequently, to an ice-cold solution of (*S*)-methionine methyl ester hydrochloride (19 g; 95.14 mmol), $NaHCO_3$ (48 g; 570.84 mmol) in H_2O (500 mL) and EtOAc (500 mL) was added dropwise benzyl chloroformate (17 g; 99.9 mmol). The reaction mixture was stirred for 4h at RT, the organic layer was seperated, washed with 2M HCl (500 mL) and H_2O (500 mL), dried (Na_2SO_4) and concentrated. Crystallisation from petroleum ether afforded pure product **5** (24.78 g; 88%) as a white solid. R_f = 0.72 (DCM/MeOH, 50/1, v/v); ^{1}H-NMR ($CDCl_3$, 300 MHz): δ = 7.33 (m. 5H, Ar-H), 5.63 (d, J=8.0 Hz, 1H, NH), 5.10 (s, 2H, O*C*H_2Ar), 4.50-4.46 (m, 1H, αCH), 3.72 (s, 3H, OCH_3), 2.51 (t, J= 7.4 Hz, 2H, γCH_2), 2.15-2.01 (m, 1H, βCH_2), 2.06 (s, 3H, SCH_3), 2.0-1.91 (m, 1H, βCH_2) ppm; ^{13}C-NMR ($CDCl_3$, 75.5 MHz): δ = 172.6 (MeO-*C*O), 156.0 (NH*C*O), 136.2 (Ar-C), 128.6, 128.2 and 128.1 (Ar-CH), 67.1 (O*C*H_2Ar), 53.2 (αCH), 52.5 (OCH_3), 31.9 and 29.9 (CH_2), 15.4 (SCH_3).

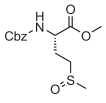

(*S*)-methyl-2-(benzyloxycarbonylamino)-4-(methylsulfinyl)butanoate (6)[3,4]
A solution of $NaIO_4$ (19 g; 88.78 mmol) in H_2O (100 mL) was added dropwise to an ice cooled solution of **5** (24 g; 80.71 mmol) in MeOH (250 mL). The cooling bath was removed and the foamy mixture stirred for 3 h. The precipitated sodiumiodate was filtered off and washed with MeOH, and the filtrate was partially concentrated in vacuo. Then, the mixture was extracted with DCM (3× 200 mL), the organic layer washed with H_2O (400 mL) and brine (400 mL), dried (Na_2SO_4), filtered and concentrated in *vacuo*. The resulting oil was dried, yielding sulfoxide **6** (25 g; 99%) as a waxy solid. R_f =

0.24 (DCM/MeOH, 50/1, v/v); ^{1}H-NMR ($CDCl_3$, 300 MHz): δ = 7.35 (m. 5H, Ar-H), 5.85-5.76 (m, 1H, NH), 5.11 (s, 2H, O*CH*$_2$Ar), 4.51-4.47 (m, 1H, αCH), 3.76 (s, 3H, OCH_3), 2.79-2.66 (m, 2H, γCH_2), 2.54 (s, 3H, SCH_3), 2.44-2.32 (m, 1H, βCH_2), 2.20-2.09 (m, 1H, βCH_2) ppm; ^{13}C-NMR ($CDCl_3$, 75.5 MHz): δ = 171.9 (MeO-*C*O), 156.2 (NH*C*O), 136.2 (Ar-C), 128.6, 128.2 and 128.1 (Ar-CH), 67.2 (O*CH*$_2$Ar), 53.2 (αCH), 52.8 (OCH_3), 50.2 (γCH_2), 38.5 (SCH_3), 25.7 (βCH_2).

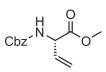

Cbz-(*S*)-vinylglycine methyl ester (7)[15]

A solution of sulfoxide **6** (15.7 g; 50.2 mmol) was refluxed in mesitylene (50 mL) for 20 h. After cooling to RT, the entire reaction was directly loaded onto a silica gel column and eluted with hexanes to remove mesitylene and then Hexane/EtOAc (4/1, v/v) to elute the product. Pure product **7** (8.11 g; 65%) was obtained as a yellowish oil. R_f = 0.33 (Hexane/EtOAc, 4/1, v/v); ^{1}H-NMR ($CDCl_3$, 300 MHz): δ = 7.36 (m, 5H, Ar-H), 6.00-5.85 (m, 1H, βCH=), 5.45 (br d, 1H, NH), 5.36 (dd, J=17.1 Hz, 1H, CH=*CH*$_{trans}$), 5.28 (dd, J=10.2 Hz, 1H, CH=*CH*$_{cis}$), 5.13 (s, 2H, O*CH*$_2$Ar), 4.99-4.89 (m, 1H, αCH), 3.77 (s, 3H, OCH_3) ppm; ^{13}C-NMR ($CDCl_3$, 75.5 MHz): δ = 171.9 (MeO-*C*O), 155.9 (NH*C*O), 136.2 (Ar-C), 132.4 (βCH=), 128.7, 128.3 and 128.2 (Ar-CH), 117.9 (γCH_2=), 67.2 (O*CH*$_2$Ar), 56.2 (αCH), 52.9 (OCH_3).

(*S*)-Vinylglycine (3)[3]

A mixture of Cbz-(*S*)-vinylglycine methyl ester **7** (8.11 g; 32.54 mmol) in 6 M HCl (165 mL) was refluxed for 1.5 h. The solution was cooled, extracted with DCM (2× 100 mL) and evaporated to dryness. Crystallization of the residue was achieved by refluxing in acetone (165 mL) to give vinylglycine **3** (2.89 g; 65%). ^{1}H-NMR (D_2O, 300 MHz): δ = 6.00-5.85 (m, 1H, βCH=), 5.58 (dd, J=13.2 Hz, 1H, γCH_2=), 4.60 (d, J=7.4 Hz, 1H, αCH) ppm; ^{13}C-NMR (D_2O, 75.5 MHz): δ = 173.8 (CO), 130.8 (βCH=), 125.6 (γCH_2=), 57.9 (αCH).

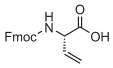

Fmoc-(*S*)-vinylglycine (10)

Vinylglycine **3** (3.58 g; 26 mmol) was dissolved in H_2O (150 mL) and the pH of the solution was adjusted to 9 with Et_3N. A solution of Fmoc-OSu (8.78 g; 26 mmol) in MeCN (150 mL) was added to this mixture. Stirring was continued for 2 h, and the pH was kept between 8 and 8.5 by adding Et_3N. Acetonitrile was removed and the residue was acidified to pH of 1-2 with 1M $KHSO_4$. The product precipitated from the mixture and was collected by filtration to afford **10** as white solid (6.25 g, 74 %). R_f = 0.33 (DCM/MeOH/AcOH, 20/1/0.1, v/v/v); ^{1}H-NMR ($CDCl_3$, 300 MHz): δ = 10.42 (bs, 1H, OH), 7.44 (d, J=7.4 Hz, 2H, Ar-H), 7.60-7.52 (m. 2H, Ar-H), 7.38 (t, J=7.3 Hz, 2H, Ar-H), 7.29 (t, J=7.3 Hz, 2H, Ar-H), 6.01-5.89 (m, 1H, βCH=), 5.32 (dd, J=17.8 Hz, 1H, CH=*CH*$_{trans}$), 5.24 (dd, J=9.1 Hz, 1H, CH=*CH*$_{cis}$), 5.0 (m, 1H, αCH), 4.64 (m, 1H, NH), 4.47-4.39 (m, 2H, CH_2Fmoc), 4.21 (t, J=6.5 Hz, 1H, CH Fmoc) ppm; ^{13}C-NMR ($CDCl_3$, 75.5 MHz): δ = 175.1 (CO), 156.0 (CO Fmoc), 143.8 and 141.5 (Ar-C), 131.9 (βCH=), 128.0, 127.3, 125.2 and 120.2 (Ar-CH), 118.5 (γCH_2=), 67.5 (CH_2 Fmoc), 56.2 (αCH), 47.3 (CH Fmoc).

(*E*)-methyl 2-acetamidobut-2-enoate (15)

Polystyrene resin functionalized with a 2-chlorotrityl chloride linker (1.10 mmol/g; 1g; 1.10 mmol) was loaded with Fmoc-VGly-OH **10** (711.35 mg; 1.10 mmol) in DCM (10 mL) in the presence of DiPEA (766 μL; 4.4 mmol) for 16h. After drying *in vacuo* overnight, the amount of Fmoc-VGly-OH coupled to the resin was determined by an Fmoc determination according to Meienhofer et al.[28] and was found to be 0.485 mmol/g.

Subsequently, unreacted tritylchloride moieties were capped with methanol (DCM/MeOH/DiPEA; 3× 5 mL, each 2 min; 17/2/1; v/v/v). The Fmoc group was cleaved and the free amines were acetylated by treatment with capping reagent according to the general procedure for solid phase peptide synthesis. The linear peptide was released from the resin by treatment of the resin with HFIP/DCM (6 mL, 1/1, v/v) for 2h and concentrated. The peptide was then dissolved in MeOH (2 mL) and TMS-diazomethane (1 mL) was added until the reaction mixture remained yellow. The reaction mixture was purified by column chromatography (DCM/MeOH/AcOH, 9/1/0.1, v/v/v) to afford peptide **15** (78.4 mg; 45%). R_f = 0.62 (DCM/MeOH/AcOH, 9/1/0.1, v/v/v); ^{1}H-NMR ($CDCl_3$, 300 MHz): δ = 6.79-6.72 (m, 1H, C=*CH*CH_3), Ar-H), 3.69 (s, 3H, OCH_3), 2.05 (s, 3H, CH_3 Ac), 1.70 (d, J=7.2 Hz, 3H, C=CH*CH_3*) ppm.

Ac-Ala-VGly-NH_2 (18)

Fmoc-Rink-Tentagel resin (1 g; 0.24 mmol) was loaded with Fmoc-VGly-OH (155.2 mg; 0.48 mmol) according to the general procedure for solid phase peptide synthesis. After drying *in vacuo* overnight, the amount of Fmoc-VGly-OH coupled to the resin was determined by an Fmoc determination according to Meienhofer[28] and was found to be 0.21 mmol/g. The dipeptide was synthesized further following the general procedure for solid phase peptide synthesis and released from the resin by treatment with TFA/TIS/H_2O (3 mL, 95/2.5/2.5, v/v/v) for 2h. The peptide was precipitated in MTBE/hexane (1/1), the supernatant was removed and the crude peptide was washed twice with MTBE/hexane (1/1) and dried in vacuo. According to NMR a mixture of **17** and **18**.

Ac-VGly-Ala-OMe (21)

A polystyrene resin functionalized with a 2-chlorotrityl chloride linker (1.10 mmol/g; 1g; 1.10 mmol) was loaded with Fmoc-Ala-OH (684.9 mg; 1.10 mmol) in DCM (10 mL) in the presence of DiPEA (766 μL; 4.4 mmol) for 16h. After drying *in vacuo* overnight, the amount of Fmoc-Ala-OH coupled to the resin was determined by an Fmoc determination according to Meienhofer[28] and was found to be 0.428 mmol/g. Subsequently, unreacted tritylchloride moieties were capped with methanol (DCM/MeOH/DiPEA; 3× 5 mL, each 2 min; 17/2/1; v/v/v). Then, following the general procedure for solid phase peptide synthesis, the Fmoc group was cleaved, Fmoc-VGly-OH coupled, followed by again cleavage of the Fmoc and acetylation of the free amines by treatment with capping reagent. The linear peptide was released from the resin by treatment of the resin with HFIP/DCM (6 mL, 1/1, v/v) for 2h and concentrated. The peptide was then dissolved in MeOH (2 mL) and TMS-diazomethane (1.15 mL) was added until the reaction mixture remained yellow. The reaction mixture was purified by column chromatography to afford the conjugated product **20** (49.2 mg; 27%) and the desired dipeptide **21** (67.8 mg; 20%). R_f **20**= 0.53 (DCM/MeOH/AcOH, 9/1/0.1, v/v/v); ^{1}H-NMR ($CDCl_3$, 300 MHz): δ = 7.78 (s, 1H, NH), 7.05 (d, J=6.9 Hz, 1H, NH Ala), 6.46-6.39 (q, 1H, C=*CH*CH_3), 4.62-4.54 (m, 1H, αCH Ala), 3.75 (s, 3H, OCH_3), 2.10 (s, 3H, CH_3 Ac), 1.70 (d, J=7.2 Hz, 3H, C=CH*CH_3*), 1.42 (d, J=7.2 Hz, 3H, CH_3 Ala) ppm; ^{13}C-NMR ($CDCl_3$, 75.5 MHz): δ = 173.9, 169.7 and 165.3 (CO), 130.1 (*C*=$CHCH_3$), 129.1 (C=*CH*CH_3), 52.6 (OCH_3), 48.6 (αCH Ala) 23.2 (CH_3 Ac), 18.0 (CH_3 Ala), 13.8 (C=CH*CH_3*). R_f **21**= 0.57 (DCM/MeOH/AcOH, 9/1/0.1, v/v/v); ^{1}H-NMR ($CDCl_3$, 300 MHz): δ = 7.49 (d, J=7.2 Hz, 1H, NH Ala), 7.14 (d, J=7.7 Hz, 1H, NH VGly), 5.92-5.81 (m, 1H, βCH= VGly), 5.39 (dd, J=16.2 Hz, 1h, $CH=CH_{trans}$), 5.26 (dd, J=11.2 Hz, 1H, $CH=CH_{cis}$), 5.23-5.19 (m, 1H, αCH Vgly), 4.58-4.48 (m, 1H, αCH Ala), 3.74 (s, 3H, OCH_3), 2.04 (s, 3H, CH_3 Ac), 1.42 (d, J=7.2 Hz, 3H, CH_3 Ala) ppm; ^{13}C-NMR ($CDCl_3$, 75.5 MHz): δ =

173.1, 170.2 and 170.0 (C=O), 133.6 (βCH= VGly), 118.2 (γCH_2= VGly), 55.5 (αCH Vgly), 52.5 (OCH_3), 48.5 (αCH Ala), 23.1 (CH_3 Ac), 17.9 (CH_3 Ala).

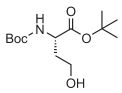

Boc-(*S*)-homoserine *t*-butyl ester (24)[21]

To a cooled solution of Boc-Asp-O*t*Bu **23** (10.81 g; 37.35 mmol) in THF (40 mL) at -15°C NMM (4.11 mL; 37.35 mmol) and isobutylchloroformate (4.84 mL; 37.35 mmol) were added. After an activation period of 10 min, the precipitate NMM.HCl was removed by filtration and the solid washed with cold THF. $NaBH_4$ (2.83 g; 74.70 mmol) was added to the solution in one portion followed by the dropwise addition of MeOH (40 mL) at 0°C over 1h. A solution of 1 N HCl (50 mL) was added and the mixture was extracted with Et_2O (3× 100 mL). The combined organic layer was washed with 1 N HCl (3× 100 mL), 5% $NaHCO_3$ (3× 100 mL), and H_2O (3× 100 mL). The organic layer was dried (Na_2SO_4), filtered and concentrated in *vacuo* yielding product **24** (8.05 g; 78%) as a clear oil. R_f = 0.52 (Hexane/acetone, 7/3, v/v); ^{1}H-NMR ($CDCl_3$, 300 MHz): δ = 5.38 (d, J=7.7 Hz, 1H, NH), 4.39-4.32 (m, 1H, αCH), 3.76-3.60 (m, 2H, γCH), 2.20-2.09 (m, 1H, βCH_2), 1.59-1.49 (m, 1H, βCH_2), 1.47 (s, 9H, *t*Bu), 1.45 (s, 9H, *t*Bu) ppm; ^{13}C-NMR ($CDCl_3$, 75.5 MHz): δ = 172.2 (CO *t*Bu), 156.8 (CO Boc), 82.5 and 80.5 (C *t*Bu), 58.4 (γCH_2), 51.0 (αCH), 36.7 (βCH_2), 28.4 and 28.2 (CH_3).

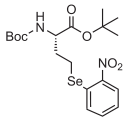

(*S*)-*tert*-Butyl 2-Boc-amino-4-(2-nitrophenylselenyl)butanoate (25)[7]

To a solution of 2-NO_2PhSeCN (19.92 g; 87.71 mmol) and homoserine derivative **24** (8.05 g; 29.24 mmol) in THF (distilled over $LiAlH_4$, 350 mL) under N_2 a solution of Bu_3P (8.87 g; 43.85 mmol) in THF (distilled over $LiAlH_4$, 250 mL) was added dropwise over 30 min. The reaction was stirred for 16h and the mixture was concentrated in vacuo. The residue was redissolved in Et_2O (350 mL) and washed with brine (2× 350 mL) and H_2O (350 mL). The combined organic layers were dried (Na_2SO_4), filtered and concentrated in *vacuo*. Pure product **25** (9.9 g; 74%) was obtained after column chromatography (Hexanes/Et_2O, 9/1, v/v) as a yellow solid. R_f = 0.23 (Hexane/Et_2O, 7/3, v/v); ^{1}H-NMR ($CDCl_3$, 300 MHz): δ = 8.31-8.28 (m, 1H, Ar-H), 7.56-7.46 (m, 2H, Ar-H), 7.35-7.27 (m, 1H, Ar-H), 5.23 (bs, 1H, NH), 4.31 (bs, 1H, αCH), 3.03-2.85 (m, 2H, γCH_2), 2.33-2.25 (m, 1H, βCH), 2.12-2.02 (m, 1H, βCH), 1.49 (s, 9H, *t*Bu), 1.47 (s, 9H, *t*Bu) ppm; ^{13}C-NMR ($CDCl_3$, 75.5 MHz): δ = 171.0 (CO *t*Bu), 155.6 (CO Boc), 147.0 and 133.2 (Ar-C), 133.9, 128.9, 126.7 and 125.7 (Ar-CH), 82.8 and 80.2 (C *t*Bu), 54.6 (αCH), 32.5 (γCH_2), 28.5 and 28.2 (CH_3), 21.5 (βCH_2).

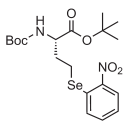

(*S*)-2-Fmoc-amino-4-(2-nitrophenylselenyl)butanoate (22)

A mixture of DCM/TFA (2/1, v/v, 50 mL) was added dropwise to a solution of **25** (2.68 g; 5.83 mmol) in dry DCM (30 mL). The mixture was stirred overnight and concentrated. H_2O (100 mL) was added and washed with Et_2O (100 mL) to remove the *tert*-butyl impurities. The H_2O layer was concentrated to a minimal amount and stored at 4 °C overnight. The yellow precipitate was filtered off to afford pure product (1.41 g; 80%) as a yellow solid. R_f = 0.29 (DCM/MeOH/AcOH, 9/1/0.1, v/ v/v). To a suspension of the unprotected hSec(*o*NO_2)Ph (1.41 g; 4.65 mmol) was in H_2O (20 mL) Et_3N was added untill the pH of the solution was 9. A solution of Fmoc-OSu (1.57 g; 4.65 mmol) in MeCN (10 mL) was added to this mixture. The suspension was stirred overnight. Acetonitrile was removed and the residue was acidified to a pH of 1-2 with 1M HCl and extracted with

EtOAc (3× 20 mL). The combined organic layers were dried (Na_2SO_4), filtered and concentrated in *vacuo*. Pure Fmoc-derivative **22** (1.81 g; 74%) was obtained by crystallization in EtOAc. R_f = 0.62 (DCM/MeOH/AcOH, 9/1/0.1, v/v/v); ^{1}H-NMR (DMSO, 300 MHz): δ = 8.28 (dd, J=8.3 Hz, 1H, Ar-H), 7.90 (d, J=7.7 Hz, 1H, Ar-H), 7.80-7.64 (m, 5H, Ar-H + NH), 7.50-7.29 (m, 5H, Ar-H), 4.34-4.11 (m, 4H, CH + CH_2 Fmoc, αCH), 3.04 (t, J=7.6 Hz, 2H, γCH_2), 2.10-2.04 (m, 2H, βCH_2) ppm; ^{13}C-NMR (DMSO, 75.5 MHz): δ = 173.2 and 156.2 (CO), 146.5, 143.7, 140.7 and 131.6 (Ar-C), 134.5, 129.5, 127.6, 127.0, 126.4, 126.2, 125.2 and 120.1 (Ar-CH), 65.6 (CH_2 Fmoc), 53.8 (αCH), 46.7 (CH Fmoc), 30.2 and 22.1 (CH_2).

Ac-VGly-Alg-NH_2 (27)

Linear peptide Ac-[*o*NO_2PhSe]VGly-Alg-NH_2 (**26**) was synthesized on Fmoc-Rink-Tentagel resin (1 g; 0.25 mmol) according to the general procedure for solid phase peptide synthesis. A trial cleavage of **26** and analysis on TLC showed an R_f value of 0.50 (DCM/MeOH/AcOH, 9/1/0.1,v/ v/v). Subsequently, the resulting yellow resin-bound peptide **26** (200 mg; 50 μmol) in THF (2 mL) was cooled to -2°C and treated with H_2O_2 (30%; 0.5 mL). The mixture was shaken overnight and the resin was washed with THF (6×) and DCM (6×). The yellow color of the resin disappeared during these washing steps. The peptide was cleaved from the resin by treatment with TFA/TIS/H_2O (2 mL, 95/2.5/2.5, v/v/v) for 2h. The peptide was precipitated in MTBE/hexane (1/1), the supernatant was removed and peptide **27** was washed twice with MTBE/hexane (1/1) and dried in vacuo.

R_f = 0.21 (DCM/MeOH/AcOH, 9/1/0.1,v/ v/v); ^{1}H-NMR (DMSO, 300 MHz): δ = 8.20 (d, J=7.7 Hz, 1H, NH VGly), 7.98 (d, J=8.0 Hz, 1H, NH Alg), 7.30 (s, 1H, NH_2), 7.07 (s, 1H, NH_2), 5.90-5.81 (m, 1H, βCH= VGly), 5.79-5.64 (m, 1H, γCH= Alg), 5.30-5.00 (m, 4H, δCH_2= Alg, γCH_2= VGly), 4.89 (t, J=6.0 Hz, 1H, αCH VGly), 4.27-4.21 (m, 1H, αCH Alg), 2.45-2.25 (m, 2H, βCH_2 Alg), 1.88 (s, 3H, CH_3 Ac) ppm; ^{13}C-NMR (DMSO, 75.5 MHz): δ = 172.5, 169.3 and 169.1 (C=O), 134.5 and 134.1 (CH=), 117.4 and 116.4 (CH_2=), 55.2 and 52.0 (αCH), 36.2 (βCH Alg), 22.4 (CH_3 Ac).

Ac-*Cyclo*[Alg-Pro-Gly-Alg]-Lys-NH_2 (31)

The linear peptide Ac-Alg-Pro-Gly-Alg-Lys-NH_2 (2**8**) was synthesized on Fmoc-Rink-Tentagel resin (1 g; 0.25 mmol) according to the general procedure for solid phase peptide synthesis. ESI-MS calcd for TFA deprotected **28** $C_{25}H_{41}N_7O_6$: 535.31, found: m/z 538.85 $[M+H]^+$; R_f = 0.67 ($CHCl_3$/MeOH/NH_3, 60/45/20, v/v/v). The resulting resin-bound peptide **28** was subjected to the general microwave-assisted RCM procedure under the following conditions: Resin-bound peptide (200 mg; 50 μmol), DCM (2 mL), LiCl/DMA (degassed; 0.4M; 0.18 mL), Grubbs II (10 mol%; 4.2 mg; 5 μmol), 100 °C for 60 min.[23] The peptide was cleaved from the resin by treatment with TFA/TIS/H_2O (2 mL, 95/2.5/2.5, v/v/v) for 2h. The peptide was precipitated in MTBE/hexane (1/1), the supernatant was removed and peptide **31** was washed twice with MTBE/hexane (1/1) and dried in vacuo. ESI-MS calcd for **31** $C_{23}H_{37}N_7O_6$: 507.28, found: m/z 508.30 $[M+H]^+$; R_f = 0.49 ($CHCl_3$/MeOH/NH_3, 60/45/20, v/v/v).

Ac-VGly-Pro-Gly-Alg-Lys-NH_2 (32)

The linear peptide Ac-[*o*NO_2PhSe]VGly-Pro-Gly-Alg-Lys-NH_2 (**29**) was synthesized on Fmoc-Rink-Tentagel resin (1 g; 0.25 mmol) according to the general procedure for solid phase peptide synthesis. ESI-MS calcd for TFA deprotected **29** $C_{30}H_{44}N_8O_8Se$: 724.24, found: m/z 725.20 $[M+H]^+$. Subsequently, the resulting yellow resin-bound peptide **29** (200 mg; 50

μmol) in THF (2 mL) was cooled to -2°C and treated with H_2O_2 (30%; 0.5 mL). The mixture was shaken overnight and the resin was washed with THF (6×) and DCM (6×). The yellow color of the resin disappeared during these washing steps. And the resin bound peptide was subjected to the general microwave-assisted RCM procedure under the following conditions: Resin-bound peptide (200 mg; 50 μmol), DCM (2 mL), LiCl/DMA (degassed; 0.4M; 0.18 mL), Grubbs II (10 mol%; 4.2 mg; 5 μmol), 100 °C for 60 min. The peptide was released from the resin by treatment with TFA/TIS/H_2O (2 mL, 95/2.5/2.5, v/v/v) for 2h. The peptide was precipitated in MTBE/hexane (1/1), the supernatant was removed and peptide **32** was washed twice with MTBE/hexane (1/1) and dried in vacuo. ESI-MS calcd for **32** $C_{24}H_{39}N_7O_6$: 521.30, found: m/z 523.20 $[M+H]^+$.

Ac-VGly-Pro-Gly-VGly-Lys-NH_2 (33)

Peptide **33** was obtained analogous to peptide **32**. Only during the oxidation step the resin was treated with a double amount of H_2O_2 (30%; 1 mL) due to the presence of two [*o*NO_2PhSe]VGly residues. ESI-MS calcd for TFA deprotected **30** $C_{35}H_{47}N_9O_{10}Se_2$: 913.18, found: m/z 913.90 $[M+H]^+$. ESI-MS calcd for **33** $C_{23}H_{37}N_7O_6$: 507.28, found: m/z 508.27 $[M+H]^+$; ^{1}H-NMR (D_2O, 500 MHz): δ = 5.99-5.91 (m, 1H, βCH= VGly), 5.91-5.85 (m, 1H, βCH= VGly), 5.50-5.38 (m, 4H, 2x, γCH_2= VGly), 5.15 (d, J=6.3 Hz, 1H, αCH VGly), 4.91 (d, J=6.3 Hz, 1H, αCH VGly), 4.48 (t, 1H, αCH Pro), 4.31 (q, 1H, αCH Lys), 3.99 (s, 2H, αCH_2 Gly), 3.85-3.80 (m, 1H, δCH_2 Pro), 3.69-3.65 (m, 1H, δCH_2 Pro), 3.02 (t, J=7.6 Hz, 2H, εCH_2 Lys), 2.37-2.30 (m, 1H, βCH_2 Pro), 2.09-2.03 (m, 2H, δCH_2 Lys), 2.06 (s, 3H, CH_3 Ac), 2.01-1.96 (m, 1H, βCH_2 Pro), 1.92-1.87 (m, 1H, γCH_2 Pro), 1.83-1.76 (m, 1H, γCH_2 Pro), 1.74-1.68 (m, 2H, βCH_2 Lys), 1.53-1.44 (m, 2H, γCH_2 Lys) ppm; ^{13}C-NMR (D_2O, 125 MHz): δ = 131.0 and 130.1 (βCH= VGly), 120.5 and 120.1 (γCH_2= VGly), 60.6 (αCH Pro), 56.1 and 54.3 (αCH VGly), 53.0 (αCH Lys), 47.3 (δCH_2 Pro), 42.0 (αCH_2 Gly), 38.7 (εCH_2 Lys), 29.7 (γCH_2 Pro), 28.7 (βCH_2 Pro), 25.6 (βCH_2 Lys), 24.1 (δCH_2 Lys), 21.6 (γCH_2 Lys), 21.0 (CH_3 Ac).

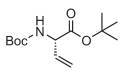

Boc-(*S*)-vinylglycine *tert*-butyl ester (34)

Selenide **25** (4.08 g; 8.88 mmol) was dissolved in THF (300 mL), cooled to -5°C, and treated with H_2O_2 (30%; 75 mL). After 30 min the reaction mixture was quenched with $Na_2S_2O_3$, H_2O (200 mL) was added and the solution extracted with Et_2O (3× 200 mL). The combined organic layers were dried (Na_2SO_4), filtered and concentrated in *vacuo*. Pure product **34** (1.78 g; 77%) was obtained after column chromatography (Hexane/Et_2O, 7/3, v/v). R_f = 0.56 (Hexane/Et_2O, 7/3, v/v); ^{1}H-NMR ($CDCl_3$, 300 MHz): δ = 5.95-5.80 (m, 1H, βCH=), 5..33 (dd, J=17.1 Hz, 1H, CH=CH_{trans}), 5.22 (dd, J=10.5 Hz, 1H, CH=CH_{cis}), 4.80-4.68 (m, 1H, αCH), 1.47 (s, 9H, *t*Bu), 1.45 (s, 9H, *t*Bu) ppm.

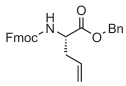

Fmoc-(*S*)-allylglycine benzyl ester (36)

To a stirred solution of Fmoc-Alg-OH **35** (10 g; 29.6 mmol) in dry DMF (150 mL), $NaHCO_3$ (6.23 g; 74.1 mmol) and benzyl bromide (10.6 mL; 88.9 mmol) were added. The reaction mixture was stirred for 48h, diluted with H_2O (200 mL) and extracted with DCM (3× 150 mL). The combined organic layer was washed with H_2O (2× 150 mL), sat $NaHCO_3$ (150 mL) and brine (150 mL) and then dried (Na_2SO_4), filtered and concentrated in *vacuo*. The product was precipitated by adding cold hexane (250 mL) and stirring vigourously untill precipitation was complete to afford **36** as a white solid (11.47 g, 91 %). R_f = 0.33 (Hexane/EtOAc, 5/1, v/v); ^{1}H-NMR ($CDCl_3$, 300 MHz): δ = 7.75 (d, J=7.4 Hz, 2H, Ar-H), 7.58

(d, J=7.2 Hz, 2H, Ar-H), 7.42-7.24 (m. 9H, Ar-H), 5.70-5.59 (m, 1H, γCH=), 5.35 (d, J=7.7 Hz, 1H, NH), 5.23-5.06 (m, 4H, OCH_2Ar, δCH_2=), 4.53-4.49 (m, 1H, αCH), 4.38 (d, J=6.9 Hz, 2H, CH_2Fmoc), 4.22 (t, J=6.6 Hz, 1H, CH Fmoc), 2.61-2.52 (m, 2H, βCH_2) ppm; ^{13}C-NMR ($CDCl_3$, 75.5 MHz): δ = 171.8 (BnO-CO), 155.9 (CO Fmoc), 143.9, 141.5 and 135.4 (Ar-C), 132.1 (γCH=), 128.8, 128.7, 128.6, 127.9, 127.2, 125.3 and 120.2 (Ar-CH), 119.7 (δCH_2=), 67.4 and 67.3 (CH_2 Fmoc and OCH_2Ar), 53.5 (αCH), 47.3 (CH Fmoc), 36.9 (βCH_2).

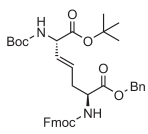

(2*S*,6*S*,*E*)-7-benzyl 1-*tert*-butyl 6-(Fmoc-amino)-2-(Boc-amino)hept-3-ene-dioate (37)

Grubbs II catalyst (28 mg; 0.033 mmol) was added to a solution of Fmoc-Alg-OBn **36** (140.9 mg; 0.33 mmol) and Boc-VGly-O*t*Bu **34** (169.6 mg; 0.66 mmol) in DCM (2 mL). The reaction mixture was refluxed overnight and concentrated. Pure cross metathesis product **37** (98 mg; 45%) was obtained after column chromatography (Hexane/EtOAc, 7/1, v/v). ^{1}H-NMR ($CDCl_3$, 300 MHz): δ = 7.75 (d, J=7.4 Hz, 2H, Ar-H), 7.60 (d, J=7.2 Hz, 2H, Ar-H), 7.42-7.26 (m. 9H, Ar-H), 5.75-5.60 (m, 2H, 2× CH=), 5.55 (d, 1H, NH), 5.20 (d, 2H, OCH_2Ar), 5.10 (m, 1H, NH), 5.0-4.92 (m, 1H, αCH VGly), 4.45-4.34 (m, 2H, CH_2Fmoc), 4.32-4.18 (m, 2H, CH Fmoc, αCH Alg), 2.62-2.50 (m, 1H, βCH_2 Alg), 2.50-2.38 (m, 1H, βCH_2 Alg), 1.48 (s, 9H, *t*Bu), 1.45 (s, 9H, *t*Bu) ppm.

References and notes

1. Mulder, M.P.C.; Kruijtzer, J.A.W.; Breukink, E.J.; Kemmink, J.; Pieters, R.J., Liskamp, R.M.J. *Bioorg. Med. Chem.*, **2011**, *19*, 6505-6517.
2. Baldwin, J.E.; Haber, S.B.; Hoskins, C.; Kruse L.I. *J. Org. Chem.*, **1977**, *42*, 1239-1241.
3. Afzaliardakani, A.; Rapoport, H. *J. Org. Chem.*, **1980**, *45*, 4817-4820.
4. Carrasco, M.; Jones, R.J.; Kamel, S.; Rapoport, H.; Truong, T. *Org. Synth.*, **1992**, *70*, 29-31.
5. Küchenthal, C.H.; Migenda, J.; Polednia, M.; Maison, W. *Amino Acids*, **2010**, *39*, 443-448.
6. Itaya, T.; Shimizu, S.; Nakagawa, S.; Morisue, M. *Chem. Pharm. Bull.*, **1994**, *42*, 1927-1930.
7. Siebum, A.H.G.; Woo, W.S.; Raap, J.; Lugtenburg, J. *Eur. J. Org. Chem.*, **2004**, 2905-2913.
8. Hanessian, S.; Sahoo, S.P. *Tetrahedron Lett.*, **1984**, *25*, 1425-1428.
9. Barton, D.H.R.; Crich, D.; Hervé, Y.; Potier, P.; Thierry, J. *Tetrahedron*, **1985**, *41*, 4347-4357.
10. Krol, W.J.; Mao, S.S.; Steele, D.L.; Townsend, C.A. *J. Org. Chem.*, **1991**, *56*, 728-731.
11. Beaulieu, P.L.; Duceppe, J.S.; Johnson, C. *J. Org. Chem.*, **1991**, *56*, 4196-4204.
12. Rose, N.G.W.; Blaskovich, M.A; Wong, A.; Lajoie, G.A. *Tetrahedron*, **2001**, *57*, 1497-1507.
13. Badorrey, R.; Cativiela, C.; Díaz-de-Villegas, M.; Gálvez, J. *Synthesis*, **1997**, 747-749.
14. Chandrasekhar, S.; Raza, A.; Takhi, M. *Tetrahedron Asymmetr.*, **2002**, *13*, 423-428.
15. Bartley, D.M.; Coward, J.K. *J. Org. Chem.*, **2005**, *70*, 6757-6774.
16. Kaiser, E.; Colescott, R.L.; Bossinger, L.D.; Cook, P.I. *Anal. Biochem.*, **1970**, *34*, 595-598.
17. Brantley, S.E.; Gerlach, B.; Olmstead, M.M.; Smith, K.M. *Tetrahedron Lett.*, **1997**, *38*, 937-940.

18. Gerlach, B.; Brantley, S.E.; Smith, K.M. *J. Org. Chem.*, **1998**, *63*, 2314-2320.
19. Sharpless, K. B.; Young M.W. *J. Org. Chem.*, **1975**, *40*, 947 - 949.
20. Grieco, P.A.; Gilman, S.; Nishizawa, M. *J. Org. Chem.*, **1976**, *41*, 1485-1486.
21. Soai, K.; Yokoyama, S.; Mochida, K. *Synthesis*, **1987**, 647-648.
22. Ghalit, N.; Reichwein, J.F.; Hilbers, H.W.; Breukink, E.; Rijkers, D.T.S; Liskamp, R.M.J. *ChemBioChem*, **2007**, *8*, 1540-1554.
23. Robinson, A.J.; Elaridi, J.; van Lierop, B.J.; Mujcinovic, S.; Jackson, W.R. *J. Pept. Sci.*, **2007**, *13*, 280-285.
24. Biagini, S.C.G.; Gibson, S.E.; Keen, S.P. *J.Chem. Soc. Perkin Trans.*, **1998**, *1*, 2485-2499.
25. Miller, S.J.; Blackwell, H.E.; Grubbs, R.H. *JACS*, **1996**, *118*, 9606-9614.
26. Chowdhurry, A.R.; Boons, G-J. *Tetrahedron Lett.*, **2005**, 46, 1675-1678.
27. Vojkovsky, T. *Pept. Res.*, **1995**, *8*, 236-237.
28. Meienhofer, J.; Waki, M.; Heimer, E.P.; Lambros, T.J.; Makofske, R.C.; Chang, C.-D. *Int. J. Peptide Protein Res.*, **1979**, *13*, 35.

CHAPTER 4

Synthesis of Photoaffinity Label Containing Analogues of the Echinocandin Antifungal Compounds

4.1 Introduction

The echinocandin antifungal class of compounds are known to bind to the glucan synthase catalytic subunit, however the exact mechanism of inhibition is not understood.[1] Although several genes[2,3] have been identified that are involved in resistance to the echinocandins[4,5], their direct role is still unknown. A synthetic molecular probe that may bind to the products of these genes, leading to their identification, may contribute to the elucidation of the mechanism of action of the echinocandin antifungal compounds.

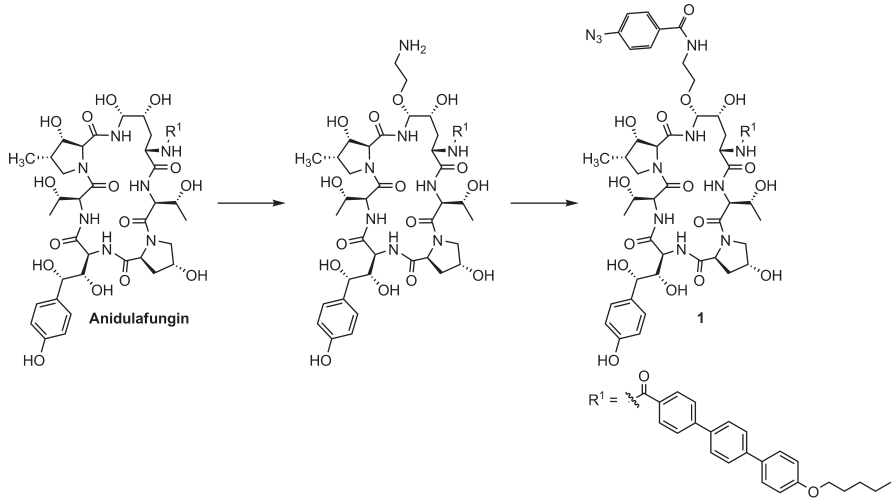

Scheme 1. Schematic presentation of the synthesis of a photoaffinity probe containing analogue (**1**) of an aryl azide photolabel.

So far only Radding et al have reported the use of a photoaffinity probe containing echinocandin analogue (**1**, Scheme 1).[6] This analogue was prepared by coupling the N-hydroxysuccinimide ester of 4-azidobenzoic acid to the free amine, resulting from aminoethylation of the aminal hydroxyl group of anidulafungin as shown in Scheme 1. The obtained azidobenzoate derivative **1** maintained *in vitro* microbiological activity against *Candida albicans* and was radiolabeled by solid-phase iodination of the homotyrosine residue. The resulting ^{125}I-labeled echinocandin probe was then used in photoaffinity experiments to label membrane preparations of *C. albicans* possessing glucan synthase activity. Two major proteins of 40 and 18 kDa were specifically labeled by the photoaffinity probe. This labelling could be effectively suppressed by unlabeled echinocandin analogs. Labelling of the 40-kDa protein was sufficient to allow purification but unfortunately the echinocandin-cross-linked 40 kDa *C. albicans* was not further characterized.[6]

To elucidate in more detail the molecular mechanism of action of the echinocandin antifungal compounds alternative photoaffinity containing analogs may be interesting. A chemical probe-based method as shown in Figure 1 was envisioned. This requires the construction of a chemical probe consisting of a photoreactive group for photoaffinity cross-linking and a so called reporter tag (e.g fluorescein) for read out. The idea of this concept is that the protein of interest (glucan synthase) is incubated with the chemical probe. Next, the sample

is irradiated with UV-light (366 nm), which will cross-link the probe to the target protein. Then, a fluorescent reporter is clicked to the alkyne moiety of the chemical probe.[7] This two-step labelling process has been developed because of the hydrophobicity, bulkyness and difficult cellular uptake of reporter molecules such as fluorescein.[8] Thus, the alkyne moiety permits post-labelling readout of captured echinocandin-binding protein targets, thereby excluding contributions of the reporter molecule. Introduction of a fluorescent label via 'click' chemistry allows the labelled proteins to be visualized in a gel. The whole complex can be resolved on SDS-page, and the gel scanned for fluorescence.[7]

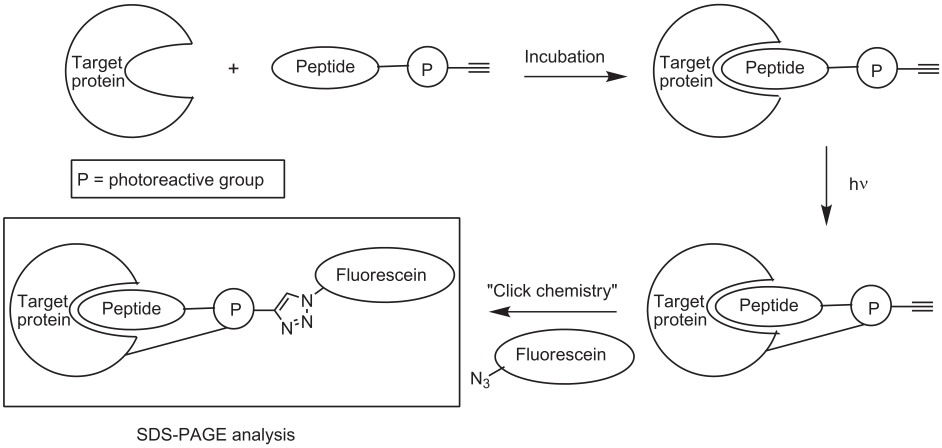

Figure 1. Schematic representation of the use of a chemical probe, consisting of a photo reactive group and an alkyne moiety, in protein labelling.

Due to the structural importance of the cyclic hexapeptide nucleus of the echinocandins, it may be advisable to construct the chemical probe as part of the fatty acid side chain. The side chain of the echinocandins has been studied extensively. Several articles have described semisynthetic analogues of the echinocandins by enzymatic deacetylation and chemical reacetylation of the side chain.[9-14] It has been shown that increasing the length of the side chain, increased the activity (from C-12 to C-18).[9] Moreover, lipophilic aroyl groups can replace the natural fatty acid moieties.[10] In addition, insertion of additional phenyl groups in the side chain led to alkoxybiphenyl and terphenoyl analogues with excellent anti-*Candida* activity.[12] However, these phenylic moieties have to be near the carbonyl moiety at the head of the side chain for the best activity and a rigid geometry of the side chain is preferable.[12] Finally, it has been shown that the lipophilicity of the side chains was important for antifungal activity. Using ClogP values to describe and compare the lipophilicities of the side chain fragments, it has been shown that values of >3.5 were required for expression of antifungal activity.[12]

Based on these earlier studies and the requirements of the chemical probe a set of probes is proposed, consisting of a benzophenone photoaffinity label and alkyn moiety as is shown in Figure 2. Next, these probes will be coupled to the cyclic peptide to obtain a series of echinocandin based photoaffinity analogues. These analogues will be tested for their biological activity and if active they can be used in a labelling experiment as illustrated in Figure 1.

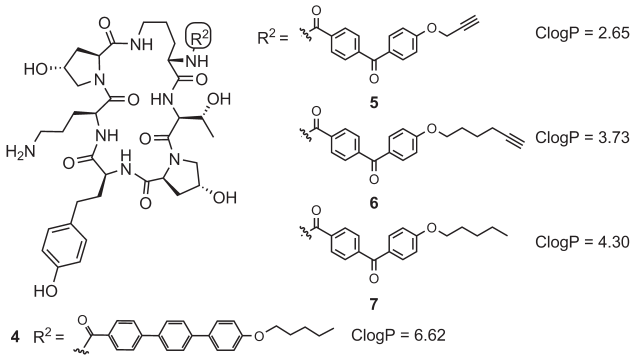

Figure 2. Proposed probes (**5**-**7**) for the synthesis of a serie of echinocandin based photoaffinity analogues and previously described echinocandin analogue (**4**).

Photoaffinity labels **5**[15,16] and **6** are benzophenone containing labels with different lengths of the alkyne moiety. Photoaffinity label **7** was included as a reference, this probe lacks the alkyne moiety and instead a 4-pentyloxy group, as in the terphenyl tail of analog **4** (previously described in chapter 2, as mimic **13b**), was incorporated. When coupled to the peptide, this probe will serve as a reference to investigate whether the changes to the relatively rigid terphenyl side chain of **4** will be detrimental to the activity of the echinocandin peptide analogues. Debono et al[12] have shown that introduction of a spacer consisting of a single oxygen or carbon atom between biphenyl aroyl groups resulted in compounds that are less active. One major structural consequence of these modifications is conversion of the linear shape of the biphenyl aryl groups to a bent one with angle of ca 120°. However, elongating this bridge by yet another atom restored the antifungal activity back to the same level. This elongation relaxed the angular shape and permitted a more linear orientation and thereby restored its activity. This result showed that there is some room for altering the linear structure of the side chains as in **4**. The benzophenone (**5**-**7**) containing labels also show a more angular relationship between the biphenyl aroyl groups. However, these structures are more flat than the inactive compounds described by Debono et al. In addition, probes **6** and **7** fulfil the criteria of a ClogP value greater than 3.5.[17]

4.2 Results and discussion

This work started with the synthesis of the photoaffinity label containing side chains, followed by the solid phase synthesis of the echinocandin peptide analogues.

The preparation of the benzophenone containing side chains is summarized in Scheme 2. Phenol (**8**) was alkylated by propargylbromide or 1-bromopentane in the presence of a base to give **10** and **12**, respectively. For the synthesis of **11**, phenol **8** was reacted with hex-5-ynyl methanesulfonate (**9**). Then, ethers **10**-**12** were subjected to Friedel-Crafts acylation. Terephtalic acid monomethyl ester (**13**) was converted to its acid chloride **14** and reacted with the corresponding ethers **10**-**12** in the presence of $AlCl_3$ to afford the benzophenone esters **15-17**. Finally, saponification gave access to the corresponding acids **5**-**7**.

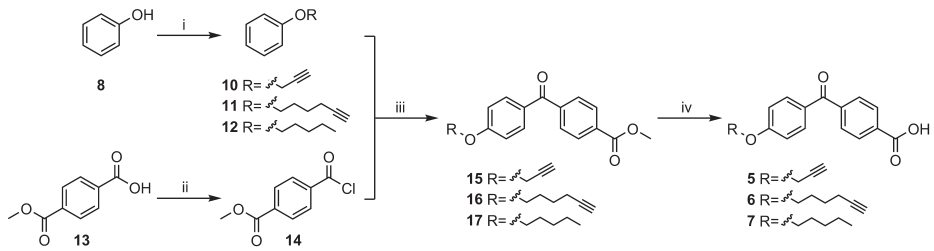

Scheme 2. Reagents and conditions: (i) **10**: K_2CO_3, propargylbromide, acetone, 20h, 70%; **11**: (1) NaOH, H_2O, 60°C; (2) hex-5-ynyl methanesulfonate (**9**), THF, Δ, 18h, 62%; **12**: 1-bromopentane, K_2CO_3, KI, DMF, 4h, 90%; (ii) $SOCl_2$, Δ, 6h, quant.; (iii) $AlCl_3$, DCM, Δ, 4h, **15**: 32%, **16**: 19%, **17**: 44%; (iv) LiOH, MeOH, Δ, 18h, 87-95%.

The echinocandin based photoaffinity analogues were synthesized as is outlined in Scheme 3. The linear hexapeptide precursor **18** was synthesized by SPPS using the trityl resin. Removal of the ε-Fmoc group from ornithine, followed by coupling of the photolabel containing side chains **5**-**7** and mild acidolytic cleavage of the Mtt group liberated the peptide chain from the resin to give the linear fully protected peptide precursor **19**. Solution-phase cyclization followed by protecting group removal afforded the macrocyclic peptides **20**-**22** in overall yields of 7-17% after purification by preparative HPLC.

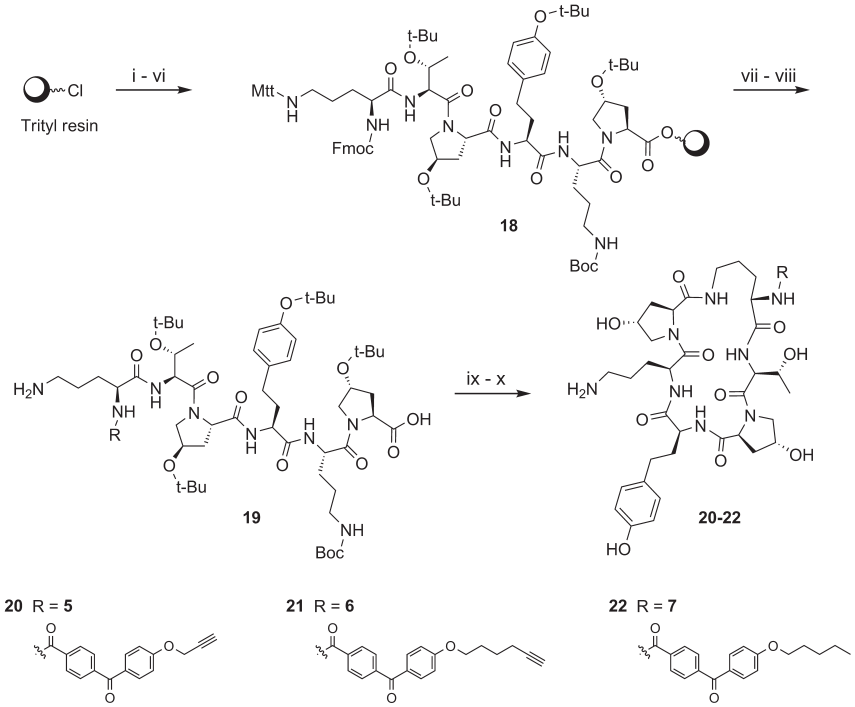

Scheme 3. Reagents and conditions: (i) Fmoc-Hyp(*t*Bu)-OH, DIPEA, DCM; (ii-vi) (1) 20% piperidine in NMP; (2) Fmoc-Xxx-OH, BOP, DiPEA, NMP; (vii) (1) 20% piperidine in NMP; (2) photolabel containing side chain **5**-**7**, HATU, DiPEA, NMP; (viii) TFE/AcOH/DCM (2/1/7; v/v/v); (ix) BOP, DiPEA, DMF; (x) TFA/TIS/H_2O (95/2.5/2.5; v/v/v).

The antifungal activity of each echinocandin analogue was evaluated by broth microdilution using Caspofungin[18] as a reference compound. Minimum inhibitory concentrations (MICs) were inspected visually and thereby quantified as the lowest concentration of compound resulting in inhibition of yeast growth after overnight incubation at 30 °C (Table 1). In addition, the MIC value of the previously described head-to-tail mimic **4** with a terphenyl chain was included in Table 1.

Table 1. Antifungal activity of the photoaffinity probe echinocandin analogues in μg/mL.

	Candida albicans CBS 9975
Caspofungin	0.025
20	>100
21	>100
22	>100
4	0.14

Unfortunately, none of the photoaffinity probe echinocandin analogues showed antifungal activity up to 100 μg/mL. Replacement of the linear terphenyl chain (**4**) with benzophenone based labels (**20**-**22**) completely abolished the activity. This might be due to the presence of a bent side chain in mimics **20**-**22** instead of a straight one as in mimic **4**. Although our mimics, with a ketone spacer between the biphenyl groups are more constrained and rigid, in comparison to the freely rotatable oxygen or carbon spacers described by Debono[12] the antifungal activity had completely disappeared. These observations further support the hypothesis that the side chain has to be straight and relatively rigid for optimal antifungal potency.

4.3 Conclusion

Novel photoaffinity probe containing echinocandin analogues were synthesized. Fatty acids containing a photoaffinity label were designed and synthesized. Although synthesis of the mimics **20**-**22** was successful, evaluation of their antifungal properties showed no measurable activity. These findings stress the importance of the nature of the fatty acid side chain in relation to antifungal potency.

4.4 Experimental section

4.4.1 Reagents, materials and analysis methods

Unless stated otherwise, all chemicals were obtained from commercial sources and used as supplied, with the exception of DMF, NMP and DCM, which were dried on molecular sieves (4Å) prior to use. HPLC grade solvents were purchased from Biosolve B.V. (Valkenswaard, The Netherlands). Fmoc protected amino acids were purchased from GL Biochem Ltd. (Shanghai, China). Protected homotyrosine (H-hTyr(*t*Bu)-OH) was purchased from Advanced Chemtech (Louisville, United States) and furnished with the Fmoc group. The 2-chlorotritylchloride PS resin was purchased from Hecheng Chemicals (Shanghai, China). All other reagents were

purchased from Merck (Darmstadt, Germany), Sigma-Aldrich (Munich, Germany) and Acros (Geel, Belgium) and were used without further purification.

All Reactions were carried out at room temperature unless stated otherwise. Solid phase synthesis was performed in plastic syringes with a polyethylene frit. Reactions were monitored by TLC on Merck pre-coated Silica 60 plates. Spots were visualized by UV light, ninhydrin or K_2CO_3/$KMnO_4$. Solid phase reactions were monitored with the chloranil test[19] in case of secondary amines or with the Kaiser test[20] in case of primary amines. Column chromatography was performed using Silicycle UltraPure silicagel (40-63 μm).

^{1}H NMR spectra were recorded on a Varian G-300 (300 MHz) spectrometer and chemical shifts are given in ppm relative to TMS (0.00 ppm). ^{13}C NMR spectra were recorded using the attached proton test (APT) sequence on a varian G-300 (75.5 MHz) spectrometer and chemical shifts are given in ppm relative to $CDCl_3$ (77.0 ppm). For measurements in DMSO, the residual solvent peak was used as a reference. For the peptides ^{1}H NMR, TOCSY, ^{1}H-^{13}C HSQC and ROESY spectra were recorded using a Varian INOVA-500 spectrometer (500 MHz).

The purity of the peptides was confirmed by analytical HPLC using an Alltima C8 column. Analytical HPLC was performed on a Shimadzu automated HPLC system equipped with an evaporative light scattering detector (PL-ELS 1000) and a UV/Vis detector operated at 220/254 nm. A flow rate of 0.5 mL/min with a linear gradient of buffer B (100% in 40 min) from 100% buffer A was used. Preparative HPLC runs were performed using a C8 Altima column on an Applied Biosystems 400 solvent delivery system with an Applied Biosystems 757 UV/VIS absorbance detector. A flow rate of 6 mL/min with a linear gradient of buffer B (100% in 80 min) from 100% buffer A was used. The buffer system will be referred to as *i*-PrOH/MeOH/H_2O buffer and consists of buffer A: 0.1 % TFA in *i*-PrOH/MeOH/H_2O, 5/5/90, v/v/v and buffer B: 0.1% TFA in *i*-PrOH/MeOH/H_2O, 45/50/5, v/v/v.

ESI-MS spectra were obtained in the positive ion mode on a Shimadzu QP8000 single quadrupole mass spectrometer. Peptides were characterized by high resolution mass spectrometry (HRMS) analyses performed on a MALDI TOF/TOF (Applied Biosystems).

4.4.2 Chemistry

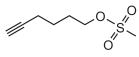

Hex-5-ynyl methanesulfonate (9)

Methanesulfonyl chloride (1.0 mL; 13.0 mmol) was added dropwise to a solution of 5-hexyn-1-ol (1.37 mL; 12.4 mmol) and TEA (1.90 mL; 13.7 mmol) in dry DCM (120 mL). The reaction mixture was stirred for 2.5 h. The mixture was washed with 1 M $KHSO_4$ (150 mL) and H_2O (150 mL). The organic layer was dried (Na_2SO_4), filtered and concentrated in *vacuo*. Pure product **9** (2.17 g; 99%) was obtained after column chromatography (DCM/MeOH, 200/1, v/v) as a clear oil. R_f = 0.15 (DCM/MeOH, 200/1, v/v); ^{1}H-NMR ($CDCl_3$, 300 MHz): δ = 4.29 (t, J=6.3 Hz, 2H, OCH_2), 3.02 (s, 3H, CH_3), 2.24-2.29 (m, 2H, *CH*$_2$C), 1.98 (t, J=2.6 Hz, 1H, C≡CH), 1.85-1.92 (m, 2H, CH_2), 1.64-1.71 (m, 2H, CH_2) ppm; ^{13}C-NMR ($CDCl_3$, 75.5 MHz): δ = 83.8 (*C*≡CH), 69.7 (OCH_2), 68.2 (≡CH), 37.9 (CH_3), 28.1 and 24.4 (CH_2), 21.6 (CH_2CH≡CH).

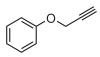

1-(prop-2-ynoxy)benzene (10)

Phenol (3.0 g; 31.9 mmol) was dissolved in dry acetone (30 mL), K_2CO_3 (13.2 g; 95.6 mmol) was added and propargylbromide (4.3 mL; 47.8 mmol) was added dropwise to the mixture. The mixture was stirred overnight and the K_2CO_3 filtered off. Subsequently, the filtrate was co-evaporated with toluene (3×) *in vacuo*. Pure product **10** (2.95 g; 70%) was obtained after column chromatography (DCM/MeOH, 250/1, v/v) as a clear oil. R_f = 0.90 (DCM/MeOH, 200/1, v/v); ^{1}H-NMR ($CDCl_3$, 300 MHz): δ = 7.30 (t, J=0.8 Hz, 2H, Ar-H), 7.01-6.96 (m, 3H, Ar-H), 4.68 (d, J=2.2 Hz, 2H, OCH_2), 2.50 (d, J=0.8Hz, 1H, C≡CH) ppm; ^{13}C-NMR ($CDCl_3$, 75.5 MHz): δ = 157.7 (Ar-C), 129.7, 121.8 and 115.1 (Ar-CH), 76.9 (C≡CH), 75.7 (C≡*CH*), 56.0 (OCH_2).

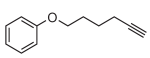

1-(hex-5-ynoxy)benzene (11)

To a solution of NaOH (1.72 g; 43.1 mmol) in H_2O (100 mL) phenol (4.06 g; 43.1 mmol) was added. The mixture was stirred for 1h, subsequently the mixture was heated at 60°C for an additional 3h. After filtration, pure sodium phenoxide (5.11 g; 100%) was obtained by crystallization from EtOH. Hex-5-ynyl methanesulfonate **(9)** (510 mg; 2.89 mmol) was added dropwise to a solution of sodium phenoxide (310 mg; 2.63 mmol) in dry THF (4 mL). The reaction mixture was refluxed overnight. The mixture was then washed with H_2O (10 mL) and extracted with Et_2O (10 mL). The organic layer was washed with H_2O (10 mL), brine (10 mL) and then dried (Na_2SO_4), filtered and concentrated in *vacuo*. Pure product **11** (0.31 g; 62%) was obtained after column chromatography (DCM/MeOH, 300/1, v/v) as a clear oil. R_f = 0.90 (DCM/MeOH, 250/1, v/v); ^{1}H-NMR ($CDCl_3$, 300 MHz): δ = 7.27 (t, J=0.8 Hz, 2H, Ar-H), 6.95-6.87 (m, 3H, Ar-H), 3.97 (t, J=6.2 Hz, 2H, OCH_2), 2.30-2.24 (m, 2H, *CH_2*C≡CH), 1.97-1.86 (m, 3H, CH_2 and C≡CH), 1.77-1.70 (m, 2H, CH_2) ppm; ^{13}C-NMR ($CDCl_3$, 75.5 MHz): δ = 159.4 (Ar-C), 129.6, 120.8 and 114.7 (Ar-CH), 68.8 (*C*≡CH), 67.3 (OCH_2), 28.5, 25.3 and 18.4 (CH_2).

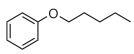

1-(pentanoxy)benzene (12)

Phenol (0.90 g; 9.13 mmol), 1-bromopentane (2.07 g; 13.7 mmol), K_2CO_3 (3.80 g; 27.40 mmol) and KI (317 mg; 1.83 mmol) were stirred in dry DMF (20 mL) at 150°C for 4h. The reaction was cooled and filtered. Subsequently, the solid was washed with acetone. The amount of DMF was reduced to ca 25% by evaporation. A 1N HCl solution was added to give a precipitate and the acidified mixture was extracted with DCM (2x 50 mL). The combined organic layers were dried (Na_2SO_4), filtered and concentrated in *vacuo*, yielding a brownish solid. Pure product **12** (1.43 g; 90%) was obtained after column chromatography (DCM/MeOH, 250/1, v/v) as a clear oil. R_f = 0.98 (DCM/MeOH), 250/1, v/v); ^{1}H-NMR ($CDCl_3$, 300 MHz): δ = 7.26 (t, J=6.9 Hz, 2H, Ar-H), 6.94-6.87 (m, 3H, Ar-H), 3.94 (t, J=6.6 Hz, 2H, OCH_2), 1.82-1.73 (m, 2H, *CH_2*CH_3), 1.46-1.34 (m, 4H, OCH_2*CH_2*, OCH_2CH_2*CH_2*), 0.93 (t, J= 6.5 Hz, 3H, CH_3) ppm; ^{13}C-NMR ($CDCl_3$, 75.5 MHz): δ = 159.4 (Ar-C), 129.6, 120.7 and 114.7 (Ar-CH), 68.1 (OCH_2), 29.3, 28.5 and 22.7 (CH_2), 14.3 (CH_3) ppm.

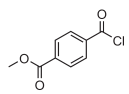

Methyl 4-(chlorocarbonyl)benzoate (14)

Terephthalic acid monomethylester **13** (4.55 g; 25.25 mmol) was dissolved in $SOCl_2$ (55 mL) and refluxed for 6h. $SOCl_2$ was removed by evaporation followed by coevaporation with toluene (3×) to afford the acid chloride **14**. ^{1}H-NMR (DMSO, 300 MHz): δ = 8.07 (s, 4H, Ar-H), 3.90 (s, 3H, OCH_3) ppm; ^{13}C-NMR (DMSO, 75.5 MHz): δ =

166.7 and 165.7 (C=O), 134.9 and 133.2 (Ar-C), 129.7 and 129.5 (Ar-CH), 52.6 (OCH_3) ppm.

General procedure of Friedel-Crafts acylation

To a solution of alkylated phenol and acid chloride (1.1 equiv.) in dry DCM (3 mL/mmol) $AlCl_3$ (2 equiv.) was added. The reaction mixture was refluxed for 4 h. Then, the mixture was cooled to RT, poured on ice, and extracted with EtOAc. The organic layer was washed with aq. $NaHCO_3$ (5%), H_2O and brine. After drying over Na_2SO_4, the solvent was evaporated under reduced pressure and the crude product purified by column chromatography (Hex/EtOAC, 9/1, v/v) to give methyl ester **15**, **16** and **17**.

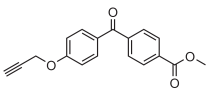

Methyl 4-(4-(prop-2-ynoxy)benzoyl)benzoate (15)

Methyl ester **15** was obtained according to the general procedure for Friedel-Crafts acylation using phenol **10** (449 mg; 3.40 mmol), methyl 4-(chlorocarbonyl)benzoate (**14**) (728 mg; 3.74 mmol) and $AlCl_3$ (906 mg; 6.80 mmol). Pure product **15** (320 mg; 32%) was obtained as a white solid. R_f = 0.41 (Hex/EtOAc, 9/1, v/v); ^{1}H-NMR ($CDCl_3$, 300 MHz): δ = 8.16 (d, J=8.5 Hz, 2H, Ar-H), 7.85-7.78 (m, 4H, Ar-H), 7.08 (d, J=9.1 Hz, 2H, Ar-H), 4.79 (d, J=2.2 Hz, 2H, OCH_2), 3.97 (s, 3H, OCH_3), 2.58 (s, 1H, ≡CH) ppm; ^{13}C-NMR ($CDCl_3$, 75.5 MHz): δ = 195.2 (C=O), 166.6 (C(O)CH_3), 161.6, 142.2 and 132.7 (Ar-C), 129.7 and 114.8 (Ar-CH), 77.6 (C≡), 76.8 (CH≡), 56.1 (OCH_2), 52.7 (OCH_3).

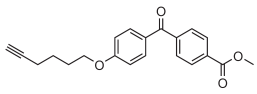

Methyl 4-(4-(hex-5-ynoxy)benzoyl)benzoate (16)

Methyl ester **16** was obtained according to the general procedure for Friedel-Crafts acylation using phenol **11** (282 mg; 1.49 mmol), methyl 4-(chlorocarbonyl)benzoate (**14**) (435 mg; 2.24 mmol) and $AlCl_3$ (396 mg; 2.97 mmol). Pure product **16** (93 mg; 19%) was obtained as a white solid. R_f = 0.38 (Hex/EtOAc, 9/1, v/v); ^{1}H-NMR (DMSO, 300 MHz): δ = 8.12 (d, J=8.5 Hz, 2H, Ar-H), 7.81-7.74 (m, 4H, Ar-H), 7.12 (d, J=8.8 Hz, 2H, Ar-H), 4.12 (t, J=6.5 Hz, 2H, OCH_2), 3.91 (s, 3H, OCH_3), 2.51 (t, J= 1.8 Hz, 1H, ≡CH), 2.28-2.22 (m, 2H, CH_2C≡CH), 1.87-1.82 (m, 2H, CH_2), 1.64-1.58 (m, 2H, CH_2) ppm; ^{13}C-NMR (DMSO, 75.5 MHz): δ = 193.9 (C=O), 165.7 (C(O)CH_3), 162.8, 141.8, 132.2 and 128.7 (Ar-C), 132.4, 129.4 and 114.5 (Ar-CH), 84.3 (C≡), 71.5 (CH≡), 67.5 (OCH_2), 52.5 (OCH_3), 27.6, 24.5 and 17.4 (CH_2).

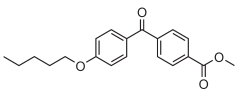

Methyl 4-(4-(pentanoxy)benzoyl)benzoate (17)

Methyl ester **17** was obtained according to the general procedure for Friedel-Crafts acylation using phenol **12** (503 mg; 3.06 mmol), methyl 4-(chlorocarbonyl)benzoate (**14**) (669 mg; 3.37 mmol) and $AlCl_3$ (817 mg; 6.13 mmol). Pure product **17** (442 mg; 44%) was obtained as a white solid. R_f = 0.34 (Hex/EtOAc, 9/1, v/v); ^{1}H-NMR ($CDCl_3$, 300 MHz): δ =8.15 (d, J=8.3 Hz, 2H, Ar-H), 7.83-7.77 (m, 4H, Ar-H), 6.97 (d, J=8.8 Hz, 2H, Ar-H), 4.04 (t, J=6.6 Hz, 2H, OCH_2), 3.96 (s, 3H, OCH_3), 1.87-1.78 (m, 2H, CH_2CH_3), 1.51-1.36 (m, 4H, OCH_2CH_2, $OCH_2CH_2CH_2$), 0.94 (t, J= 6.9 Hz, 3H, CH_3) ppm; ^{13}C-NMR ($CDCl_3$, 75.5 MHz): δ = 195.0 (C=O), 166.6 (C(O)CH_3), 163.5, 142.5 and 132.9 (Ar-C), 132.8, 129.6 and 114.4 (Ar-CH), 68.6 (OCH_2), 52.6 (OCH_3), 29.0, 28.3 and 22.6 (CH_2), 14.2 (CH_3).

General procedure for saponification of methyl esters (15-17) to carboxylic acids (5-7)
A solution of the methyl ester in MeOH/H_2O (9/1, v/v) was treated with LiOH (2 equiv.). The reaction mixture was refluxed overnight. The mixture was cooled to RT, acidified with 2M HCl, and extracted with EtOAC (3×). The combined organic layers were washed with H_2O and brine. After drying over $NaSO_4$, the solvent was removed *in vacuo* to afford the free acid.

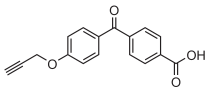

4-(4-(prop-2-ynoxy)benzoyl)benzoic acid (5)
Acid **5** was obtained following the general procedure for saponification using: ester **15** (175 mg; 0.60 mmol) and LiOH (49 mg; 1.19 mmol). Product **5** (156 mg; 94%) was obtained as an off-white solid. R_f = 0.31 (DCM/MeOH/AcOH, 97/2/1, v/v); ^{1}H-NMR (DMSO, 300 MHz): δ = 8.10 (d, J=7.7 Hz, 2H, Ar-H), 7.80 (d, J=8.8 Hz, 4H, Ar-H), 7.17 (d, J=8.3 Hz, 2H, Ar-H), 4.95 (d, J=1.9 Hz, 2H, OCH_2), 3.66 (s, 1H, ≡CH) ppm; ^{13}C-NMR (DMSO, 75.5 MHz): δ = 194.0 (C=O), 166.7 (*C*(O)CH_3), 161.1, 141.3, 133.6 and 129.6 (Ar-C), 132.2, 129.3 and 114.9 (Ar-CH), 78.8 (CH≡), 55.8 (OCH_2).

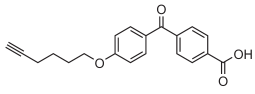

4-(4-(hex-5-ynoxy)benzoyl)benzoic acid (6)
Acid **6** was obtained following the general procedure for saponification using: ester **16** (233 mg; 0.69 mmol) and LiOH (58 mg; 1.39 mmol). Product **6** (194 mg; 87%) was obtained as an off-white solid. R_f = 0.29 (DCM/MeOH/AcOH, 97/2/1, v/v); ^{1}H-NMR (DMSO, 300 MHz): δ = 8.11 (d, J=8.5 Hz, 2H, Ar-H), 7.79-7.75 (m, 4H, Ar-H), 7.11 (d, J=8.8 Hz, 2H, Ar-H), 4.11 (t, J=6.3 Hz, 2H, OCH_2), 2.80 (t, J= 2.6 Hz, 1H, ≡CH), 2.28-2.23 (m, 2H, *CH_2*C≡CH), 1.87-1.82 (m, 2H, CH_2), 1.65-1.60 (m, 2H, CH_2) ppm; ^{13}C-NMR (DMSO, 75.5 MHz): δ = 193.9 (C=O), 166.7 (*C*(O)CH_3), 162.7, 141.4, 133.4 and 128.8 (Ar-C), 132.3, 129.2 and 114.4 (Ar-CH), 84.0 (C≡), 71.4 (CH≡), 67.4 (OCH_2), 27.6, 24.5 and 17.4 (CH_2).

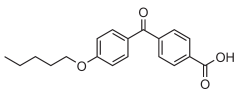

4-(4-(pentanoxy)benzoyl)benzoic acid (7)
Acid **7** was obtained following the general procedure for saponification using: ester **17** (442 mg; 1.35 mmol) and LiOH (112 mg; 2.70 mmol). Product **7** (401 mg; 95%) was obtained as a white solid. R_f = 0.27 (DCM/MeOH/AcOH, 97/2/1, v/v); ^{1}H-NMR (DMSO, 300 MHz): δ = 8.11 (d, J=8.5 Hz, 2H, Ar-H), 7.79-7.74 (m, 4H, Ar-H), 7.10 (d, J=8.8 Hz, 2H, Ar-H), 4.08 (t, J=6.5 Hz, 2H, OCH_2), 1.77-1.73 (m, 2H, *CH_2*CH_3), 1.43-1.32 (m, 4H, OCH_2*CH_2*, OCH_2CH_2*CH_2*), 0.90 (t, J= 7.0 Hz, 3H, CH_3) ppm; ^{13}C-NMR (DMSO, 75.5 MHz): δ = 193.9 (C=O), 166.7 (*C*(O)CH_3), 162.8, 141.5, 133.5 and 128.7 (Ar-C), 132.3, 129.3 and 114.4 (Ar-CH), 67.9 (OCH_2), 28.2, 27.6 and 21.8 (CH_2), 13.9 (CH_3).

General Procedure for Solid phase peptide synthesis
Peptides were synthesized manually in 50 mL syringes with polyethylene frit. Each synthetic cycle consisted of the following steps:
Fmoc removal: The resin was treated with a 20% solution of piperidine in NMP (3×, each 10 min). The solution was removed by filtration and the resin was washed with NMP (3×, each 3 min) and DCM (3×, each 3 min).
Coupling step: A mixture of Fmoc-Xxx-OH (3 equiv.), BOP (3 equiv.) and DiPEA (6 equiv.) in NMP (10mL/mmol)) was added to the resin and N_2 was bubbled through the mixture for 2h. The solution was removed by filtration and the resin washed with NMP (3×, each 3 min) and DCM (3×, each 3 min). Completion of the coupling was checked with Kaiser or chloranil

test.

Capping of the remaining free amines: Capping solution [Ac_2O (50 mmol, 4.7 mL), HOBt (1.9 mmol, 220 mg), DiPEA (12.5 mmol, 2.2 mL) in 100 mL NMP] was added to the resin and N_2 was bubbled through the mixture for 20 min The solution was removed by filtration and the resin was washed with NMP (3×, each 3 min) and DCM (3×, each 3 min).

General procedure for the preparation of the echinocandin analogues (20-22)

A polystyrene resin functionalized with a 2-chloro Trityl linker (3.0 g; initial loading: 1.1 mmol/g) was loaded with Fmoc-Hyp(tBu)-OH (3.69 g; 9.0 mmol) in DCM (30 mL) in the presence of DiPEA (3.14 mL; 18 mmol) for 16h. The solution was removed by filtration and the resin washed with DCM (3× 4 mL, each 3 min). After drying *in vacuo* overnight, the amount of Fmoc-Hyp(tBu)-OH coupled to the resin was determined by a Fmoc determination according to Meienhofer[21] and was found to be 0.610 mmol/g. Subsequently, unreacted tritylchloride moieties were capped with methanol (DCM/MeOH/DiPEA; 3× 5 mL, each 2 min; 17/2/1; v/v/v). The peptide sequence was synthesized according to the general procedure for solid phase peptide synthesis. The resin-bound peptide **18** was divided in portions for the synthesis of the analogues **20**-**22**. The Fmoc group was cleaved and the photoaffinity label containing side chain (**5**-**7**) (3 equiv.) was coupled in the presence of HATU (3 equiv.) and DiPEA (6 equiv.) in NMP (3 mL). The mixture was shaken overnight. Subsequently the coupling solution was removed by filtration and the resin washed with NMP (3× 4 mL, each 3 min) and DCM (3× 4 mL, each 3 min). Completion of the coupling was checked with the Kaiser test. Then, mild acidolytic cleavage, by treatment with TFE/AcOH/DCM (2/1/7, v/v/v, 5 mL) for 2 hours, of the Mtt group as well as cleavage from the resin gave protected peptide precursor **19.** The mixture was concentrated *in vacuo* and the peptide was precipitated in MTBE/Hex (3×, 1/1, v/v). The linear peptide was then subjected to head-to-tail cyclization by dissolving it in dry DMF (2 mL/μmol) followed by the addition of BOP (4 equiv.) and DiPEA (4 equiv.). The mixture was stirred for 48h and then evaporated *in vacuo*. The product was redissolved in EtOAc and washed with 1M $KHSO_4$ (2×), $NaHCO_3$ (2×) and H_2O (2×). The organic layer was dried over Na_2SO_4, filtered and concentrated *in vacuo*. Final protecting group removal by treatment with a mixture of TFA/TIS/H_2O (2 mL, 95/2.5/2.5, v/v/v) for 2h and precipitation in MTBE/hexanes (3×, 1/1, v/v) afforded the crude peptide. After lyophilization from *tert*-BuOH/H_2O (1/1, v/v) the peptide was purified by preparative HPLC.

***Cyclo*[-(propynoxy-benzophenone)-Orn-Thr-Hyp-hTyr-Orn-Hyp] (20)**

Peptide **20** was obtained according to the general procedure for the preparation of the echinocandin analogues, using **5** in the coupling of the side chain. After lyophilization, peptide **20** (3.5 mg; 7%) was obtained as a white solid. Purity was confirmed by analytical HPLC and was found to be to be higher than 99% (R_t = 32.15 min). ESI-MS calcd for $C_{50}H_{59}N_7O_{14}$: 981.41, found: m/z 982.46 $[M+H]^+$; HRMS calcd for $C_{50}H_{59}N_7O_{14}$ $[M+H]^+$ 982.4198, found 982.4180; ^{1}H-NMR (DMSO, 500 MHz): δ Orn-1: 8.58 (NH), 4.54 (αCH), 1.91/1.53 (βCH), 1.52 (γCH), 3.09/3.02 (δCH); Thr-2: 8.04 (NH), 4.31 (αCH), 4.08 (βCH), 1.24 (γCH); Hyp-3: 4.42 (αCH), 2.12/1.83 (βCH), 4.40 (γCH), 3.77 (δCH); hTyr-4: 8.41 (NH), 3.67 (αCH), 2.17/2.13 (βCH), 2.43/2.36 (γCH), 6.95/6.66 (Ar-H); Thr-5: 7.48 (NH), 4.79(αCH), 4.15 (βCH), 1.05 (γCH); Hyp-6: 4.36 (αCH), 2.12/1.83 (βCH), 4.29 (γCH), 3.65 (δCH); Tail: 3.67 (≡CH), 4.95 (OCH_2), 7.16/7.76 (Ar-H Ph-2), 7.78/8.03 (Ar-H Ph-1) ppm. ^{13}C-NMR (DMSO, 125 MHz): δ Orn-1:52.1 (αCH), 28.2 (βCH), 24.1 (γCH), 38.0 (δCH); Thr-2: 58.5 (αCH), 66.6 (βCH), 19.3 (γCH); Hyp-3: 60.2

(αCH), 37.7 (βCH), 69.2 (γCH), 56.5 (δCH); hTyr-4: 53.6 (αCH), 31.2 (βCH), 31.2 (γCH), 129.9/115.5 (Ar-H); Thr-5: 56.5 (αCH), 67.4 (βCH), 19.0 (γCH); Hyp-6: 59.3 (αCH), 37.7 (βCH), 69.1 (γCH), 56.2 (δCH); Tail: 56.0 (OCH_2), 79.1 (≡CH), 115.3/129.7 (Ar-H Ph-2), 132.7/128.3 (Ar-H Ph-1).

***Cyclo*[-(hexynoxy-benzophenone)-Orn-Thr-Hyp-hTyr-Orn-Hyp] (21)**

Peptide **21** was obtained according to the general procedure for the preparation of the echinocandin analogues, using **6** in the coupling of the side chain. After lyophilization, peptide **21** (4.1 mg; 8%) was obtained as a white solid. Purity was confirmed by analytical HPLC and was found to be to be higher than 99% (R_t = 35.72 min). ESI-MS calcd for $C_{53}H_{65}N_7O_{14}$: 1023.46, found: m/z 1024.64 $[M+H]^+$; HRMS calcd for $C_{53}H_{65}N_7O_{14}$ $[M+H]^+$ 1024.4668, found 1024.4690.

***Cyclo*[-(pentanoxy-benzophenone)-Orn-Thr-Hyp-hTyr-Orn-Hyp] (22)**

Peptide **22** was obtained according to the general procedure for the preparation of the echinocandin analogues, using **7** in the coupling of the side chain. After lyophilization, peptide **22** (9.0 mg; 17%) was obtained as a white solid. Purity was confirmed by analytical HPLC and was found to be to be higher than 95% (R_t = 38.68 min). ESI-MS calcd for $C_{52}H_{67}N_7O_{14}$: 1013.47, found: m/z 1014.50 $[M+H]^+$; HRMS calcd for $C_{52}H_{67}N_7O_{14}$ $[M+H]^+$ 1014.4824, found 1014.4832; ^{1}H-NMR (DMSO, 500 MHz): δ Orn-1: 8.57 (NH), 4.54 (αCH), 1.90/1.55 (βCH), 1.51 (γCH), 3.08/3.01 (δCH); Thr-2: 8.02 (NH), 4.36 (αCH), 4.07 (βCH), 1.24 (γCH); Hyp-3: 4.42 (αCH), 2.11/1.83 (βCH), 4.40 (γCH), 3.77 (δCH); hTyr-4: 8.41 (NH), 3.66 (αCH), 2.18/2.12 (βCH), 2.44/2.35 (γCH), 6.95/6.66 (Ar-H); Thr-5: 7.47 (NH), 4.79(αCH), 4.15 (βCH), 1.05 (γCH); Hyp-6: 4.31 (αCH), 2.11/1.83 (βCH), 4.29 (γCH), 3.64 (δCH); Tail: 0.91 (CH_3), 1.37 (CH_2), 1.41 (CH_2), 1.75 (CH_2), 4.09 (OCH_2), 7.10/7.74 (Ar-H Ph-2), 7.75/8.03 (Ar-H Ph-1) ppm. ^{13}C-NMR (DMSO, 125 MHz): δ Orn-1:52.1 (αCH), 28.3 (βCH), 24.2 (γCH), 38.0 (δCH); Thr-2: 59.3 (αCH), 66.6 (βCH), 19.2 (γCH); Hyp-3: 60.2 (αCH), 37.7 (βCH), 69.2 (γCH), 56.5 (δCH); hTyr-4: 53.6 (αCH), 31.2 (βCH), 31.2 (γCH), 129.8/ 115.5 (Ar-H); Thr-5: 56.6 (αCH), 67.4 (βCH), 19.0 (γCH); Hyp-6: 58.5 (αCH), 37.7 (βCH), 69.1 (γCH), 56.2 (δCH); Tail: 13.9 (CH_3), 21.9 (CH_2), 27.7 (CH_2), 28.3 (CH_2), 68.2 (OCH_2), 114.9/129.6 (Ar-H Ph-2), 132.9/128.2 (Ar-H Ph-1).

4.4.3 Biology

Candida MIC Assay

Antifungal activity was evaluated by broth microdilution. The media used in this assay was Yeast Extract Peptone Dextrose (YPD) containing 1% yeast extract, 2% peptone, 1% dextrose in distilled water. Test compounds were dissolved in 10% DMSO to a concentration of 1 mg/mL. After solubilization each compound was diluted 5 times in YPD medium rendering a stock solution of 200 μg/mL. Caspofungin[18], purchased from Merck Sharp & Dohme B.V. (Haarlem, Netherlands), was included as a reference. Serial 2-fold dilutions of the test compounds in YPD medium were prepared as follows. To each well of a sterile Greiner bio-one Cellstar 96 well, U bottomed microtiter plate, 100 μl of YPD was dispensed. Manually, 100 μl of stock compounds was delivered to each well in column 1. Then using a 8-channel pipet, compounds in column 1 were serially diluted 2-fold over the microtiter plate until column 11. The last column of the plate contained drug-free wells dedicated for growth and sterility controls.

The plates containing the diluted compounds were inoculated with 100 µl of *C. albicans* CBS9975. A stock culture of the *C. albicans* strain in liquid media (YPD + 15% glycerol) was maintained at -80°C. For use in this assay, the yeast culture was streaked on an YPD agar plate and incubated for 24h at 30°C. Then, using a sterile disposable loop, cells from a colony were suspended in 5 mL of YPD media and aerated for 24h at 30°C on a shaker set at 300 rpm. The broth culture was diluted 10 times with media and the optical density of this suspension was measured at a wavelength of 600 nm. The suspension was further diluted to an OD_{600} of 0.01 resulting in a concentration of 3×10^6 cfu/mL. This suspension was further diluted 1:100 in YPD media to yield 3×10^4 cfu/mL. This final dilution was used for inoculating the plates. The final volume/well, including organism and compound was 200 µl. Thus, the final number of cells per well is approximately $15x10^3$ cells/mL. Tests were incubated overnight at 30 °C prior to recording MICs. The in vitro activity was determined visually at 24h of incubation as the lowest concentration of compound resulting in full inhibition of yeast growth.

References and notes

1. S.M. Bowman, S.J. Free, *Bioessays*, **2006**, *28*, 799-808.
2. Balashov, S.V.; Park, S.; Perlin, D.S. *Antimicrob. Agents Chemother.*, **2006**, *50*, 2058-2063.
3. Garcia-Effron, Chua, D.J., Tomada, J.R.; Dispersio, J.; Perlin, D.S.; Ghannoam M.; Bonilla, H. *Antimicrob. Agents and Chemother.*, **2010**, *54*, 2225-2227.
4. Perlin, D.S. *Drug Resistance Updates*, **2007**, *10*, 121-130.
5. Walker, L.A.; Crow, N.A.R.; Munro, C.A. *Fungal Genetics and Biology*, **2010**, *47*, 117-126.
6. Radding, J.A.; Heidler, S.A.; Turner, W.W. *Antimicrob. Agents Chemother.*, **1998**, 1187-1194.
7. Ballell, L.; Alink, K.J.; Slijper, M.; Versluis, C.; Liskamp, R.M.J.; Pieters, R.J. *ChemBioChem*, **2005**, *6*, 291-295.
8. Speers, A.E.; Adam, G.C.; Cravatt, B.F. *J. Am. Chem. Soc.*, **2003**, *125*, 4686-4687.
9. Debono, M.; Abbott, B.J.; Turner, J.R.; Howard, L.C.; Gordee, R.S.; Hunt, A.S.; Barnhart, M.; Molloy, R.M.; Willard, K.E.; Fukuda, D.; Butler, T.F.; Zeckner, D.J. *Ann. N.Y. Acad. Sci.*, **1988**, *544*, 152-163.
10. Debono, M.; Abbott, B.J.; Fukuda, D.S.; Barnhart, M.; Willard, K.E.; Molloy, R.M.; Michel, K.H.; Turner, J.R.; Butler, T.F.; Hunt, A.H. *J. Antibiot.*, **1989**, *XLII*, 389-397.
11. Taft, C.S.; Selitrennikoff, C.P. *J. Antibiot.*, **1990**, *XLIII*, 433-437.
12. Debono, M.; Turner, W.W.; LaGrandeur, L.; Burkhardt, F.J.; Nissen, J.S.; Nichols, K.K.; Rodriguez, M.J.; Zweifel, M.J.; Zeckner, D.J.; Gordee, R.S.; Tang, J.; Parr, T.R. *J. Med. Chem.*, **1995**, *38*, 3271-3281.
13. Jamison, J.A.; Zeckner, D.J.; Rodriguez, M.J. *J. Antibiot.*, **1997**, *50*, 562-566.
14. Jamison, J.A.; Rodriguez, M.J.; Vasudevan, V. *US Patent 6,670,324*, **2003**.
15. Scherpenzeel, M.; Moret, E.E.; Ballell, L.; Liskamp, R.M.J.; Nilsson, U.J.; Leffler, H.; Pieters, R.J. *ChemBioChem,* **2009**, *10*, 1724-1733.
16. Bandyopadhyay, S.; Bong, D. *Eur. J. Org. Chem.*, **2011**, 751-758.
17. For each proposed analogue the structure of the side chain (**5**-**7**) amide was drawn and a calculation performed by a computer assisted method to provide a ClogP value.[22,23] This methodology was based on the work of Debono et al.[12]

18. Caspofungin is present in and commercially available as “Cancidas” from Merck.
19. Vojkovsky, T. *Pept. Res.*, **1995**, *8*, 236-237.
20. Kaiser, E.; Colescott, R.L.; Bossinger, L.D.; Cook, P.I. *Anal. Biochem.*, **1970**, *34*, 595-598.
21. Meienhofer, J.; Waki, M.; Heimer, E.P.; Lambros, T.J.; Makofske, R.C.; Chang, C.-D. *Int. J. Peptide Protein Res.***1979**, *13*, 35.
22. Tetko, I. V.; Gasteiger, J.; Todeschini, R.; Mauri, A.; Livingstone, D.; Ertl, P.; Palyulin, V. A.; Radchenko, E. V.; Zefirov, N. S.; Makarenko, A. S.; Tanchuk, V. Y.; Prokopenko, V. V. *J. Comput. Aid. Mol. Des.*, **2005**, 19, 453-63.
23. VCCLAB, Virtual Computational Chemistry Laboratory, http:/www.vcclab.org, XLOGP2 program, feb 2012.

CHAPTER 5

Mutual Influence of Backbone Proline Substitution and Lipophilic Tail Character on the Biological Activity of Simplified Analogues of Caspofungin

Parts of this chapter have been published:

*Mulder, M.P.C.; *Fodran, P.; Kemmink, J.; Breukink, E.J.; Kruijtzer, J.A.W.; Minnaard, A.J.; Liskamp, R.M.J., *Org. Biomol. Chem.*, **2012**, *10*, 7491-7502. *) equal contributors

5.1 Introduction

As was described in chapter 1 the echinocandins represent the most recent class of antifungal drugs that has reached the market in the last decade.[1] The first licensed echinocandin was caspofungin (**1**, Figure 1), a semi-synthetic compound based on pneumocandin B_0, in 2001. Since then, two other semi-synthetic echinocandins, micafungin (2005) and anidulafungin (2006), have been approved by the Food and Drug Administration (FDA).[2] These clinically relevant echinocandins are all semisynthetic derivatives of the natural fermentation products.[3-5]

The complex chemical structures of the echinocandins have led to extensive structure activity relationship (SAR) studies by semisynthetic modification of the natural product.[6] This approach relies on the availability of the lipopeptides in large quantities from fermentation and of course these semisynthetic modifications cannot access a complete SAR of the echinocandins. With respect to this, synthetic approaches offer an opportunity to obtain valuable additional SAR information.

In 1992 the first total synthesis of simplified echinocandin analogues was described by Zambias et al.[7] Structure activity relationship data of these analogues showed that several of the functional groups, primarily the hydroxyl groups, were not essential for antifungal activity.[7] Partly inspired by this work, Klein et al. reported a similar study in 2000.[8] The total synthesis approach has provided valuable echinocandin SAR data that would be difficult or impossible to obtain via modification of the natural products themselves.[9]

These reports and the results described in chapter 2[10] showed that the role of the fatty acid tail is very dominant. These observations enticed us to synthesize simplified analogues of caspofungin to investigate the role of the methyl groups in the natural dimethylmyristoyl chain[11] of caspofungin **1**, which is described in this chapter.

Our previous analogues (e.g. **3**, Figure 1) were designed to contain a palmitoyl chain[10], instead of the dimethylmyristoyl chain, which is consistent with SAR studies showing that a regular C12-C18 fatty acid side chain gives an optimal activity.[12] Unfortunately, mimics equipped with this chain showed low to no activity. Therefore, based on previous work by Klein et al[8], simplified head-to-tail analogues were synthesized equipped with a terphenyl fatty acid side chain (e.g. **2** Figure 1). Terphenyl lipophilic tail containing analogue **2** was 30-fold more active than mimic **3** with a palmitoyl chain.[10] Other reports in the literature discussed the importance of both the stereochemistry and methyl branching patterns of fatty acids in biological recognition.[13,14] This raised the interest in an investigation of the influence of the presence and stereochemistry of methyl groups in the dimethylmyristoyl chain on the antifungal activity.

Although extensive structure-activity studies have been performed in the past on the nature of the fatty acid side chain and its influence on the activity of the echinocandins,[15-19] the role of the stereochemistry and number of methyl groups in the natural dimethylmyristoyl chain of caspofungin (**1**) has not been investigated so far.

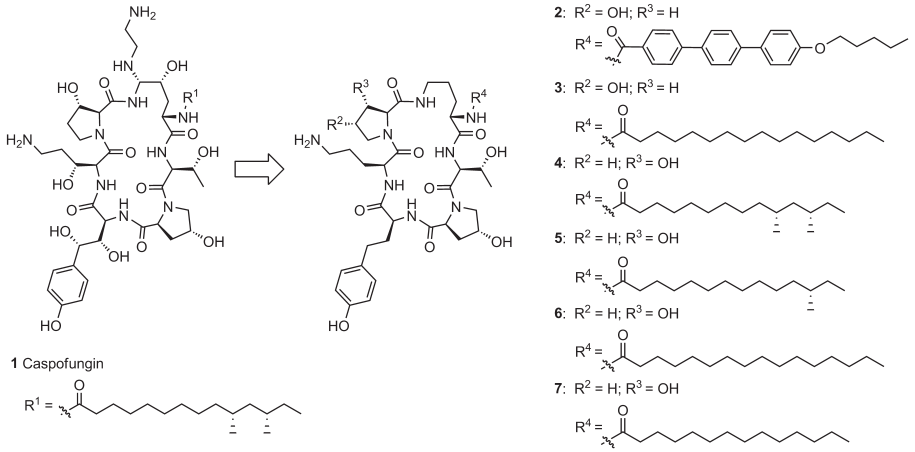

Figure 1. Structures of caspofungin (**1**), previously described mimics (**2** and **3**)[10] and the designed synthetic caspofungin analogues (**4**-**7**).

In this chapter the synthesis and antifungal activity is described of a simplified caspofungin analogue (**4**) bearing its natural (10*R*, 12*S*)-dimethylmyristoyl chain.[20] In addition, the influence of the methyl groups in this chain on antifungal activity was determined by synthesis of several analogues and evaluation of their antifungal activity. Also analogues were included with either one (**5**) or no (**6**,**7**) methyl groups (Figure 1).

5.2 Results and Discussion

5.2.1 Chemistry

Both the relative and absolute configuration of the fatty acid side chain of caspofungin (**1**) have been elucidated by Leonard et al.[20] Their reported stereoselective synthesis of the (*R*,*S*)-enantiomer was conducted in 8 steps, starting from (*R*)-propionyl-2-pyrrolidinemethanol (**10**), and provided (10*R*,12*S*)-dimethylmyristic acid **8** in a 90:10 (*syn*/*anti*) ratio of diastereomers (Scheme 1).[20] According to the reported synthesis the construction of the fatty acid side chain **8** was started with the acylation of L-prolinol **9** with propionic anhydride affording **10** in 71% after bulb-to-bulb distillation.

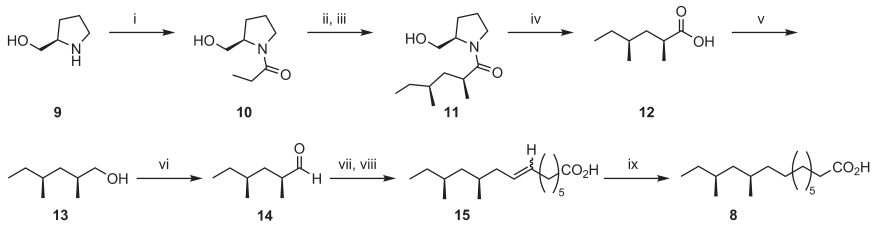

Scheme 1. Reported synthesis by Leonard et al.[15] of the dimethylmyristoyl side chain of caspofungin. Reagents and conditions: (i) propionic anhydride, 70 °C, 10 min (71%); (ii) 1) LDA, THF, 15 min; 2) HMPA, -67 °C, 135 min; (iii) (*S*)-(+)-1-iodo-2-methylbutane, 65 h; (iv) 1) 1M HCl, Δ; 2) cinchonidine, H_2O/acetone, 70 °C to RT, two times; (v) Et_2O/THF, $LiAlH_4$, 5 °C; (vi) DCM, Swern, -70 to 0 °C; (vii) $Br^-Ph_3P^+CH_2(CH_2)_6CO_2H$, THF, 0 °C, LiHMDS, 30 min; viii) Wittig 0 °C to RT, 4h; (ix) H_2, Pd/C.

The alkylation of **10** with optically pure 1-iodo-(2*S*)-methylbutane for obtaining **11** was unsuccessful. The reaction towards **11** was performed several times, but did not yield any product. In order to synthesize compound **11**, pyrrolidine **10** had to be deprotonated with LDA in the presence of HMPA, which stabilizes the dianion formed. Then the dianion was reacted with (*S*)-(+)-1-iodo-2-methylbutane. To determine if the dianion had been formed at all in the reaction, several test reactions with different bases and also with THP protected **10** were performed. These test reactions were quenched with D_2O to identify formation of dianion by NMR. The results of these test reactions are summarized in Table 1.

Table 1. Results test reactions for dianion formation.

	St. material	Base	% Dianion	% St. material
10a	**10**	LDA*	5	95
10b	**10**	LDA**	15	85
10c	THP protected 10	LDA**	32	68
10d	**10**	LHMDS	27	73
10e	**10**	KHMDS	13	87

* commercially available
** freshly made from diisopropylamine (2.2 eq) and nBuLi (2.1 eq) in THF at 0 °C

As is shown in Table 1, the dianion was formed only in low amounts. Therefore it was decided to move on to another route in collaboration with the group of prof. Minnaard of the University of Groningen. In this group an efficient asymmetric synthesis was designed using the copper/Josiphos[21,22] catalysed addition of methylmagnesium bromide for the construction of the stereogenic centers (Scheme 2).[21,22]

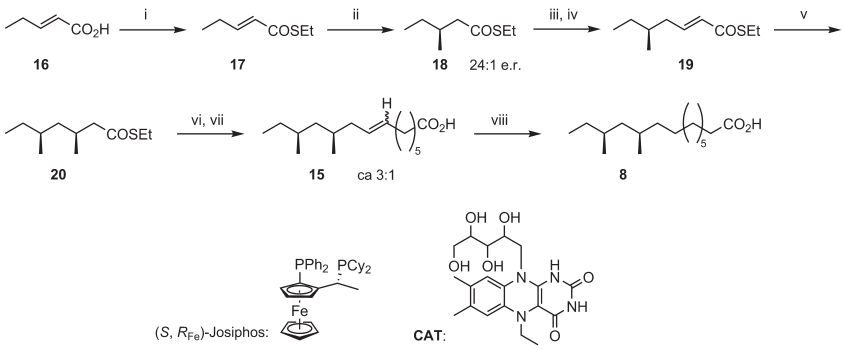

Scheme 2. Synthesis of (10*R*,12*S*)-dimethylmyristic acid **8**. i) EtSH, DCC, DMAP, DCM, 0-21°C, 3h, 95%; ii) MeMgBr, CuBr/(S,R_{Fe})-Josiphos, MTBE, –78°C, 16h, 92%; iii) DIBAL-H, DCM, –50°C, 1h; iv) $(MeO)_2P(O)CH_2COSEt$, *n*BuLi, THF, 0-21°C, 16h, 70%; v) MeMgBr, CuBr/(S,R_{Fe})-Josiphos, MTBE, –78°C, 16h, 80%; vi) DIBAL-H, DCM, –50°C, 1h; vii) $Br^-Ph_3P^+(CH_2)_6CO_2H$, LiHMDS, THF, 21°C, 20 min, 47%; viii) $NH_2NH_2.H_2O$, O_2, Cat, EtOH, 21°C, 70%.

Commercially available (*E*)-pent-2-enoic acid **16** was converted into thioester **17** under Steglich conditions.[23] This thioester underwent copper/Josiphos catalyzed enantioselective conjugate addition by MeMgBr smoothly, affording the desired compound **18** in 92% yield with a high e.r. (24:1).[22] Subsequent DIBAL-H reduction followed by Horner-Wadsworth-Emmons[22] reaction gave the elongated thioester **19** in good yield (80%) with an excellent *E*:*Z*

ratio (20:1). After separation of the unwanted *Z*-stereoisomer with column chromatography, the α,β-unsaturated thioester **19** was subjected to a second conjugate addition. This reaction afforded a 20:1 mixture of C3-epimers which was separable again by column chromatography. The desired diastereomer **20** was isolated in 80% yield. After DIBAL-H reduction and Wittig reaction with a carboxylate functionalized ylide, a mixture of double bond isomers **15** in an approximate 3:1 ratio was obtained in 47% combined yield. In order to avoid any epimerization of the nearby stereocenter, the double bond of **15** was subsequently reduced by diimide, *in situ* formed by catalytic oxidation of hydrazine,[24] affording **8** in 70% yield.

Overall, the side chain **8** of caspofungin was synthesized in a linear 8 step synthesis with an overall yield of 16%. The catalytic enantioselective conjugate addition in combination with a Wittig reaction using a carboxylate functionalized ylide, represents an efficient approach towards methyl-branched fatty acids. It is important to mention, that several of the intermediates in the synthesis were rather volatile, which complicated isolation.

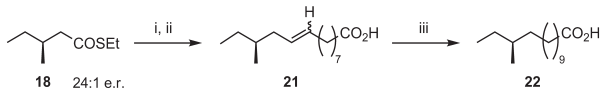

Scheme 3. Synthesis of (12*S*)-methylmyristic acid **22**. Reagents and conditions: i) DIBAL-H, DCM, –50°C, 1h; ii) $Br^-Ph_3P^+(CH_2)_8CO_2H$, LiHMDS, THF, 21°C, 20 min, 60% over two steps; iii) $NH_2NH_2.H_2O$, O_2, Cat, EtOH, 21°C, 80%.

The synthesis of the mono methyl analogue **22** was performed in similar manner (Scheme 3). Thioester (**18**) was reduced by DIBAL-H and after a Wittig reaction, a mixture of *E* and *Z* isomers (**21**) was isolated in 60% yield. Reduction of the resulting double bond was achieved by *in situ* generated diimide[24] giving **22** in 80% yield.

Now that we had both the (10*R*,12*S*)-dimethylmyristic acid **8** and its mono methyl analogue (12*S*)-methylmyristic acid **22** in hand, the attention was turned to the synthesis of the head-to-tail mimics.

First, the required building block Fmoc-3-Hyp(*t*Bu)-OH[25] **23** was synthesized starting from the commercially available (2*S*,3*S*)-*trans*-proline **24**. Protection of the amino group of **24** using FmocOSu proceeded smoothly to give Fmoc-protected amino acid derivative **25**. Allyl ester **26** was prepared under acidic conditions using a Dean-Stark apparatus. Subsequently, **26** was converted to the tert-butyl ether protected analogue **27** after which the desired Fmoc-3-Hyp(*t*Bu)-OH **23** was obtained by Pd-assisted removal of the allyl group.

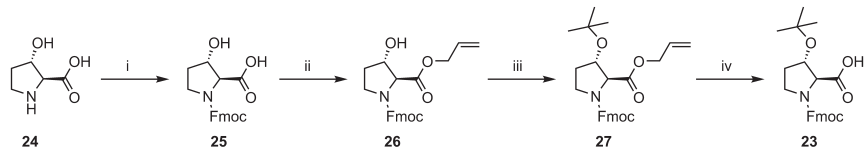

Scheme 4. Reagents and conditions: i) (1) FmocOSu, H_2O/dioxane, $NaHCO_3$, 20h, 99%; ii) allyl alcohol, toluene, p-toluenesulfonic acid, Dean-Stark, 1h Δ, 75%; iii) isobutene, H_2SO_4, DCM, 72h, 90%; iv) $Pd(PPh_3)_4$, $PhSiH_3$, DCM, 2h, 52%.

The synthesis of the head-to-tail mimics proceeded readily and is outlined in Scheme 5 for mimic **4**. Linear precursor **23** was prepared by SPPS using the trityl resin. Removal of the ε-Fmoc group from ornithine was followed by coupling of dimethylmyristic acid **8**. Mild acidolytic cleavage of the Mtt group liberated the peptide chain from the resin and gave the linear fully protected peptide precursor **24**. Solution-phase cyclization followed by protecting group removal afforded the macrocyclic peptide **4** in an overall yield of 51% after purification by preparative HPLC. Synthesis of macrocyclic peptides **5**-**7** was performed analogously to the synthesis of mimic **4** in Scheme 5. For the preparation of peptides **5**-**7** other fatty acids methylmyristic acid, palmitic acid and myristic acid were coupled, respectively in step viii) instead of the dimethylmyristic acid **8** as is shown in Scheme 5. Peptides **5**-**7** were obtained in overall yields of 48-88% after purification by preparative HPLC.

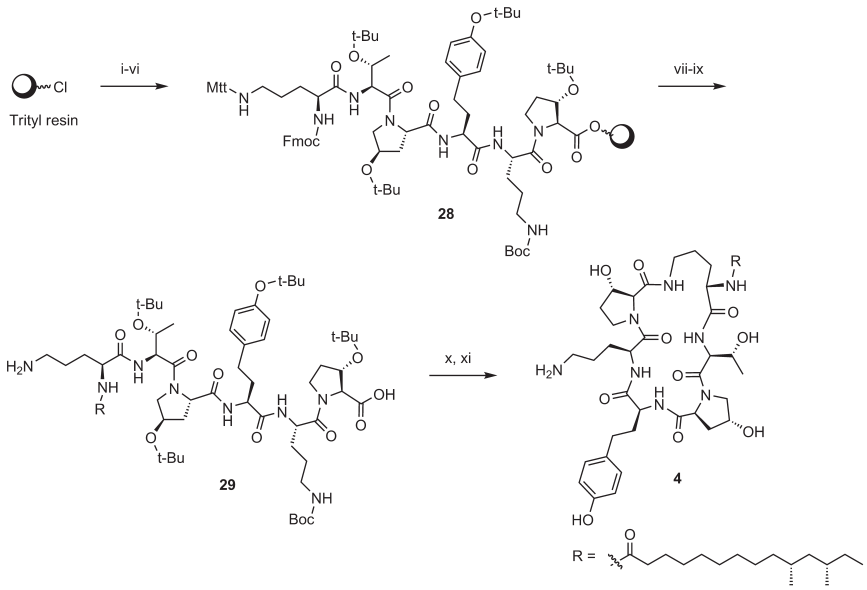

Scheme 5. Reagents and conditions: i) (1) Fmoc-3-Hyp(*t*Bu)-OH **23**, DIPEA, DCM; (2) DCM/MeOH/DiPEA (17/2/1, v/v/v); ii)-vi) (1) 20% piperidine in NMP; (2) Fmoc-Xxx-OH, BOP, DiPEA, NMP; vii) 20% piperidine in NMP; viii) dimethylmyristic acid **8**, HATU, DIPEA, NMP; ix) TFE/AcOH/DCM (2/1/7, v/v/v); x) BOP, DiPEA, DMF; xi) TFA/TIS/H_2O (95/2.5/2.5, v/v/v).

5.2.2 Structure Activity Relationships

The antifungal activity of each analogue (**4**-**7**) was evaluated using a broth microdilution microtiter assay against a panel of common *Candida* species.[26] This panel included *C. dubliniensis*, *C. glabrata*, *C. tropicalis*, *C. parapsilosis*, *C. krusei* and two strains of *C. albicans*. Caspofungin **1**[27] was used as a reference compound and our previous described compounds (**2** and **3**)[10] were also included in the test for comparison. The results of these tests are expressed as the minimum inhibitory concentration (MIC) value, the minimum concentration of compound which completely inhibits visible fungal growth, and are shown in Table 2.

Table 2. Screen against a panel of candida strains. (MIC value in μg/mL).

	Candida albicans CBS9975	*Candida albicans* CBS8758	*Candida dubliniensis* CBS7987	*Candida glabrata* CBS138	*Candida krusei* CBS573	*Candida parapsilosis* CBS604	*Candida tropicalis* CBS94
caspofungin	0.023	0.039	0.014	0.027	0.006	0.281	0.006
2	0.14	0.156	0.063	0.188	0.078	>4.25	0.063
3	4.38	4.38	0.938	3.8	3.8	>10	3.8
4	0.117	0.188	0.07	0.469	2.25	>4.25	0.094
5	0.188	0.281	0.047	0.625	1.875	>4.25	0.188
6	0.313	0.406	0.102	0.234	0.375	3.5	0.109
7	0.203	0.25	0.047	0.438	0.813	>4.25	0.063

The simplified caspofungin analogue **4**, bearing the natural side chain, showed substantial antifungal activity against the *Candida* strains (0.07 – 0.19 μg/mL) with a somewhat higher MIC value for *C. krusei* (2.25 μg/mL) and proved to be inactive against *C. parapsilosis*. Only a 5-fold decrease in the inhibitory activity of **4**, compared with that of caspofungin (**1**), was observed against *C. albicans* and the closely related *C. dubliniensis*.[28] In addition, analogue **4** proved to have a more selective antifungal spectrum than caspofungin (**1**).

In order to assess the contribution of the methyl groups in the dimethylmyristoyl chain **8** of caspofungin (**1**), the mono methyl derivative methylmyristic acid **22**, as well as non-methylated palmitic and myristic fatty acid chains were incorporated as a replacement for **8** in analogue **4** to give analogues **5**, **6** and **7**, respectively.

Remarkably, all of the analogues in the series showed substantial antifungal activity against *Candida*. Similar to analogue **4**, these analogues were more selective than caspofungin, having higher MIC values for *C. krusei* and showing no activity against *C. parapsilosis.* These results showed that there is no obvious relationship between the presence of the methyl groups in the dimethylmyristoyl chain **8** of caspofungin (**1**) and antifungal activity. Most surprisingly, analogue **6** with a palmitoyl chain, as is also present in analogue **3**, showed a 10-35 fold increase in antifungal activity against *Candida*. The only difference between these analogues is the position of the hydroxyl group in the left-upper hydroxyproline (residue Hyp-6) of the cyclic hexapeptide (R^2 and R^3 in Figure 1).

These findings did not justify further investigation into the role of the methyl groups in the fatty acid side chain for example by preparation of additional enantiomers or diastereomers derivatives. However, the somewhat surprising influence of the hydroxyl position in the proline residue warranted the synthesis of three additional analogues. The synthesis of these macrocyclic peptides **30**-**32** was performed analogously to the synthesis of mimic **4** in Scheme 5 and their antifungal activity was evaluated and expressed as MIC values as is shown in Table 3.

Table 3. Screen against a panel of candida strains. (MIC value in μg/mL).

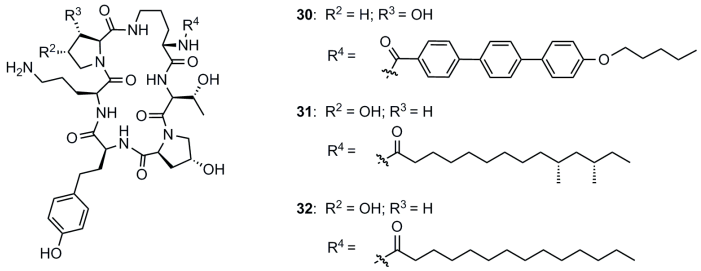

	Candida albicans CBS9975	*Candida albicans* CBS8758	*Candida dubliniensis* CBS7987	*Candida glabrata* CBS138	*Candida krusei* CBS573	*Candida parapsilosis* CBS604	*Candida tropicalis* CBS94
30	0.051	0.039	0.031	0.027	0.027	0.75	0.141
31	1.63	3	1.5	2.5	>4.25	>4.25	2.5
32	>4.25	>4.25	3	>4.25	>4.25	>4.25	>4.25

These analogues confirm the finding that the position of the hydroxyl group in the top-left proline residue (R^2 and R^3 in Hyp-6) is crucial for antifungal activity. Analogues **3**, **31** and **32** (R^2=OH) bearing the same lipophilic tail as analogue **6**, **4** and **7** (R^3=OH) respectively, were practically inactive or showed a tremendous decrease in antifungal activity against *Candida*. Clearly R^2= OH is only allowed in caspofungin derivative **2** bearing a terphenyl fatty acid side chain. Here analogue **30** with R^3= OH and analogue **2** with R^2= OH both showed substantial antifungal activity against *Candida*. Analogue **30** was even more active than analogue **2** and had activities comparable to those of caspofungin (**1**). In addition the selectivity of inhibition of *Candida parapsilosis* by **30** was remarkable and was not shown by any of the other analogues (See Tables 2 and 3).

These results suggest that the position of the hydroxyl group in the top-left hydroxyproline of the cyclic hexapeptide backbone (R^2 and R^3 in Hyp-6, Figure 1) in combination with the character of the lipophilic fatty acid chain was a crucial factor for antifungal activity. In attempts to interpret this finding we evaluated the analogues by circular dichroism (CD) in order to probe their conformational properties.

5.2.3. Circular dichroism spectroscopy

In addition to secondary structure prediction, circular dichroism spectroscopy can give valuable insights into peptide structure.[29] As was described by Ovchinnikov and Ivanov[30], CD spectra can provide evidence for the perturbation or alteration of the conformational state in a series of related peptides.[29] Therefore, CD may provide an attractive technique to evaluate our analogues and determine whether the observed antifungal activity can be correlated with the conformational state.

Thus, the secondary structure of caspofungin (**1**) and analogues (**2**-**7**, **30**-**33**) was investigated by circular dichroism as presented in Figure 2. In addition to measurements in MeCN/H_2O,

CD spectra were measured in TFE/H_2O, since TFE is known to enhance secondary structure formation of peptides.[31]

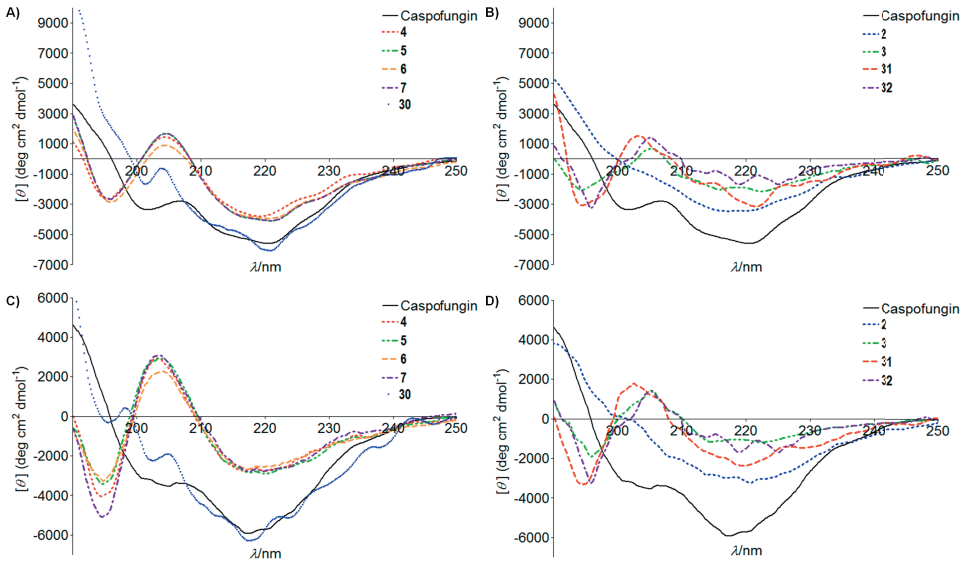

Figure 2. CD spectra of caspofungin and analogues (**2**-**7**, **30**-**32**). A) + B) Measured in MeCN/H_2O (1/1, v/v); C) + D) Measured in TFE/H_2O (1/1, v/v). All peptides were measured at 0.1 mM concentration.

As is shown in Figure 2, spectra of the cyclic peptides **4**-**7** in both MeCN/H_2O and TFE/H_2O are similar. Peptides **4**-**7** are characterized by a negative band at ca. 220 nm and a positive band at 205 nm. In general, these peptides (**4**-**7**) showed CD spectra characteristic for a type II β-turn.[32-35] However, their pattern below 215 nm is clearly different from caspofungin (**1**). This difference may be explained by the deletion of several hydroxyl groups in our analogues. Moreover, analogue **30** showed a distinctly different pattern at wavelengths below 210 nm and higher ellipticities of the band compared to peptides **4**-**7**. This observation may be explained by a large contribution of the aromatic residues present in the side chain of analogue **30** as is supported by CD spectra of other analogues (see chapter 6).

Remarkably, cyclic peptides **3**, **32** and **32** (R^2=OH; Figure 2B and D) exhibit different spectra than series **4**-**7** (R^3=OH; Figure 2A and C). Differences are apparent from the ellipticities of the bands, which could indicate that these peptides have a more disordered structure with less β-turn character. The only structural difference between these analogues is the position of the hydroxyl group in the left-upper hydroxyproline of the hexapeptide ring (R^2 and R^3 in Hyp-6, Figure 1). Apparently, merely the position of the OH-function was responsible for the largely different CD-spectra and possibly conformational behaviour of the peptides.

For further insights into the influence of the OH-function on the conformation of our analogues, models were built and superimposed on the reported crystal structure of Echinocandin B (ECBN)[5] as is shown in Figure 3. Overall, the more active analogue **6** appeared to have a better superimposition with the crystal structure. Analogue **3** had a more puckered structure with the Hyp-6 residue situated more in the back of the molecule as compared

to analogue **6**. In addition, the Orn-5 residue was pointing out more to the front of the macrocyclic peptide ring structure in **3**, These models support the finding that the position of the OH-function in Hyp-6 induces subtle changes in the conformation of the peptides. Apparently, these add up and were sufficient for a large effect on the biological activity.

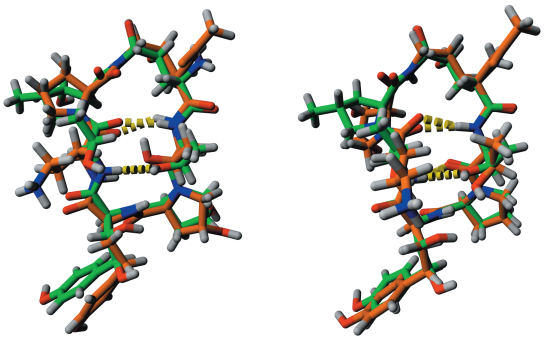

Figure 3. Superimposition of ECBN (carbons colored green) with analogues **3** (right) and **6** (left) (carbons colored orange). The backbone atoms have been used for superimposition.

5.3 Conclusions

A versatile approach for the rapid enantioselective synthesis of the dimethylmyristoyl chain of caspofungin and a one-methyl group containing analogue is described. These fatty acids were coupled to simplified analogues of the caspofungin skeleton. In this way access was obtained to new fully synthetic derived caspofungin mimics with high and selective antifungal activities against *Candida*. Unexpectedly, no obvious relationship between the presence of the methyl groups in the dimethylmyristoyl tail **8** of caspofungin (**1**) and antifungal activity was observed. The dimethyl containing lipophilic tail derivative **4** did not lead to significant improvement of its bioactivity as compared to that of the non-methylated lipophilic chain. In fact the activities of non-methylated derivatives **6** and **7** and the methylated derivatives **4** and **5** were quite similar in most species. The position of the hydroxyl group in the top-left proline residue (R^2 and R^3 in Hyp-6) was apparently more crucial: derivative **3** (R^2= OH) having the same tail as derivative **6** (R^3= OH) was practically inactive. Clearly R^2= OH is only allowed in caspofungin derivative **2** bearing a terphenyl fatty acid side chain. Thus, the position of the hydroxyl group in the top-left hydroxyproline of the cyclic hexapeptide backbone (R^2 and R^3 in Hyp-6, Figure 1) in combination with the character of the lipophilic fatty acid chain was a crucial factor for antifungal activity. The position of the hydroxy group turned out to be very important for the general activity against *Candida* species as was shown by the higher activity of analogue **30** compared to analogue **2**, but also for selectivity of inhibition. Compound **30** was capable of a much more selective inhibition of *Candida parapsilosis* than analogue **2**.

CD measurements showed subtle but distinctive changes indicative of structural changes in the conformation of these cyclic peptides. The results of this investigation suggest that the top-left proline residue somehow plays an important role in the bio-active conformation of the macrocyclic peptide ring structure. Finally, we have observed that the choice of the fatty acid derivative (rigid as in **2** or flexible as in **3**) in combination with the conformational character of the ring may be a determining factor for antifungal activity.

5.4 Experimental section

5.4.1 Reagents, materials and analysis methods

Unless stated otherwise, all chemicals were obtained from commercial suppliers and used without further purification. HPLC grade solvents were purchased from Biosolve B.V. (Valkenswaard, The Netherlands) and used directly, with the exception of DMF, NMP and DCM, which were dried on molecular sieves (4Å). Fmoc protected amino acids were purchased from GL Biochem Ltd. (Shanghai, China). Protected homotyrosine (H-hTyr(*t*Bu)-OH) was purchased from Advanced Chemtech (Louisville, United States) and furnished with the Fmoc group. Fmoc-Orn(Mtt)-OH was obtained from Nova Biochem. The 2-chlorotritylchloride PS resin cross-linked with 1% DVB (200-400 mesh) was purchased from Hecheng Chemicals (Shanghai, China) (theoretical loading: 1.10 mmol/g).

All Reactions were carried out at room temperature unless stated otherwise. Solid phase synthesis was performed in plastic syringes with a polyethylene frit. Synthesis in solution was monitored by TLC on Merck pre-coated Silica 60 plates. Spots were visualized by UV light, K_2CO_3/$KMnO_4$, ninhydrin or Seebach stain (phosphomolybdic acid/cerium sulphate).[36] Solid phase reactions were monitored with the chloranil test[37] in case of secondary amines or with the Kaiser test[38] in case of primary amines. Column chromatography was performed using Silicycle UltraPure silicagel (40-63 μm).

^{1}H NMR spectra were recorded on a Varian AMX 400 MHz spectrometer or Varian G-300 (300 MHz) spectrometer and chemical shifts are given in ppm relative to TMS (0.00 ppm). ^{13}C NMR spectra were recorded using the attached proton test (APT) sequence on a Varian AMX 400 (101 MHz) or a Varian G-300 (75.5 MHz) spectrometer and chemical shifts are given in ppm relative to $CDCl_3$ (77.0 ppm). For measurements in DMSO, the residual solvent peak was used as a reference. For the peptides, ^{1}H NMR, TOCSY, ^{1}H-^{13}C HSQC and ROESY spectra were recorded using a Varian INOVA-500 spectrometer (500 MHz).

Purity of the peptides was confirmed by analytical HPLC using an Alltima C8 column (4.6 × 250 mm; 5 μm) at a flow rate of 0.5 mL/min using a linear gradient of buffer B (100% in 40 min) from 100% buffer A. Analytical HPLC was performed on a Shimadzu automated HPLC system equipped with an evaporative light scattering detector (PL-ELS 1000) and a UV/Vis detector operated at 220/254 nm. Preparative HPLC runs were performed using an Alltima C8 column (22 × 250 mm; 10 μm) at a flow rate of 6 ml/min with a linear gradient of buffer B (100% in 80 min) from 100% buffer A on an Applied Biosystems 400 solvent delivery system with an Applied Biosystems 757 UV/VIS absorbance detector. The buffer system used consists out of buffer A: 0.1 % TFA in MeCN/H_2O, 20/80, v/v and buffer B: 0.1% TFA in *i*-PrOH/MeCN/H_2O, 45/50/5, v/v/v.

ESI-MS spectra were obtained in the positive ion mode on a Shimadzu QP8000 single quadrupole mass spectrometer. HRMS analyses were performed on a MALDI TOF/TOF (Applied Biosystems).

CD spectroscopy
CD spectra were recorded at 298 K on a JASCO J-810 spectrometer using 0.1 cm path length quartz cells. The CD spectra are an average of four scans, collected at 0.2 nm intervals between 190 and 250 nm. The peptides were prepared at concentrations of 0.1 mM in MeCN/H_2O (1/1, v/v) or 0.1 mM in TFE/H_2O (1/1, v/v). Ellipticity is reported as the mean residue ellipticity [θ] in degrees.cm^2/$dmol^{-1}$.

YASARA modelling
Modeling of the structures was accomplished using the YASARA Structure 10.5.2.1 software package. Structures were energy minimized using the simulated annealing protocol employing the AMBER99[39] force field. Of each structure a 2500 ps MD-simulation in water was run. After an equilibration period of 250 ps, the structure with the lowest energy was selected from the trajectory between 250-2500 ps and saved as a yob file. Molecules were superimposed on the reported crystal structure of ECBN[5], by minimizing the rmsd between the backbone atoms in the ring.

5.4.2 Chemistry

General Procedures for solid phase synthesis
Peptides were synthesized manually. Each synthetic cycle consisted of the following steps:
Fmoc-group removal: The resin was treated with a 20% solution of piperidine in NMP (3×, each 10 min). The solution was removed by filtration and the resin was washed with NMP (3×, each 3 min) and DCM (3×, each 3 min).
Coupling step: A mixture of Fmoc-Xxx-OH (3 equiv.), BOP (3 equiv.) and DiPEA (6 equiv.) in NMP (10 mL/ mmol)) was added to the resin and N_2 was bubbled through the mixture for 2h. The solution was removed by filtration and the resin washed with NMP (3×, each 3 min) and DCM (3×, each 3 min). Completion of the coupling was checked with Kaiser or chloranil test.
Capping of the remaining free amines: Capping solution [Ac_2O (50 mmol, 4.7 mL), HOBt (1.9 mmol, 220 mg), DiPEA (12.5 mmol, 2.2 mL) in 100 mL NMP] (10 mL/ mmol) was added to the resin and N_2 was bubbled through the mixture for 20 min. The solution was removed by filtration and the resin was washed with NMP (3×, each 3 min) and DCM (3×, each 3 min).

General procedure for the preparation of the caspofungin analogues (4-7)
A polystyrene resin functionalized with a 2-chloro Trityl chloride linker (550 mg; initial loading: 1.1 mmol/g) was loaded with Fmoc-3-Hyp(*t*Bu)-OH **23** (999 mg; 2.44 mmol) in DCM (5 mL) in the presence of DiPEA (850 μL; 4.88 mmol) for 16h. The solution was removed by filtration and the resin washed with DCM (6× 5 mL, each 3 min). After drying *in vacuo* overnight, the amount of Fmoc-3-Hyp(*t*Bu)-OH coupled to the resin was determined by a Fmoc determination according to Meienhofer[40] and was found to be 0.520 mmol/g. Subsequently, unreacted tritylchloride moieties were capped with methanol (DCM/MeOH/DiPEA; 3× 5 mL, each 2 min; 17/2/1; v/v/v). The peptide sequence was synthesized according to the general procedure for solid phase peptide synthesis. The resin-bound peptide **28** was divided in portions for the synthesis of the analogues **4**-**7**. The Fmoc group was cleaved and the fatty acid side chain was coupled by adding the tail (3 equiv.), HATU (3 equiv.) and DiPEA (6 equiv.) in NMP (3 mL) to the resin. The mixture was shaken overnight, subsequently the

coupling solution was removed by filtration and the resin washed with NMP (3× 4 mL, each 3 min) and DCM (3× 4 mL, each 3 min). Completion of the coupling was checked with the Kaiser test. Then, mild acidolytic cleavage, by treatment with TFE/AcOH/DCM (2/1/7, v/v/v, 5 mL) for 2 hours, of the Mtt group as well as cleavage from the resin gave protected peptide precursor **29**. The mixture was concentrated *in vacuo* and the peptide was precipitated in MTBE/Hexanes (3×, 1/1, v/v). The linear peptide was then subjected to head-to-tail cyclization by dissolving it in dry DMF (2 mL/μmol) followed by the addition of BOP (4 equiv.) and DiPEA (8 equiv.). The mixture was stirred for 48h and then evaporated *in vacuo*. The product was redissolved in EtOAc and washed with 1M $KHSO_4$ (2×), $NaHCO_3$ (2×) and H_2O (2×). The organic layer was dried over Na_2SO_4, filtered and concentrated *in vacuo*. Final protecting group removal by treatment with a mixture of TFA/TIS/H_2O (2 mL, 95/2.5/2.5, v/v/v) for 2h and precipitation in MTBE/hexanes (3×, 1/1, v/v) afforded the crude peptide. After lyophilization from *tert*-BuOH/H_2O (1/1, v/v) the peptide was purified by preparative HPLC.

***Cyclo*[-(DMT-Myr)-Orn-Thr-Hyp-hTyr-Orn-3-Hyp] (4)**

Peptide **4** was obtained according to the general procedure for the preparation of the caspofungin analogues using 149.4 μmol of **28**. After lyophilization, peptide **4** (74.5 mg; 51%) was obtained as a white solid. Purity was confirmed by analytical HPLC and was found to be higher than 99% (R_t = 41.28 min). ESI-MS calcd for $C_{50}H_{82}N_8O_{11}$: 970.61, found: m/z 971.90 $[M+H]^+$; HRMS calcd for $C_{50}H_{82}N_8O_{11}$ $[M+H]^+$ 971.6181, found 971.6124; ^{1}H-NMR (CD_3OH, 500 MHz): δ Orn-1: 8.34 (NH), 4.48 (αCH), 2.31/1.79 (βCH), 1.68 (γCH), 3.60/2.85 (δCH); Thr-2: 8.73 (NH), 4.90 (αCH), 4.53 (βCH), 1.22 (γCH); Hyp-3: 4.49 (αCH), 2.27/1.97 (βCH), 4.50 (γCH), 3.78/3.70 (δCH); hTyr-4: 7.62 (NH), 4.81 (αCH), 1.96/1.67 (βCH), 2.98/2.92 (γCH), 6.92/6.69 (Ar-H); Orn-5: 7.50 (NH), 4.30 (αCH), 2.21/1.92 (βCH), 2.17 (γCH), 2.57 (δCH); Hyp-6: 4.28 (αCH), 4.08 (βCH), 2.27/1.97 (γCH), 3.78/3.71 (δCH); Tail: 2.25 (C(O)CH_2), 1.81/1.75 (CH_2), 1.67/1.61 (CH_2), 1.49, 1.42, 1.35, 1.33/1.27, 1.31/1.06, 1.28 (CH_2), 1.24/0.92 (CHCH_2CH), 1.09, 0.87 (CH_3), 0.85 (CH_3) ppm. ^{13}C-NMR (CD_3OH, 125 MHz): δ Orn-1: 53.1 (αCH), 38.1 (βCH), 24.0 (γCH), 37.6 (δCH); Thr-2: 57.9 (αCH), 68.9 (βCH), 19.7 (γCH); Hyp-3: 62.4 (αCH), 34.2 (βCH), 71.4 (γCH), 56.9 (δCH); hTyr-4: 50.8 (αCH), 30.0 (βCH), 40.6 (γCH), 130.7/ 116.5 (Ar-H); Orn-5: 54.7 (αCH), 34.4 (βCH), 27.0 (γCH) 32.6 (δCH); Hyp-6: 74.5 (αCH), 69.4 (βCH), 34.2 (γCH), 46.5 (δCH); Tail: 45.7 (CHCH_2CH), 37.8, 36.7 (C(O)CH_2), 32.6, 30.9, 30.0, 27.7, 26.9 (CH_2), 23.9 (CH_2), 30.8 (CH_2), 30.1, 20.05 (CH_3), 11.2 (CH_3).

***Cyclo*[-(Me-Myr)-Orn-Thr-Hyp-hTyr-Orn-3-Hyp] (5)**

Peptide **5** was obtained according to the general procedure for the preparation of the caspofungin analogues using 38.9 μmol of resin bound peptide **28**. After lyophilization, peptide **5** (17.9 mg; 48%) was obtained as a white solid. Purity was confirmed by analytical HPLC and was found to be higher than 95% (R_t = 40.48 min). ESI-MS calcd for $C_{49}H_{80}N_8NaO_{11}$: 979.58, found: m/z 979.85 $[M+Na]^+$; HRMS calcd for $C_{49}H_{80}N_8O_{11}$: $[M+H]^+$ 957.6025, found 957.6016; ^{1}H-NMR (CD_3OH, 500 MHz): δ Orn-1: 8.15 (NH), 8.33 (εNH), 4.48 (αCH), 2.30/1.79 (βCH), 1.67 (γCH), 3.59/2.84 (δCH); Thr-2: 8.72 (NH), 4.89 (αCH), 4.53 (βCH), 1.22 (γCH); Hyp-3: 4.48 (αCH), 2.27/1.96 (βCH), 4.49 (γCH), 3.77/3.70 (δCH); hTyr-4: 7.72 (NH), 4.80 (αCH), 1.95/1.66 (βCH), 2.98/2.91 (γCH), 6.99/6.68 (Ar-H); Orn-5: 7.52 (NH), 4.30 (αCH), 2.20/1.91 (βCH), 2.17 (γCH), 2.56 (δCH); Hyp-6: 4.28 (αCH), 4.07 (βCH), 2.27/1.96 (γCH), 3.77/3.70 (δCH); Tail: 2.24 (C(O)CH_2), 1.80/1.75 (CH_2), 1.66/1.59 (CH_2), 1.32 (CH_2), 1.30, 1.30/1.27,

1.30/1.09, 1.29 (CH_2), 1.27 (CH_2), 1.13, 0.87 (CH_3), 0.85(CH_3) ppm. ^{13}C-NMR (CD_3OH, 125 MHz): δ Orn-1: 53.1 (αCH), 38.1 (βCH), 24.0 (γCH), 37.6 (δCH); Thr-2: 57.9 (αCH), 68.9 (βCH), 19.8 (γCH); Hyp-3: 62.3 (αCH), 34.2 (βCH), 71.3 (γCH), 56.8 (δCH); hTyr-4: 50.8 (αCH), 30.0 (βCH), 40.6 (γCH), 130.7/ 116.5 (Ar-H); Orn-5: 54.6 (αCH), 34.4 (βCH), 26.9 (γCH) 32.6 (δCH); Hyp-6: 74.5 (αCH), 69.4 (βCH), 34.2 (γCH), 46.5 (δCH); Tail: 37.6, 36.6 (C(O)*C*H_2), 35.4, 30.7 (CH_2), 30.3, 30.1 (CH_2), 27.9, 26.9 (CH_2), 23.9 (CH_2), 23.8 (CH_2), 19.3 (CH_3), 11.4 (CH_3).

***Cyclo*[-(Palm)-Orn-Thr-Hyp-hTyr-Orn-3-Hyp] (6)**

Peptide **6** was obtained according to the general procedure for the preparation of the caspofungin analogues using 38.9 μmol of resin bound peptide **28**. After lyophilization, peptide **6** (24.5 mg; 65%) was obtained as a white solid. Purity was confirmed by analytical HPLC and was found to be higher than 99% (R_t = 42.28 min). ESI-MS calcd for $C_{50}H_{82}N_8O_{11}$: 971.23, found: m/z 972.45 $[M+H]^+$; HRMS calcd for $C_{50}H_{82}N_8O_{11}$ $[M+H]^+$ 971.6181, found 971.6197; ^{1}H-NMR (CD_3OH, 500 MHz): δ Orn-1: 8.16 (NH), 4.48 (αCH), 2.30/1.78 (βCH), 1.67 (γCH), 3.59/2.84 (δCH); Thr-2: 8.72 (NH), 4.88 (αCH), 4.52 (βCH), 1.21 (γCH); Hyp-3: 4.49 (αCH), 2.26/1.96 (βCH), 4.49 (γCH), 3.77/3.70 (δCH); hTyr-4: 7.72 (NH), 4.81 (αCH), 1.96/1.66 (βCH), 2.97/2.91 (γCH), 6.99/6.68 (Ar-H); Orn-5: 7.52 (NH), 4.30 (αCH), 2.20/1.91 (βCH), 2.17 (γCH), 2.57 (δCH); Hyp-6: 4.28 (αCH), 4.07 (βCH), 2.26/1.96 (γCH), 3.77/3.71 (δCH); Tail: 2.24 (C(O)*CH*$_2$), 1.78/1.75 (CH_2), 1.66/1.60 (CH_2), 1.31 (CH_2), 1.30 (CH_2), 1.28 (CH_2), 1.27 (CH_2), 0.89 (CH_3) ppm. ^{13}C-NMR (CD_3OH, 125 MHz): δ Orn-1: 53.1 (αCH), 38.1 (βCH), 24.0 (γCH), 37.6 (δCH); Thr-2: 58.0 (αCH), 68.9 (βCH), 19.7 (γCH); Hyp-3: 62.3 (αCH), 34.2 (βCH), 71.3 (γCH), 56.9 (δCH); hTyr-4: 50.8 (αCH), 30.0 (βCH), 40.6 (γCH), 130.7/ 116.5 (Ar-H); Orn-5: 54.6 (αCH), 34.4 (βCH), 27.0 (γCH) 32.7 (δCH); Hyp-6: 74.5 (αCH), 69.4 (βCH), 34.2 (γCH), 46.5 (δCH); Tail: 36.7 (C(O)*C*H_2), 32.8 (CH_2), 30.5 (CH_2), 30.0 (CH_2), 27.0 (CH_2), 23.9 (CH_2), 23.4 (CH_2), 14.1 (CH_3).

***Cyclo*[-(Myr)-Orn-Thr-Hyp-hTyr-Orn-3-Hyp] (7)**

Peptide **7** was obtained according to the general procedure for the preparation of the caspofungin analogues using 38.9 μmol of resin bound peptide **28**. After lyophilization, peptide **7** (32.4 mg; 88%) was obtained as a white solid. Purity was confirmed by analytical HPLC and was found to be higher than 99% (R_t = 39.33 min). ESI-MS calcd for $C_{48}H_{78}N_8O_{11}$: 942.58, found: m/z 944.00 [M+H]+; HRMS calcd for $C_{48}H_{78}N_8O_{11}$ [M+H]+ 943.5868, found 943.5867; ^{1}H-NMR (CD_3OH, 500 MHz): δ Orn-1: 8.16 (NH), 8.34 (εNH), 4.48 (αCH), 2.31/1.78 (βCH), 1.67 (γCH), 3.59/2.85 (δCH); Thr-2: 8.72 (NH), 4.89 (αCH), 4.53 (βCH), 1.22 (γCH); Hyp-3: 4.49 (αCH), 2.27/1.97 (βCH), 4.50 (γCH), 3.78/3.70 (δCH); hTyr-4: 7.62 (NH), 4.81 (αCH), 1.96/1.66 (βCH), 2.97/2.92 (γCH), 6.99/6.69 (Ar-H); Orn-5: 7.53 (NH), 4.30 (αCH), 2.21/1.92 (βCH), 2.17 (γCH), 2.57 (δCH); Hyp-6: 4.28 (αCH), 4.08 (βCH), 2.27/1.96 (γCH), 3.78/3.71 (δCH); Tail: 2.25 (C(O)*CH*$_2$), 1.81/1.75 (CH_2), 1.66/1.60 (CH_2), 1.32 (CH_2), 1.31 (CH_2), 1.29 (CH_2), 1.27 (CH_2), 0.90 (CH_3) ppm. ^{13}C-NMR (CD_3OH, 125 MHz): δ Orn-1: 53.1 (αCH), 38.1 (βCH), 24.0 (γCH), 37.6 (δCH); Thr-2: 58.0 (αCH), 69.0 (βCH), 19.7 (γCH); Hyp-3: 62.3 (αCH), 34.2 (βCH), 71.3 (γCH), 56.9 (δCH); hTyr-4: 50.8 (αCH), 29.9 (βCH), 40.6 (γCH), 130.7/ 116.5 (Ar-H); Orn-5: 54.7 (αCH), 34.4 (βCH), 27.0 (γCH) 32.7 (δCH); Hyp-6: 74.5 (αCH), 69.4 (βCH), 34.2 (γCH), 46.5 (δCH); Tail: 36.7 (C(O)*C*H_2), 32.9 (CH_2), 30.4 (CH_2), 30.0 (CH_2), 27.0 (CH_2), 23.9 (CH_2), 23.4 (CH_2), 14.2 (CH_3).

(*R*)-Propionyl-2-pyrrolidinemethanol (10)[41]
Propionic anhydride (12.6 mL, 98.3 mmol) was added drop wise to L-prolinol **9** (9.0 g, 89.3 mmol). Then, the mixture was heated at 70°C for 10 min and basified to pH=9 with 2 M NaOH. The solution was extracted with DCM (3x), the combined organic layers were dried over Na_2SO_4 and concentrated *in vacuo*. The crude was purified by bulb-to-bulb distillation (1.5 mbar, 139 °C) to afford **10** (9.95 g; 71%) as a colourless liquid. R_f = 0.65 (DCM/MeOH/AcOH 9/1/0.1, v/v/v); ^{1}H NMR ($CDCl_3$, 300 MHz): δ 1.16 (t, J= 7.4 Hz, 3H, CH_3), 1.57-1.65 (m, 1H, βCH_2), 1.83-2.10 (m, 3H, βCH_2 and γCH_2), 2.33 (q, 2H, CH_2), 3.42-3.67 (m, 4H, δCH_2 and CH_2OH), 4.18-4.26 (m, 1H, αCH), 5.46 (bs, 1H, OH) ppm; ^{13}C NMR ($CDCl_3$, 75.5 MHz): δ 9.06 (CH_3), 24.54 (γCH_2), 28.43 (βCH_2), 48.11 (δCH_2), 61.32 (αCH), 67.66 (CH_2OH), 175.31 (C=O).

General procedure for test reactions concerning the formation of a dianion of 10.
Glassware was dried in the oven and cooled down under argon prior to use. Syringes were dried over P_2O_5 in a desiccator overnight and put on a flask with nitrogen prior to use. The amide (**10**) was dried overnight at an oil-pump prior to use. Diisopropylamine was distilled from KOH and degassed with nitrogen. In case of the use of freshly prepared LDA, this was prepared first by reacting diisopropylamine (2.2 eq) with nBuLi (2.1 eq) in THF at 0 °C. **10** was dissolved in THF and cooled to -78 °C. Hereafter, the base was added to the solution. The reaction mixture was stirred for 1-2 hours. The reaction was quenched with D_2O (3 mL/mmol amide) and extracted with Et_2O (3x). The combined organic layers were dried over Na_2SO_4 and concentrated *in vacuo*. ^{1}H NMR ($CDCl_3$, 300 MHz): δ 1.14 (t, J= 7.4 Hz 3H, CH_3,), 1.68-1.73 (m, 1H, βCH_2), 1.86-2.05 (m, 3H, βCH_2 and γCH_2), 2.35 (q, 2H, CH_2CH_3), 2.41 (m, 2H, CH_2CH_3 deuterated product), 3.47-3.53 (m, 2H, δCH_2), 3.59 (d, J = 5.5 Hz, 2H, CH_2OH), 3.95 (m, 1H, αCH deuterated product), 4.18 (m, 1H, αCH) ppm; ^{13}C NMR ($CDCl_3$, 75.5 MHz): δ 8.5 (CH_3), 9.3 (CH_3 deuterated product), 21.5 (γCH_2 deuterated product), 24.0 (γCH_2), 27.3 ($CHDCH_3$ deuterated product), 27.7 (CH_2CH_3 and βCH_2), 45.4 (δCH_2 deuterated product), 47.6 (δCH_2), 58.9 (αCH deuterated product), 60.4 (αCH), 63.0 (CH_2OH deuterated product), 65.8 (CH_2OH), 173.0 (C=O deuterated product), 174.4 (C=O).

10a
Compound **10** (843 mg, 5.4 mmol) and commercially available LDA (2.0 M in THF, 11.8 mL, 23.6 mmol) were reacted according to the general procedure for test reactions concerning the formation of a dianion over 2 hours. 5% of deuterated product was formed; 95% of starting material was left.

10b
Compound **10** (750 mg, 4.8 mmol) and freshly prepared LDA (10 mmol) were reacted according to the general procedure for test reactions concerning the formation of a dianion over 1 hour. 15% of deuterated product was formed; 85% of starting material was left.

THP protected 10c
To a solution of **10** (5.08 g, 50.2 mmol) in dry DCM (100 mL) DHP (6 mL, 66.2 mmol) and CSA (152 mg; 0.66 mmol) were added. The solution was stirred overnight and subsequently quenched with Na_2CO_3 (643 mg) while stirring for an additional 30 min. H_2O (100 mL) was added and the mixture was extracted with DCM (3× 100 mL). The combined organic layers were dried and evaporated and the crude was purified by column chromatography (Hexanes:

EtOAC) and afforded the THP protected intermediate **10c** (8.48 g, 70%) as a colourless liquid. ^{1}H NMR ($CDCl_3$, 300MHz): δ 1.08-1.17 (m, 3H, CH_3), 1.52-1.55 (m, 1H, βCH_2), 1.64-1.80 (m, 6H, CH_2 THP), 1.84-2.10 (m, 3H, βCH_2 and γCH_2), 2.24-2.30 (m, 2H, *CH_2*CH_3), 3.23-3.54 (m, 2H, CH_2 THP), 3.61 (m, 2H, δCH_2), 3.82 (m, 2H, CH_2OTHP), 4.35 (m, 1H, αCH), 4.82 (m, 1H, CH THP) ppm; ^{13}C NMR ($CDCl_3$, 75.5 MHz): δ 8.7 (CH_3), 19.7 (CH_2 THP), 22.0 (CH_2 THP), 25.5 (γCH_2), 27.8 (CH_2 THP), 30.7 (CH_2CH_3 and βCH_2), 47.2 (δCH_2), 56.7 (αCH), 62.2 (CH_2 THP), 67.9 (CH_2OTHP), 99.2 (CH THP), 172.6 (C=O).
Then, the THP derivative **10c** (734 mg, 3.0 mmol) and freshly prepared LDA (6.4 mmol) were reacted according to the general procedure for test reactions concerning the formation of a dianion over 1 hour. 32% of deuterated product was formed; 68% of starting material was left. ^{1}H NMR ($CDCl_3$, 300MHz): δ 1.08-1.16 (m, 3H, CH_3), 1.53-1.55 (m, 1H, βCH_2), 1.64-1.81 (m, 6H, CH_2 THP), 1.84-2.10 (m, 3H, βCH_2 and γCH_2), 2.24-2.30 (m, 2H, *CH_2*CH_3), 2.32-2.48 (m, 2H, *CH_2*CH_3 deuterated product), 3.23-3.54 (m, 2H, CH_2 THP), 3.61 (m, 2H, δCH_2), 3.82 (m, 2H, CH_2OTHP), 4.12 (m, 1H, αCH deuterated product), 4.35 (m, 1H, αCH), 4.82 (m, 1H, CH THP) ppm; ^{13}C NMR ($CDCl_3$, 75.5 MHz): δ 8.9 (CH_3), 19.7 (CH_2 THP), 22.0 (CH_2 THP), 24.4 (γCH_2 deuterated product), 25.5 (γCH_2), 27.8 (CH_2 THP), 29.0 (CH_2CH_3 and βCH_2 deuterated product), 30.7 (CH_2CH_3 and βCH_2), 45.6 (δCH_2 deuterated product), 47.4 (δCH_2), 56.7 (αCH), 62.2 (CH_2 THP), 67.9 (CH_2OTHP), 69.1 (CH_2OTHP deuterated), 99.2 (CH THP), 172.6 (C=O).

10d
Compound **10** (797 mg, 5.1 mmol) and LHMDS (22.3 mL, 22.3 mmol) were reacted according to the general procedure for test reactions concerning the formation of a dianion over 1.5 hours. 27% of deuterated product was formed; 73% of starting material was left.

10e
Compound **10** (708 mg, 4.5 mmol) and KHMDS (2.0 M in THF, 9.9 mL, 19.8 mmol) were reacted according to the general procedure for test reactions concerning the formation of a dianion over 1.5 hours. 13% of deuterated product was formed; 87% of starting material was left.

(*E*)-S-ethyl pent-2-enethioate (17)
To a cooled solution (0°C) of (*E*)-pentenoic acid **16** (5.01 g; 50 mmol), DCC (11.35 g; 55 mmol) and DMAP (611 mg; 5 mmol, 10 mol%) in pentane (500 mL), neat EtSH (7.22 mL; 100 mmol) was added dropwise. The mixture was allowed to slowly reach room temperature and stirred for 16 h. After filtration through a short silica pad, volatiles were evaporated. The crude residue was distilled (Kugelrohr) and afforded product **17** as a colorless liquid (6.85 g; 95%). ^{1}H NMR (400 MHz, $CDCl_3$): δ 6.96 – 6.84 (m, 1H), 6.06 (dd, J = 15.5, 1.5 Hz, 1H), 2.95 – 2.84 (m, 2H), 2.18 (qd, J = 7.2, 3.7 Hz, 2H), 1.28 – 1.01 (m, 3H), 0.99 (s, 3H) ppm. ^{13}C NMR (101 MHz, $CDCl_3$): δ 190.03 (Cq), 146.46 (CH), 127.79(CH), 25.18(CH_2), 22.95 (CH_2), 14.78(CH_3), 12.05 (CH_3). Spectral data correspond to literature.[21]

(*S*)-S-ethyl 3-methylpentanethioate (18)
(S,R_{Fe})-Josiphos.EtOH adduct (43.2 mg; 67 µmol) and CuBr.Me_2S (12.8 mg; 62 µmol) were stirred in freshly distilled MTBE (56 mL) until the mixture remained homogeneous (typically 10-30 min). Then the mixture was cooled to –78°C and after 10 min a solution of MeMgBr in Et_2O (2.7 mL; 8.1 mmol) was added dropwise during 10 min. After 15 min

of stirring a solution of thioester **17** (721 mg; 5 mmol) in MTBE (6.2 mL) was added over 3 h by a syringe pump. The reaction mixture was stirred for an additional 16 h at –78°C, quenched with EtOH (5 ml) and allowed to reach ambient temperature. Then a solution of NH_4Cl (1 M; 50 mL) was added. The organic layer was separated and the aqueous layer extracted with Et_2O (3× 20 mL). The combined organic layers were dried over $MgSO_4$ and carefully evaporated (the product is volatile). The residual yellow liquid was purified by flash chromatography (Et_2O: pentane; 1:4) to afford (*S*)-S-ethyl 3-methylpentanethioate **18** (800 mg; 80%) as a colorless liquid. HRMS: calcd for $C_8H_{16}OS$ $[M+H]^+$ 161.0994, found 161.0996; ^1H NMR (400 MHz, $CDCl_3$): δ 2.87 (q, *J* = 7.4 Hz, 2H), 2.53 (dd, *J* = 14.4, 6.1 Hz, 1H), 2.34 (dd, *J* = 14.4, 8.1 Hz, 1H), 2.17 – 1.72 (m, 1H), 1.45 – 1.30 (m, 1H), 1.24 (t, *J* = 7.4 Hz, 4H), 1.08 – 0.72 (m, 6H) ppm. ^{13}C NMR (101 MHz, $CDCl_3$): δ 199.36, 51.01, 32.63, 29.23, 23.24, 19.02, 14.78, 11.21. NMR spectra contain traces of solvents (≈5%). Spectral data corresponded to literature.[21] The enantiomeric ratio was determined on the corresponding methyl ester by chiral stationary phase gas chromatography on a Chiraldex G-TA column (30 m x 0.25 mm), 60 °C, retention times: 5.94 (*R*) / 6.05 (*S*) min: 85:1 (e.r.), 97% ee (as reported in literature[21]) $[\alpha]_D$ = +8.4 (c=1.0 in $CHCl_3$).

The absolute configuration was determined on the alcohol[21]: 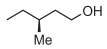

$[\alpha]_D$ = +7.4 (c=0.95 in $CHCl_3$).

Literature[42] reports the opposite enantiomer with α_D= –8.5 (c=1 in $CHCl_3$).

(*S*,*E*)-S-ethyl 5-methylhept-2-enethioate (19)

A solution of (*S*)-S-ethyl 3-methylpentanethioate **18** (801 mg; 5 mmol) in DCM (50 mL) was cooled to –55 °C and then a solution of DIBAL (1 M in DCM; 6 mL; 6 mmol) was added. The mixture was stirred until complete conversion of starting material (ca 1.5 h). Subsequently, the mixture was poured into a saturated Rochelles salt (potassium sodium tartrate) solution and stirred until the phases separated (mostly within 2 h). Layers were separated and the aqueous layer was extracted with DCM (3×15 mL). The combined layers were dried and carefully evaporated (the product is volatile) until the weight corresponded to quantitative yield (501 mg). To a cooled solution (0 °C) of HWE reagent (1.8 g; 7.5 mmol) in THF (25 mL) a solution of *n*-BuLi (1.6 M in hexanes; 3.44 mL; 5.55 mmol) was added dropwise. The reaction mixture was stirred for 20 min at 0 °C. Then (*S*)-3-methylpentanal (501 mg; 5 mmol) in a small amount of THF (0.3 ml) was added and the reaction mixture was stirred overnight (16 h). The reaction was quenched with water (10 mL). Layers were separated and the aqueous layer extracted with Et_2O (3× 15 mL). The combined organic layers were dried over $MgSO_4$ and carefully evaporated (the product is volatile). The residue was purified by flash chromatography on SiO_2 (MTBE : pentane; 250:1) and afforded (*S*,*E*)-S-ethyl 5-methylhept-2-enethioate **19** (510 mg; 55%) as a colorless liquid. HRMS calcd for $C_{10}H_{18}OS$ $[M+H]^+$ 187.1151, found 187.1152; $[\alpha]_D$= +8.2 (c=1.8 in $CHCl_3$); ^1H NMR (400 MHz, $CDCl_3$): δ 6.85 (dtd, *J* = 8.6, 7.6, 1.2 Hz, 1H), 6.08 (dd, *J* = 15.5, 1.3 Hz, 1H), 3.05 – 2.83 (m, 2H), 2.17 (ddd, *J* = 7.2, 6.5, 3.5 Hz, 1H), 2.09 – 1.91 (m, 1H), 1.53 (dq, *J* = 13.3, 6.9 Hz, 1H), 1.36 (dt, *J* = 14.5, 6.8 Hz, 1H), 1.26 (ddd, *J* = 7.4, 4.9, 1.2 Hz, 3H), 0.86 (td, *J* = 7.0, 3.2 Hz, 6H) ppm. ^{13}C NMR (101 MHz, $CDCl_3$): δ 189.95, 144.27, 129.69, 39.21, 34.19, 29.18, 22.99, 19.14, 14.79, 11.34 + 2 peaks at 65.81 and 15.24 as Et_2O residues.

(3*S*,5*S*)-S-ethyl 3,5-dimethylheptanethioate (20)

(S,R_{Fe})-Josiphos-CuBr complex (29.1 mg; 39 μmol) was dissolved in freshly distilled MTBE (23.7 mL) until the mixture remained homogeneous (typically 10-30 minutes). Then the mixture was cooled to –78°C and after 10 min a solution of MeMgBr (3 M in Et_2O; 1.1 mL; 3.42 mmol) was added dropwise.[43] After 15 min of stirring, a solution of thioester **19** (490 mg; 2.63 mmol) in MTBE (2.6 mL) was added over 3 h by a syringe pump. The mixture was stirred for an additional 16 h at –78°C. The reaction was quenched by addition of EtOH (2 mL) and the mixture was allowed to reach ambient temperature. Then an aqueous solution of NH_4Cl (1 M, 30 mL) was added, the organic layer separated and the aqueous layer extracted with Et_2O (3× 20 mL). The combined organic layers were dried over $MgSO_4$ and carefully evaporated (the product is volatile). The residual yellow liquid was purified by flash chromatography (MTBE/pentane, 1/250, v/v) to afford (3*S*,5*S*)-S-ethyl 3,5-dimethylheptanethioate **20** (417.7 mg; 78%) as a colourless liquid. HRMS: calcd for $C_{11}H_{22}OS$ $[M+H]^+$ 203.14, found 203.11; $[\alpha]_D$= +4.2 (c=1.4 in $CHCl_3$); ^{1}H NMR (400 MHz, $CDCl_3$): δ 2.86 (q, *J* = 7.4 Hz, 2H), 2.52 (dd, *J* = 14.4, 5.4 Hz, 1H), 2.28 (dd, *J* = 14.4, 8.5 Hz, 1H), 1.43 – 1.27 (m, 2H), 1.24 (t, *J* = 7.4 Hz, 4H), 1.14 – 0.94 (m, 3H), 0.92 (d, *J* = 6.6 Hz, 3H), 0.85 (d, *J* = 6.5 Hz, 6H) ppm. ^{13}C NMR (101 MHz, $CDCl_3$): δ 199.33, 51.29, 44.07, 31.53 (CH1), 29.00, 28.66 (CH1), 23.23, 20.15 (CH_3), 19.48 (CH_3), 14.79 (CH_3), 11.07 (CH_3).

(10*S*,12*S*)-dimethyltetradec-7-enoic acid (15)

A solution of (*S*)-S-ethyl 3-methylpentanethioate (417 mg; 2.06 mmol) in DCM (20 mL) was cooled to –55 °C and a solution of DIBAL (1 M in DCM; 2.5 mL; 2.5 mmol) was added. The mixture was stirred until complete conversion of starting material (ca 1.5 h), then poured into saturated aqueous Rochelles salt solution and stirred until phases separated (mostly within 2 h). Layers were separated and the aqueous layer was extracted with DCM (3×15 mL). The combined layers were dried and carefully evaporated (the product is volatile) to a weight corresponding to quantitative yield (294 mg). To a stirred suspension of 7-(bromotrip henylphosphoranyl) heptanoic acid (1.65 g; 3.5 mmol) in THF (2 mL) at ambient temperature a solution of LiHMDS (1 M in THF; 6.2 mL; 6.18 mmol) was added dropwise. The mixture was stirred until the suspension turned into a deep red solution. Then a solution of (3*S*,5*S*)-dimethylheptanal (293 mg; 2 mmol) in a small amount of THF (300 μL) was added and the reaction mixture was stirred until complete consumption of starting material (2 h). The mixture was acidified to pH=1 by dilute aq. HCl and extracted with Et_2O (3× 20 mL). The combined organic layers were dried and evaporated. The resulting thick liquid was purified by column chromatography (Et_2O : pentane; 1:4) and afforded **15** (331 mg; 47%) as a colorless liquid (a mixture of *E* and *Z* isomers). HRMS: calcd for $C_{16}H_{30}O_2$ $[M+H]^+$ 255.2324, found 255.2347; $[\alpha]_D$= +12.2 (c=1.8 in $CHCl_3$); ^{1}H NMR (400 MHz, $CDCl_3$): δ 5.51 – 5.22 (m, 2H), 2.35 (t, *J* = 7.5 Hz, 2H), 2.13 – 0.55 (m, 25H) ppm. ^{13}C NMR (101 MHz, $CDCl_3$): δ 131.22, 130.17, 129.03, 128.67, 44.23, 44.00, 39.77, 34.26, 34.03, 32.35, 31.61, 31.55, 30.70, 30.42, 29.29, 29.16, 28.72, 28.49, 27.08, 24.57, 24.51, 20.16, 20.06, 19.68, 11.14. – additional peaks were observed due to the inseparable *E*/*Z* mixture. Spectral data corresponded to literature.[20]

(10*R*,12*S*)-dimethyltetradecanoic acid (8)

To a vigorously stirred solution of (10*R*,12*S*)-dimethyltetradec-7-enoic acid **15** (310.1 mg; 1.2 mmol) and flavine catalyst (49.6 mg; 0.12 mmol, 10 mol%) in EtOH (1 mL) under oxygen atmosphere, hydrazine hydrate (1.6 mL; 31.7 mmol) was added in one portion. Vigorous

stirring continued for 16 h. Then the reaction mixture was acidified to pH=1 by dilute aq. HCl and extracted with Et_2O (3× 20 mL). The combined organic layers were dried and evaporated. The residual red liquid was purified by column chromatography (Et_2O : pentane; 1:4) and afforded **8** (524 mg; 81%) as a colorless thick liquid. $[\alpha]_D$= +14.1 (c=1.3 in $CHCl_3$); ^{1}H NMR (400 MHz, $CDCl_3$): δ 11.20 (bs, 1H), 2.34 (t, *J* = 7.5 Hz, 2H), 1.95 – 1.51 (m, 1H), 1.57 – 0.32 (m, 31H) ppm. ^{13}C NMR (101 MHz, $CDCl_3$): δ 180.15 (Cq), 44.70, 36.85, 34.21, 31.56 (CH), 30.00 (CH), 29.93, 29.46, 29.24, 29.20, 29.07, 26.86, 24.73, 20.26 (CH_3), 19.72 (CH_3), 11.17(CH_3). Spectral data corresponded to literature.[20]

(*S*)-12-methyltetradec-9-enoic acid (21)

To a stirred solution of (*S*)-S-ethyl 3-methylpentanethioate **18** (80 mg; 0.5 mmol) in DCM (0.75 mL) at –50°C, DIBAL-H was added. After complete conversion of the thioester (2 h), the reaction mixture was poured into a saturated solution of Rochelle salt. After clear layer separation, the organic layer was separated and the aqueous layer extracted with Et_2O (3× 10 mL). The combined organic layers were dried and carefully evaporated until the weight corresponded to a quantitative yield (43 mg). Then, to a stirred suspension of 9-(bromotriphenyl phosphoranyl)nonanoic acid (425 mg; 0.85 mmol) in THF (0.75 mL) a solution of LiHMDS (1 M in THF; 1.5 mL; 1.5 mmol) was added until the solution stayed deep red. To this solution, 3-methyl-pentanal in a small amount of THF (300 µL) was added. The reaction mixture was stirred until complete conversion of the starting material (2 h) and acidified to pH=1 by dilute aq. HCl. The resulting solution was extracted with Et_2O (3× 20 mL) and the combined organic layers were dried and evaporated. The resulting thick liquid was purified by column chromatography (Et_2O: pentane; 1:4) and afforded **21** (65.9 mg; 55%) as a colorless liquid (as a mixture of *E* and *Z* isomers). HRMS: calcd for $C_{15}H_{29}O_2$ $[M+H]^+$ 241.216, found 241.217; $[\alpha]_D$= +0.3 (c=0.5 in $CHCl_3$); ^{1}H NMR (400 MHz, $CDCl_3$): δ 5.37 (dt, *J* = 6.0, 4.6 Hz, 2H), 2.35 (t, *J* = 7.5 Hz, 2H), 2.01 (d, *J* = 5.4 Hz, 2H), 1.68 – 1.59 (m, 2H), 1.40 – 1.21 (m, 14H), 0.96 – 0.80 (m, 6H) ppm. ^{13}C NMR (101 MHz, $CDCl_3$): δ 177.89, 130.32, 128.66, 35.11, 34.13, 33.63, 29.69, 29.46, 29.19, 28.94, 28.88, 27.19, 24.64, 19.11, 11.55.

(*S*)-12-methyltetradecanoic acid (22)

To a vigorously stirred solution of (12*S*)-methyltetradec-9-enoic acid **21** (60 mg; 0.25 mmol) and flavine catalyst (10 mg; 25 µmol, 10 mol%) in EtOH (1 mL) under oxygen atmosphere, hydrazine hydrate (375 µl; 7.5 mmol) was added in one portion. Vigorous stirring was continued for 16 h and the mixture was acidified to pH=1 by dilute aq. HCl and extracted with Et_2O (3× 20 mL). The combined organic layers were dried and evaporated. The residual red liquid was purified by column chromatography (Et_2O: pentane; 1:4) and afforded **22** (50 mg, 83%) as a colourless thick liquid. HRMS: calcd for $C_{15}H_{31}O_2$ $[M+H]^+$ 243.231, found 243.233; $[\alpha]_D$= +0.3 (c=0.5 in $CHCl_3$); ^{1}H NMR (400 MHz, $CDCl_3$): δ 2.34 (t, *J* = 7.5 Hz, 2H), 1.65 – 1.60 (m, 2H), 1.32 – 1.23 (m, 20H), 0.87 – 0.81 (m, 6H) ppm. ^{13}C NMR (101 MHz, $CDCl_3$): δ 220.66, 36.62, 34.38, 34.07, 29.99, 29.66, 29.58, 29.48, 29.42, 29.23, 29.05, 27.09, 24.66, 19.20, 11.39.

Fmoc-3-Hyp-OH (25)

trans-3-Hydroxy-L-proline (**24**) (2.0 g; 15.25 mmol) was added to a vigorously stirred, ice-cooled solution of $NaHCO_3$ (2.56 g; 30.5 mmol) in H_2O (20 mL). A solution of FmocOSu (5.66 g, 16 mmol) in dioxane (15 mL) was added dropwise over 1h. Then, the ice-cooling

was removed and the reaction mixture stirred for 20h. Additional H_2O (40 mL) was added, the reaction mixture was washed with EtOAc (2× 50 mL) and the combined organic layers discarded. Subsequently, the aqueous phase was acidified with 1N HCl to a pH of 2, providing a thick opaque mixture. The mixture was extracted with EtOAc (2× 50 mL). The combined organic layers were dried and evaporated providing Fmoc-3-Hyp-OH **25** (5.37 g, 99%) as a white solid. R_f = 0.49 (DCM/MeOH/AcOH, 19/1/0.1, v/v/v); Analysis by ^{1}H- and ^{13}C-NMR showed the presence of rotamers around the 3° amide bond. ^{1}H NMR (300 MHz, DMSO): δ 7.92-7.88 (m, 2H, Ar-H), 7.69-7.63 (m, 2H, Ar-H), 7.45-7.30 (m, 4H, Ar-H), 5.58/5.51 (2bs, 1H, NH), 4.37-4.05 (m, 5H, αCH, βCH, CH_2 + CH Fmoc), 3.54-3.49 (m, 2H, δCH_2), 1.99-1.84 (m, 2H, γCH_2) ppm. ^{13}C NMR (75.5 MHz, DMSO): δ 172.1/171.8 (COOH), 154.2/154.0 (NCOO), 143.8 and 140.7 (Ar-C), 127.8, 127.1, 125.2 and 120.2 (Ar-CH), 73.9/72.7 (βCH), 68.2/67.9 (αCH), 67.0/66.7 (CH_2 Fmoc), 46.6 (CH Fmoc), 44.9/44.3 (δCH_2), 31.3/30.8 (γCH_2).

Fmoc-3-Hyp-OAll (26)

Fmoc-3-Hyp-OH **25** (5.35 g; 15.14 mmol) was dissolved in toluene (40 mL) and the flask connected to a Dean-Stark apparatus. Allyl alcohol (9.8 mL; 143.8 mmol) was added followed by *p*-toluenesulfonic acid monohydrate (2.94 g; 15.44 mmol). The reaction mixture was refluxed for 1h, cooled and DCM (150 mL) was added. The organic layer was washed with $NaHCO_3$ (150 mL), 0.1N HCl (150 mL) and brine (150 mL), then dried and concentrated. The crude was purified by column chromatography (Hexanes/ EtOAc; 2/1) and afforded Fmoc-3-Hyp-OAllyl **26** (4.48 g, 75%) as a colorless oil. R_f= 0.38 (Hexanes/EtOAc, 3/1, v/v); HRMS: calcd for $C_{23}H_{23}NO_5$ $[M+H]^+$ 394.1654, found 394.1648; Analysis by ^{1}H- and ^{13}C-NMR showed the presence of rotamers around the 3° amide bond. ^{1}H NMR (300 MHz, $CDCl_3$): δ 7.77-7.73 (m, 2H, Ar-H), 7.63-7.52 (m, 2H, Ar-H), 7.41-7.24 (m, 4H, Ar-H), 5.93-5.79 (m, 1H, CH=), 5.35-5.18 (m, 2H, CH_2=), 4.65-4.10 (m, 7H, αCH, βCH, CH_2 + CH Fmoc, CH_2 allyl), 3.79-3.68 (m, 2H, δCH_2), 2.70/2.59 (2bs, 1H, OH), 2.20-1.95 (m, 2H, γCH_2) ppm. ^{13}C NMR (75.5 MHz, $CDCl_3$): δ 170.3 (*C*OOCH_2), 155.4/154.9 (NCOO), 144.2 and 141.5 (Ar-C), 131.7 (CH=), 127.9, 127.3, 125.3 and 120.1 (Ar-CH), 119.0 (CH_2=), 75.5 (βCH), 74.3 (αCH), 67.9 (CH_2 Fmoc), 66.2 (CH_2 allyl), 47.4 (CH Fmoc), 45.1/44.8 (δCH_2), 32.8/32.1 (γCH_2).

Fmoc-Hyp(*t*Bu)-OAll (27)

Fmoc-3-Hyp-OAllyl **26** (915 mg; 2.33 mmol) was dissolved in dry DCM (10 mL) in a 20 mL glass pressure tube and cooled to -20°C. Concentrated H_2SO_4 (80 μL) was added and isobutene (~ 6 mL) was condensed into the solution. The tube was sealed and stirred at RT for 92h. The sealed tube was cooled to -20 °C for 16h and vented carefully. Then, the mixture was allowed to reach RT while excess of isobutene evaporated from the reaction mixture. DCM (50 mL) was added and the organic layer was washed with saturated $NaHCO_3$ (3× 50 mL), then brine (50 mL) and dried. The mixture was concentrated to give Fmoc-3-Hyp(*t*Bu)-OAllyl **27** (936 mg; 90%) as a clear oil. R_f= 0.57 (Hexanes/EtOAc, 2/1, v/v); HRMS: calcd for $C_{27}H_{31}NO_5$ $[M+H]^+$ 450.2280, found 450.2295; Analysis by ^{1}H- and ^{13}C-NMR showed the presence of rotamers around the 3° amide bond. ^{1}H NMR (300 MHz, $CDCl_3$): δ 7.78-7.70 (m, 2H, Ar-H), 7.65-7.55 (m, 2H, Ar-H), 7.42-7.28 (m, 4H, Ar-H), 5.95-5.81 (m, 1H, CH=), 5.38-5.18 (m, 2H, CH_2=), 4.72-4.22 (m, 7H, αCH, βCH, CH_2 + CH Fmoc, CH_2 allyl), 3.77-3.65 (m, 2H, δCH_2), 2.18-2.01 (m, 1H, γCH_2), 1.93-1.84 (m, 1H, γCH_2), 1.24 (s, 9H, *t*Bu) ppm. ^{13}C NMR (75.5 MHz, $CDCl_3$): δ 171.0 (*C*OOCH_2), 155.2/154.7 (NCOO), 144.4/144.1 and 141.5 (Ar-C), 131.7 (CH=), 127.9, 127.2, 125.4 and 120.1 (Ar-CH), 119.0 (CH_2=), 75.2 (C *t*Bu), 74.3 (βCH), 68.1

(αCH), 67.8 (CH_2 Fmoc), 66.0 (CH_2 allyl), 47.5 (CH Fmoc), 45.7/45.3 (δCH_2), 33.4/32.5 (γCH_2), 28.4 (CH_3 *t*Bu).

Fmoc-3-Hyp(*t*Bu)-OH (23)

Fmoc-3-Hyp(*t*Bu)-OAllyl **27** (2.1 g; 4.68 mmol) was dissolved in dry DCM (20 mL). Under argon $Pd(PPh_3)_4$ (108.1 mg; 0.094 mmol) was added to the stirred solution, followed by phenyltrihydrosilane (1.15 mL; 9.36 mmol). After 2h, DCM (150 mL) was added and the organics washed with 0.01 N HCl (150 mL), brine (150 mL) and dried (Na_2SO_4). The solvents were removed in vacuo and the crude solid was purified by column chromatography (Hexanes: EtOAc; 2:1). Fmoc-3-Hyp(*t*Bu)-OH **23** (996 mg; 52%) was obtained as a white solid. HRMS: calcd for $C_{24}H_{27}NO_5$ $[M+H]^+$ 410.1967, found 410.1974; Analysis by ^{1}H- and ^{13}C-NMR showed the presence of rotamers around the 3° amide bond. ^{1}H NMR (300 MHz, $CDCl_3$): δ 7.78-7.64 (m, 2H, Ar-H), 7.62-7.49 (m, 2H, Ar-H), 7.46-7.24 (m, 4H, Ar-H), 4.50-4.14 (m, 5H, αCH, βCH, CH_2 + CH Fmoc), 3.69-3.63 (m, 2H, δCH_2), 2.16-2.00 (m, 1H, γCH_2), 1.91-1.80 (m, 1H, γCH_2), 1.23 (s, 9H, *t*Bu) ppm. ^{13}C NMR (75.5 MHz, $CDCl_3$): δ 175.9/174.2 (COOH), 156.4/154.7 (NCOO), 144.3/144.0 and 141.5 (Ar-C), 128.0, 127.3, 125.2 and 120.2 (Ar-CH), 75.3 (C *t*Bu), 73.7 (βCH), 68.3 (αCH), 67.9 (CH_2 Fmoc), 47.3 (CH Fmoc), 45.6 (δCH_2), 33.3/32.5 (γCH_2), 28.3 (CH_3 *t*Bu).

***Cyclo*[-(Ter)-Orn-Thr-Hyp-hTyr-Orn-3-Hyp] (30)**

Peptide **30** was obtained according to the general procedure for the preparation of the caspofungin analogues using 39 μmol of resin bound peptide **28**. After lyophilization, peptide **30** (18 mg; 43%) was obtained as a white solid. Purity was confirmed by analytical HPLC and was found to be higher than 95% (R_t = 21.55 min). ESI-MS calcd for $C_{58}H_{74}N_8O_{12}$: 1074.54, found: *m/z* 1075.85 $[M+H]^+$; HRMS calcd for $C_{58}H_{74}N_8O_{12}$ $[M+H]^+$ 1075.5504, found 1075.5529; ^{1}H-NMR (DMSO, 500 MHz): δ Orn-1: 8.59 (NH), 7.98 (εNH), 4.53 (αCH), 2.15/1.68 (βCH), 1.77 (γCH), 3.45/2.73 (δCH); Thr-2: 8.22 (NH), 4.76 (αCH), 4.39 (βCH), 1.13 (γCH); Hyp-3: 4.33 (αCH), 2.16/1.76 (βCH), 4.38 (γCH), 3.74/3.69 (δCH); hTyr-4: 7.55 (NH), 4.04 (αCH), 2.08/1.87 (βCH), 2.46/2.37 (γCH), 6.95/6.66 (Ar-H); Orn-5: 7.59 (NH), 4.70 (αCH), 1.84/1.69 (βCH), 1.59 (γCH), 2.88/2.83 (δCH); Hyp-6: 4.13 (αCH), 4.02 (βCH), 2.12/1.87 (γCH), 3.65 (δCH); Ter: 0.92 (CH_3), 1.37 (CH_2), 1.41 (CH_2), 1.75 (CH_2), 4.00 (OCH_2), 7.67/7.05 (Ar-H Ph-3), 7.83/7.75 (Ar-H Ph-2), 8.03/7.81 (Ar-H Ph-1) ppm. ^{13}C-NMR (DMSO, 125 MHz): δ Orn-1: 51.1 (αCH), 25.2 (βCH), 22.7 (γCH), 35.1 (δCH); Thr-2: 55.5 (αCH), 65.6 (βCH), 18.7 (γCH); Hyp-3: 59.9 (αCH), 36.4 (βCH), 68.4 (γCH), 54.8 (δCH); hTyr-4: 51.4 (αCH), 32.5 (βCH), 30.2 (γCH), 128.5/ 114.1 (Ar-H); Orn-5: 48.2 (αCH), 28.0 (βCH), 22.1 (γCH), 37.9 (δCH); Hyp-6: 71.5 (αCH), 66.7 (βCH), 32.5 (γCH), 44.1 (δCH); Ter: 13.2 (CH_3), 21.1 (CH_2), 26.9 (CH_2), 27.6 (CH_2), 67.2 (OCH_2), 126.8/114.1 (Ar-H Ph-3), 125.3/125.8 (Ar-H Ph-2), 127.6/126.6 (Ar-H Ph-1) ppm.

***Cyclo*[-(DMT-Myr)-Orn-Thr-Hyp-hTyr-Orn-Hyp] (31)**

Peptide **31** was obtained analogously to peptide **4**, except for the amino acid sequence, using 31 ìmol of resin bound peptide **28**. The first amino acid coupled was Fmoc-Hyp(*t*Bu)-OH instead of Fmoc-3-Hyp(*t*Bu)-OH. After lyophilization, peptide **31** (12 mg; 40%) was obtained as a white solid. Purity was confirmed by analytical HPLC and was found to be higher than 99% (R_t = 23.25 min). ESI-MS calcd for $C_{50}H_{82}N_8O_{11}$: 970.61, found: *m/z* 971.75 $[M+H]^+$; HRMS calcd for $C_{50}H_{82}N_8O_{11}$ $[M+H]^+$ 971.6181, found 971.6123; ^{1}H-NMR (DMSO, 500 MHz): δ Orn-

1: 8.07 (NH), 7.91 (εNH), 4.35 (αCH), 2.02/1.43 (βCH), 1.65 (γCH), 3.40/2.66 (δCH); Thr-2: 8.21 (NH), 4.74 (αCH), 4.38 (βCH), 1.07 (γCH); Hyp-3: 4.31 (αCH), 2.15/1. 75 (βCH), 4.34 (γCH), 3.72 (δCH); hTyr-4: 7.53 (NH), 4.03 (αCH), 2.06/1.84 (βCH), 2.45/2.36 (γCH), 6.94/6.65 (Ar-H); Orn-5: 7.61 (εNH), 7.39 (NH), 4.66 (αCH), 1.79/1.59 (βCH), 1.55 (γCH), 2.79 (δCH); Hyp-6: 4.34 (αCH), 1.99/1.82 (βCH), 4.36 (γCH), 3.68/3.47 (δCH); Tail: 2.12 ($C(O)CH_2$), 1.47, 1.45/1.22, 1.39, 1.31/1.06, 1.26/1.21, 1.25/1.02, 1.19/0.89, 0.83 (CH_3), 0.82 (CH_3) ppm. ^{13}C-NMR (DMSO, 125 MHz): δ Orn-1: 49.4 (αCH), 25.1 (βCH), 22.2 (γCH), 34.6 (δCH); Thr-2: 55.4 (αCH), 68.4 (βCH), 18.6 (γCH); Hyp-3: 59.9 (αCH), 36.4 (βCH), 68.0 (γCH), 54.7 (δCH); hTyr-4: 51.2 (αCH), 32.5 (βCH), 30.2 (γCH), 128.5/ 114.1 (Ar-H); Orn-5: 48.7 (αCH), 27.9 (βCH), 21.8 (γCH) 37.9 (δCH); Hyp-6: 58.1 (αCH), 36.8 (βCH), 65.5 (γCH), 55.0 (δCH); Tail: 43.3, 35.4, 34.3 ($CHCH_2CH$), 30.2, 28.6, 27.8, 27.6, 25.5, 24.6, 19.1 (CH_3), 10.2 (CH_3).

***Cyclo*[-(Myr)-Orn-Thr-Hyp-hTyr-Orn-Hyp] (32)**

Peptide **32** was obtained analogously to peptide **7**, except for the amino acid sequence, using 31 ìmol of resin bound peptide **28**. The first amino acid coupled was Fmoc-Hyp(*t*Bu)-OH instead of Fmoc-3-Hyp(*t*Bu)-OH. After lyophilization, peptide **32** (6 mg; 20%) was obtained as a white solid. Purity was confirmed by analytical HPLC and was found to be higher than 95% (R_t = 22.25 min). ESI-MS calcd for $C_{48}H_{78}N_8O_{11}$: 942.58, found: *m/z* 943.65 $[M+H]^+$; HRMS calcd for $C_{48}H_{78}N_8O_{11}$ $[M+H]^+$ 943.5868, found 943.5870; ^{1}H-NMR (DMSO, 500 MHz): δ Orn-1: 8.07 (NH), 7.91 (εNH), 4.29 (αCH), 1.96/1.37 (βCH), 1.58 (γCH), 3.34/2.60 (δCH); Thr-2: 8.21 (NH), 4.68 (αCH), 4.31 (βCH), 1.01 (γCH); Hyp-3: 4.24 (αCH), 2.09/1. 69 (βCH), 4.27 (γCH), 3.66 (δCH); hTyr-4: 7.57 (NH), 3.97 (αCH), 2.39/2.30 (βCH), 2.00/1.78 (γCH), 6.88/6.69 (Ar-H); Orn-5: 7.65 (εNH), 7.39 (NH), 4.59 (αCH), 1.72/1.52 (βCH), 1.49 (γCH), 2.73 (δCH); Hyp-6: 4.27 (αCH), 1.93/1.76 (βCH), 4.30 (γCH), 3.62/3.41 (δCH); Tail: 2.06 ($C(O)CH_2$), 1.41, 1.20, 1.17/1.01, 1.14, 0.87 (CH_3), 0.80 (CH_3) ppm. ^{13}C-NMR (DMSO, 125 MHz): δ Orn-1: 49.4 (αCH), 25.1 (βCH), 22.1 (γCH), 34.6 (δCH); Thr-2: 55.4 (αCH), 68.4 (βCH), 18.6 (γCH); Hyp-3: 59.9 (αCH), 36.4 (βCH), 67.9 (γCH), 54.7 (δCH); hTyr-4: 51.2 (αCH), 32.5 (βCH), 30.2 (γCH), 128.5/ 114.1 (Ar-H); Orn-5: 48.6 (αCH), 27.9 (βCH), 21.9 (γCH) 37.9 (δCH); Hyp-6: 58.0 (αCH), 36.8 (βCH), 65.5 (γCH), 55.1 (δCH); Tail: 34.3 ($C(O)CH_2$), 28.1, 27.5, 24.7, 21.3, 18.0 (CH_3), 13.2 (CH_3).

5.4.3 Biology

Candida MIC Assay:

Antifungal activity was evaluated by broth microdilution. The media used in this assay was Yeast Extract Peptone Dextrose (YPD) containing 1% yeast extract, 2% peptone, 1% dextrose in distilled water. Test compounds were dissolved in distilled water or 10% DMSO, depending on the solubility of the compounds, to a concentration of 1 mg/mL. After dissolving each compound was diluted 20 times in YPD medium rendering a stock solution of 50 μg/mL. Caspofungin[27], purchased from Merck Sharp & Dohme B.V. (Haarlem, Netherlands), was included as a reference. Serial 2-fold dilutions of the test compounds in YPD medium were prepared as followed. To each well of a sterile Greiner bio-one Cellstar 96 well, U bottomed microtiter plate 100 μl of YPD was dispensed. Manually, 100 μl of stock compounds was delivered to each well in column 1. Then using an 8-channel pipette, compounds in column 1 were serially diluted 2-fold over the microtiter plate until column 11. The last column of the plate contained drug-free wells dedicated for growth and sterility controls for each

organism tested.

The plates containing the diluted compounds were inoculated with 100 μl of the appropriate microorganism. The yeast strains used were isolates obtained from the CBS-KNAW Fungal Biodiversity Centre (Utrecht, The Netherlands). The collection included *C. dubliensis*, *C. glabrata*, *C. tropicalis*, *C. parapsilosis*, *C. krusei* and two strains of *C. albicans*. Stock cultures of the yeast strains in liquid media (YPD + 15% glycerol) were maintained at -80°C. For use in this assay, yeast cultures were streaked on YPD agar plates and incubated for 24h at 30°C. Then, using a sterile disposable loop, cells from a colony were suspended in 5 mL of YPD media and aerated for 24h at 30°C on a shaker set at 300 rpm. The broth cultures were diluted 10 times with media and the optical density of this suspension was measured at a wavelength of 600 nm. The suspension was further diluted to an OD_{600} of 0.01 resulting in a concentration of (1-5) $\times$ 10^6 cfu/mL. This suspension was further diluted 1:100 in YPD media to yield (1-5) $\times$ 10^4 cfu/mL. This final dilution was used for inoculating the plates. Plates containing the diluted compounds were inoculated with 100 μL/well of the appropriate microorganism using an 8-channel pipette. The final volume/well, including organism and compound was 200 μl. Thus, the final number of cells per well was approximately 5-25 x10^3 cfu/mL. Tests were incubated overnight at 30 °C prior to recording MICs. The in vitro activity was determined visually at 24h of incubation as the lowest concentration of compound resulting in full inhibition of yeast growth.

References and notes

1. Denning, D.W. *J. Antimicrob. Chemother.*, **2002**, *49*, 889-891.
2. Sucher, A.J.; Chahine, E.B.; Balcer, H.E. *Ann. Pharmacother.*, **2009**, *43*, 1647-1656.
3. Leonard, W.R.; Belyk, K.M.; Conlon, D.A.; Bender, D.R.; DiMichele, L.M.; Liu, J.; Hughes, D.L. *J. Org. Chem.*, **2007**, *72*, 2335-2343.
4. Tomishima, M.; Ohki, H.; Yamada, A.; Maki, K.; Ikedia, F. *Bioorg. Med. Chem. Lett.*, **2008**, *18*, 2886-2890.
5. Norris, T.; VanAlsten, J.; Hubbs, S.; Ewing, M.; Cai, W.; Jorgensen, M.L.; Bordner, J.; Jensen G.O. *Org. Process Res. Dev.*, **2008**, *12*, 447-455.
6. For an excellent review of the total and semisynthetic approaches, see Renslo, A.R. *Anti-Infect. Agents Med. Chem.*, 2**007**, *6*, 201-212.
7. Zambias, R.A.; Hammond, M.L.; Heck, J.V.; Bartizal, K.; Trainor, C.; Abruzzo, G.; Schmatz, D.M.; Nollstadt, K. M. *J. Med. Chem.*, **1992**, *35*, 2843-2855.
8. Klein, L.L.; Li, L.; Chen, H.; Curty, C.B.; DeGoey, D.A.; Grampovnik, D.J.; Leone, C.L.; Thomas, S.A.; Yeung, C.M.; Funk, K.W.; Kishore, V.; Lundell, E.O.; Wodka, D.; Meulbroek, J.A.; Alder, J.D.; Nilius, A.M.; Lartey, P.A.; Plattner, J.J. *Bioorg. Med. Chem. Lett.*, **2000**, *8*, 1677-1696.
9. a) Yao, J.; Liu, H.; Zhou, T.; Chen, H.; Miao, Z.; Dong, G.; Wang, S.; Sheng, C.; Zhang, W. *Tetrahedron*, **2012**, *68*, 3074-3085; b) Yao, J.; Liu, H.; Zhou, T.; Chen, H.; Miao, Z.; Sheng, C.; Zhang, W. *Eur. J. Med. Chem.*, **2012**, *50*, 196-208.
10. Mulder, M.P.C.; Kruijtzer, J.A.W.; Breukink, E.J.; Kemmink, J.; Pieters, R.J., Liskamp, R.M.J. *Bioorg. Med.Chem.*, **2011**, *19*, 6505-6517.
11. Adefarati, A.A.; Giacobbe, R.A.; Hensens, O.D.; Tkacz, J.S. *J. Am. Chem. Soc.*, **1991**, *113*, 3542-3545.

12. Debono, M.; Abbott, B.J.; Turner, J.R.; Howard, L.C.; Gordee, R.S.; Hunt, A.S.; Barnhart, M.; Molloy, R.M.; Willard, K.E.; Fukuda, D.; Butler, T.F.; Zeckner, D.J. *Ann. N.Y. Acad. Sci.,* **1988**, *544*, 152-163.
13. Jong, de A.; Arce, E.C.; Cheng, T.-Y.; Summeren, van R.P.; Feringa, B.L.; Dudkin, V.; Crich, D.; Matsunaga, I.; Minnaard, A.J.; Moody, D.B. *Chem. Biol.*, **2007**, *14*, 1232-1242.
14. Guiard, J.; Collmann, A.; Garcia-Alles, L.F.; Mourey, L.; Brando, T.; Mori, L.; Gilleron, M.; Prandi, J.; De Libero, G.; Puzo, G. *J. Immunol.*, **2009**, *182*, 7030-7037.
15. Debono, M.; Abbott, B.J.; Fukuda, D.S.; Barnhart, M.; Willard, K.E.; Molloy, R.M.; Michel, K.H.; Turner, J.R.; Butler, T.F.; Hunt, A.H. *J. Antibiot.*, **1989**, *XLII*, 389-397.
16. Taft, C.S.; Selitrennikoff, C.P. *J. Antibiot.*, **1990**, *XLIII*, 433-437.
17. Debono, M.; Turner, W.W.; LaGrandeur, L.; Burkhardt, F.J.; Nissen, J.S.; Nichols, K.K.; Rodriguez, M.J.; Zweifel, M.J.; Zeckner, D.J.; Gordee, R.S.; Tang, J.; Parr, T.R. *J. Med. Chem.*, **1995**, *38*, 3271-3281.
18. Jamison, J.A.; Rodriguez, M.J.; Vasudevan, V. *US Patent 6,670,324*, **2003**.
19. Jamison, J.A.; Zeckner, D.J.; Rodriguez, M.J. *J. Antibiot.*, **1997**, *50*, 562-566.
20. Leonard W.R., Belyk K.M., Bender D.R., Conlon D.A. Hughes D.L., Reider P.J. *Org. Lett* **2002**, *4*, 4201-4204.
21. Mazery R., Pullez M., López F., Harutyunyan S.R., Minnaard A.J., Feringa B.L. *J. Am. Chem. Soc.* **2005**, *127*, 9966-9967.
22. López F. Harutyunyan S.R., Meetsma A., Minnaard A.J., Feringa B.L. *Angew. Chem., Int. Ed*. **2005**, *44*, 2752-2756.
23. Höfle G., Steglich W., Vorbrüggen H., *Angew. Chem., Int. Ed*. *Engl.* **1978**, *17*, 569–583.
24. a) Smit C., Fraaije M., Minnaard A.J., *J. Org. Chem.* **2008**, *73*, 9482–9485; b) Teichert, J. F.; den Hartog, T.; Hanstein, M.; Smit, C.; ter Horst, B.; Hernandez-Olmos, V.; Feringa, B. L.; Minnaard, A. J. *ACS Catalysis* **2011**, *1*, 309.
25. Quibell, M.; Benn, A.; Flinn, N.; Monk, T.; Ramjee, M.; Wang, Y.; Watts, J. *Bioorg. Med. Chem.*, **2004**, *12*, 5693.
26. Pfaller, M.A.; Diekema, D.J. *Clin. Microbiol. Rev.*, **2007**, *20*, 133-163.
27. Caspofungin is present in and commercially available as “Cancidas” from Merck.
28. Jackson, A. P.; Gamble, J. A.; Yeomans, T.; Moran, G. P.; Saunders, D.; Harris, D.; Aslett, M.; Barrell, J.F.; Butler, G.; Citiulo, F.; Coleman, D.C.; Groot, de P.W.J; Goodwin, T.J.; Quail, M.A.; McQuillan, J.; Munro, C.A.; Pain, A.; Poulter, R.T.; Rajandream, M.; Renauld, H.; Spiering, M.J.; Tivey, A.; Gow, N.A.R.; Barrell, B.; Sullivan, D.J.; Berriman, M. *Genome Res.*, **2009**, *19*, 2231-2244.
29. Kelly, S.M.; Price, N.C. Curr. Protein Pept. Sci., **2000**, 1, 349-384.
30. Ovchinnikov, Y.A.; Ivanov, V.T. *Tetrahedron*, **1975**, *31*, 2177-2209.
31. Sönnichsen, F.D.; van Eyk, J.E.; Hodges, R.S.; Sykes, B.D. *Biochemistry*, **1992**, *31*, 8790-8798.
32. Woody, R.W. *Peptides, Polypeptides, and Proteins Proc. Int. Symp.*, **1974**, eds. Blout, E. R., Bovey, F. A., Goodman, M. & Lotan, N. (Wiley, New York), 338-350.
33. Bandekar, J.; Evans, D.J.; Krimm, S.; Leach, S.J.; Lee, S.; McQuie, J.R.; Minasian, E.; Némethy, G.; Pottle, M.S.; Sheraga, H.A.; Stimson, E.R.; Woody, R.W. *Int. J. Peptide Protein Res.*, **1982**, *19*, 187-205.
34. Perczel, A.; Hollósi, M.; Sándor, P.; Fasman, G.D. *Int. J. Peptide Protein Res.*, **1993**, *41*, 223-236.
35. Woody, R.W.; *Method Enzymol.*, **1995**, *246*, 34-71.

36. http://www.scripps.edu/finn/Scipdfiles/TLC%20Staining.pdf, retrieved July 8, 2012.
37. Vojkovsky, T. *Pept. Res.*, **1995**, *8*, 236-237.
38. Kaiser, E.; Colescott, R.L.; Bossinger, L.D.; Cook, P.I. *Anal. Biochem.*, **1970**, *34*, 595-598.
39. Ponder, J.W.; Case, D.A. *Adv. Protein Chem*., **2003**, *66*, 27-85.
40. Meienhofer, J.; Waki, M.; Heimer, E.P.; Lambros, T.J.; Makofske, R.C.; Chang, C.-D. *Int. J. Peptide Protein Res.***1979**, *13*, 35.
41. Evans, D.A.; Dow, R.L.; Shih, T.L.; Takacs, J.M.; Zahler, R. *JACS*, **1990**, *112*, 5290-5313.
42. Roeder, M.; Spiegelstein, O.; Schurig, V.; Bialer, M.; Yagen, B. *Tetrahedron: Asymm.*, **1999**, *10*, 841.
43. Occasionally yellow precipitate was formed.

CHAPTER 6

Structural Investigations on Macrocyclic Peptide Analogues of the Echinocandins: Implications of the Ring Size on Antifungal Activity

6.1 Introduction

In the previous chapters it became clear that the size and thereby the conformational behaviour of the macrocyclic ring structure of the echinocandins in combination with the choice of the fatty acid side chain as well as crucial substituents are determining factors for antifungal activity. As is described in chapter 2 even small variations of the size of the macrocyclic ring structure can completely abrogate antifungal activity. In addition, the results described in chapter 5 also indicate that small variations in the position of a (hydroxyl) substituent have a large influence on the antifungal activity. Even expansion of the peptide macrocycle with just one carbon atom completely abolished antifungal activity. Since this finding was rather unexpected in view of the limited added flexibility to the already flexible peptide 21-membered macrocycle,[1] it was attempted to evaluate the conformational behaviour and possible ensuing influence of ring size on antifungal activity. With respect to this, larger ring sizes may disrupt any trans-annular hydrogen bonds that may be important for stabilizing bio-active conformations. To address this hypothesis we applied nuclear magnetic resonance (NMR) and circular dichroism (CD) techniques were applied in attempts to elucidate solution conformations of the analogues described in the previous chapters. In the NMR studies parameters such as temperature coefficients of NH protons and NOEs were investigated. In the CD studies the Far UV region (250-190 nm), which corresponds to peptide-amide bond absorption, was measured to analyze the content of secondary structures.

6.2 Results and discussion

6.2.1 NMR studies

Temperature coefficients

Amide proton temperature coefficients are an attractive and simple way to detect and confirm the presence of hydrogen bonds.[3] Since the early years of peptide NMR it has been known that the chemical shifts of amide proton resonances display a temperature dependence.[4] This can be quantified by the temperature coefficient ($\Delta\delta_{NH}/\Delta T$). The value of the amide temperature coefficient has been used to predict hydrogen bond donors, with hydrogen-bonded amides generally showing smaller temperature coefficients than non-hydrogen bonded amides.[3,5-8]

Generally, the analysis of temperature coefficients is performed in water. Due to solubility problems of the analogues bearing a terphenyl side chain these could not be measured. Therefore, a first attempt was made with a simplified mimic of caspofungin with a dimethylmyristic side chain. Although soluble in H_2O, NMR measurements showed that aggregates were formed and therefore it was impossible to study the structure of this peptide. Probably the lipophilic tail of this analogue is responsible for the aggregation effect and therefore analogues were used with a shortened acetyl “tail” as are shown in Figure 1. Their syntheses are outlined in Scheme 1 and Scheme 2.

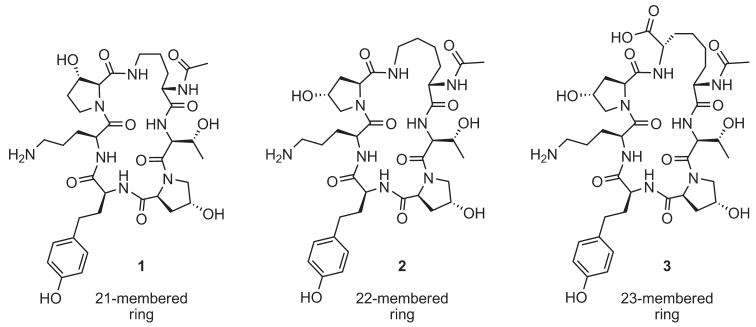

Figure 1. Ring size analogues (**1**-**3**) with an acetyl tail.

For the 21- and 22- membered rings the linear hexapeptide precursors **4** and **5** were synthesized by SPPS using the trityl resin as shown in Scheme 1. Removal of the ε-Fmoc group from ornithine in **4** and lysine in **5**, followed by treatment with capping reagent (Ac_2O/HOBt/DiPEA/NMP) and mild acidolytic cleavage of the Mtt group liberated the peptide chain from the resin to give the linear fully protected peptide precursors **6** and **7**. Solution-phase cyclization followed by protecting group removal resulted in macrocyclic peptides **1** and **2** in overall yields of 20-53% after purification by preparative HPLC.

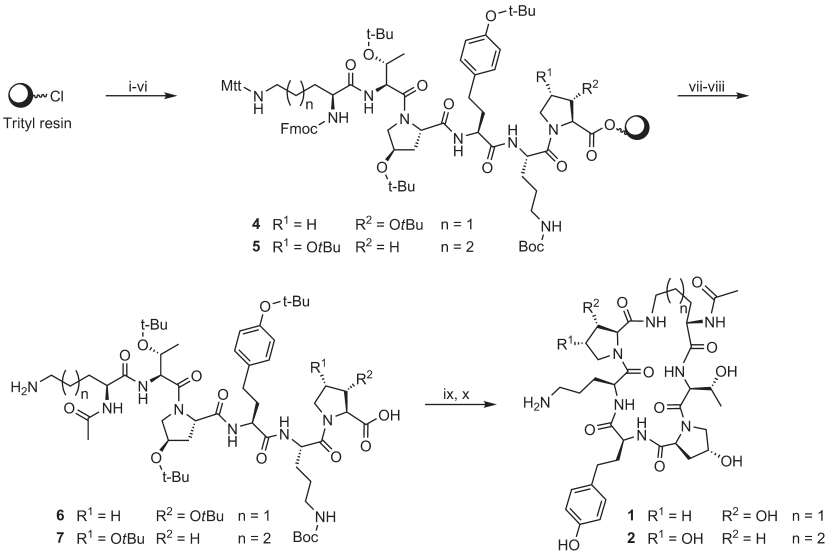

Scheme 1. Reagents and conditions: (i) 4: Fmoc-3-Hyp(*t*Bu)-OH, DIPEA, DCM; 5: Fmoc-Hyp(*t*Bu)-OH, DIPEA, DCM; (ii-vi) (1) 20% piperidine in NMP; (2) Fmoc-Xxx-OH, BOP, DiPEA, NMP; (vii) (1) 20% piperidine in NMP; (2) Capping solution: Ac_2O/HOBt/DiPEA/NMP; (viii) TFE/AcOH/DCM (2/1/7; v/v/v); (ix) BOP, DiPEA, DMF; (x) TFA/TIS/H_2O (95/2.5/2.5; v/v/v).

As is shown in Scheme 2 the linear precursor **8** of the 23-membered cyclic peptide **3** was prepared by SPPS on the Wang resin. Removal of the N-terminal Fmoc group, treatment with capping reagent followed by RCM reaction of the resin-bound peptide using a 10 mol% solution of Grubbs II catalyst in DCM (containing 10 vol% 0.4M LiCl in DMA) under microwave irradiation resulted in the ring-closed product. Cleavage from the resin with

concomitant removal of side chain protecting groups gave cyclic peptide **9** as a mixture of *cis/trans* isomers in an overall yield of 6% after purification by preparative HPLC. After reduction of the double bond in the *cis*/*trans* mixture of peptide **9**, macrocyclic peptide **3** was obtained.

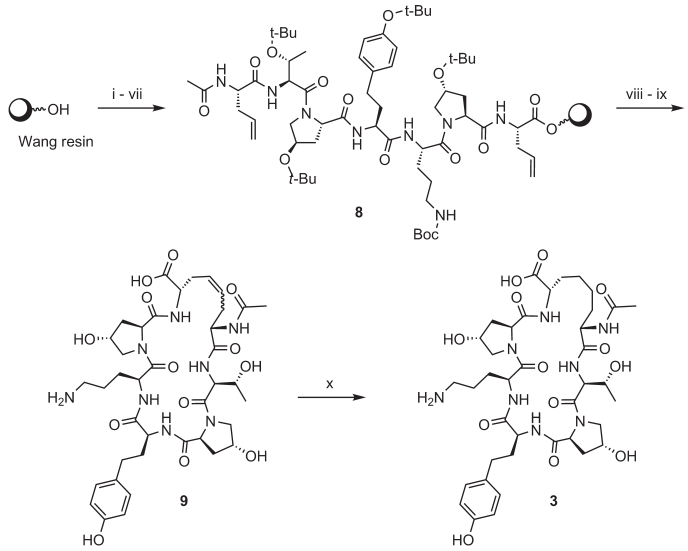

Scheme 2. Reagents and conditions: (i) Wang resin: (1) Fmoc-Alg-OH, pyridine, DCBC, DMF; (2) Ac_2O/NMI/DiPEA/DMF (2/1/1/6, v/v/v); (ii-vi) (1) 20% piperidine in NMP; (2) Fmoc-Xxx-OH, BOP, DiPEA, NMP; (vii) (1) 20% piperidine in NMP; (2) Capping solution: Ac_2O/HOBt/DiPEA/NMP; (viii) Grubbs II (10 mol%), 10 vol% LiCl/DMA (0.4M), MW, 60 min, 100 °C, DCM; (ix) TFA/TIS/H_2O (95/2.5/2.5, v/v/v), (x) H_2, 10% Pd/C, EtOH, rt, 36h.

The ring size analogues **1**-**3** with an acetyl "tail" were studied by NMR spectroscopy (Figure 2- 4). One- and two- dimensional[9] (NOESY[10], TOCSY[11] and ^{13}C-^{1}H HSQC[12]) NMR experiments were used for the complete proton and carbon resonance assignments of these peptides.

Inspection of the amide region in the 1D spectra of the three analogues, showed differences in chemical shift of the amides around the site, which was varied (upper amino acid, O1, K1, Alg respectively). Most interestingly, increasing the ring size from 21 (Figure 2) to 22 (Figure 3) also showed an effect on the chemical shift of the homotyrosine amide (Y4), suggesting a conformational change. This could indicate that the amide proton of Y4 in cyclic peptide **2** is more shielded by the aromatic ring of this residue.

To analyze changes in the hydrogen bonding network of these cyclic peptides the amide temperature coefficients ($\Delta\delta_{NH}/\Delta T$) were measured. The temperature dependence of the amide proton chemical shifts was determined with one dimensional ^{1}H NMR experiments over the temperature range of 273-318 K. In the 1D-spectra of the 23-membered analogue **3** the amide protons overlapped (Figure 4). Therefore, two-dimensional TOCSY experiments were used, in addition to the 1D spectra, to determine the temperature coefficients of these amides. The experimental data are presented in Figure 5 and the temperature coefficients are listed in Table 1.

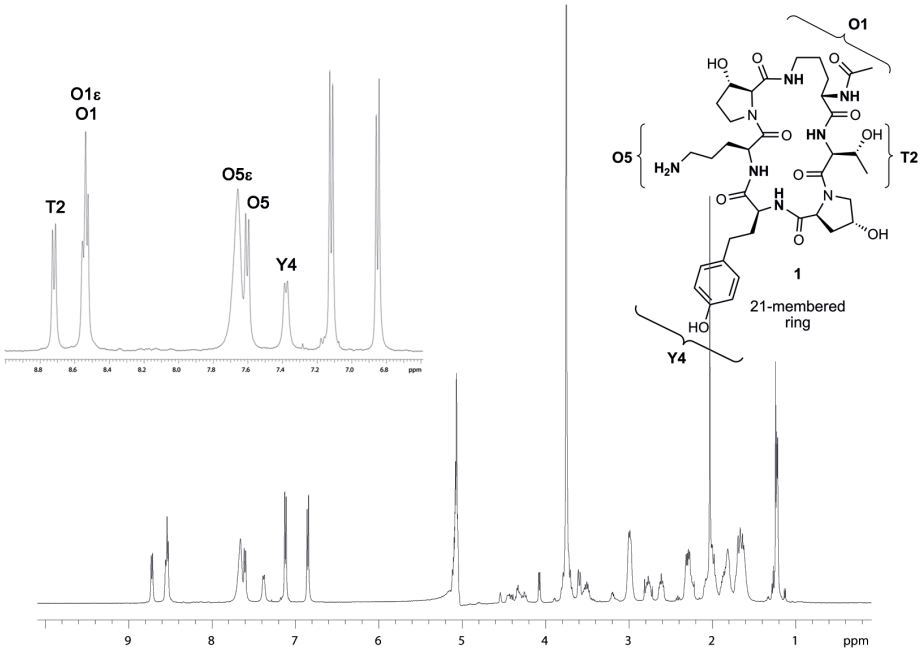

Figure 2. ^{1}H-NMR spectrum at 278K of the 21-membered ring size analogue **1**, in the expanded region of the spectra are all six NH protons.

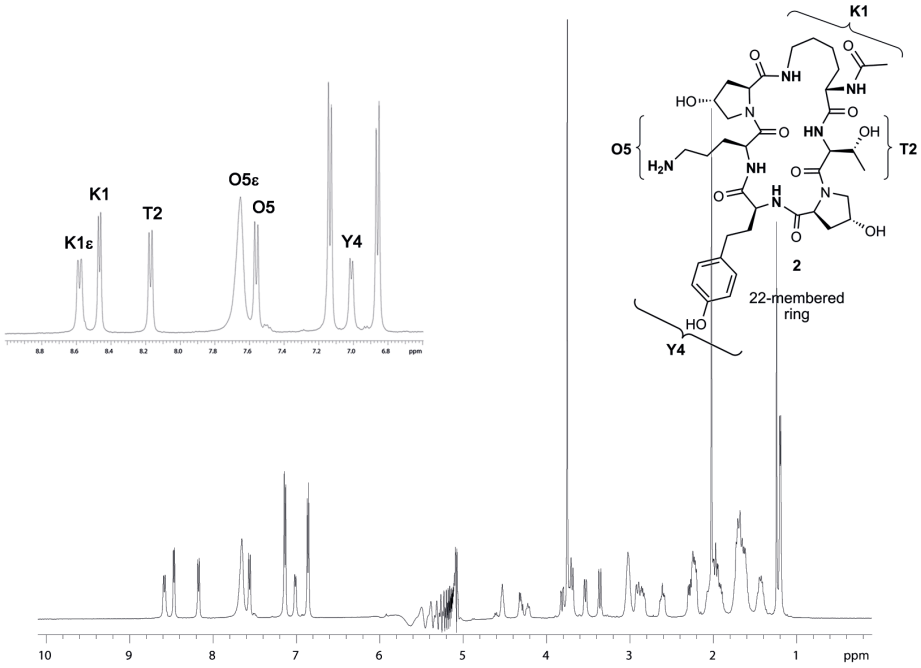

Figure 3. ^{1}H-NMR spectrum at 278K of the 22-membered ring size analogue **2**, in the expanded region of the spectra are all six NH protons.

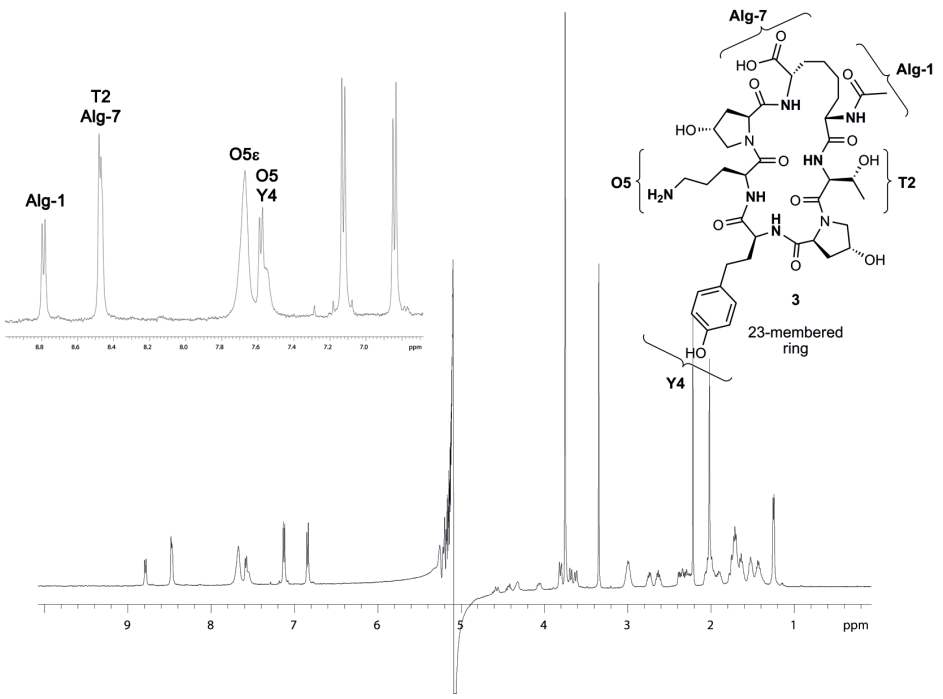

Figure 4. ^{1}H-NMR spectrum at 278K of the 23-membered ring size analogue **3**, in the expanded region of the spectra are all six NH protons.

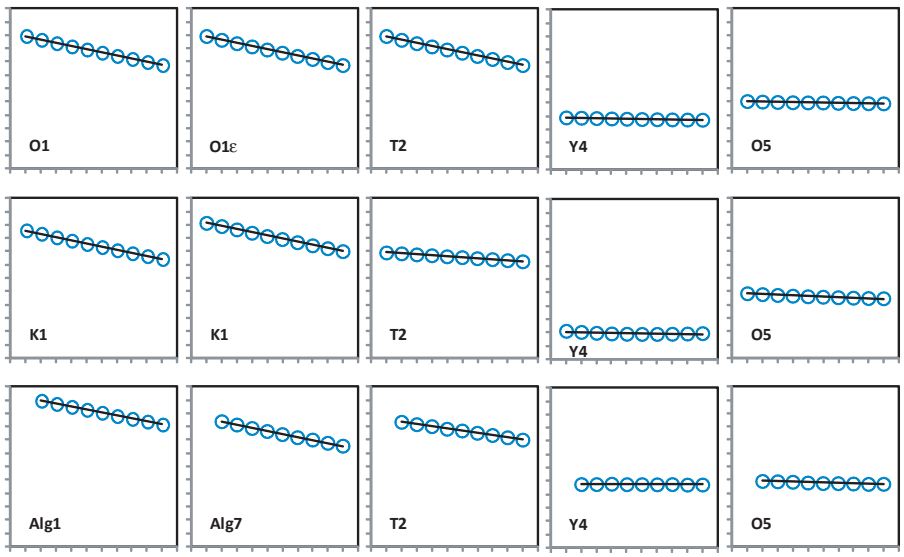

Figure 5. Dependence of chemical shifts on temperature for the amide protons. A) 21-membered ring size analogue **1**; B) 22-membered ring size analogue **2**; C) 23-membered ring size analogue **3**. The x-axis for each graph displays the range 268- 323 K with marks at 5° intervals. The scaling on the y-axis is identical for each plot; the mark interval corresponds to 0.2 ppm.

Most proton chemical shifts display a linear temperature dependence (Figure 5), although it is noticeable that the amide proton Y4 shows a non-linear behaviour, especially in the 22-membered analogue **2**. This result could indicate that at least two species in this region of the peptide are in fast exchange over the temperature range studied.[7]

Table 1. Temperature coefficients in ppb/K.

1: 21-membered ring		**2: 22-membered ring**		**3: 23-membered ring**	
	Amide-NH		Amide-NH		Amide-NH
Residue	$\Delta\delta/\Delta T$	Residue	$\Delta\delta/\Delta T$	Residue	$\Delta\delta/\Delta T$
O1	-9.61	**K1**	-9.56	**Alg-1**	-8.90
O1ε[a]	-9.19	**K1**ε[a]	-9.45	**Alg-7**	-9.10
T2	-6.37	**T2**	-2.93	**T2**	-6.60
Y4	-0.76	**Y4**	-0.72	**Y4**	-0.20
O5	-0.75	**O5**	-1.65	**O5**	-1.20

[a] Amide NH of the side chain in this residue.

Values of amide proton temperature coefficients measured for the ring size analogues (**1**-**3**), as listed in Table 1, ranged from -9.61 to -0.20 ppb/K. From literature it is known that amide protons with temperature coefficients more positive than -4.6 ppb/K are hydrogen bonded, whereas high coefficients (i.e. $\Delta\delta_{NH}/\Delta T$ < -4.6 ppb/K) suggest that the amide is not hydrogen-bonded.[3,7,8] Analysis of the temperature coefficients of the data sets showed that the backbone amides of Y4 and O5 are involved in intramolecular hydrogen bonds. Notably, only for the 22-membered analogue **2**, the $\Delta\delta_{NH}/\Delta T$ value indicates that also the backbone amide proton of T2 might be involved in hydrogen bonding.

For comparison purposes the temperature coefficients of the three analogues were depicted in a bar diagram as shown in Figure 6. This clearly shows that the ring size has almost no effect on the temperature coefficients of the amides, except for T2. This may suggest that the backbone amide proton of T2 in the 22-membered analogue **2** is involved in hydrogen bonding.

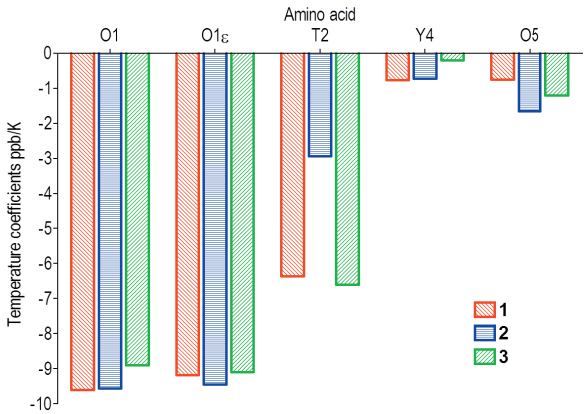

Figure 6. Bar diagram showing a comparison in temperature coefficient values of NH resonances in peptides **1**-**3**.

NOEs

More detailed structural information can be obtained from NOESY experiments.[13] Therefore, in addition to the temperature coefficients NOE signals were evaluated. As NOEs depends on the *through-space* interaction they can be directly related to the peptide conformation.[14] While backbone NH(i+1)-Cα(i) and NH(i+1)-side-chain(i) NOEs support the ^{1}H-NMR sequential assignments and determine the order of the amino acids in the peptide sequence, sequential NH(i)-NH(i+1) and non-sequential NOEs are an indication for non-random coil conformations of the poly-peptide chain.[2,5,14]

2D NOE spectra of the ring size analogues (**1**-**3**) contain predominantly sequential NOEs, but a few long-range contacts could be identified as well. These are shown in Figure 7. Similar NOE patterns were observed for all three ring size analogues. Two interesting NOE connectivities were observed for analogues **1** and **2**: between residues T2 and O5 NH(2)-NH(5) and residues Y4 and O5 NH(4)-NH(5), respectively. For analogue **3** only the NOE between T2 and O5 NH(2)-NH(5) was observed. A possible NOE between the NHs of Y4 and O5 is masked by overlap. However, we did observe this NOE in the precursor (**9**) of this mimic. In addition, we observed a weak NOE between the Cα of P3 and the NH of O5 in analogues **1** and **2**.

The NOE data also demonstrate that all other peptide bonds than those involving the amine of the proline residues are in the *trans* configuration.

Discussion

The structure of macrocyclic peptide echinocandin analogues **1**-**3** has been characterized by NMR spectroscopy. These studies indicate the presence of non-random conformations.

In general cyclic peptides are known to form turn-like conformations and the NH(2)-NH(5) NOE connectivity observed in all peptides (**1**-**3**) establishes the presence of a turn at this site of our analogues. The presence of two proline residues greatly facilitates the formation of turns.

Cyclic hexapeptides have long been known to favor the conformation of a β-turn.[15,16] Detection of a β-turn stabilized by an intramolecular 4 → 1 hydrogen bond by NMR relies upon three types of evidence: (*i*) A low temperature coefficient for the NH of residue 4 of the turn, indicating the 4 → 1 backbone amide-carbonyl hydrogen bond; (*ii*) The chain reversal associated with a β-turn results in short proton-proton distance NOE connectivity between residue 3 and 4 of the turn; (*iii*) Observation of a $d_{\alpha N}$(2,4) NOE connectivity.[2,5,17]

A summary of the observed NOEs and temperature coefficients for the peptides **1**-**3** is given in Figure 8. Indeed a low temperature coefficient was found for the NH of residue 4 (O5) in all three macrocyclic ring size analogues. In addition, for cyclic peptides **1** and **2** a short distance NOE connectivity was observed, between residue 3 (Y4) and 4 (O5) of the turn. This NOE was not observed for the 23-membered cyclic peptide **3**, due to overlap of the amide signals. Moreover, a weak $d_{\alpha N}$ NOE connectivity between P3 CHα and NH O5 was observed for cyclic peptides **1** and **2**. As was described by Dyson et al.[5] this connectivity was only observed for peptides with the highest population of β-turns.

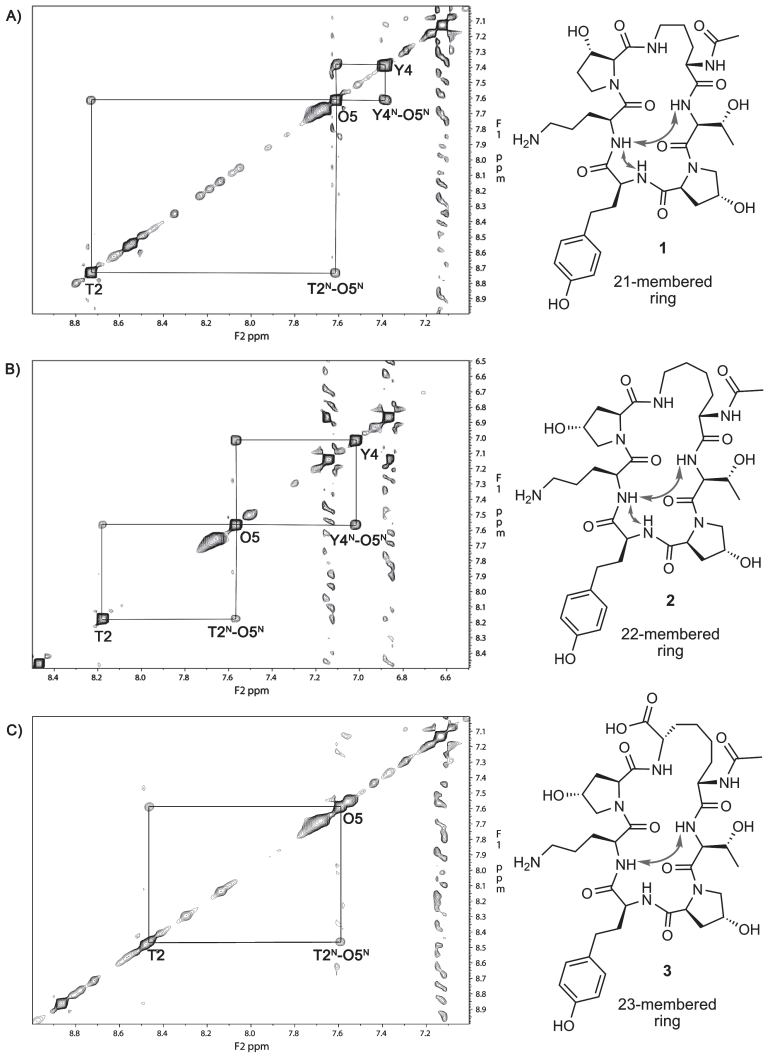

Figure 7. NH-NH NOEs observed in ring size analogues (**1**-**3**). Left: Amide region of NOESY spectra of A) 21-membered analogue (**1**); B) 22-membered analogue (**2**); C) 23-membered analogue (**3**). Right: NOEs are indicated in the chemical structures by arrows.

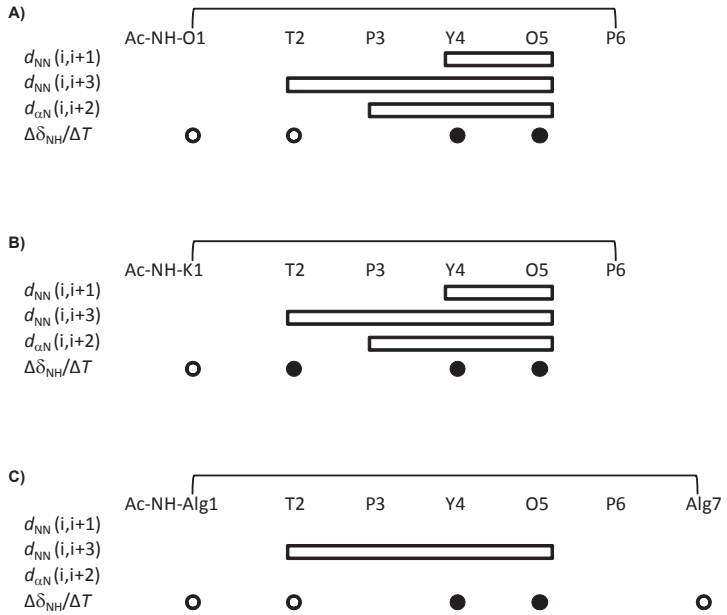

Figure 8. Summary of observed non-sequential NOEs and temperature coefficients. 21-membered analogue (**1**); B) 22-membered analogue (**2**); C) 23-membered analogue (**3**). Closed circles correspond to $\Delta\delta_{NH}/\Delta T > -4.6$ ppb/K and open circles to $\Delta\delta_{NH}/\Delta T < -4.6$ ppb/K.

Thus, the NMR data showed comparable conformational behaviour of ring size analogues **1**-**3**. To corroborate the β-turn like structures observed by NMR, CD spectra were measured (*vide infra*).

6.2.2 CD studies

Circular dichroism (CD) spectroscopy can give valuable insights into peptide structure. In the Far UV region (250-190 nm), which corresponds to peptide-amide bond absorption, the CD spectrum can be analyzed with respect to the content of secondary structures.[18] In addition to secondary structure prediction changes in CD spectra are indicators of changes in conformation. As first discussed by Ovchinnikov and Ivanov[19], CD spectra may provide evidence of perturbations or alterations of the accessible conformational states in a series of *related* peptides.[18,20] In order to investigate the secondary structure and structural changes of cyclic peptides **1**-**3**, CD spectra were recorded (Figure 9).

In addition to measuring in aqueous systems, CD can be measured in organic solvents e.g. ethanol[21], methanol[21], trifluoroethanol (TFE)[22]. The latter has the advantage to enhance secondary structure formation of peptides. Therefore CD measurements were carried out in water and water-TFE (1/1, v/v) mixtures. The data were normalized with respect to the amount of amide bonds present (6 in **1** and **2** and 7 in **3**, respectively) and reported as mean residue ellipticities.

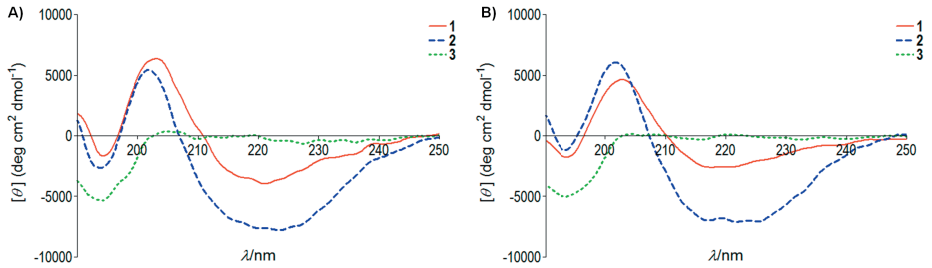

Figure 9. CD spectra of ring size analogues (**1**-**3**). A) Measured in H_2O; B) Measured in TFE/H_2O (1/1, v/v). All peptides were measured at 0.1 mM concentration.

The CD spectra of cyclic peptides **1**-**3** are almost identical in water and water-TFE mixtures. While the CD spectra of cyclic peptides **1** and **2** were similar, the spectra of cyclic peptide **3** were very different from those of **1** and **2**.

The CD spectrum of cyclic peptide **3**, with a very low ellipticity above 210 nm and a negative band at 195 nm, resembled the spectrum of a random coil conformation.[17,18] The CD spectra of cyclic peptide **1** showed characteristics for mixtures of conformers with a considerable turn population. For **1** negative ellipticity maxima at ca 220 nm and positive bands at ca 205 nm were observed suggesting that the cyclic peptide formed a significant proportion of a folded structure with an absorption profile reminiscent of a β-turn (type II).[17,20-24] The CD curve of cyclic peptide **2** exhibited a more pronounced negative molar ellipticity curve combined with a broader negative band compared to **1**, which can indicate a different backbone conformation.

In chapter 5 it was mentioned, that the position of the OH function in the left upper hydroxyproline of the cyclic hexapeptide ring (residue Hyp-6) influenced the shape of the CD spectra of these compounds.[25] To exclude this possible additional structural effect on the CD spectra of the 21- and 22-membered cyclic peptides **1** and **2** CD spectra of cyclic peptides **10** and **11** (Figure 10) were measured (Figure 11). These cyclic peptides **10** and **11** only differed in ring size, thereby allowing a comparison of merely the effect of size on CD.

As is shown in Figure 11, cyclic peptides **10** and **11** exhibited similar CD spectra as cyclic peptides **1** and **2**, with a more negative molar ellipticity curve for peptide **11**. In addition, a distinctly different pattern in the CD spectra of these analogues was observed, at wavelenghts below 210 nm, compared to ring size analogues **1** and **2** in Figure 9. This agrees with the observation discussed in chapter 5 regarding the considerable influence of the terphenyl side chain on CD spectra, possibly caused by the aromatic residues.

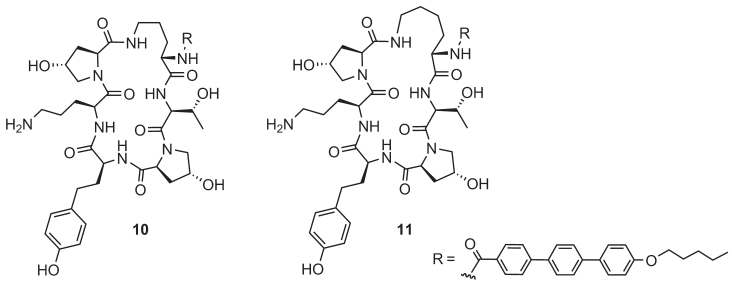

Figure 10. 21-membered ring size analogue **10** and 22- membered analogue **11** with terphenyl side chain.

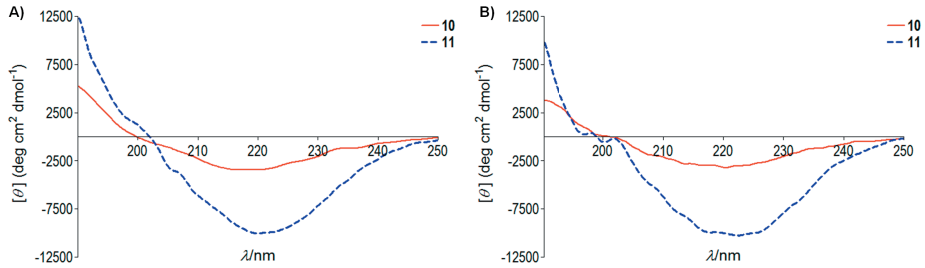

Figure 11. CD spectra of ring size analogues **10** and **11** bearing a terphenyl side chain. A) Measured in MeCN/H_2O (1/1, v/v); B) Measured in TFE/H_2O (1/1, v/v). All peptides were measured at 0.1 mM concentration.

6.2.3 Modeling

Recently, a single crystal X-ray structure of the cyclic peptide nucleus **13** (ECBN.HCl) of echinocandin B (**12**) has been reported.[26] Echinocandin B (**12**) was deacylated enzymatically, to remove the linoleoyl function from the α-amino group of the dihydroxyornithine residue to yield cyclic peptide **13**, isolated as the hydrochloride salt (Scheme 3).

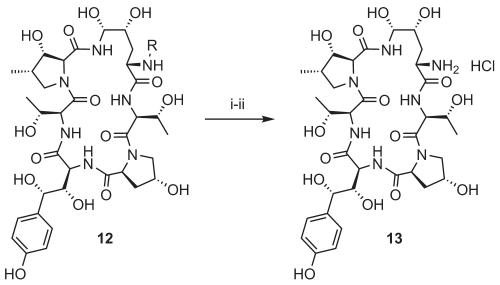

Scheme 3. Enzymatic cleavage of the linoleoyl tail of Echinocandin B (**12**). (i) ECB deacylase; (ii) aq. HCl. R= linoleoyl side chain. Single crystal X-Ray data were obtained directly from crystals selected from bulk material produced by recovery from the fermentation process biomass.[26]

Single crystal X-Ray data were obtained directly from crystals selected from bulk material produced by recovery from the fermentation process biomass.[26]

In addition to the NMR and CD measurements previously described, models of the cyclic peptides described in this chapter were constructed and superimposed on the reported crystal structure of **13**. These models may provide further insights into the influence of the ring size on the conformation(s) of the macrocyclic lipopeptides.

Thus, molecular models of the cyclic peptides (**1**-**3**) were constructed using the YASARA program.[27] Molecular dynamics (MD) simulations were carried out for each structure in a box filled with water. The lowest energy conformation of each peptide **1**-**3** was superimposed with the crystal structure of **13** (Figure 12).

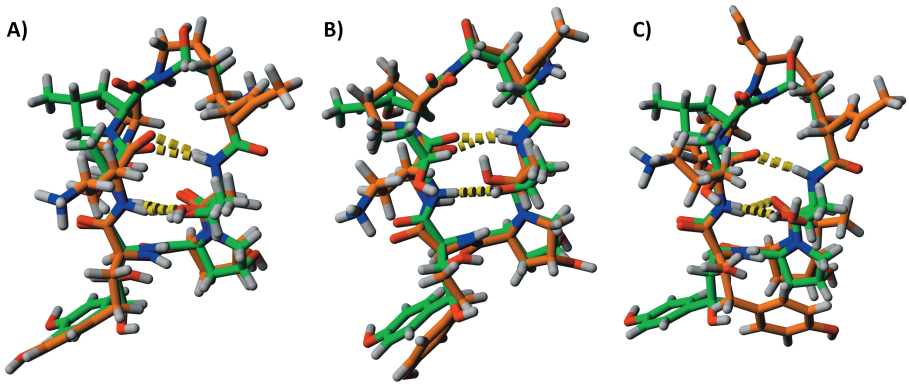

Figure 12. Superimposition of **13**[26] (ECBN, carbons colored green) with cyclic peptides **1**-**3** (carbons colored orange).[27] A) 21-membered ring cyclic peptide (**1**); B) 22-membered ring cyclic peptide (**2**); C) 23-membered ring cyclic peptide (**3**). The backbone atoms have been used as fixed coordinates for superimposition.

It appears that cyclic peptide **1** and **2** resemble the structure of **13**, while analogue **3** is more different.

6.2.4 Crystallization attempts

So far no crystal structure of any semisynthetic or synthetic echinocandin analogue has been reported. The only available crystal structure is that of cyclic peptide part **13** (ECBN.HCl).[26]

In an attempt to obtain further structural information on our echinocandin mimics several analogues were sent to the University of Santiago de Compostela in Spain where they were included in a crystallization assay.[28] The approach used was microbatch crystallization under oil.[29] This allows the use of small samples which are protected from evaporation, contamination and physical shock by the oil and generates a rapid screening to determine solubility properties.

Very thin colorless needle-shaped crystals were obtained with cyclic peptide **14** in the well where 20% dimethylsulfoxide in methanol crystallization solution was added (Figure 13). Unfortunately, these crystals did not diffract with the laboratory X-ray source and did not grow further after slow evaporation performed during several months. The other cyclic peptides included in this assay did not show any crystal growth.

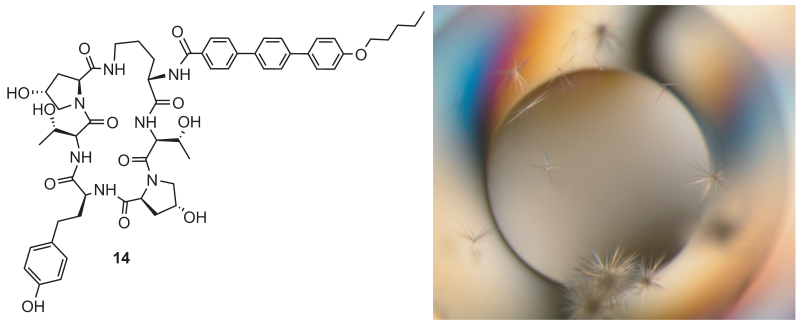

Figure 13. Crystals obtained for cyclic peptide **14**.

6.3 Conclusions

In this chapter an attempt was made to rationalize the complete loss in activity as a result of increasing the ring size of echinocandin analogues. Even expansion of the peptide macrocycle by merely one carbon atom completely abolished antifungal activity. It was hypothesized that larger ring sizes may disrupt the transannular hydrogen bonds that are thought to be important for adoption of the biologically active conformation. Therefore the 21-membered analogue **1**, having the same ring size as echinocandin as well as the 22-membered analogue **2** and 23-membered analogue **3** were prepared. To facilitate the NMR studies these cyclic peptides contained an acetyl group instead of the long lipophilic tail.

NMR studies showed comparable conformational behaviour of all three macrocyclic peptides. Non-sequential NOEs and low NH temperature coefficients were all indicative of β-turn like structures in the T2-O5 regions of these peptides. CD spectroscopy confirmed the similarities in secondary structure preferences of ring size analogues **1** and **2** and showed characteristics for mixtures of conformers with a considerable amount of turn-like populations. In contrast, the spectrum of analogue **3** seemed characteristic of a more disordered structure. These findings were in agreement with molecular modeling studies.

These results seem to indicate that the 23-membered ring contains a smaller population of turn conformation compared to the native 21-membered ring. However, the slightly larger ring of the 22-membered analogue **2** displays the same characteristic conformational features as the 21-membered ring.

These findings suggest that apart from the backbone conformation of the echinocandin ring also other features contribute to efficient antifungal activity.

6.4 Experimental section

6.4.1 Reagents, materials and methods:

Unless stated otherwise, all chemicals were obtained from commercial sources and used as supplied, with the exception of DMF, NMP and DCM, which were dried on molecular sieves (4Å) prior to use. HPLC grade solvents were purchased from Biosolve B.V. (Valkenswaard, The Netherlands). Fmoc protected amino acids were purchased from GL Biochem Ltd. (Shanghai, China). Fmoc-Orn(Mtt)-OH was obtained from Nova Biochem. The *tert*-butyl side chain protected homotyrosine (H-hTyr(*t*Bu)-OH) was purchased from Advanced Chemtech (Louisville, United States) and subsequently protected with the Fmoc group. The 2-chlorotritylchloride PS resin was purchased from Hecheng Chemicals (Shanghai, China). Tentagel S PHB was purchased from RAPP Polymere (Tübingen, Germany). All other reagents were purchased from Merck (Darmstadt, Germany), Sigma-Aldrich (Munich, Germany) and Acros (Geel, Belgium) and were used without further purification.

Solid phase synthesis was performed in plastic syringes with a polyethylene frit. Reactions were monitored with the chloranil test[30] in case of secondary amines or with the Kaiser test[31] in case of primary amines.

Purity of the peptides was confirmed by analytical HPLC using a Prosphere C18 column at a flow rate of 1 mL/min using a linear gradient of buffer B (100% in 20 min) from 100% buffer A. Analytical HPLC was performed on a Shimadzu automated HPLC system equipped with an evaporative light scattering detector (PL-ELS 1000) and a UV/Vis detector operated at 220/254 nm. Preparative HPLC runs were performed using a Prosphere C18 column at a flow rate of 12 ml/min with a linear gradient of buffer B (100% in 80 min) from 100% buffer A on an Applied Biosystems 400 solvent delivery system with an Applied Biosystems 757 UV/VIS absorbance detector. The buffer system used consists out of buffer A: 0.1 % TFA in H_2O and buffer B: 0.1% TFA in MeCN/H_2O, 80/20, v/v.

HRMS analyses were performed on a MALDI TOF/TOF (Applied Biosystems).

NMR spectroscopy

^{1}H NMR, TOCSY, ^{1}H-^{13}C HSQC and ROESY spectra were recorded on a Varian INOVA-500 spectrometer (500 MHz) at 278K. Data were processed with NMRpipe[32] and chemical shifts were assigned using the Sparky program (T. D. Goddard and D. G. Kneller, University of California, San Francisco). Chemical shifts are given in ppm relative to dioxane (^{1}H 3.75 ppm; ^{13}C 69.3 ppm)[33], which was used as an internal reference in the mixed H_2O/D_2O solutions.

YASARA modelling

Modeling of the structures was accomplished using the YASARA Structure 10.5.2.1 software package.[27] Structures were energy minimized using the simulated annealing protocol employing the AMBER99[34] force field. Of each structure a 2500 ps MD-simulation in water was run. After an equilibration period of 250 ps, the structure with the lowest energy was selected from the trajectory between 250-2500 ps and saved as a yob file. Molecules were superimposed by minimizing the rmsd between the backbone atoms in the ring.

CD spectroscopy

CD spectra were recorded at 298 K on a JASCO J-810 spectrometer using 0.1 cm path length quartz cells. The CD spectra are an average of four scans, collected at 0.2 nm intervals between 190 and 250 nm. The peptides were prepared at concentrations of 0.1 mM in MeCN/H_2O (1/1, v/v) or 0.1 mM in TFE/H_2O (1/1, v/v). Ellipticity is reported as the mean residue ellipticity [θ] in degrees.cm^2/dmol calculated from the following equation: [θ]=(100*θobs)/(C_{MR}*l), where θobs is the observed ellipticity in degrees, C_{MR} is the mean residue molar concentration, and l the optical path length of the cell in cm. The mean residue concentration C_{MR} is the concentration of peptide (c) in molar multiplied by the number of amino acids (N) in the peptide: C_{MR}= c*N. The factor of 100 converts to a pathlength in m.

Microbatch Crystallization[28]

Droplets (72 x 2 μL) of a solution of each compound in methanol (5-20 mg/mL) were placed in a 72 wells Terasaki plate filled with decane (8 mL). To each well, 2 μl of one of the 72 crystallization conditions of a homemade crystallization screening kit (made with a variety of concentrations in methanol of water, ethanol, i-propanol, n-butanol, dimethylsulfoxide, dimethylformamide, polyethylene glycol 600, hexylene glycol, sodium acetatate or tris-hydroxymethyl-aminomethane hydrochloride) were added; the decane was removed and the plate was filled with mineral oil (8 mL). Slow evaporation of solvents were performed at 296 K in a temperature controlled chamber. Very narrow colorless needle-shaped crystals were obtained with compound **14** in the well where 20% dimethylsulfoxide in methanol crystallization solution was added. These crystals did not diffract with a laboratory X-ray source and did not grow after slow evaporation performed during several months.

6.4.2 Chemistry

General Procedures

Solid phase peptide synthesis: Peptides were synthesized manually. Each synthetic cycle consisted of the following steps:

Fmoc removal: The resin was treated with a 20% solution of piperidine in NMP (3×, each 10 min). The solution was removed by filtration and the resin was washed with NMP (3×, each 3 min) and DCM (3×, each 3 min).

Coupling step: A mixture of Fmoc-Xxx-OH (3 equiv.), BOP (3 equiv.) and DiPEA (6 equiv.) in NMP (10mL/mmol resin bound peptide derivative) was added to the resin and N_2 was bubbled through the mixture for 2h. The solution was removed by filtration and the resin washed with NMP (3×, each 3 min) and DCM (3×, each 3 min). Completion of the coupling was checked with Kaiser or chloranil test.

Capping of the remaining free amines: Capping solution [Ac_2O (50 mmol, 4.7 mL), HOBt (1.9 mmol, 220 mg), DiPEA (12.5 mmol, 2.2 mL) in 100 mL NMP] was added to the resin and N_2 was bubbled through the mixture for 20 min The solution was removed by filtration and the resin was washed with NMP (3×, each 3 min) and DCM (3×, each 3 min).

Head-to-tail cyclization: The peptide was dissolved in dry DMF (2 mL/μmol) and BOP (4 equiv.) and DiPEA (8 equiv.) were added. The mixture was stirred overnight followed by evaporation *in vacuo*. The product was redissolved in EtOAc and washed with 1M $KHSO_4$ (2×), $NaHCO_3$ (2×) and H_2O (2×). The organic layer was dried over Na_2SO_4, filtered and

concentrated *in vacuo*.

Microwave-assisted RCM: A microwave vessel containing a magnetic stirrer bead was loaded under argon with resin peptide, catalyst and solvent. The vessel was capped and irradiated at 100 °C. At the end of the reaction period the resin-bound peptide was washed with DMF (3× 3 mL, each 3 min) DCM (3× 3 mL, each 3 min) and MeOH (3× 3 mL, each 3 min).

Hydrogenation: To a solution of the olefenic peptide in *t*BuOH/H_2O (1 mL, 3/1, v/v) 10% Pd/C was added. The reaction mixture was stirred under H_2 at atmospheric pressure overnight. The mixture was then filtered through a path of celite and washed extensively with *tert*-BuOH. The mixture was concentrated and lyophilized from *tert*-BuOH/H_2O (1/1, v/v).

General procedure for the preparation of the cyclic peptide analogues (1-2)

The linear peptides **4** and **5** were synthesized on trityl resin according to the general procedure for solid phase peptide synthesis. Then, the Fmoc group was cleaved and the resin was treated with capping solution Ac_2O/HOBt/DiPEA/NMP as described in the general procedures. Subsequently the capping solution was removed by filtration and the resin washed with DMF (3× 4 mL, each 3 min) and DCM (3× 4 mL, each 3 min). Completion of the coupling was checked with the Kaiser test. Then, mild acidolytic cleavage, by treatment with TFE/AcOH/DCM (2/1/7, v/v/v, 5 mL) for 2 hours, of the Mtt group as well as cleavage from the resin gave protected peptide precursors **6** and **7.** The mixture was concentrated *in vacuo* and the peptides were precipitated in MTBE/Hexanes (3×, 1/1, v/v).

The linear peptide was then subjected to head-to-tail cyclization by dissolving it in dry DMF (2 mL/μmol) followed by the addition of BOP (4 equiv.) and DiPEA (4 equiv.). The mixture was stirred for 48h and then evaporated *in vacuo*. The product was redissolved in EtOAc and washed with 1M $KHSO_4$ (2×), $NaHCO_3$ (2×) and H_2O (2×). The organic layer was dried over Na_2SO_4, filtered and concentrated *in vacuo*. Final protecting group removal by treatment with a mixture of TFA/TIS/H_2O (2 mL, 95/2.5/2.5, v/v/v) for 2h and precipitation in MTBE/hexanes (3×, 1/1, v/v) afforded the crude peptide. After lyophilization from *tert*-BuOH/H_2O (1/1, v/v) the peptide was purified by preparative HPLC.

***Cyclo*[-(Ac)-Orn-Thr-Hyp-hTyr-Orn-3-Hyp] (1)**

Cyclic peptide **1** was obtained according to the general procedure for the preparation of the ring size analogues using 33 μmol of **4**. After lyophilization, peptide **1** (13.5 mg; 53%) was obtained as a white solid. Purity was confirmed by analytical HPLC and was found to be to be higher than 99% (R_t = 15.53 min). HRMS calcd for $C_{36}H_{54}N_8O_{11}$ $[M+H]^+$ 775.3990, found 775.3986; ^{1}H-NMR (H_2O/D_2O, 500 MHz): δ Orn-1: 8.56 (εNH), 8.54 (NH), 4.33 (αCH), 2.06/1.69 (βCH), 1.81 (γCH), 3.52/3.00 (δCH); Thr-2: 8.73 (NH), 4.91 (αCH), 4.45 (βCH), 1.23 (γCH); Hyp-3: 4.42 (αCH), 2.30/1.68 (βCH), 4.55 (γCH), 3.76/3.60 (δCH); hTyr-4: 7.39 (NH), 4.26 (αCH), 2.26/2.01 (βCH), 2.77/2.62 (γCH), 7.12/6.86 (Ar-H); Orn-5: 7.68 (εNH), 7.61 (NH), 4.81 (αCH), 1.86/1.70 (βCH), 1.63 (γCH), 3.00 (δCH); Hyp-6: 4.09 (αCH), 4.34 (βCH), 2.32/2.01 (γCH), 3.80/3.72 (δCH); Ac: 2.04 ppm. ^{13}C-NMR (H_2O/D_2O, 125 MHz): δ Orn-1: 55.2 (αCH), 28.5 (βCH), 24.8 (γCH), 39.2 (δCH); Thr-2: 59.6 (αCH), 70.2 (βCH), 21.0 (γCH); Hyp-3: 63.2 (αCH), 38.8 (βCH), 72.9 (γCH), 57.9 (δCH); hTyr-4: 57.2 (αCH), 34.8 (βCH), 34.2 (γCH), 132.8/ 118.4 (Ar-H); Orn-5: 52.1 (αCH), 31.5 (βCH), 25.4 (γCH) 41.8 (δCH); Hyp-6: 70.1 (αCH), 75.6 (βCH), 34.6 (γCH), 48.1 (δCH); Ac: 23.9.

***Cyclo*[-(Ac)-Lys-Thr-Hyp-hTyr-Orn-Hyp] (2)**

Peptide **2** was obtained according to the general procedure for the preparation of the ring size analogues using 45 μmol of **5**. After lyophilization, peptide **2** (7 mg; 20%) was obtained as a white solid. Purity was confirmed by analytical HPLC and was found to be to be higher than 99% (R_t = 15.93 min). HRMS calcd for $C_{37}H_{56}N_8O_{11}$ $[M+H]^+$ 789.4147, found 789.4153; ^{1}H-NMR (H_2O/D_2O, 500 MHz): δ Lys-1: 8.58 (εNH), 8.47 (NH), 4.54 (αCH), 2.06/1.68 (βCH), 1.72/1.42 (γCH), 1.71/1.46 (δCH), 3.71/2.92 (εCH); Thr-2: 8.18 (NH), 4.89 (αCH), 4.32 (βCH), 1.19 (γCH); Hyp-3: 4.31 (αCH), 2.28/1.67 (βCH), 4.54 (γCH), 3.70/3.53 (δCH); hTyr-4: 7.01 (NH), 4.24 (αCH), 2.85/2.61 (βCH), 2.22/1.97 (γCH), 7.14/6.87 (Ar-H); Orn-5: 7.45 (εNH), 7.56 (NH), 4.61 (αCH), 1.91/1.69 (βCH), 1.61 (γCH), 3.00 (δCH); Hyp-6: 4.52 (αCH), 2.21/1.97 (βCH), 4.53 (γCH), 3.82/3.36 (δCH); Ac: 2.02 ppm. ^{13}C-NMR (H_2O/D_2O, 125 MHz): δ Lys-1: 56.4 (αCH), 33.4 (βCH), 26.5 (γCH), 27.9 (δCH), 43.2 (εCH); Thr-2: 59.3 (αCH), 70.6 (βCH), 20.9 (γCH); Hyp-3: 63.2 (αCH), 38.8 (βCH), 72.9 (γCH), 57.9 (δCH); hTyr-4: 58.2 (αCH), 34.3 (βCH), 34.6 (γCH), 132.9/ 118.5 (Ar-H); Orn-5: 53.0 (αCH), 30.2 (βCH), 25.8 (γCH) 41.8 (δCH); Hyp-6: 62.6(αCH), 39.5 (βCH), 72.4 (γCH), 57.9 (δCH); Ac: 24.0.

***Cyclo*[-(Ac)-Alg-Thr-Hyp-hTyr-Orn-Hyp-Alg]-OH (9)**

Wang-Tentagel S PHB resin (4 g; 1.04 mmol) and Fmoc-Alg-OH (1.09 g, 4.16 mmol) were dried *in vacuo* overnight over P_2O_5. DMF (20 mL) and pyridine (555 μL, 6.86 mmol) were added and the resin was shaken for 10 min untill total dissolution of the reagents. DCBC (596 μL, 4.16 mmol) was added and the resin was shaken for two days. The resin was drained and washed with DMF (5× 30 mL, each 2 min) and DCM (5× 30 mL, each 2 min). Subsequently, unreacted hydroxyl functions of the resin were acetylated by treatment with Ac_2O/NMI/DiPEA/DMF (30 mL; 2/1/1/6; v/v/v) for 30 min. The resin was drained and washed with DMF (3× 30 mL, each 2 min) and DCM (3× 30 mL, each 2 min). The peptide sequence was synthesized according to the general procedure for solid phase peptide synthesis. Hyp was coupled as part of the dipeptide Fmoc-Orn(Boc)-Hyp(*t*Bu)-OH. Part of the resin bound peptide (0.58 mmol) was used in the next steps. Removal of the Fmoc group was followed by treatment with capping solution Ac_2O/HOBt/DiPEA/NMP as described in the general procedures. Subsequently the capping solution was removed by filtration and the resin was washed with NMP (3× 15 mL, each 3 min) and DCM (3× 15 mL, each 3 min). The resin-bound peptide **8** was subjected to the microwave-assisted RCM procedure under the following conditions: Resin peptide (0.58 mmol), DCM (20 mL), LiCl/DMA (degassed; 0.4M; 2.0 mL), Grubbs II (10 mol%; 49 mg; 58 μmol), 100 °C for 60 min (performed in two batches due to the size (20 mL) of the microwave vessel). Final treatment with a mixture of TFA/TIS/H_2O (4 mL, 95/2.5/2.5, v/v/v) for 2h and precipitation in MTBE/hexanes (3×, 1/1, v/v) afforded the crude peptide. After lyophilization from *tert*-BuOH/H_2O (1/1, v/v) the peptide was purified by preparative HPLC. After preparative HPLC and lyophilization, peptide **9** (28 mg; 6%) was obtained as a white solid. Purity of this mixture of *E/Z* stereoisomers was confirmed by analytical HPLC and was found to be higher than 95% (R_t = 15.63 min). HRMS calcd for $C_{39}H_{56}N_8O_{13}$ $[M+H]^+$ 845.4045, found 845.4064; ^{1}H-NMR (H_2O/D_2O, 500 MHz): δ Alg-1: 8.60 (NH), 4.58 (αCH), 2.76/2.44 (βCH), 5.71 (γCH); Thr-2: 8.29 (NH), 4.85 (αCH), 4.40 (βCH), 1.25 (γCH); Hyp-3: 4.40 (αCH), 2.30/1.73 (βCH), 4.57 (γCH), 3.78/3.64 (δCH); hTyr-4: 7.52 (NH), 7.12/6.84 (Ar-H), 4.17 (αCH), 2.28/2.02 (βCH), 2.73/2.63 (γCH); Orn-5: 7.68 (εNH), 7.65 (NH), 4.78 (αCH), 1.92/1.70 (βCH), 1.60 (γCH), 3.00 (δCH); Hyp-6: 4.61 (αCH), 2.38/2.05 (βCH), 4.55 (γCH), 3.81/3.59 (δCH); Alg-7: 8.81 (NH), 4.36 (αCH), 2.76/2.44 (βCH), 5.71 (γCH); Ac: 2.01 ppm.

^{13}C-NMR (H_2O/D_2O, 125 MHz): δ Alg-1: 56.3 (αCH); Thr-2: 59.3 (αCH), 70.0 (βCH), 21.0 (γCH); Hyp-3: 63.0 (αCH), 38.9 (βCH), 72.7 (γCH), 57.9 (δCH); hTyr-4: 57.1 (αCH), 34.2 (βCH), 34.0 (γCH), 132.9/118.4 (Ar-H); Orn-5: 53.1 (αCH), 30.9 (βCH), 25.6 (γCH) 41.6 (δCH); Hyp-6: 61.2 (αCH), 39.5 (βCH), 72.5 (γCH), 58.1 (δCH); Alg-7: 55.7 (αCH); Ac: 23.9.

***Cyclo*[-(Ac)-Alg-Thr-Hyp-hTyr-Orn-Hyp-Alg]-OH (3)**

Hydrogenation of the cyclic unsaturated peptide **9** (21.9 mg; 25.9 μmol) was carried out using the hydrogenation procedure in the presence of 10 mg 10% Pd/C. After lyophilization from *tert*-BuOH/H_2O (1/1, v/v) the peptide was purified by preparative HPLC. After preparative HPLC and lyophilization, saturated peptide **3** (8.9 mg; 48%) was obtained as a white solid. Purity was confirmed by analytical HPLC and was found to be higher than 99% (R_t = 15.67 min). HRMS calcd for $C_{39}H_{58}N_8O_{13}$ $[M+H]^+$ 847.4202, found 847.4197; ^{1}H-NMR (H_2O/D_2O, 500 MHz): δ Alg-1: 8.79 (NH), 4.38 (αCH), 1.99 (βCH), 1.44 (γCH); Thr-2: 8.47 (NH), 4.84 (αCH), 4.32 (βCH), 1.25 (γCH); Hyp-3: 4.43 (αCH), 2.32/1.76 (βCH), 4.57 (γCH), 3.81/3.62 (δCH); hTyr-4: 7.56 (NH), 4.06 (αCH), 2.26/2.03 (βCH), 2.74/2.64 (γCH), 7.12/6.84 (Ar-H); Orn-5: 7.67 (εNH), 7.59 (NH), 4.81 (αCH), 1.90/1.74 (βCH), 1.64 (γCH), 3.00 (δCH); Hyp-6: 4.60 (αCH), 2.37/2.04 (βCH), 4.57 (γCH), 3.81/3.68 (δCH); Alg-7: 8.48 (NH), 4.42 (αCH), 1.71 (βCH), 1.53 (γCH); Ac: 2.02 ppm. ^{13}C-NMR (H_2O/D_2O, 125 MHz): δ Alg-1: 54.5 (αCH), 31.8 (βCH), 26.0 (γCH); Thr-2: 59.4 (αCH), 70.1 (βCH), 20.9 (γCH); Hyp-3: 62.7 (αCH), 39.1 (βCH), 72.6 (γCH), 58.2 (δCH); hTyr-4: 57.7 (αCH), 34.2 (βCH), 34.4 (γCH), 133.0/ 118.5 (Ar-H); Orn-5: 53.3 (αCH), 31.4 (βCH), 25.5 (γCH) 41.8 (δCH); Hyp-6: 61.6(αCH), 39.6 (βCH), 72.6 (γCH), 58.2 (δCH); Alg-7: 56.9 (αCH), 34.1 (βCH), 27.1 (γCH); Ac: 23.8.

References and notes

1. Mulder, M.P.C.; Kruijtzer, J.A.W.; Breukink, E.J.; Kemmink, J.; Pieters, R.J., Liskamp, R.M.J. *Bioorg. Med.Chem.*, **2011**, *19*, 6505-6517.
2. Dyson, H.J.; Wright, P.E. *Annu. Rev. Biophys. Biophys. Chem.*, **1991**, *20*, 519-538.
3. Cierpicki, T.; Otlewski, J. *J. Biomol. NMR*, **2001**, *21*, 249-261.
4. Ohnishi, M.; Urry, D.W. *Biochem. Biophys. Res. Commun.*, **1969**, *36*, 194-202.
5. Dyson, H.J.; Rance, M.; Houghten, R.A.; Lerner, R.A.; Wright, P.E. *J. Mol. Biol.*, **1988**, *201*, 161-200.
6. Rothemund, S.; Weiβhoff, H.; Beyermann, M.; Krause, E.; Bienert, M.; Mügge, C.; Sykes, B.D., Sönnischsen, F.D. *J. Biomol. NMR*, **1996**, *8*, 93-97.
7. Baxter, N.J.; Williamson, M.P. *J. Biomol. NMR*, **1997**, *9*, 359-369.
8. Wang, C.K., Hu, S-H.; Martin, J.L., Sjögren, T.; Hajdu, J.; Bohlin, L.; Claeson, P.; Göransson, U.; Rosengren, K.J.; Tang, J.; Tan, N-H; Craik, D.J. *J. Biol. Chem.*, **2009**, *284*, 10672-10683.
9. Aue, W.P.; Bartholdi, E.; Ernst, R.R. *J.Chem.Phys.*, **1976**, *64*, 2229-2246.
10. Kumar, A., Ernst, R.R., Wüthrich, K. *Biochem. Biophys. Res. Commun.*, **1980**, *95*, 1-6.
11. Rance, M. *J. Magn. Reson.*, **1987**, *74*, 557-564.
12. Bodenhausen, G.; Ruben, D.J. *Chem. Phys. Lett.*, **1980**, *69*, 185-189.
13. Wüthrich, K. *J. Biol. Chem.*, **1990**, 265, 22059-22062.
14. Wúthrich, K.; Billeter, M.; Braun, W. *J. Mol. Biol.*, **1984**, *180*, 715-740.
15. Rose, G.D.; Gierasch, L.M.; Smith, J.A. *Adv. Protein Chem.*, **1985**, *17*, 1-109.
16. Venkatachalam, C.M. *Biopolymers*, **1968**, *6*, 1425-1436.

17. Perczel, A.; Hollósi, M.; Sándor, P.; Fasman, G.D. *Int. J. Peptide Protein Res.*, **1993**, *41*, 223-236.
18. Kelly, S.M.; Price, N.C. Curr. Protein Pept. Sci., **2000**, 1, 349-384.
19. Ovchinnikov, Y.A.; Ivanov, V.T. Tetrahedron, **1975**, 31, 2177-2209
20. Woody, R.W.; *Method Enzymol.*, **1995**, *246*, 34-71.
21. Shibata, A.; Yamamoto, M.; Yamashita, T.; Chiou, J-S.; Kamaya, H.; Ueda, I. *Biochemistry*, **1992**, *31*, 5728-5733.
22. Sönnichsen, F.D.; van Eyk, J.E.; Hodges, R.S.; Sykes, B.D. *Biochemistry*, **1992**, *31*, 8790-8798.
23. Woody, R.W. *Peptides, Polypeptides, and Proteins Proc. Int. Symp.*, **1974**, eds. Blout, E. R., Bovey, F. A., Goodman, M. & Lotan, N. (Wiley, New York), 338-350.
24. Bandekar, J.; Evans, D.J.; Krimm, S.; Leach, S.J.; Lee, S.; McQuie, J.R.; Minasian, E.; Némethy, G.; Pottle, M.S.; Sheraga, H.A.; Stimson, E.R.; Woody, R.W. *Int. J. Peptide Protein Res.*, **1982**, *19*, 187-205.
25. Mulder, M.P.C.; Fodran, P.; Kemmink, J.; Breukink, E.J.; Kruijtzer, J.A.W.; Minnaard, A.J.; Liskamp, R.M.J. *Org. Biomol. Chem*, **2012**, *10*, 7491-7502.
26. Norris, T.; VanAlsten, J.; Hubbs, S.; Ewing, M.; Cai, W.; Jorgensen, M.L.; Bordner, J.; Jensen G.O. *Org. Process Res. Dev.*, **2008**, *12*, 447-455.
27. Modelling has been performed with the yasara software (www.yasara.org). (18-05-2012).
28. The echinocandin analogues have been sent to the University of Santiago in Spain (Departamento de Bioquímica y Biología Molecular, Facultad de Farmacia). Dr José M. Otero has included them in a crystallization assay.
29. Chayen, N.E.; Shaw Stewart, P.D.; Blow, D.M. *J. Cryst. Growth*, **1992**, *122*, 176-180.
30. Vojkovsky, T. Pept. Res., **1995**, 8, 236-237.
31. Kaiser, E.; Colescott, R.L.; Bossinger, L.D.; Cook, P.I. Anal. Biochem., **1970**, 34, 595-598.
32. Delaglio, F.; Grzesiek, S.; Vuister, G.W.; Zhu, G.; Pfeifer, J.; Bax, A. *J. Biomol. NMR*, **1995**, *6*, 277-293.
33. Wishart, D.S.; Bigam, C.G.; Yao, J.; Dyson, H.J.; Oldfield, E.; Markley, J.L.; Sykes, B.D. *J. Biol. NMR*, **1995**, *6*, 135-140.
34. Ponder, J.W.; Case, D.A. *Adv. Protein Chem*., **2003**, *66*, 27-85.

Appendices

Summary

Samenvatting

Leken Samenvatting

Curriculum Vitae

List of Publications

Summary

Fungi are increasingly recognised as major additional pathogens in already critically ill patients. Invasive fungal infections represent a growing threat and over the past two decades the incidence and diversity of fungal infections has increased enormously, especially among immunocompromised patients and patients hospitalized with serious underlying diseases. *Candida* spp. and *Cryptococcus* spp. are the yeasts most frequently isolated in clinical practice. The most frequent filamentous fungi (moulds) isolated are *Aspergillus* spp., but *Fusarium* spp., *Scedosporium* spp., and Zygomycetes are increasingly seen. Despite advances in antifungal therapies, the morbidity and mortality associated with these severe opportunistic fungal infections is substantial. Several reasons have been proposed for the increase in invasive fungal infections, including the wide use of broad-spectrum antibiotics and the still expanding population of immunocompromised patients. Resistance against and toxicity of the current antifungal agents underscores the urgent need for development of new antifungal compounds preferentially acting on novel targets.

The echinocandins represent the most recent contribution to the arsenal of antifungal compounds that have reached the market in the last decade and act on a novel target. These fungal secondary metabolites are composed of a complex cyclic hexapeptide core whose *N*-terminus is acylated by a lipid side chain. The echinocandins interfere with the synthesis of β-(1,3)-glucan, the major component of the framework of the fungal cell wall, by inhibiting the β-(1,3)-glucan synthase enzyme. They exhibit the most promising pharmacological, and toxicological profiles of the current arsenal of antifungal agents, as β-1,3-glucan is only found in fungi and not in mammalian cells. As a consequence fewer toxic side effects are observed, as compared to the other classes of antifungal agents. Moreover, the clinically approved agents for this class have rarely shown fungal resistance selection. Despite these advantages, the echinocandin class of compounds has its own limitations. Firstly, due to their semisynthetic nature, they are costly. Secondly their mechanism of action is still unknown and the interaction site of FKs1p/FKs2p with echinocandins has not yet been determined.

The research described in this Thesis aims at the exploration of the crucial structural features necessary for the antifungal activity of the echinocandin compounds, by synthesizing new derivatives for structure activity studies. This information can be used for the development of improved drugs and may contribute to elucidation of the mode of action.

In **chapter 1** a general introduction to this thesis is presented in which an overview of the current available antifungal agents is given. Additionally, an overview is offered of previous SAR studies on the echinocandins and their mode of action.

In **chapter 2** the development of a convenient strategy for the solid phase synthesis of new echinocandin derivatives (**2**, Figure 1) was described. In order to probe the influence of the cyclic peptide backbone on the antifungal activity novel echinocandins analogues by on-resin ring closing metathesis or disulfide bond formation were synthesized. The specific minimum inhibitory activity of each mimic was determined against *Candida albicans*. It was found that the analogues were not active at concentrations up to 100 μg/mL. However, analogues bearing a terphenyl side chain did show a dose-dependent effect on antifungal growth at

concentrations starting at 5 μg/mL. Remarkably, a slight enlargement of the macrocyclic peptide ring from a 21- to a 22-membered system completely abolishes antifungal activity, which was not expected in view of the resulting limited added flexibility to the peptide macrocycle. These results indicated that ring size is an crucial factor for antifungal activity.

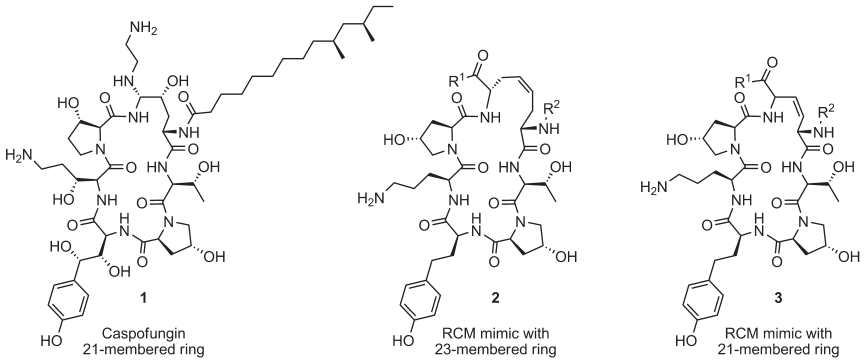

Figure 1. Structures of the semi-synthetic echinocandin Caspofungin (**1**) and the designed RCM mimics **2** and **3**.

Therefore, the preparation of other larger derivatives by either RCM or disulfide formation seemed an unattractive avenue. This somewhat unexpected finding enticed us to investigate the synthesis of smaller RCM-derived mimics (**3,** Figure 1). Attempts towards the preparation of smaller RCM mimics were outlined in **chapter 3**. The synthesis of vinylglycine and its application in the preparation of smaller caspofungin mimics involving RCM was described herein. It was demonstrated that vinylglycine had a tendency to isomerize to the conjugated α,β-unsaturated derivative due to its acidic Cα proton. Therefore, the direct incorporation of vinylglycine into peptides turned out to be problematic. Alternatively, facile, site-specific and chemoselective incorporation of vinylglycine can be achieved via oxidative elimination of (2-nitro)-phenylselenohomocysteine. This 'masked'' amino acid was readily prepared in three steps and conveniently incorporated into peptides through SPPS. Although a successful strategy for the synthesis of vinylglycine containing peptides was described, their use in metathesis reactions, for the construction of smaller RCM echinocandin mimics by RCM, proved to be unsuccessful. It was found that the vinylglycine derivatives were not or less reactive under RCM and cross metathesis conditions as compared to allylglycine derivatives.

Chapter 4 reported an approach to echinocandin based photoaffinity analogues. To elucidate in more detail the molecular mechanism of action of the echinocandin antifungal compounds photoaffinity containing analogues were interesting. Due to the structural importance of the cyclic hexapeptide nucleus of the echinocandins, the chemical probe was constructed as part of the fatty acid side chain. A set of benzophenone containing labels (**4**-**6**, Figure 2) was prepared and novel photoaffinity probe containing echinocandin analogues were synthesized. Although synthesis of these mimics was successful, evaluation of their antifungal properties showed no measurable activity. These findings stress the importance of the nature of the fatty acid side chain in relation to antifungal potency. These observations further supported the hypothesis that the side chain has to be straight and relatively rigid for optimal antifungal potency.

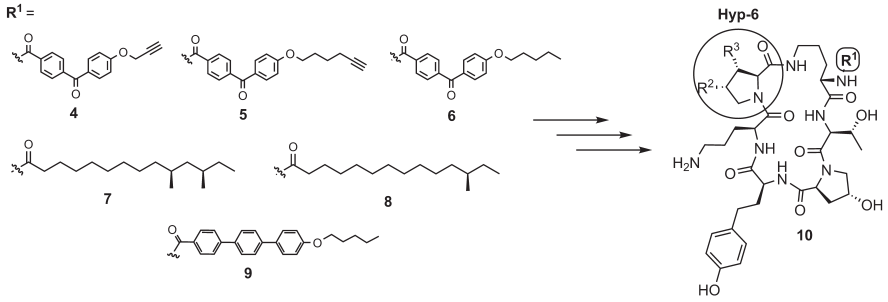

Figure 2. Structures of side chains **4**-**9** used for the synthesis of echinocandin mimics. The set of benzophenone containing labels (**4**-**6**) lead to echinocandin based photoaffinity analogues. Tails **7** and **8** lead to new fully synthetic derived caspofungin mimics **10**.

The research described in **chapter 5** entailed the study on the role of methyl groups in the lipophilic tail of analogues of caspofungin. A successful strategy for the rapid enantioselective synthesis of the branched fatty acid chain (**7**) of caspofungin and analogues (e.g. **8**) was developed (Figure 2). These fatty acids were coupled to simplified analogues of the caspofungin skeleton. In this way access was obtained to new fully synthetic derived caspofungin mimics with high and selective antifungal activities against *Candida*. Unexpectedly, no obvious relationship between the presence of the methyl groups in the dimethylmyristoyl tail of caspofungin and antifungal activity was observed. The position of the hydroxyl group in the top-left proline residue (R^2 and R^3 in Hyp-6 of analogue **10**, Figure 2) was apparently more crucial. The results of this investigation, in combination with the obtained CD spectra, suggest that the top-left proline residue somehow plays an important role in the bio-active conformation of the macrocyclic peptide ring structure. It was observed that the choice of the fatty acid derivative (rigid as in **9** or flexible as in **7** and **8**) in combination with the conformational character of the ring was a determining factor for antifungal activity.

In **chapter 6** the conformational behaviour of the echinocandin analogues was evaluated. In the previous chapters it became clear that the size, choice of the fatty acid side chain as well as crucial substituents were determining factors for antifungal activity. Here, it was attempted to rationalize the complete loss in activity as a result of increasing the ring size of echinocandin analogues. To elucidate solution conformations of the analogues described earlier in this thesis nuclear magnetic resonance (NMR) and circular dichroism (CD) techniques were applied. In the NMR studies parameters such as temperature coefficients of NH protons and NOEs were investigated. In the CD studies the Far UV region (250-190 nm), which corresponds to peptide-amide bond absorption, was measured to analyze the content of secondary structures. These studies showed comparable conformational behaviour of all three macrocyclic peptides. However, the 23-membered ring seemed to contain a smaller population of turn conformations compared to the native 21-membered ring. The slightly larger ring of the 22-membered analogue displayed the same characteristic conformational features as the 21-membered ring.

Nederlandse samenvatting

Schimmels worden steeds meer gezien als belangrijke additionele ziekteverwekkers bij reeds ernstig zieke patiënten. Invasieve schimmelinfecties vormen een toenemend gevaar en in de afgelopen twee decennia is de incidentie en de diversiteit van schimmelinfecties, vooral bij immuungecompromitteerde patiënten, enorm toegenomen. De gisten *Candida* spp. en *Cryptococcus* spp. worden het meest geïsoleerd in de klinische praktijk. De meest voorkomende geïsoleerde filamenteuze schimmels zijn *Aspergillus* spp., echter *Fusarium* spp., *Scedosporium* spp. en *Zygomycetes* worden steeds meer aangetroffen. Ondanks de vooruitgang in antischimmelbehandelingen, is het risico op morbiditeit en mortaliteit ten gevolge van deze ernstige opportunistische schimmelinfecties nog altijd aanzienlijk. Verschillende redenen kunnen hiervoor worden aangegeven, o.a het veelvuldig gebruik van breed-spectrum antibiotica en de nog steeds groeiende populatie van immuungecompromitteerde patiënten. Resistentie tegen en de toxiciteit van de huidige antischimmelmiddelen onderstrepen de dringende noodzaak voor de ontwikkeling van nieuwe antischimmelverbindingen bij voorkeur werkend op nieuwe targets.

De echinocandinen vertegenwoordigen de meest recente bijdrage aan het arsenaal van antischimmelverbindingen die de markt hebben bereikt in het laatste decennium en aangrijpen op een nieuw target. Deze secundaire metabolieten van schimmels bestaan uit een complex cyclisch hexapeptide kern met een geacyleerde *N*-terminus voorzien van een lipide zijketen. De echinocandinen verhinderen de synthese van β-(1,3)-glucan, de belangrijkste component van de schimmel celwand, door het inhiberen van het enzym β-(1,3)-glucansynthase. Zij vertonen de meest veelbelovende farmacologische en toxicologische profielen van het huidige arsenaal aan antischimmelmiddelen, aangezien β-1,3-glucan alleen te vinden is in de celwand van schimmels en niet in humane cellen. Als gevolg worden, in vergelijking met de andere klassen van antischimmelmiddelen, minder toxische bijwerkingen waargenomen. Bovendien tonen de schimmels tegen de klinisch goedgekeurde middelen van deze klasse zelden resistentie. Ondanks deze voordelen kent ook de echinocandin klasse van verbindingen zijn beperkingen. Ten eerste is de productie van deze middelen erg duur door het semisynthetische karakter van deze verbindingen. Ten tweede is hun mechanisme van werking nog onbekend. De plaats van interactie van FKs1p/FKs2p met de echinocandinen is nog niet gevonden.

Het in dit proefschrift beschreven onderzoek richtte zich op het bepalen van cruciale structurele kenmerken van de echinocandin verbindingen die nodig zijn voor een optimale antischimmelactiviteit. Dit werd bewerkstelligd door het synthetiseren van nieuwe derivaten en de evaluatie van hun antischimmelactiviteit. Deze informatie kan gebruikt worden voor het ontwikkelen van verbeterde geneesmiddelen en kan helpen bij het ophelderen van het werkingsmechanisme.

In **hoofdstuk 1** is een algemene inleiding tot dit proefschrift beschreven en is er een overzicht gegeven van de huidige beschikbare antischimmelmiddelen. Daarnaast werden eerdere structuur activiteits studies van de echinocandinen beschreven en werd het werkingsmechanisme besproken.

In **hoofdstuk 2** is de ontwikkeling van een strategie voor de synthese van nieuwe echinocandin derivaten (**2**, Figuur 1) op de vaste drager beschreven. De invloed van de cyclische peptide basisstructuur op de antischimmelactiviteit werd geëvalueerd door synthese van nieuwe echinocandin analoga op de hars met behulp van een ringsluiting metathese (RCM) reactie of vorming van een disulfidebrug. De minimaal inhiberende concentratie (MIC) van elk derivaat werd bepaald tegen *Candida albicans.* De derivaten bleken niet actief te zijn in concentraties tot 100 μg/mL. Echter, analoga met een terfenyl zijketen toonden een dosis-afhankelijk effect op antischimmelgroei bij concentraties vanaf 5 μg/mL. Opmerkelijk is dat de antischimmelactiviteit volledig verdwijnt bij een kleine vergroting van de macrocyclische peptide ring van een 21- naar een 22-atomige systeem. Dit was onverwacht, gezien de geringe extra flexibiliteit van het grotere cyclische peptide. Deze resultaten gaven aan dat ringgrootte een essentiële factor is voor antischimmelactiviteit.

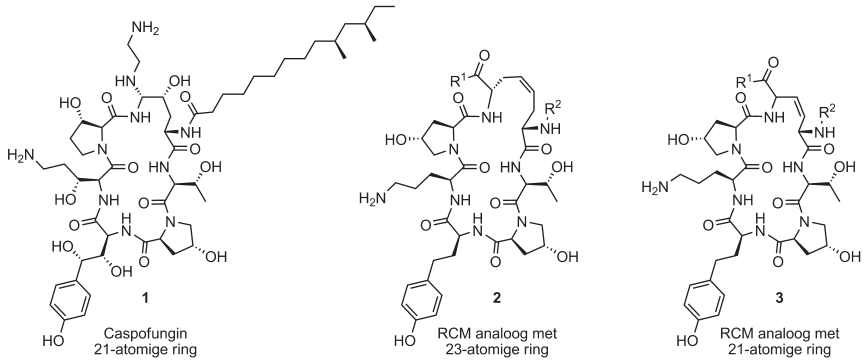

Figuur 1. Structuren van de semisynthetische echinocandin Caspofungin **(1)** en de ontworpen RCM analoga **2** en **3.**

De synthese van andere grotere derivaten via RCM of door disulfide-vorming bleek een onaantrekkelijke strategie en leidde daarom tot onderzoek naar de synthese van kleinere analoga (**3**, Figuur 1) die met behulp van RCM verkregen zouden kunnen worden. Pogingen tot de synthese van deze analoga werden beschreven in **hoofdstuk 3.** De synthese en toepassingen van vinylglycine in deze synthese werd hier beschreven. Er werd aangetoond dat vinylglycine isomeriseerde naar het geconjugeerde α,β-onverzadigde derivaat. Daarom was het direct inbouwen van vinylglycine in peptiden problematisch. Site-specifieke en chemoselectieve inbouw van vinylglycine residuen werd bereikt door het inbouwen van 2-nitro-phenylselenohomocysteine en oxidatieve verwijdering van de seleen beschermgroep. Dit 'gemaskeerde' aminozuur kon gemakkelijk bereid worden in drie stappen en werd m.b.v. SPPS ingebouwd in peptiden. Hoewel een succesvolle strategie voor de synthese van peptiden met vinylglycine residuen in de sequentie werd beschreven bleek het gebruik er van in metathesereacties geen succes voor de constructie van kleinere RCM echinocandin analoga. De vinylglycine derivaten bleken minder reactief in RCM en cross metathese reacties ten opzichte van allylglycine derivaten.

In **hoofdstuk 4** werd een strategie voor foto-affiniteit derivaten van echinocandin beschreven. Foto-affiniteit analoga zijn interessant om in meer detail het mechanisme van inhibitie van de echinocandinen te kunnen onderzoeken. De chemische fotolabel werd geïntroduceerd als deel van de vetzuur zijketen, aangezien het belang van de juiste

structuur van de cyclische hexapeptide kern van de echinocandinen al aangetoond was. Een set van labels met benzofenon groep (**4**-**6**, Figuur 2) werd gesynthetiseerd en nieuwe fotoaffiniteit analoga van echinocandin werden opgebouwd. Hoewel de synthese van deze derivaten succesvol bleek, vertoonden ze geen van allen meetbare antischimmelactiviteit. Deze resultaten benadrukken het belang van de aard van de vetzuur zijketen met betrekking tot antischimmelactiviteit. Deze bevindingen ondersteunden de hypothese dat de zijketen een relatief rigide en lineaire structuur moet bezitten voor een optimale activiteit.

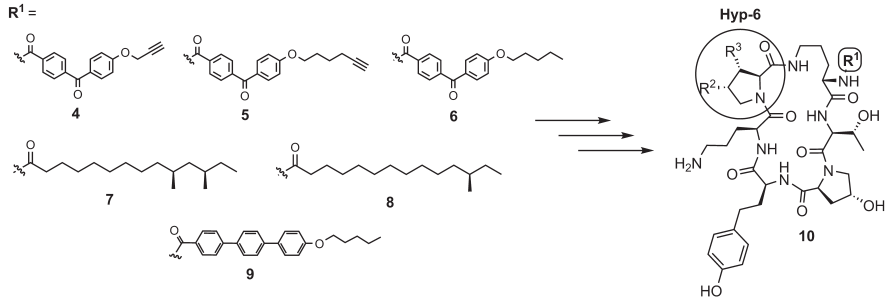

Figuur 2. Structuren van zijketens **4-9** gebruikt voor de synthese van echinocandin analoga. De set van labels met benzofenon (**4**-**6**) leiden tot foto-affiniteit derivaten van echinocandin. Staarten **7** en **8** leiden tot nieuwe, volledig synthetische caspofungin mimetica (**10**).

Het onderzoek beschreven in **hoofdstuk 5** omvat een studie over de rol van methylgroepen in de lipofiele staart van caspofungin derivaten. Een succesvolle strategie voor de snelle enantioselectieve synthese van de vertakte vetzuurketen (**7**) van caspofungin en analoga (bijv. **8**) werd ontwikkeld (Figuur 2). Deze vetzuren zijn gekoppeld aan het skelet van vereenvoudigde analoga van caspofungin. Op deze manier werd toegang verkregen tot nieuwe, volledig synthetische caspofungin derivaten met een hoge en selectieve antischimmelactiviteit tegen *Candida.* Onverwacht werd er geen duidelijk verband tussen de aanwezigheid van de methylgroepen in de dimethylmyristoyl staart van caspofungin en antischimmelactiviteit waargenomen. De positie van de hydroxylgroep in het proline residue (R^2 en R^3 in Hyp-6 van analoog **10**, Figuur 2) was blijkbaar belangrijker. Het proline residue aan de linkerkant van het molecuul bleek een belangrijke rol te spelen in de bio-actieve conformatie van de macrocyclische peptide ringstructuur. De keuze van het vetzuurderivaat (met rigide structuur zoals in **9** of een meer flexibele structuur zoals in **7** en **8**) in combinatie met het conformationele karakter van de ring leek bepalend te zijn voor antischimmelactiviteit.

In **hoofdstuk 6** werd het conformationele gedrag van de echinocandin analoga geëvalueerd. In de voorgaande hoofdstukken was gebleken dat de grootte, de keuze van de vetzuur zijketen, evenals cruciale substituenten een belangrijke rol speelden in de antischimmelactiviteit van de analoga. In dit hoofdstuk werd getracht het volledige verlies van de activiteit als gevolg van de grotere ringgrootte van echinocandin analoga te verklaren. Hiervoor werden nucleaire magnetische resonantie (NMR) en circulaire dichroïsme (CD) technieken toegepast. In het NMR onderzoek werden factoren als de temperatuur coëfficiënten van de amide protonen en NOE's onderzocht. In de CD werd het verre UV gebied (250-190 nm), met daarin de peptide-amidebinding absorptie, gemeten om de secundaire structuur te bestuderen. Deze studies toonden vergelijkbaar conformationeel gedrag aan van de drie macrocyclische

peptiden. Echter lijkt de 23-atomige ring een geringere populatie van ‘β-turn’ conformaties te bevatten in vergelijking met de oorspronkelijke 21-atomige ring. Terwijl voor de 22-ring analogon dezelfde karakteristieke conformationele ‘β-turn’ eigenschappen als voor de 21-ledige ring gevonden werden.

Samenvatting voor de geïnteresseerde leek

In deze sectie heb ik mijn promotieonderzoek in lekentaal samengevat. Deze samenvatting is vooral bedoeld voor mensen die minder bekend zijn met mijn vakgebied.

Jaarlijks sterven in Nederlandse ziekenhuizen tientallen patiënten met een verzwakt immuunsysteem aan de gevolgen van agressieve schimmelinfecties. Deze schimmels zijn steeds vaker niet of nauwelijks te bestrijden, omdat ze veroorzaakt worden door schimmels die resistent zijn voor het huidige arsenaal aan antischimmel medicijnen.

Iedereen kent wel de oppervlakkige schimmelinfecties die de huid of nagels aantasten. Denk daarbij maar aan de reclames met 'schimpie de schimmel'. Daarnaast ademen we allemaal dagelijks de sporen in van aspergillus schimmelsoorten. Deze schimmels vormen voor gezonde mensen geen gevaar. Echter kunnen ze bij patiënten met een verzwakt immuunsysteem diepe, zogeheten invasieve (inwendige) schimmelinfecties veroorzaken die levensbedreigend kunnen zijn.

Patiënten met leukemie, en binnen die groep vooral de patiënten die beenmergtransplantatie of stamceltherapie hebben gehad, lopen het grootste risico om een dergelijke schimmelinfectie op te lopen. Ook patiënten die een orgaantransplantatie hebben ondergaan en behandeld worden met corticosteroïden lopen een verhoogd risico op invasieve schimmelinfecties. Datzelfde geldt voor mensen die hiv-positief zijn en patiënten met aids.

Problemen als resistentie (ongevoeligheid) en toxiciteit (giftigheid) van de huidige geneesmiddelen onderstrepen de dringende noodzaak voor nieuwe antischimmelmedicijnen. Een ideaal geneesmiddel grijpt aan op een specifiek punt dat de schimmel wel heeft en de gastheer (de mens) niet.

De echinocandinen vertegenwoordigen de meest recente bijdrage aan het arsenaal van antischimmelmedicijnen die de markt hebben bereikt. Ze werken op een ander specifiek punt (target) van de schimmel dan de andere medicijnen. Zij vertonen de meest veelbelovende eigenschappen van de huidige geneesmiddelen aangezien hun target, in tegenstelling tot die van de andere medicijnen, alleen te vinden is in de celwand van schimmels en niet in menselijke cellen. Als gevolg daarvan worden er bij het gebruik van echinocandinen minder toxische bijwerkingen waargenomen. Bovendien tonen de schimmels zelden resistentie bij deze nieuwe klasse van medicijnen.

Het onderzoek waar ik de afgelopen jaren aan heb gewerkt richtte zich op het bepalen van de belangrijke structurele eigenschappen van de echinocandin verbindingen die nodig zijn voor het bestrijden van schimmels. Dit werd bereikt door het maken (synthetiseren) van nieuwe varianten van deze verbindingen en de evaluatie van hun antischimmelactiviteit. De verkregen kennis kan gebruikt worden voor het ontwikkelen van verbeterde geneesmiddelen en het ophelderen van het exacte werkingsmechanisme van deze middelen. Hieronder zal ik meer uitleggen over hoe ik dit bereikt heb.

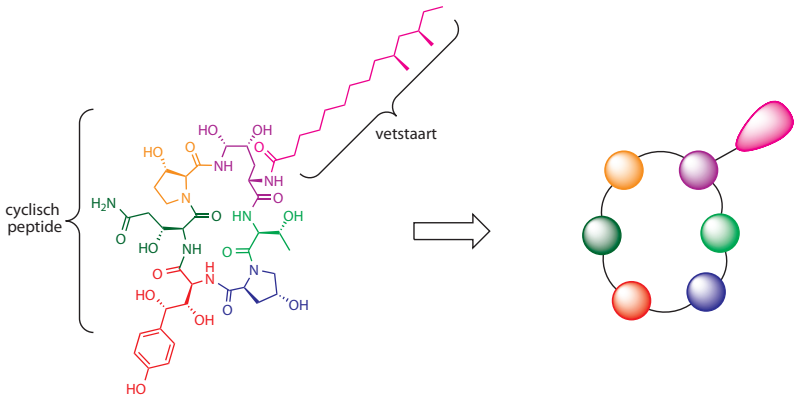

Figuur 1. De structuur van een echinocandin en de representatie als ketting.

De echinocandinen zijn cyclische peptides met een vetstaart (zie figuur 1). De bouwstenen van deze peptides zijn aminozuren. Het maken van deze cyclische peptides kun je vergelijken met het maken van een kralenketting. Voor het maken van een peptide voeg je steeds een aminozuur toe, zoals je bij een ketting een kraal toevoegt. De ketting van aminozuren die je aan het eind krijgt heet een peptide. Vervolgens willen we deze peptide cyclisch maken. Hier kunnen we verschillende 'sluitingen' gebruiken van onze ketting. De uiteindes van het peptide kunnen op verschillende manieren aan elkaar gebonden worden. Elke 'sluiting' heeft zijn eigen kenmerken. Het maken van deze eerste serie echinocandin derivaten wordt beschreven in hoofdstuk 2. Hieruit bleek dat de 'lengte van de ketting' erg belangrijk is voor de activiteit (effectiviteit van het medicijn). Wanneer de ketting te groot wordt verliest deze zijn antischimmelactiviteit.

Na dit resultaat wordt in hoofdstuk 3 een poging beschreven tot het inbouwen van een 'kleinere' kraal. Hiermee proberen we wel de 'sluiting' te gebruiken die we beschreven hebben in hoofdstuk 2, maar dan wel zonder de ketting te groot te maken. Hiermee zouden we dan de antischimmelactiviteit kunnen behouden. De synthese van dit aminozuur was succesvol, maar helaas is het niet mogelijk gebleken om met deze nieuwe kraal een cyclisch peptide te maken.

Vervolgens wordt in hoofdstuk 4 een strategie beschreven waarmee we meer informatie wilden verkrijgen over de manier waarop de echinocandinen precies werken. Er is een poging gedaan om de chemische structuur van de echinocandinen zo aan te passen zodat deze, na het binden aan hun target, fluorescerend gemaakt konden worden. De lichtgevende target-echinocandinen combinaties zouden dan vervolgens apart bekeken en geïdentificeerd kunnen worden. Deze poging was niet geslaagd omdat de aangepaste echinocandinen niet actief waren en dus niet bonden met hun target op de schimmel.

In hoofdstuk 5 bekijken we een ander deel van de structuur van de echinocandinen, namelijk de vetstaart, in meer detail. Deze vetstaart kan vergeleken worden met de hanger aan onze ketting (zie figuur 1). Zoals eerder beschreven is de samenstelling van het peptide, dus de kralen aan de ketting, erg belangrijk voor de activiteit van de echinocandinen. In dit hoofdstuk zijn we gaan kijken hoe belangrijk de hanger aan de ketting is voor activiteit.

In het vorig hoofdstuk is al gebleken dat deze staart een relatief stevige (niet flexibele) en rechte structuur moet hebben voor een goede activiteit van de echinocandinen. Uit andere onderzoeken bleek de lengte van de vetstaart al belangrijk te zijn. Wij zijn gaan kijken hoe belangrijk de vertakkingen zijn die in deze vetstaarten voorkomen. Er zijn verschillende vetstaarten gemaakt en gekoppeld aan de peptides, waarna ze getest zijn voor hun antischimmelactiviteit. Hieruit bleek dat vooral de combinatie van de hanger en één van de kralen in de ketting zeer belangrijk was voor de activiteit. Wanneer deze kraal vervangen werd voor een ander was de vetstaart niet actief. Terwijl als we de goede kraal in de ketting hadden onze hanger wel actief was.

De bevindingen uit voorgaande hoofdstukken dat de lengte van de ketting evenals de keuze van hanger in combinatie met de juiste kraal in de ketting erg belangrijk zijn voor de activiteit van de echinocandinen zorgden voor nieuwe vraagtekens. Deze resultaten suggereerde namelijk dat de conformatie van de echinocandinen erg belangrijk is voor de activiteit. Met de conformatie bedoelen we de 'vorm' van de ketting. Immers als de ketting groter wordt of als we andere kralen gebruiken kan de ketting een hele andere vorm krijgen. Om te kijken of dit dan ook het geval is voor onze aangepaste echinocandinen hebben we in hoofdstuk 6 het conformationele gedrag ('de vorm') van deze verbindingen onderzocht. Hier zijn verschillende technieken voor gebruikt, waarbij we de 3D-structuur van onze verbindingen hebben geprobeerd op te helderen. Hierbij blijkt inderdaad dat de grotere peptides andere conformationele eigenschappen hebben, ofwel dat deze ketting een iets andere ruimtelijke vorm heeft.

Curriculum Vitae

Monique Mulder werd geboren op 1 november 1983 te Zeist. In 2001 behaalde zij haar HAVO diploma aan de Lage Waard te Papendrecht. Hetzelfde jaar begon zij de studie Chemie op het HLO te Rotterdam. Daarvoor werd in 2005 een afstudeeropdracht uitgevoerd bij de Lead Optimalization Unit van N.V. Organon in Oss waar werd gewerkt aan het project "Synthesis of Er α,β active furan compounds". Na het behalen van haar diploma, begon zij in september 2005 aan met de master studie Drug Innovation aan de Universiteit Utrecht. In het kader van haar major stage verrichte zij onderzoek in de groep van Prof Dr. Rob Liskamp op de afdeling Medicinal Chemistry. Hier werd onderzoek verricht naar de synthese van triazacyclophaan (TAC) derivaten als nieuwe HIV inhibitoren, begeleid door Dr. Cristina Chamorro. Haar externe stage werd vervolgens uitgevoerd bij de afdeling Biomolecular Engineering van Philips te Eindhoven o.l.v Dr. Johan Lub. Hier werkte zij aan de synthese van polymeren voor de fabrikatie van Ultrasound Contrast Agents. In april 2007 studeerde ze Cum Laude af aan de Universiteit Utrecht. Vlak daarna keerde zij terug als promovendus in de groep Medicinal Chemistry & Chemical Biology. De resultaten van dit promotieonderzoek staan beschreven in dit proefschrift. Tijdens deze periode werden de behaalde onderzoeksresultaten gepresenteerd op nationale en internationale congressen, zoals de Dutch Peptide Meeting (April 2010, Leiden) en het 31st European Peptide Symposium (September 2010, Kopenhagen, Denemarken). Vanaf januari 2012 is de auteur werkzaam als post-doc in de groep van Dr. H. Ovaa bij het Nederlands Kanker Instituut - Antoni van Leeuwenhoek Ziekenhuis (NKI-AvL).

List of publications

Synthesis and evaluation of novel macrocyclic antifungal peptides. M.P.C. Mulder, J.A.W. Kruijtzer, E.J. Breukink, J. Kemmink, R.J. Pieters, R.M.J. Liskamp, *Bioorg. Med. Chem.*, **2011**, 19, 6505-6517.

Mutual influence of backbone proline substitution and lipophilic tail character on the biological activity of simplified analogues of caspofungin. *M.P.C. Mulder, *P. Fodran, J. Kemmink, E.J. Breukink, J.A.W. Kruijtzer , A.J. Minnaard, R.M.J. Liskamp, ***Org. Biomol. Chem.***, **2012**, *10*, **7491-7502** *) equal contributors

Oral Presentations and Posters

Utrecht University & Max-Planck Chemical Biology Symposium, May 2011, Utrecht, The Netherlands. Oral: "Synthesis and antifungal evaluation of novel macrocyclic peptides."

Netherlands Organization for Scientific Research – Chemical Sciences, Joint meeting of the study groups Design & Synthesis, Structure & Reactivity and Biomolecular Chemistry, October 2010, Lunteren, the Netherlands. Poster: "Synthesis of macrocyclic antifungal peptides by RCM. Towards novel antifungal agents against invasive fungal infections."

31st European Peptide Symposium, September 2010, Copenhagen, Denmark. Poster: "Synthesis of macrocyclic peptides. Towards novel antifungal agents against invasive fungal infections."

Dutch Peptide Meeting, April 2010, Leiden, the Netherlands. Oral: "Synthesis of macrocyclic antifungal peptides. Towards novel antifungal agents against invasive fungal infections."

Netherlands Organization for Scientific Research – Chemical Sciences, Joint meeting of the study groups Design & Synthesis, Structure & Reactivity and Biomolecular Chemistry, October 2009, Lunteren, the Netherlands. Oral: "Synthesis of mimics of Caspofungin. Towards novel antifungal agents against invasive fungal infections."

Utrecht University & Max-Planck Institut (MPI) Chemical Biology meeting, September 2008, Dortmund, Germany. Poster: "Synthesis of Caspofungin derivatives. Towards novel antifungal agents against invasive fungal infections."

Dankwoord

Ik kan het zelf nog niet helemaal geloven, maar het is nu echt klaar! Dit is mijn proefschrift, maar dat betekent bepaald niet dat ik het allemaal alleen heb gedaan. Dit boekje was er niet geweest zonder de hulp en steun van heel veel mensen binnen en buiten het lab. En dat brengt ons dan ook bij het meest gelezen gedeelte van het proefschrift, het dankwoord.

Ik wil eerst de mensen bedanken met wie ik de meeste uren in het lab heb doorgebracht. En dus begin ik bij mijn oud labgenootjes van Z617. Hilbert, Joeri, Nuria, Tania, Raymond en Marjolein, ik heb met heel veel plezier met jullie gewerkt. Bedankt voor alle uren samen op het lab, de praktische hulp, de gezelligheid en de wetenschappelijke en minder wetenschappelijke discussies.

Daarnaast wil ik mijn promotor Rob Liskamp bedanken voor de mogelijkheid en het vertrouwen om me als onderzoeker te kunnen ontwikkelen in jouw vakgroep. Bedankt voor alle adviezen en discussies. Dit brengt me meteen ook bij John Kruijtzer. Jou bijdrage in onze meetings zijn soms zeer waardevol gebleken en dit heeft jou dan ook als co-promotor weten te bestempelen. Ook wil ik Cristina bedanken, bij jou deed ik als masterstudent mijn eerste stapjes binnen het onderzoek bij Medchem en het leverde mij uiteindelijk een leuk plekje als AIO op.

Verder wil ik mijn studenten bedanken voor het werk dat zij gedaan hebben. Gerjan de Bruin, Timo Koopmans, Bieneke Janssen en Robbert Thissen bedankt voor jullie directe/ indirecte bijdrage aan mijn proefschrift. Drie van jullie zijn inmiddels zelf begonnen aan jullie PhD, heel veel succes daarin. En Robbert heel veel plezier en succes voor de klas als scheikunde docent.

Een aantal hoofdstukken zijn het resultaat van samenwerkingen binnen en buiten MedChem. Johan bedankt voor de eindeloze NMR metingen en modelling studies aan mijn peptides. Naast de mooie karakteriseringen van de peptides heeft dit ook geresulteerd in hoofdstuk 6. Eefjan Breukink bedankt voor alle hulp bij het opzetten van de biologische assays. Teun Boekhout bedankt voor de Candida strains en José Otero thanks for your efforts on crystallizing the peptides. Adri Minnaard and Peter Fodran our collaboration has resulted in a nice paper, thanks!

Ook wil ik alle andere (oud)-collega's van de vakgroep Medicinal Chemistry & Chemical Biology bedanken voor de goede werksfeer. Zowel op als buiten het lab was de sfeer altijd goed en ik heb hier een hele leuke periode beleeft. In het bijzonder wil ik Francesca en Rik bedanken, vooral voor hun vriendschap buiten het lab. Fran, I really enjoyed our time in Italy and our nice dinners. So let's keep doing this. En Rik wanneer gaan we nou eindelijk eens fietsen?

Ik wil alle huidige AIO's van Medchem: Hilde, Loek, Jack, Gwen, Francesca, Steffen, Helmus, Ou, Rik, Timo, Peter en Paul veel succes wensen met hun onderzoek en promotie. Jinqiang you're next in line, good luck with the final steps.

Nog even een woordje voor mijn paranimfjes. Ray, we hebben zo ongeveer sinds de start van mijn promotie samen op het lab gestaan en toen ik mijn werkplek verhuisde naar het NKI ben je me zelfs achter nagereisd. Voor mij was er dan ook geen twijfel en moest jij mijn paranimf zijn! En Patricia, mijn kleine lieve zusje, ik vind het echt super dat jij op deze grote dag mijn paranimf wil zijn. Hopelijk wordt het voor jullie net zo'n bijzondere dag als voor mij!

Alle vrienden en familie die zorgden voor de broodnodige ontspanning: bedankt voor de feestjes, etentjes, barbecues (ook al vinden die te vaak in de regen plaats), weekendjes, vakanties, concertbezoeken en klusweekenden.
José, Bram, Anoeska en Jasper, ik bof met jullie als schoonfamilie. Bedankt voor jullie interesse en steun in de afgelopen periode.
Lieve mam, bedankt voor alles! Je hebt me altijd vrij gelaten mijn eigen keuzes te maken en hebt me hierin vervolgens altijd gesteund. Zonder jou onvoorwaardelijke steun en liefde was het nooit gelukt.

Tot slot wil ik degene bedanken die mijn promotietijd het meest bijzonder heeft gemaakt. Lieve Jeroen, ik ben blij dat jij gedurende deze hectische periode er altijd voor me was. Jouw liefde, vertrouwen, relativeringsvermogen, nuchterheid, geduld en humor hebben me door de moeilijke momenten heen geholpen. Samen hebben we deze periode tot een goed einde weten te brengen. Ik hou van je!